SEQUENTIAL SUPPLEMENTARY FIRING IN NATURAL GAS COMBINED CYCLE PLANTS WITH CARBON CAPTURE FOR ENHANCED OIL RECOVERY

Abigail González Díaz

Doctor of Philosophy

School of Engineering
University of Edinburgh

2016

To my mom

Lay Summary

A novel configuration for gas-fired power plants with carbon dioxide capture is proposed, where the combustion of natural gas in a sequential manner in the steam generator increases the production of heat, work and carbon dioxide compared to a conventional configuration. This reduces capital costs and operational costs per kW of installed electric capacity and, when combined with enhanced oil recovery, a process which improves the recovery of producing oil fields, creates additional revenues. This lowers the cost of production of low-carbon electricity. A techno-economic assessment shows that the findings are robust over a range of fuel prices, carbon dioxide prices and capital costs. Efficiency improvements are then proposed by increasing the pressure of steam generation, the working fluid of the combined steam cycle of the gas-fired power plant, above its critical point. Optimum strategies for the part-load operation of this novel configuration are proposed, which maximise both electricity and CO_2 production. This novel configuration of gas-fired power plants could be attractive in Mexico, where favourable conditions for enhanced oil recovery and affordable natural gas prices will continue to exist.

Abstract

The rapid electrification through natural gas in Mexico; the interest of the country to mitigate the effects of climate change; and the opportunity for rolling out Enhanced Oil Recovery at national level requires an important R&D effort to develop nationally relevant CCS technology in natural gas combined cycle power plants. Post-combustion carbon dioxide (CO_2) capture at gas-fired power plant is identified and proposed as an effective way to reduce CO_2 emissions generated by the electricity sector in Mexico. In particular, gas-fired power plants with carbon dioxide capture and the sequential combustion of supplementary natural gas in the heat recovery steam generator can favourably increase the production of carbon dioxide, compared to a conventional configuration. This could be attractive in places with favourable conditions for enhanced oil recovery and where affordable natural gas prices will continue to exist, such as Mexico and North America.

Sequential combustion makes use of the excess oxygen in gas turbine exhaust gas to generate additional CO_2, but, unlike in conventional supplementary firing, allows keeping gas temperatures in the heat recovery steam generator below 820°C, avoiding a step change in capital costs. It marginally decreases relative energy requirements for solvent regeneration and amine degradation.

Power plant models integrated with capture and compression process models of Sequential Supplementary Firing Combined Cycle (SSFCC) gas-fired units show that the efficiency penalty is 8.2% points LHV compared to a conventional natural gas combined cycle power plant with capture. The marginal thermal efficiency of natural gas firing in the heat recovery steam generator can increase with supercritical steam generation to reduce the efficiency penalty to 5.7% points LHV. Although the efficiency is lower than the conventional configuration, the increment in the power output of the combined steam cycle leads a reduction of the number of gas turbines, at a similar power output to that of a conventional natural gas combined cycle. This has a positive impact on the number of absorbers and the capital costs of the post combustion capture plant by reducing the total volume of flue gas by half on a normalised basis. The relative reduction of overall capital costs is, respectively, 9.1 % and 15.3% for the supercritical and the subcritical combined cycle configurations with capture compared to a conventional configuration. The total revenue requirement, a metric combining levelised cost of electricity and revenue from EOR, shows that, at gas prices of 2

$/MMBTU and for CO_2 selling price from 0 to 50 $/tonne$CO_2$, subcritical and supercritical sequential supplementary firing presents favourably at 47.3-26 $/MWh and 44.6-25 $/MWh, respectively, compared with a conventional NGCC at 49.5-31.7 $/MWh.

When operated at part-load, these configurations show greater operational flexibility by utilising the additional degree of freedom associated with the combustion of natural gas in the HRSG to change power output according to electricity demand and to ensure continuity of CO_2 supply when exposed to variation in electricity prices. The optimisation of steady state part-load performance shows that reducing output by adjusting supplementary fuel keeps the gas turbine operating at full load and maximum efficiency when the net power plant output is reduced from 100% to 50%. For both subcritical and supercritical combined cycles, the thermal efficiency at part-load is optimised, in terms of efficiency, with sliding pressure operation of the heat recovery steam generator. Fixed pressure operation is proposed as an alternative for supercritical combined cycles to minimise capital costs and provide fast response rates with acceptable performance levels.

Acknowledgements

I would like to thank my supervisors Prof. Jon Gibbins and Dr. Mathieu Lucquiaud, for providing constant support, for their patient, and for sharing their knowledge with me. It was worthy to cross the Atlantic to join this research group.

I would like to give a special acknowledge to Dr. Eva Sanchez Fernandez for her supervision in the design and simulation of the capture plant and for her valuable advice and comments on this work.

Thanks to the Mexican National Council for Science and Technology (CONACyT) and the National Institute of Electricity and Clean Energy (INEEL) for funding my PhD study.

I would like to thank the UKCCSRC for the funding to attend different CCS meetings in the UK. CCPilot100+plant team for their help during my internships at SSE plc pilot plant.

Thank to Pamela Tomsky from Global CCS Institute for giving the opportunity to attend the training program Research experienced in Carbon Sequestration (RECS) in Alabama, USA.

Thanks to Dr. José Miguel González Santaló, Dr. Eduardo Preciado Delgado, and Ing. Antonio Carnero Parra from the IIE for making possible to come and study my PhD at the University of Edinburgh.

I would also like to thank to Dr. Alasdair Bruce for his help since I arrived to Edinburgh, for checking my writing most of all the time, and for being my friend. Also thank to Thomas Spitz for his help.

I sincerely appreciate the time and efforts of my examination committee members Prof. Mohamed Pourkashanian and Dr. Hannah Chalmers. Thank you so much.

Finally, thanks to my family.

Declaration

The work included in this thesis, except where specific reference is made to other sources, is the results of the work of the author alone under the guidance of the supervisors Dr. Mathieu Lucquiaud and Prof. Jon Gibbins. This PhD thesis has not been submitted in whole or in part for any other degree.

Abigail Gonzalez Diaz

Contents

List of tables

List of figures

List of publications

Peer-reviewed journal

1. **Abigail González Díaz**, E. Sánchez Fernández, J. Gibbins, and M. Lucquiaud, "Sequential supplementary firing in natural gas combined cycle with carbon capture: A technology option for Mexico for low-carbon electricity generation and CO_2 enhanced oil recovery", International Journal of Greenhouse Gas Control, 51 (2016) 330–345. Doi: 10.1016/j.ijggc.2016.06.007

1. **Abigail González Díaz**, M. O. González, J. Gibbins, and M. Lucquiaud, Priority projects for the implementation of CCS power generation with enhanced oil recovery in Mexico *(submitted)*

2. **Abigail González Díaz**, E. Sánchez Fernández, J. Gibbins, and M. Lucquiaud, Sequential supplementary firing in CCGT with carbon capture: part-load operation scenarios in the context of enhanced oil recovery *(In preparation)*

Peer-reviewed conferences

GHGT-12 and GHGT-13

1. **Abigail Gonzalez Diaz**, E. Sánchez Fernández, M. Lucquiaud, and J. Gibbins. On the integration of sequential supplementary firing in natural gas combined cycle for CO_2-Enhanced Oil Recovery: A techno-economic analysis for Mexico. Energy procedia vol. 63, 2014, pages 7558-7567. GHGT-12, Austin Texas, 6-9 October. doi:10.1016/j.egypro.2014.11.791

2. **Abigail González Díaz**, M.O González Díaz, J. Gibbins, M. Lucquiaud. Opportunities for deploying CCS – CO_2-EOR in Mexico. GHGT-13, Switzerland, November 2016

3. **Abigail González Díaz**, E. Sánchez Fernández, J. Gibbins, M. Lucquiaud. Part-load operation of sequential supplementary firing combined cycle power plant with CO_2 capture. GHGT-13, Switzerland November 2016

Presentations

1. **A. González Díaz**, J. Gibbins, M. Lucquiaud. Combustible suplementario secuencial en ciclos combinados para reducir emisiones de CO_2 y recuperación mejorada de petróleo en México. Innovation Match MX 2015-2016. 1er Foro Internacional de Talento Mexicano, Guadalajara, México, 6-8 abril 2016

2. **A. González Díaz**, J. Gibbins, M. Lucquiaud. Techno-economic assessment of sequential supplementary firing in natural gas combined cycle for co2 capture for enhanced oil recovery in Mexico. 8th Trondheim Conference on CO_2 Capture, Transport and StorageTCCS-8, Norway, 2015
3. **A. González Díaz**, M. Lucquiaud, and J. Gibbins, Mexico's new CCUS roadmap, , UKCCSRC Biannual Meeting CCS and Industry, University of Cardiff, 10-11 September 2014
4. **A. González Díaz**, Jose Miguel Gonzalez Santaló, Gas CCUS in Mexico, UKCCSRC Gas CCS Meeting at the University of Sussex, Brighton, 25 June 2014
5. **A. González Díaz**, M. Lucquiaud, and J.R. Gibbins, Opportunities for Deploying CCS in Mexico, UKCCSRC Biannual Meeting CCS in the Bigger Picture Agenda, at University of Cambridge, 02-03 April 2014
6. **A. González Díaz**, M. Lucquiaud, and J. Gibbins, CCS on Natural Gas Combined Cycle: An alternative to reduce CO2 emissions in Mexico, UKCCSRC Biannual Meeting at the University of Nottingham, 03-05 September 2014

Nomenclature

ASU	Air Separation Unit
BEC	Bared erected cost
BOP	Balance of plant
CAPEX	Capital expenditure
CCS	Carbon Capture and Storage
CCUS	Carbon Capture Use and Storage
CFE	Comisión Federal de Electricidad (Federal commission of Electricity)
CH_4	Methane
CO	Carbon monoxide
CO_2	Carbon dioxide
DCC	Direct Contact Cooler
EGR	Exhaust Gas Recirculation
EOR	Enhanced Oil Recovery
EPC	Engineering procurement and construction
GE	General Electric
GHG	Greenhouse Gas
GT	Gas Turbine
H_2	Hydrogen
HPB	High pressure boiler or evaporator
HPE	High pressure economiser
HP	High pressure
HPS	High pressure superheater
HR	Reheat
HRSG	Heat Recovery Steam Generation
IGV	Inlet Guide Vanes
IP	Intermedia pressure
IPB	Intermedia pressure boiler or evaporator
IPE	Intermedia pressure economiser
IPS	Intermedia pressure superheater
LP	Low pressure
LPB	Low pressure boiler or evaporator

LPE	Low pressure economiser
LPS	Low pressure superheater
MEA	Monoethanolamine
MRV	Monitoring, Report and Verification mechanisms
MW	Megawatts
N_2	Nitrogen
NGCC	Natural Gas Combined Cycle
O_2	Oxygen
OCGT	Open Cycle Gas Turbine
O&M	Operating and maintenance cost
OTB	Once through boiler or supercritical evaporator
PEMEX	Petróleos Mexicanos (Mexican Oil Company)
SC	Supercritical
SSFCC	Sequential supplementary firing combined cycle
SO_X	Sulfur oxide
TCR	Total capital requirement
TRR	Total revenue required
LCOE	Levelised cost of electricity
VHP	Very high pressure
Wt	percentage weight

1. Introduction

1.1 Carbon Capture and Storage and its contribution to mitigating climate change

Global CO_2 emissions have been rising significantly with the potential to cause catastrophic climate change. It has been estimated that global greenhouse gas (GHG) emissions will continue to rise by 28% from 2000 to 2030 if no action is taken (IPCC, 2013). In the recent Paris agreement on climate change a new goal was set to limit temperature rises to 2 °C (WEO, 2015). Past emissions, amounting to about 2 trillion tonnes of CO_2, caused an increment of 1°C in temperature (Hone, 2016). In order to limit temperature rises to 2 °C global CO_2 emissions must be reduced.

Mexico has undertaken actions to mitigate and prevent the effects of climate change as the Framework Convention of the United Nations on Climate Change and the Kyoto Protocol. To fulfill the targets set by the Climate Change Act, the country is committed to reducing "its greenhouse emissions by 50% below 2000 levels by 2050" (Veysey, et al, 2015; CTF/TFC, 2009). Mexico ranks thirteenth in the world based on total GHG emissions and is the second largest emitter in Latin America after Brazil. It is expected that the energy demands will grow from 301,462 GWh in 2014 to 470,432 GWh in 2029, driven mainly by expanding economic activity, a growing population, and rising standards of living (Veysey, et al, 2015; Mexican Ministry of Energy, 2015).

Due to the emergence of shale gas, natural gas reserves have increased in the past five years, and as a result, the gas price has dropped significantly. The gas price reduction plus lower capital costs, higher efficiency, and minimal SO_x emissions, has led to a significant increase in the number of natural gas combined cycle (NGCC) plants being built. In the case of Mexico, projections show that natural gas will continue being the dominant source of energy until 2029, representing 45% of the total generation (Mexican Ministry of Energy, 2015; Federal Commission of Electricity, 2014).

Although NGCC power plants have relatively low carbon intensity, the high participation of NGCC in Mexico causes them to emit large amounts of CO_2 and will require CO_2 capture technologies to mitigate GHG emissions. At the same time, production from oil sites located in the Gulf of Mexico, which are becoming depleted or less productive through traditional

extraction methods, could be extended by the injection of CO_2 for enhanced oil recovery (EOR).

Carbon capture and storage (CCS) is proposed to decarbonise the electricity market between 2020 and 2050 which would make it possible to generate electricity from coal and gas with nearly zero emissions (IPCC CCS, 2004). Three promising capture methods are currently being developed for coal and natural gas power plants: post-combustion capture, pre-combustion capture, and oxy-fuel combustion, as shown in Figure 1.1.

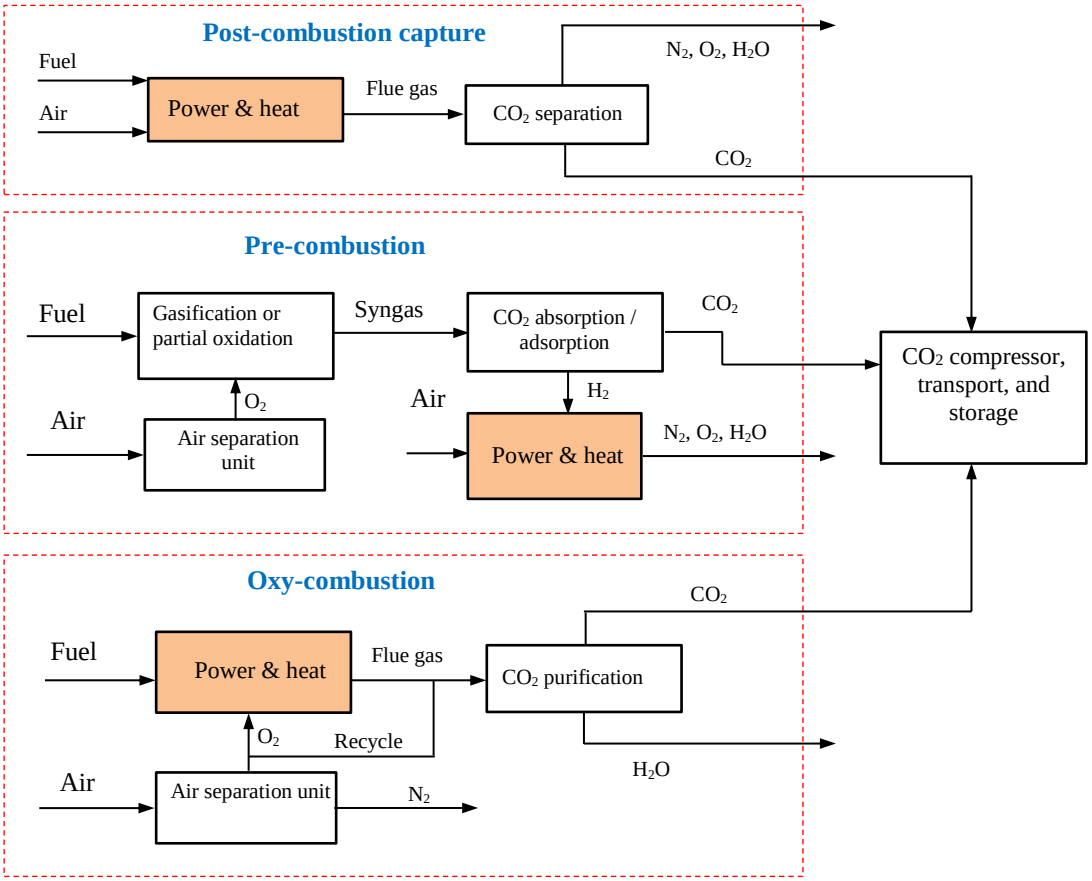

Figure 1.1. Schematics of CO_2 capture technologies for power plants (Leung et al, 2014; IPCC, 2010)

Post-combustion capture: This technology separates CO_2 from the flue gases of a power plant. Chemical absorption is used to absorb the CO_2.

Pre-combustion capture: In this process, solid, liquid or gaseous fuel is pretreated before combustion. For coal, the pretreatment involves a gasification process conducted in a gasifier under low oxygen levels forming a syngas which consists mainly of CO and H_2. The syngas then undergoes a water gas shift reaction with steam forming more H_2 while the CO gas is

converted to CO_2**.** Then the H_2/CO_2 fuel gas mixture is separated. For natural gas, it is reformed to syngas containing H_2 and CO, and then H_2/CO_2 fuel gas mixture is separated (Leung et al, 2014). Methane (CH_4), which is the main component in natural gas, is converted in a mixture of H_2 and CO in a reformer as shown in Reactions 1.1 and 1.2. The main reactions involved in steam reforming are endothermic.

$CH_4 + H_2O \longleftrightarrow CO + 3H_2$ Reaction 1.1

$CH_4 + 2H_2O \longleftrightarrow CO_2 + 4H_2$ Reaction 1.2

The syngas which consists mainly by CO and H_2 is sent to the water – gas shift reactor with steam in order to form more H_2 and to produce CO_2 as shown in Reaction 1.3 (Leung et al, 2014). In steam reforming steam is needed for the reaction. Therefore, heat is necessary to produced it. In addition, heat is required to compensate for the heat losses in the reformer and as well as for the endothermic reaction (Amann et al, 2009).

$CO + H_2O \longleftrightarrow CO_2 + H_2$ Reaction 1.3

Other option for natural gas reforming is partial oxidation. CH_4 is partly burnt in the reformer to produce H_2 as shown in reaction 1.4, in this case the reaction is exothermic (Amann et al, 2009) the air separation unit is required.

$CH_4 + ½\ O_2 \longleftrightarrow CO + 2H_2$ Reaction 1.4

The power plant has lower efficiency compared with other technologies mainly for the steam extraction, air separation unit (Amann et al, 2009). The IEAGHG, (2012) reported a techno economical study of CO_2 capture at gas fired power plants and presented six case studies including pre-combustion and pre-combustion with H_2. Both cases represented the highest levelised cost of electricity (IEAGHG, 2012). The most promising technology for pre-combustion is the auto-thermal reforming which is a combination of the two processes described previously, the heat of the exothermic reaction (partial oxidation) supplies heat to the endothermic reaction of steam reforming (Amann et al, 2009). This technology is not yet in the market, as Mexico is a developing economy, experimental units are not first priority.

Oxy-combustion: In this process, O_2, instead of air, is used for combustion. With the use of pure O_2 for the combustion, the major composition of the flue gases is CO_2, water, particulates, and SO_2. Particulates and SO_2 can be removed by conventional electrostatic precipitator and flue gas desulphurization methods, respectively. The remaining gases contain a high concentration of CO_2 around 80-90%, depending on the fuel used (Leung et al, 2014).

Table 1.1 compares the three CO_2 capture technologies described previously. Technologies which are more suitable in natural gas power plants are indicated in blue. Currently, post-combustion technology is the first commercial-scale demonstration for CO_2 capture from a power plant e.g. Boundary Dam project. This technology has been used for decades to separate CO_2 from industrial gas streams. The basic process was patented in 1930 (Merkel, 2013; Rochelle, 2009). It can be applied in an existing power plant (retrofit) without requiring excessive modifications with substantial cost reduction as well as in a new power plant (Leung et al, 2014, Herzog et al, 2009). Although the air separation unit is a mature and available technology (Table 1.1, shaded row), oxy-combustion technology is yet not in the market. As Mexico is a developing economy, experimental units are not first priority.

The main problem in post-combustion capture technology in NGCC lies in the low CO_2 partial pressure. Many studies (e.g. Hellat and Hoffmann, 2016; National Energy Technology Laboratory, 2013; Merkel et al, 2012) have shown that low CO_2 concentrations in the exhaust gas in a conventional post-combustion capture plant using amines increases the capture cost significantly. A large amount of gas must be treated because CO_2 is diluted by the nitrogen that enters with a high amount of excess of air around 200% (Merkel et al, 2012; National Energy Technology Laboratory, 2013; IEAGHG, 2012).

Some alternatives have been proposed to solve the main problems in the incorporation of CO_2 capture in natural gas, such as exhaust gas recirculation (EGR), selective exhaust gas recirculation, humidification, and supplementary firing (National Energy Technology Laboratory, 2013; Li et al, 2012; Merkel et al., 2012; IEAGHG, 2012; Aboudheir and ElMoudir, 2009). However, none of them have been close to the stoichiometric combustion. In the first two alternatives the main modification occurs in the gas turbine; in the third, the gas and steam cycle are modified; and in the last one only the HRSG. Although 35% of exhaust gas recirculation (EGR) is reasonable and allowed in a General Electric gas turbine, higher than this percentage, modifications in the design of the combustor would probably be needed. As is mentioned before, testing units are not the first interest of Mexico, especially gas turbines because Mexico has no experience in manufacturing them.

Post-gas turbine firing that uses commercially available approaches and technologies that could get close to stoichiometric levels and can be readily built in Mexico based on its experience developed in boilers e.g. CERREY company (CERREY 2016). The main purpose of sequential supplementary firing, which consists in burning fuel sequentially in the HRSG using the excess of O_2 content in the flue gas, is to increase further CO_2 concentration avoiding modifications to the gas turbine.

Table 1.1 Advantages and disadvantages of the different CO_2 capture technologies (Leung et al, 2014)

CO_2 capture technology	**Application area**	**Advantages**	**Disadvantages**
Post-combustion	Coal - fired and gas - fired plants	Technology more mature than other alternative; can easily retrofit into existing plant	Low CO_2 concentration (especially in gas) affects the capture efficiency
Pre-combustion	Coal - gasification plants	High CO_2 concentration enhanced absorption efficiency, fully developed technology, commercially deployed at the required scale in some industrial sectors; opportunity for retrofit to existing plant	Temperature associated heat transfer problem efficiency and efficiency decay issues associated with the use of hydrogen-rich gas turbine fuel; high parasitic power requirement for sorbent regeneration; inadequate experience due to few gasification plants currently operated in the market; high capital and operating cost for current sorption system
Oxy-fuel combustion	Coal - fired and gas - fired plants	Mature air separation technologies available; reduced volume of gas to be treated, hence required smaller boiler and other equipment; CO_2 is the main combustion product, which remains unmixed with N_2, thus avoiding energy intensive air separation	High efficiency drop and energy penalty; cryogenic O_2 production is costly; corrosion problem may arise
Chemical looping combustion	Coal - gasification plants	CO_2 is the main combustion product, which remains unmixed with N_2, thus avoiding energy intensive air separation	Process is still under development and inadequate large scale operation experience

Shaded rows indicate the technology suitable for natural gas combined cycle

1.2 Research aims and objectives

This thesis focuses on identifying and developing optimum configurations for post-combustion CO_2 capture in NGCC power plants in order to propose its use as an effective way to reduce CO_2 emissions generated by the electricity sector in Mexico. The development of this alternative has to be created under the specific conditions of Mexico. Important aspects that have to be considered include changes in market conditions such as the variation in future electricity demand; baseload and part-load generation which will be influenced by renewables; the price of fuel; opportunities for EOR projects; oil price; and capital expenditure in order to achieve the lowest cost per tonne of CO_2 captured for EOR (project economics based on CO_2 sales) and the lowest cost of electricity generation with CCS to abate CO_2 emissions (project economics based on electricity sales).

In achieving these objectives, as the main research is focused on NGCC power plant, the proposed alternatives have to address the three main challenges in the incorporation of post-combustion capture in NGCC: the low CO_2 concentration, the high volumetric flow, and the high concentration of O_2 in the flue gas.

1.3 Scope and outline of this thesis

This research examines different CO_2 capture technologies in order to define the most suitable alternative with appropriate configurations for Mexico. In addition, the technologies selected have to represent the lowest cost per tonne of CO_2 captured for EOR and the lowest levelised cost of electricity for higher capture rates.

- Chapter 2 gives an overview of the status of the electricity sector in Mexico. The answers to these questions are necessary before proposing an alternative for Mexico: what has been done relating to CCS; what is the capacity for EOR projects and for CO_2 storage; and what is the future plan on CCS? Here the Mexican CCUS road map is described. The main contribution of this chapter is the identification of the future power plants that are the candidates for incorporating post-combustion capture. In addition, the CO_2 emissions for new power plants are estimated; and finally a description of how power plants are operated in Mexico is given in the last section.
- Chapter 3 begins with a literature review of alternative methods to increment the CO_2 concentration and to reduce the volumetric flow and the O_2 concentration in NGCC plants in order to facilitate post-combustion capture; impact of the alternative methods on power plant and CO_2 capture plant, as well as the advantages and drawbacks in these alternatives for a

range of studies are given. After that, a literature review of the capture plant and CO_2 compressors at design and part-load conditions is provided.

- Chapter 4 introduces a novel alternative for post-combustion capture in natural gas: sequential supplementary firing combined cycle (SSFCC). The configuration of this alternative and the design principles are established. After defining the optimum alternatives, the economic analysis considering important aspects for Mexico is carried out for two supplementary firing configurations, one with a supercritical combined cycle and one with a subcritical combined cycle SSFCC. The techno-economic results at base load of the novel alternative SSFCC are compared with a conventional NGCC with CO_2 capture. The economic evaluation includes a sensitivity analysis with the gas price, CO_2 selling price, and with capital cost.
- Chapter 5 defines and evaluates the operating strategies at part-load for supercritical and subcritical supplementary firing configurations. A methodology for a rigorous assessment of each configuration at part-load is proposed and the sources of information which support the methodology are given.
- Chapter 6 shows the performance of the power plant cases at part-load for the operating strategies defined in Chapter 5. These are compared with a conventional NGCC. The main parameters that affect the efficiency of the sequential supplementary firing power plants are defined and the most efficient operating modes are selected.
- Finally, in chapter 7, conclusions are reached and recommendations for future work are suggested

1.4 Thesis contribution

An original contribution of this thesis consists in examining the relative merits of practicable high-level supplementary firing shown in Figure 1.3 vs unfired natural gas combined cycle shown in Figure 1.2 to address the research problem presented in Section 1.2.

Combined cycle gas turbine power plants with sequential supplementary firing in the heat recovery steam generator, and subcritical steam cycle effectively makes use of the excess oxygen necessary for gas turbine combustion to generate additional CO_2 and keeps a temperature of around 800-900°C, an achievable range within a heat recovery steam generator with supplementary firing (Kehlhofer et al., 2009). The last stage of supplementary firing brings oxygen close to stoichiometric limits (1% v/v). The marginal thermal efficiency of subcritical SSFCC in the heat recovery steam generator can increase with supercritical steam generation and double reheat to reduce the efficiency penalty.

The cost impacts of CO_2-EOR sales are investigated in this thesis, with a sensitivity analysis of the capital cost of the SSFCC configuration over a range of capital costs from -20% to 20%; gas prices from 2 to 6 $/MMBTU; and because of the decrease of the crude oil price, the CO_2 sale price covers a range from 0 to \$50/tonneCO_2. The subcritical SSFCC configuration is more sensitive to variations in the CO_2 selling price mainly because of the additional revenue from selling CO_2 for EOR. The total revenue requirement (TRR), which is the levelised cost of electricity considering the revenue from selling CO_2, of subcritical SSFCC, at gas price from 2 to 4 $/MMBTU, is lower than for conventional unfired NGCC for the range of capital costs and CO_2 prices specified. However, at 6 $/MMBTU, the TRR of subcritical SSFCC is lower when the CO_2 price is up to 38 $/tonne CO_2. A comparison between subcritical and supercritical SSFCC configurations shows that improvements in power plant efficiency with supercritical steam conditions consistently result in a lower TRR.

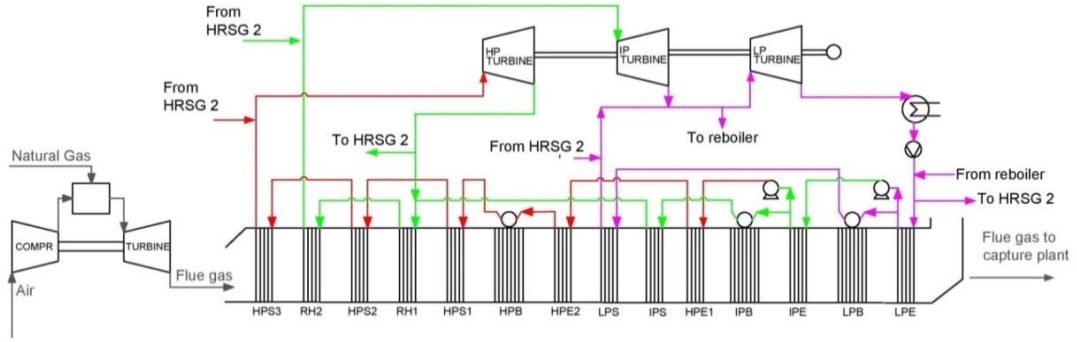

Figure 1.2. Schematic process flow diagram of the conventional natural gas combined cycle configuration with two GE 937 IFB gas turbines, two triple pressure HRSGs and one subcritical steam turbine

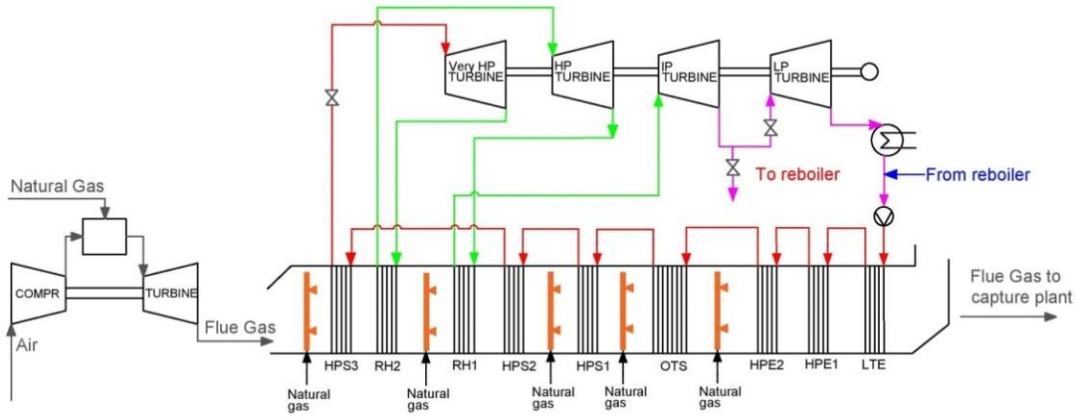

Figure 1.3. Schematic process flow diagram of a supercritical sequential supplementary firing configuration with one GE 937 IFB/single pressure HRSG train combined cycle with a double reheat steam cycle

Although there is a reduction in the capital cost of SSFCC compared with unfired NGCC, which is important, there are a large biases and uncertainties related to the real capital cost. Consequently, further work is needed to include site specific considerations and detailed capital estimates beyond the work included in this thesis.

The proposal has been identified in this thesis as an attractive alternative for the following specific conditions:

1. Markets with access to competitive natural gas prices
2. Where supply of CO_2 for EOR is important
3. Countries where the emphasis on capital cost reduction is important

Although this alternative has been evaluated for Mexico, it can be applied in countries with similar characteristics to Mexico mainly with a cheap gas price as shown in Figure 1.4 and the potential for selling CO_2 for EOR e.g. United States and Canada, where most of the EOR projects are located as indicated by the shaded rows in Table 1.2.

In addition, it has been identified that supplementary firing is an alternative to be used in installation for cogeneration of heat and power with CO_2 capture. In a cogeneration system, electricity and steam for the process are the important products and the control of the electricity and thermal output separately is very important, which is one of the main characteristic of post-GT firing (Kehlhofer et al., 2009). In 2016 the Mexican Ministry of Energy launched the new future prospective of the electricity sector 2015-2029 where cogeneration systems are included for the first time. Their participation in electricity generation is estimated to be 6.8% in 2029 (Mexican Ministry of Energy, 2015).

Finally, further work related to capture ready for SSFCC is needed for new power plants. For existing HRSG it is necessary to identify how to retrofit it using sequential combustion.

Table 1.2 List of current and planned EOR projects (Leung et al, 2014)

Project name	Location	Year of operation start	Max. CO_2 injection rate Mt/year
Jilin oil field	Jilin, China		0.10
Wayburn-Midale	Saskatchewan, Canada	2000	2.20
Paradox Basin	Utah, USA	2005	0.14
Salt Creek	Wyoming, USA	2006	2.20
Williston Basin	North Dakota, USA	2011	1.00
South Heart	North Dakota, USA	2012	0.60
Oologah	Oklahoma, USA	2012	1.50
Masdar	Abu Dhabi, United Arab Emirates	2012	1.70
Hatfield	Hatfield, UK	2013	6.50
California (DF2)	California, USA	2014	5.00
Mongstad	Mongstad, Norway	2014	1.50
Traiblazer	Texas, USA	2014	4.30
Greengen	China	2015	0.70
Genesee (EPCOR)	Alberta, Canada	2015	3.60

Shaded lines indicate EOR projects in United State and Canada

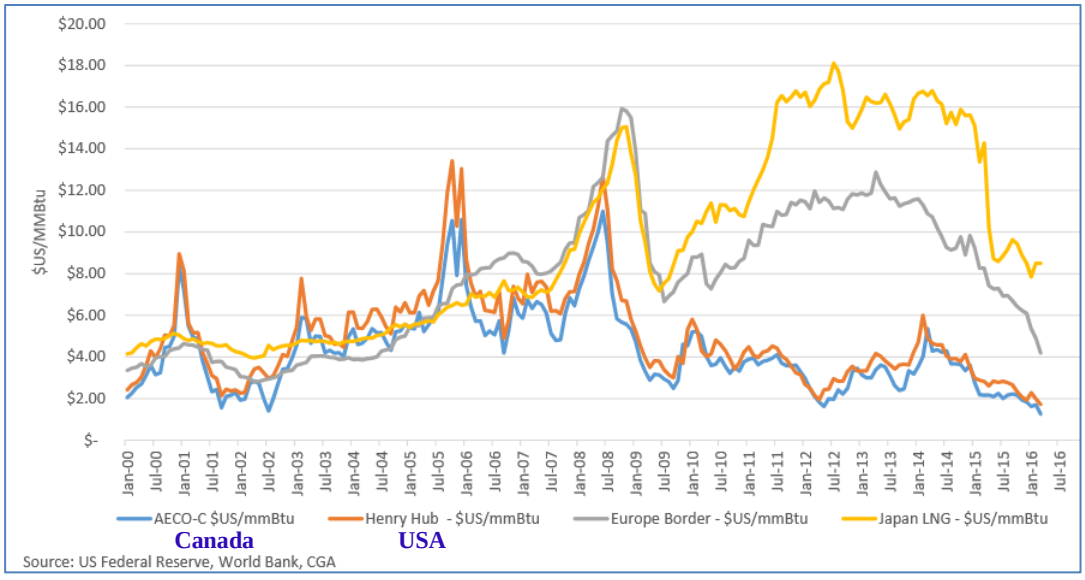

Figure 1.4 Global natural gas prices (Canadian Gas Association, 2016)

2. Status of the electricity sector and CCS – CO_2-EOR in Mexico

2.1 Introduction

The annual electricity demand in Mexico is predicted to grow by 56% from 301,462 to 470,432 GWh_e between 2014 and 2029 (Mexican Ministry of Energy, 2015). This rising demand for electricity is expected to be met by an increase in the use of both coal and gas with natural gas being the dominant energy source. The proportion of natural gas used in electricity generation in Mexico increased significantly from 17.1% (32.9 TWh_e) in 2000 to 50.4% (130.6 TWh_e) in 2011 (Mexican Ministry of Energy, 2012). In this context of rapid electrification dominated by natural gas power plants, Mexico intends to effect a parallel reduction of "its greenhouse emissions by 50% below 2000 levels by 2050" (Veysey, J., et al, 2015; CTF/TFC, 2009). In 2012, the Mexican Congress approved the General Law on Climate Change to reduce greenhouse gas emissions. One of the strategies proposed in order to reach this objective is the application of carbon capture in fossil fuel power plants for the purpose of EOR in the oil industry, which relies on the availability of large amounts of CO_2 in the Gulf of Mexico (Mexican Ministry of Energy, 2012) between 2020 and 2050. According to Lacy et al, (2013), carbon capture projects for the purpose of EOR rather than for storage only is more likely to be developed in Mexico to reduce CO_2 emissions. The main reason for this is the high cost of CCS technology. However, EOR projects could develop experience and infrastructure that would reduce the cost of the technology. In March 2014, Mexico launched its carbon capture use and utilisation (CCUS) technological roadmap containing recommendations for actions be taken at the national level up until 2024 (Mexican Ministry of Energy, 2014) focusing solely on EOR projects. The aim of this chapter is to provide an overview of the opportunities for deploying CCS and CO_2-EOR in Mexico, describing the actions which have been taken and the plans for the future. Additionally, the potential for incorporating CCS and CO_2-EOR into future power plants is outlined. An estimate is also provided for the CO_2 emissions of new natural gas power plants.

The two major energy companies in Mexico are state owned: The Mexican oil company, Petróleos Mexicanos (PEMEX), which was exclusively controlled by the State for more than 75 years; and The utility company, Comisión Federal de Electricidad (CFE). However, on

December 12, 2013, Mexican legislators approved controversial reforms to the country's energy sector to allow private investment.

The content of this chapter is organised as follows: The question "Why CCS in natural gas power plants and CO_2-EOR in Mexico?" is answered in section 2.2. A projection of electricity production and the use of natural gas, as well as the expected reservoir of shale gas in Mexico, are described briefly. In addition, future power plants are identified; the amount of CO_2 and the distance from the emitter to the oil field are quantified. Section 2.3 focusses on the current status of CO_2-EOR in the two biggest energy companies in Mexico, the oil company PEMEX and the utility company CFE. Section 2.4 basically describes Mexico's CCUS roadmap with details. Section 2.5 describes how the power plant operates in Mexico related to the electricity demand. Finally, a conclusion is reached in section 2.6.

2.2 Why implement CCS in natural gas power plants and CO_2-EOR in Mexico?

CCS will be important for Mexico for three main reasons: a rapid growth of installed capacity is anticipated, natural gas is and will remain the dominant energy source in 2028, and the oil industry will require large amounts of CO_2 for EOR.

2.2.1 Growth in electricity production

Electricity production is expected to grow from 62 GW in 2009 to 113.7 GW in 2028. Due to the expected discovery of large reserves of shale gas in Mexico (Federal commission of electricity, 2014) and North America, power generation with low capital costs, high efficiency, low CO_2 emissions, good reliability, good flexibility and positive public perception leans towards using gas rather than coal (IEAGHG, 2012). Furthermore, the share of natural gas for power production is expected to increase from 36.8% in 2012 to 58.6% in 2028, as can be seen in Figure 2.1. In 2028, new clean generation, which could include coal and gas with CCS and other renewable sources, will account for 11.5% and solar energy 1.6%. Mexico has two alternative strategies for reducing CO_2 emissions generated by new power plants (Mexican Ministry of Energy, 2012), whilst contributing to limiting cumulative global CO_2 emissions:

1. Limiting the use of fossil fuels (a reduction of 65% by 2026 compared to 2012 levels) in the electricity sector.
2. Introduce CCS in coal and natural gas power plants, represented in Figure 2.1 as new clean generation.

The information related to the Mexican plan on the energy sector is realised by the Mexican Ministry of Energy every year after being approved by the senate.

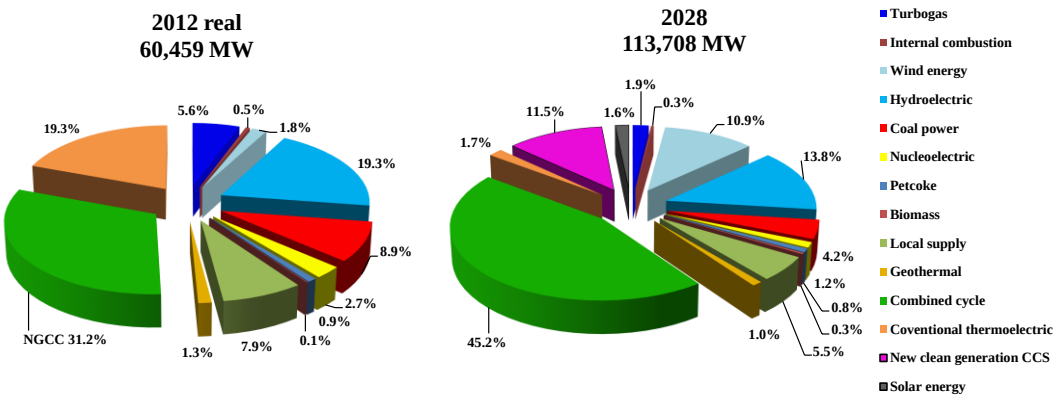

Figure 2.1. Expected electricity generation in 2028 (Federal Commission of Electricity, 2014, Aburto and Valdovinos, 2014)

2.2.2 Natural gas the dominant energy source

The use of natural gas would continue after 2028, given the expectation of large shale gas reserves in Mexico. Figure 2.2 shows the different areas where shale gas reserves are located.

Figure 2.2. Location of Shale gas in Mexico (Mexican Ministry of Energy, 2012; after Gonzalez-Santaló, 2013)

Although a significant reduction in oil production is expected in Mexico, shale gas could supply the demand for natural gas currently covered by the Cantarell and Burgos reservoirs. The use of shale gas could begin in 2016, as shown in Figure 2.3, and would reach its peak in 2026. Shale gas is expected to consist of around 600 trillion cubic feet, which means that Mexico is ranked 6th in the world in terms of the size of its deposits (Oil price, 2014). This is the main reason for believing that the cheap gas price in Mexico will continue after 2028 as shown in Figure 2.4.

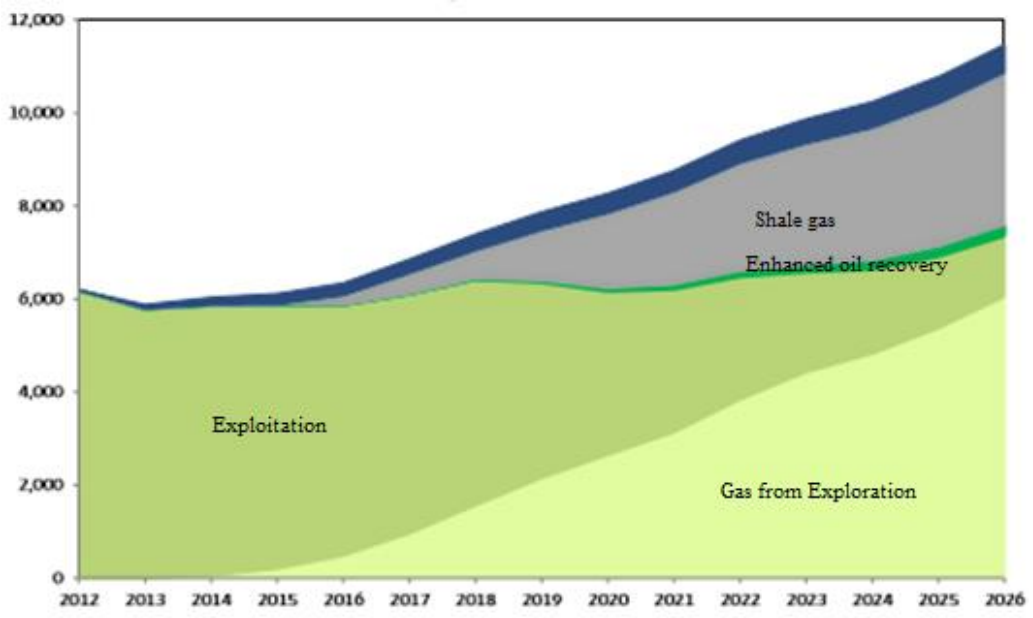

Figure 2.3. Scenarios of natural gas production 2012-2026 (Millions cubic feet per day) (Ministry of Energy, 2012)

2.2.3 CCS and CO_2-EOR Potential in Mexico

Gulf of Mexico: The region for EOR project

Production from oil sites which are becoming depleted or less productive through traditional extraction methods could be extended by the injection of CO_2 for enhanced oil recovery (EOR). CO_2 injection for EOR (CO_2-EOR) into depleted oil fields improves hydrocarbon flow and recovery rates. Lacy et al. (2013) identified industrial and power plants with CO_2 emissions above 0.5 million tonne/year located within 80 km of oil fields in the Chicontepec and Cinco Presidentes regions, as well as a demand for up to 50 million tonne of CO_2 per year for EOR in the Gulf of Mexico from the largest oil fields which are candidates for EOR shown in Figure 2.5. This region is the largest emitter of CO_2, at around 20.1 million tons of CO_2 per year as shown in Figure 2.6 (Lacy et al, 2013).

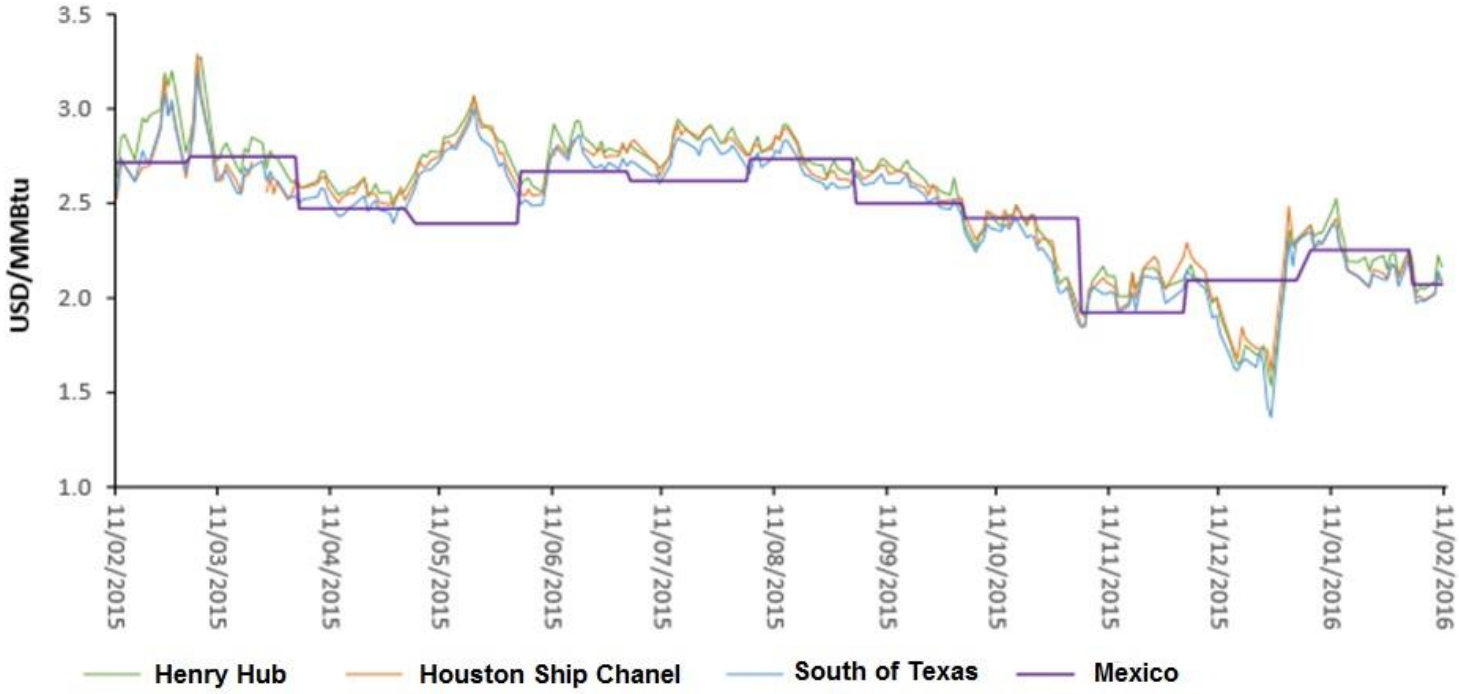

Figure 2.4. a) International gas price scenario 2016 with respect to Mexico (Dollars per million BTU) (Regulatory Commission of Energy, 2016)

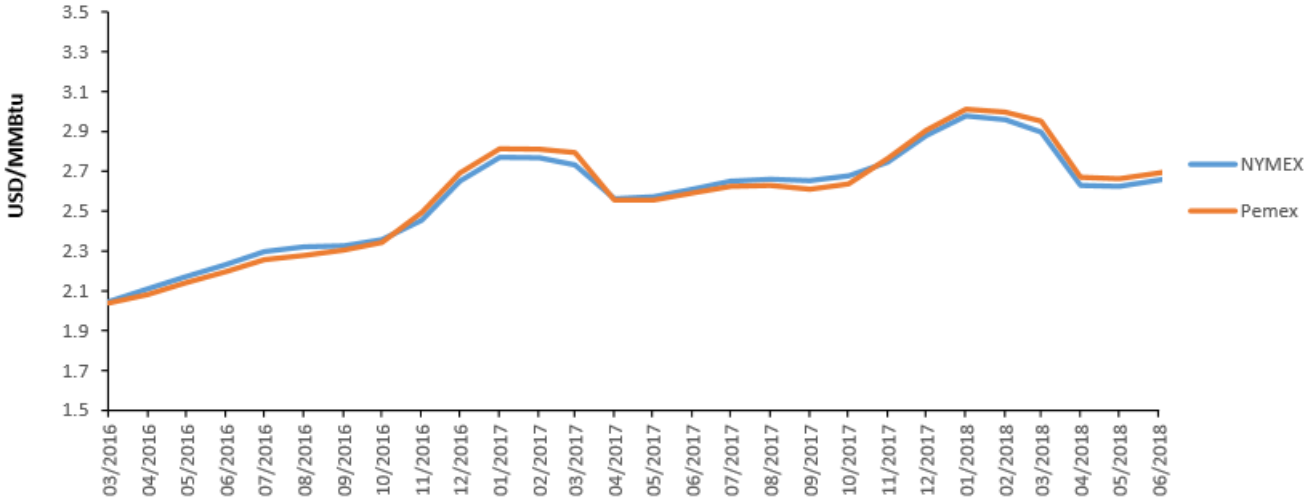

Figure 2.4. b) Gas price scenario 2016-2018 for PEMEX and NYMEX natural gas (Dollars per million BTU) (Regulatory Commission of Energy, 2016)

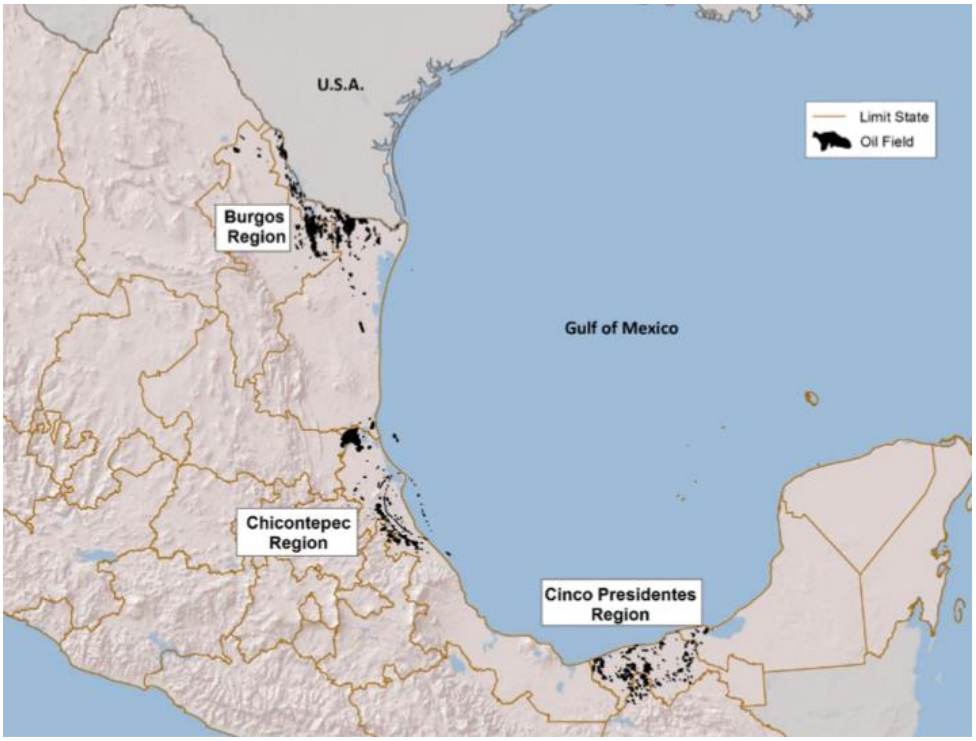

Figure 2.5. Location of the main oil reservoirs for EOR in the Gulf of Mexico region (Lacy et al., 2013)

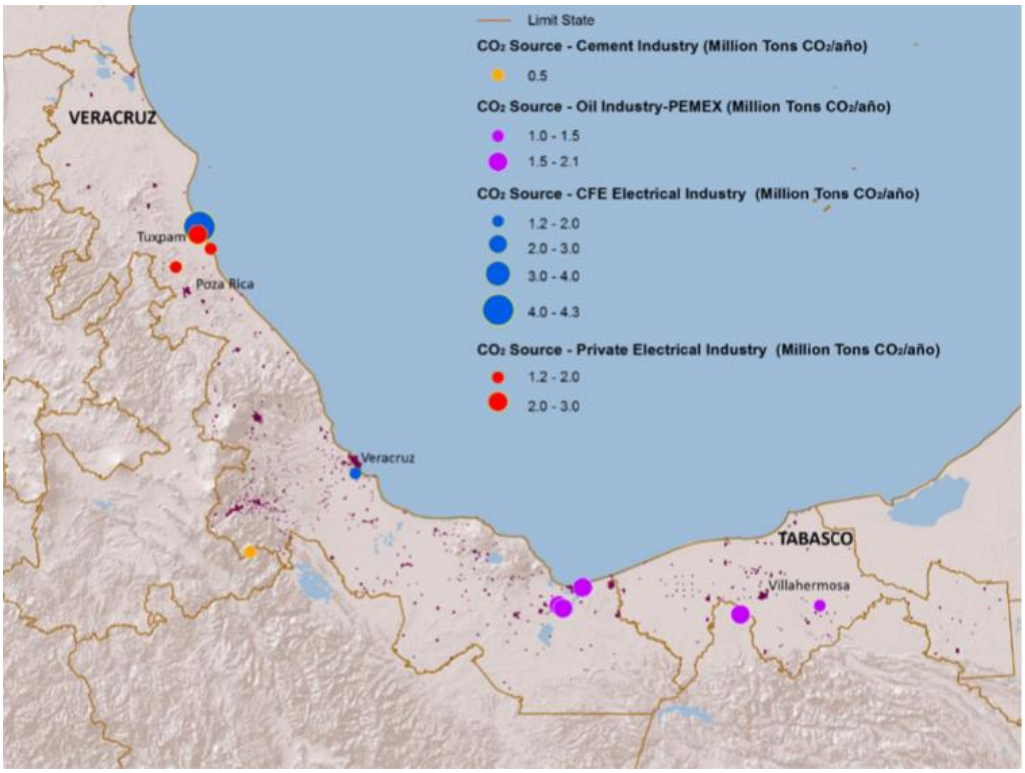

Figure 2.6. Location of the main industrial CO_2 sources in the Gulf of Mexico region (Lacy et al, 2013)

Regions for CO_2 storage

Davila et al, 2010, presented a preliminary study on the geological carbon storage possibilities in Mexico. The country is split up into seven zones based on their characteristics, i.e. the seismic, volcanic and tectonic hazards in combination with the surface geology and lithology. This work has been included in 2012 version of the North America Atlas for CCS.

The North American Carbon Storage Atlas 2012 divided Mexico into the two zones shown in Figure 2.7: the exclusion zone (red colour), which is characterised by volcanic igneous rock and is not recommended for CO_2 storage; and the inclusion zone (green colour), which is characterised as being a stable area and may be suitable for CO_2 storage in saline formations deeper than 800 metres. This zone is made up of the 11 regions shown in Figure 2.8. Regions 4, 5, 6, and 7 are located close to oil fields. This makes them suitable for simultaneous development of CCS and CO_2-EOR. A CO_2-EOR project could develop infrastructure and experience for deploying CCS in the future in order to reach the Mexican mitigation target. As a result, CO_2-EOR may provide two benefits: an increase in Mexico's oil production and a reduction in future GHG emissions (Lacy et al., 2013).

Figure 2.7. North American Carbon Storage Atlas 2012 (North American Carbon Atlas Partnership, 2012). Green - inclusion zone, red - exclusion zone

Figure 2.8. Suitable zones for CO_2 storage with good characteristics for retaining CO_2 underground and safe storage (North American Carbon Atlas Partnership, 2012; Aburto and Valdovinos, 2014)

2.2.4 Future new power plants suitable for CCS and CO_2-EOR

Although Lacy et al. (2013) identified the main existing industrial plants and power plants which emit CO_2 in the Gulf of Mexico, there was no indication of the CO_2 emissions for new power plants. In this chapter, therefore, future power plant projects are identified in order to define which of them are suitable for incorporating the carbon capture process, which of them are candidates for capture ready and which of them for retrofit and repowering, how far away from oil fields these power plants will be located, and how much CO_2 will be generated.

Before identifying the new power plants suitable for CCS and CO_2-EOR from 2013-2028, definition of capture ready and retrofit is given:

Capture ready

A capture ready power plant is one that has been designed and built for incorporation with CCS technology in future (IEAGHG, 2007). This action leads to a reduction of capital cost when CCS is incorporated in a power plant in the future, as well as the operating cost and a reduction in the energy penalty. Some of the most Important requirements in capture-ready are listed below (Jockenhövel, et al, 2009; Sinclair Knight Merz, 2009, Scottish power, 2009):

1. Sufficient space for the capture plant including CO_2 compressor, CO_2 compressor intercoolers and drying, and flue gas pre-treatment
2. Enough space for steam turbine for future modifications for the same turbine or for adapting a new steam turbine.
3. Space for routing the flue gas duct to the CO_2 capture equipment
4. Additional space for vehicle movement (amine transport etc.)
5. Additional space allocation for storage and handling of amines and CO_2
6. Routing of large piping
7. Readiness of the flue gas system for incorporation of an additional or modified blower, additional or enlarged desulfurization plant and tie-in for the capture plant
8. Possibility of extending the cooling system for additional waste heat loads and preparation for additional circulating water pumps
9. Preparation of electric auxiliary power supply and cable routing for the capture plant
10. Preparation for additional water consumption and treatment/demineralization as well as provisions for waste water disposal
11. Steam extraction for regenerating the solvent

Retrofit

In the case of existing power plants, modification will be needed for incorporating CO_2 capture. There are two important actions that have to have evaluated for existing power plant before incorporated carbon capture:

1. Retrofit
2. Repowering

The first action is related to some modification in the power plant in order to make suitable for incorporating CCS such as modification for steam extraction in the crossover and in the LP steam turbine. When carbon capture is incorporated in an existing power plant, the power output decreases due to the steam extraction to regenerate the amine and for CO_2 compression. Therefore, repowering is necessary to increase the power output at the original capacity.

The constructions of the new power plants from 2013 to 2028 are divided in four stages (Federal Commission of Electricity, 2014; Aburto and Valdovinos, 2014):

First stage

The first stage covers new power plants built by the Mexican state-owned electricity utility, Federal commission of electricity (CFE) for public service, which construction began in

2013. The total expected power generation of these new public service power plants is 3,522 MW, with 2,455 MW of capacity by NGCC and open cycle gas turbines (OCGT). Two units of 404 MW and 445 MW are located in the inclusion zone as shown in Figure 2.9. As their construction began in 2013, it is clear that no actions relating to CCUS readiness were considered. Therefore, it is unclear whether they could be retrofitted. The location of these two plants is 900 km from the oil fields candidates for EOR. If they were retrofitted with CCS, then it is clear that they would send their carbon dioxide to geological storage in non-hydrocarbon reservoirs for purely climate change purpose.

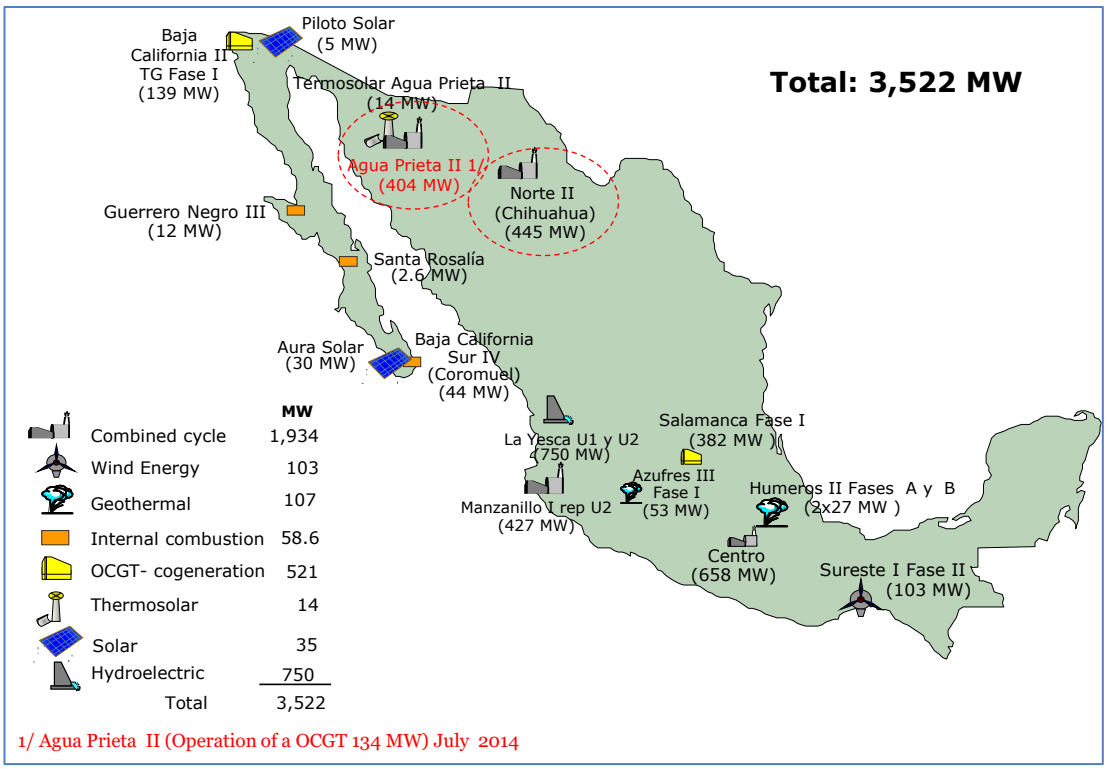

Figure 2.9. Location of the new 3,522 MW power generation projects for public service, construction started in 2013 (Federal Commission of Electricity, 2014; Aburto and Valdovinos, 2014)

Second stage

The second stage covers the power plants which construction began from 2014 to 2015. The total power expected for these new public service projects approved by the Mexican Government is 9,679 MW, with NGCC and OCGT together accounting for 7,369 MW. Two units are located within the inclusion zones shown in Figure 2.10. Likewise, projects included in this period were not considered for CCUS readiness as their construction started in 2014-2015, before the start of a National CCUS strategy in 2015. The Noreste CCGT

power plant, with a capacity of 1,034 MW is located approximately 100 km from the oil field Burgos and could be a potential candidate for a retrofit with CCS and with CO_2 injection for EOR.

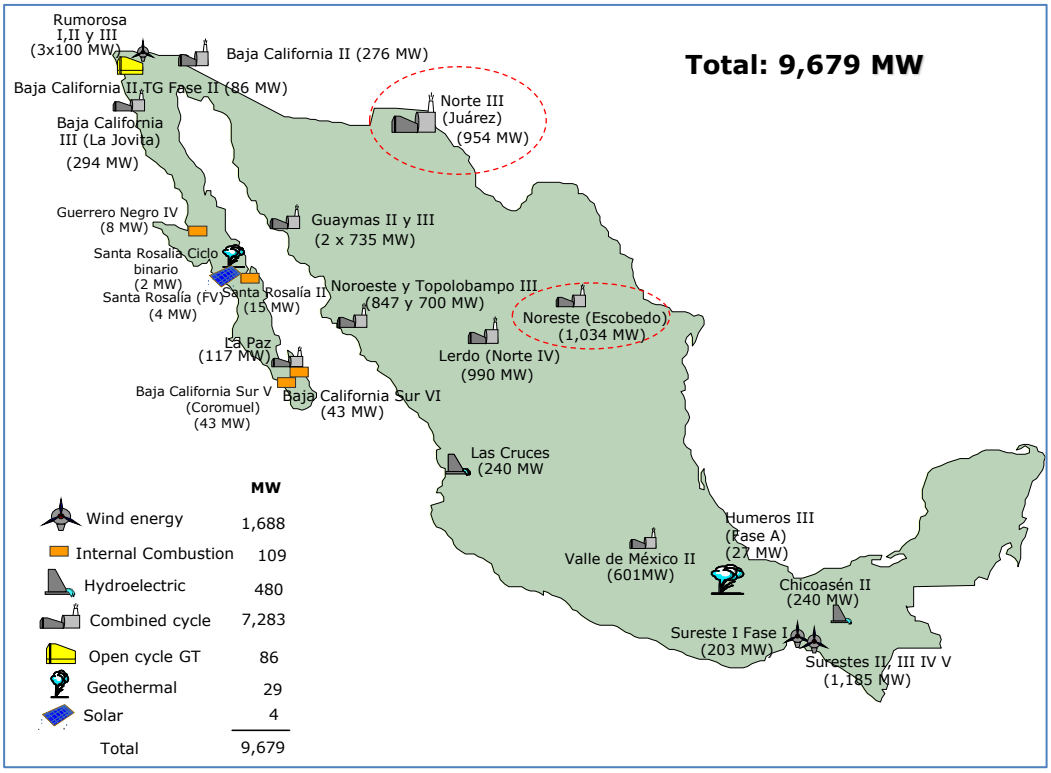

Figure 2.10. Location of the 9,679 MW of new power generation projects to cover the demand for public service from 2014 to 2015 approved by the Mexican Government (Federal Commission of Electricity, 2014; Aburto and Valdovinos, 2014)

Third stage

The third stage covers the power plants which construction is expected to begin from 2016 to 2022. Power plants built in the period ranging from 2018 to 2022 could be considered for CCUS readiness. Therefore, it is important and urgent to evaluate these power plants in a timely manner. 14,795 MW of electricity capacity for public service is expected, with NGCC plants accounting for 11,136 MW. Three NGCC and two open cycle power plant (OCGT) are located within the zone suitable for CCS and CO_2-EOR as shown in Figure 2.11. In particular, the Monterrey NGCC plant with a capacity of 1,088MW is located approximately 100 km from the oil field Burgos and is a candidate for CO_2-EOR. Merida and Valladolid IV NGCC plants could be considered for geological storage in non-hydrocarbon reservoirs. CCS on OCGT is not suitable because they are far away from oil field. In addition, they are not operated enough hours as they would use to provide backup capacity.

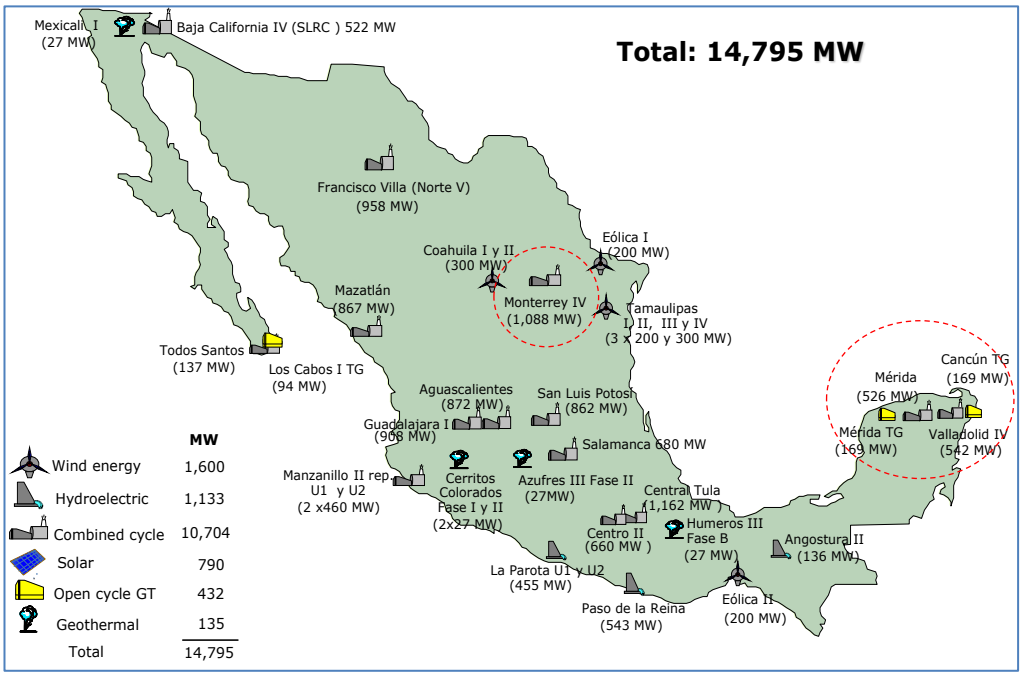

Figure 2.11. Location of the 14,795 MW of new power generation projects to cover the demand for public service from 2016 to 2022 (Federal Commission of Electricity, 2014; Aburto and Valdovinos, 2014)

Fourth stage

Finally, the fourth stage of capacity addition covers the power plants expected to start from 2023 to 2028 illustrated in Figure 2.12. The majority of the new power generation projects would be built during this period. These new power plants would have a total capacity of 26,955 MW of electricity demand for public service. NGCC capacity is expected to account for 11,107 MW. In this stage 13 GW of capacity would be provided by new clean generation alternatives, such as coal and NGCC with CO_2 capture.

Six new units are identified with the potential to incorporate CO_2 capture, mainly because they would be located within the inclusion zone for storage or CO_2-EOR. Furthermore, there is sufficient time to prepare these natural gas power stations for CCUS readiness, and in particular, Oriental l, II, III, IV, IX Y X NGCC and Tamazunchale II y III power plants, which are located less than 70 km from an oil field as shown in Figure 2.12.

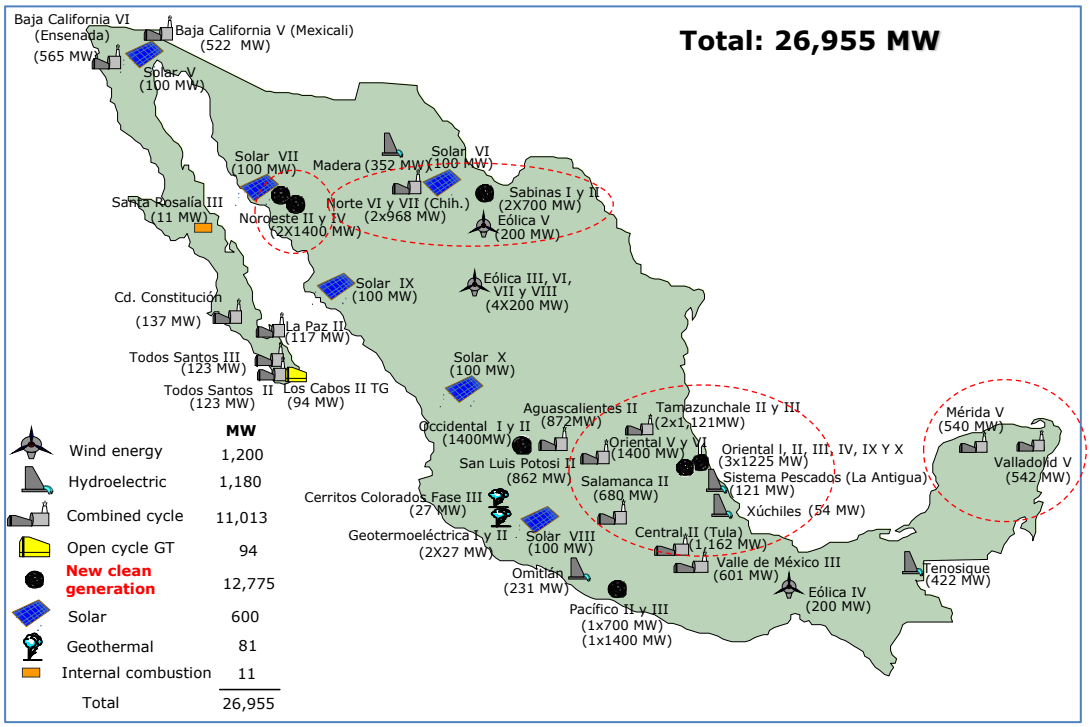

Figure 2.12. Location of the 26,955 MW of new power generation projects to cover the demand for public service from 2023 to 2028 (Federal Commission of Electricity, 2014; Aburto and Valdovinos 2014)

Table 2.1 reports the amount of CO_2 which would be produced only by the new NGCC projects located inside the inclusion zone for CCS, with most of them close to oil fields for EOR. It also identifies which plants could be candidate for a CCS retrofit or be made CCUS ready. The amount of CO_2 is calculated based on the report by the International Energy Agency Greenhouse Gas R&D Programme (IEAGHG, 2012) and (IEAGHG, 2011) considering a Load factor for new plant of 80%. A 910 MW net power NGCC produces 320 tonnes CO_2/hr; and an 800MW net power coal power plant produces 660 tonnes CO_2/hr. This value was used to extrapolate CO_2 production at different power capacities. Information reported in shaded rows represents new clean generation identified by the Federal Commission of Electricity (CFE), and includes NGCC and coal power plants with CCS. It is possible that all of these new projects would be NGCC power plants taking into account current natural gas prices and the availability of shale gas in North America. Some of these plants may well be developed as coal-fired projects if the economics of gas/coal were to change. In total, 47.7 million tonnes CO_2 / year (assuming that all thermal capacity as gas-fired) would be generated solely by new projects located in the inclusion zone, with 90% of the CO_2 generated by these power plants would be abated at the point of emission if CO_2 capture process is incorporated.

Table 2.1. CO_2 emitted by new natural gas power plants located between the inclusion zone suitable for CCS and CO_2-EOR

Power plant	Type	Unit	Capacity MW	CO_2 million tonne/year[2]	
Projects to supply electricity demand from 2013					
Agua Prieta II	NGCC	1	404	0.97	Retrofit
Norte II	NGCC	1	445	1.07	Retrofit
Projects to supply electricity demand from 2014-2015					
Norte III (Juarez)	NGCC	1	954	2.4	Retrofit
Noreste (Escobedo)	NGCC	1	1034	2.5	Retrofit
Lerdo Norte	NGCC	1	990	2.4	Retrofit
Projects to supply electricity demand from 2016-2022					
Monterrey	NGCC	1	1088	2.7	Retrofit/capture ready
Valladolid IV	NGCC	1	542	1.3	Retrofit/capture ready
Cancun	OCGT	1	169	0.4	Retrofit/capture ready
Merida	NGCC	1	526	1.3	Retrofit/capture ready
Merida TG	OCGT	1	169	0.4	Retrofit/capture ready
Projects to supply electricity demand from 2023-2028					
Noroeste II and IV	Coal or NGCC	2	2800	16.2 (coal) 6.9 (gas)	capture ready
Sabinas I and II	Coal or NGCC	2	1400	8.1 (coal) 3.5 (gas)	capture ready
Tamazunchale II and III	NGCC	2	2242	5.5	capture ready
Oriental I, II, III, IV, IX, and X	Coal or NGCC	3	3675	21.2 (coal) 9.1 (gas)	capture ready
Norte VI and VII (Chihuahua)	NGCC	2	1936	4.7	capture ready
Merida V	NGCC	1	540	1.3	capture ready
Valladolid V	NGCC	1	542	1.3	capture ready
Total[1]		**23**	**19,607**	**47.7**	

[1]New clean generation is considered only as NGCC power plants to show an average amount of CO_2 emitted (shaded lines)
[2]Unabated CO_2 emissions

The next step of this analysis is to address, at this early stage in the deployment of CCUS in Mexico, is whether the potential capacity of electricity with CCS of the power plants identified in the previous section - all located inside the inclusion zone of Figures 2.10, 2.11, and 2.12 – matches the contribution that CCS power plants are expected to make for Mexico to meet its CO_2 emission target, estimated to be of the order of 13 GW of CCS power generation in Figure 2.1.

If the capacity in the inclusion zone is lower than 13 GW, then power plants located in the exclusion zone would have to be considered for incorporating CO_2 capture or converted to renewable energy generation. The optimum configurations for CCUS readiness of new plants, the retrofit and/or repowering of non-CCUS ready existing unit plants would have to be defined in future work and is outside the scope of this analysis. Table 2.2 indicates new power plants located within a distance of less than 100 km from oil fields in the Gulf of Mexico. Capturing 90% of the CO_2 emitted by these stations would amount to approx. 17.8 million tonnes / year, which can be supplied for EOR. The remaining of the CO_2 emissions

generated by the power plants located further away from these oil fields could then be connected to existing EOR projects in a second phase, or implement geological storage in non-hydrocarbon reservoirs located in the inclusion zone. Effectively, the power plants reported in Table 2.2 could be considered as priority CCS-EOR projects as they will provide economic benefits from additional oil production and would provide experience and infrastructure for future CO_2 storage. Lacy et (2013) identified 20.1 million tonne CO_2 / year, emitted for existing power plants, industries, and refineries as potential primary sources, which, if added to the 49.9 million tonne / year from new NGCC power plants, could be used for EOR projects. It would then be possible to match the demand for CO_2 for EOR in oil fields in the Gulf of Mexico, estimated to be approximately 50 million tonne of CO_2 per year reported by Lacy et al, (2013). The remaining 28 million tonne/year would supply CO_2 for geological storage in non-hydrocarbon reservoirs.

Table 2.2. CO_2 emitted by new natural gas power plants located between the inclusion zones suitable CO_2-EOR at less than 100 km from the oil field

Power plant	**Type**	**Unit**	**Capacity (MW)**	**Approximately Distant from the oil field (km)**	**CO_2[1] Million (tonne/year)**	
Noreste (Escobedo)	NGCC	1	1034	100	2.5	Retrofit
Monterrey	NGCC	1	1088	100	2.7	Retrofit/capture ready
Tamazunchale	NGCC	2	2242	70	5.5	capture ready
Oriental I, II, III, IV, IX, and X[1]	NGCC	3	3675	>70	9.1	capture ready
Total CO_2 emissions			**8,039**		**19.8**	capture ready

[1]Unabated CO_2 emissions

2.2.5 Current status of CO_2-EOR in PEMEX-CFE

Since 2008, Mexico has taken several actions to reduce greenhouse gas emissions, as summarised below. Although Mexico is not part of the Kyoto protocol, it intends to reduce its greenhouse gas emissions voluntarily. The first action was taken in 2009, when the Mario Molina Centre and Electrical Research Institute were contracted by CFE to conduct preliminary studies for a demonstration CO_2 capture plant in a coal power plant. In the meantime, PEMEX launched a pilot test of CO_2 continuous injection in the Coyotes field in 2010 (Rodriguez De la Garza, 2014). Following positive results in this pilot plant, the Mexican Congress approved the General Law on Climate Change in 2012. One of its strategies for reaching its objective of reducing greenhouse gas emissions is the application of CCS in fossil fuel power plants and CO_2 for EOR.

2.3 Future plans for CCUS

According to the Mexican Ministry of Energy (2014), Aburto and Valdovinos (2014) and the Mexican Ministry of Environment and Natural Resources (2014), Mexico will take several actions in the near and long term related to climate change and specific to CCS and CO_2-EOR. Most of them are outlined in the Mexican CCUS Technology Roadmap. In March 2014, Mexico launched its Roadmap for CCUS-EOR and its implementation began later in 2014 (Mexican Ministry of Energy, 2014). Actions to be taken in chronological order are as follows: incubation, public policy, planning, a pilot and demonstration scale projects in the oil industry, pilot and demonstration scale projects in power plants, and commercial scale projects (Mexican Ministry of Energy, 2014). The first two steps are related to creating agreements, a new regulatory framework for CCUS projects, and resources for training people, etc. The activities in this stage are described in chronological order in Table 2.3.

Table 2.3. Public policy action taken from 2014-2024 (Mexican Ministry of Energy, 2014)

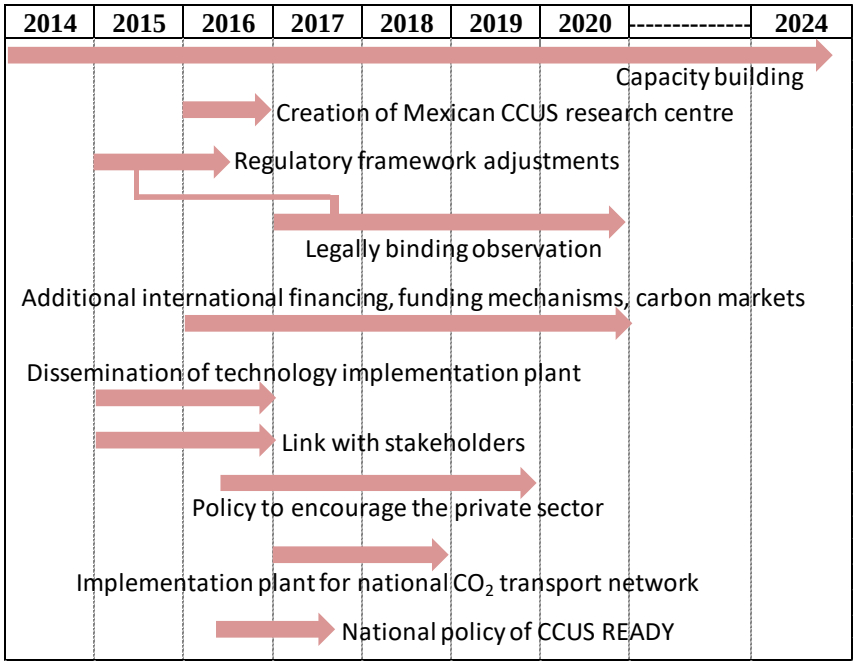

Planning activities described in Table 2.4 are related to a group of actions which the oil industry and the electricity industry need to develop jointly, basically because they need to share information related to EOR, storage capacity, and CO_2 emissions by power plants. Most of them were developed during 2014 as described in Table 2.4.

As can be seen, the activities are focused on EOR projects. However, the location of deep saline aquifers as an option for storage of unmarketable CO_2 has already been identified, but must be assessed by CFE and PEMEX.

Table 2.4. Planning activities taken from 2014-2024 (Mexican Ministry of Energy, 2014)

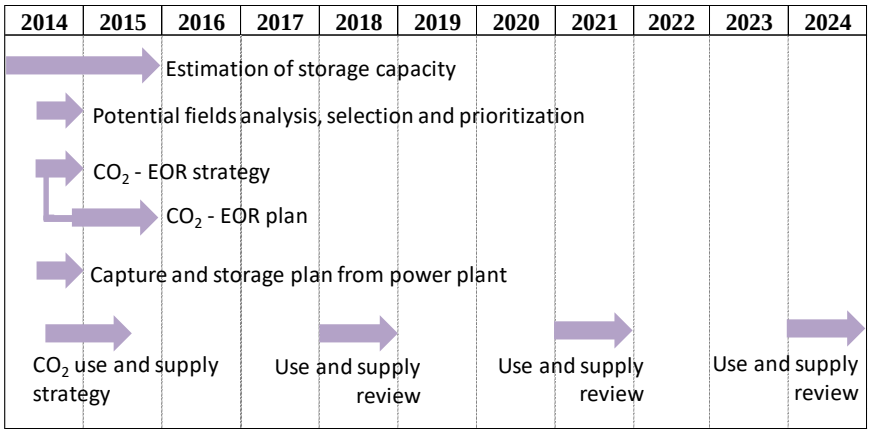

Table 2.5 describes actions related to the pilot and demonstration plants before, during and after their construction in chronological order. The PEMEX CCUS-EOR project funded by the Mexican Government began in 2015 and will finish in 2018. It consists of designing and implementing a CO_2-EOR pilot test at the Cinco Presidentes field (see Figure 2.5) by using the high purity CO_2 to be captured in the ammonia plants in the Cosoleacaque Petrochemical Centre (Rodriguez De La Garza, 2014). The plan is for a full-scale CO_2-EOR implementation to be located in the same petrochemical centre as the pilot plant, increasing the capacity by about 80 MMSCFD in order to allow for the elimination of current CO_2 emissions from this petrochemical plant. It is expected that 60-70% of the injected CO_2 could remain sequestered in the reservoir (Rodriguez De La Garza, 2014).

Table 2.5. Pilot and demonstration scale projects in oil industry activities taken from 2014-2024 (Mexican Ministry of Energy, 2014)

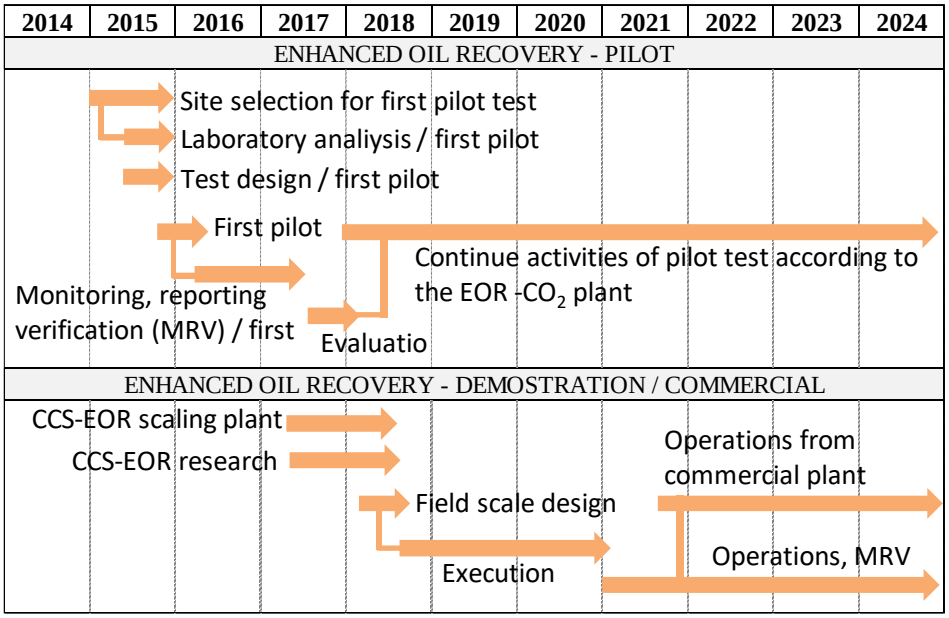

The following actions are related to pilot and demonstration scale projects in power plants. As can be seen in Table 2.6, when evaluating power plants, the integration of capture readiness for new power plants was not considered. A CO_2-ready design would avoid such risks and allow greater flexibility in the degree and timing of CCS deployment (Roadmap for Carbon Capture and Storage demonstration and deployment in the Republic of China, 2015). This could be useful for creating a technology roadmap for the design of newly built NGCC power plants and their operating requirements for EOR and to reduce CO_2 emissions. This action should be taken in parallel with the pilot project and should start in 2016 and not in 2018. The CCS roadmap focuses on the capture plant, and different solvents will be tested in the pilot plant and used in the demonstration project. Activities are described in Table 2.6 in chronological order. The capacities of the pilot plants according to Aburto and Valdovinos (2014) and the Mexican road map (Mexican Ministry of Energy, 2014) are:

1. 50 MW pilot plant to provide 5 MMSCFD of CO_2 for an EOR project funded by the Mexican Government
2. 250 MW demonstration plant to provide 25 MMSCFD CO_2 for an EOR project in a large reservoir funded by the Mexican Government
3. 2 MW pilot plant in Poza Rica, Veracruz funded by the Mexican Government – World Bank

Table 2.6. Pilot and demonstration scale projects in power plant activities taken from 2014-2024 (Mexican Ministry of Energy, 2014)

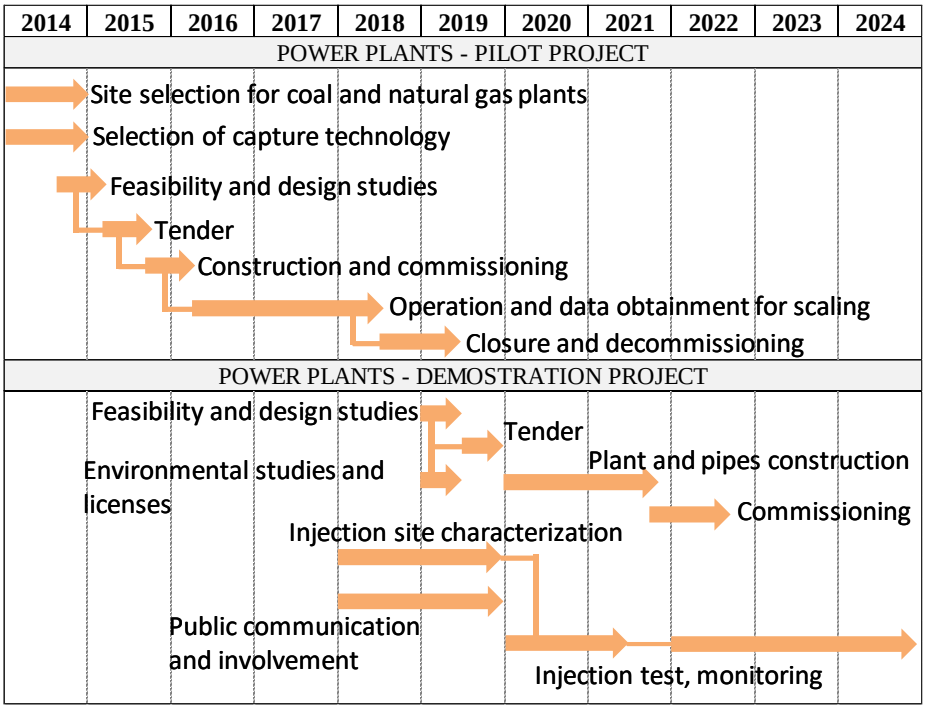

The final activities of the Mexican CCUS roadmap are described in Table 2.7. These comprise the final decisions relating to the selected CCS technology.

Table 2.7. Commercial scale activities taken from 2014-2024 (Mexican Ministry of Energy, 2014)

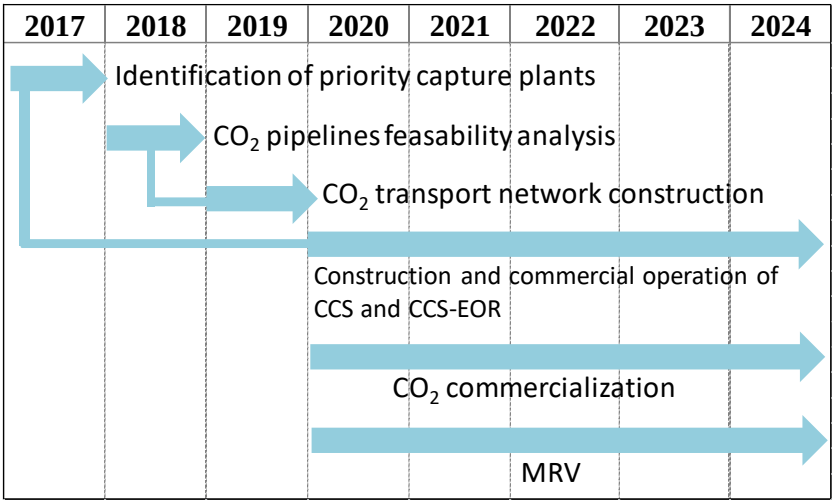

2.4 Variation in electricity demand in Mexico

Although the most efficient way to operate a power plant is at maximum possible output most of the time (called baseload plants), this does not happen to all power plants. Weather conditions, seasonal, daily and hourly, weekdays and weekend days cause variations in electricity demand that means to change their power output.

In the north of Mexico, the demand is higher due to the extreme variation in the temperature. In summer it reaches 40°C approximately, the weather is hot and there is a high demand for air conditioning, and in winter the temperature reaches in some cases 0°C which increases the demand for heaters, calefaction, and the use of hot water. In the south, there is no significant variation between the summer and winter.

In the following Figures 2.13 and 2.14 are shown the demand of electricity in a normal working day and in a holiday during the winter and summer seasons. This information confirms that any alternative for Mexico has to be evaluated at part-load in order to demonstrate its flexibility as in a NGCC.

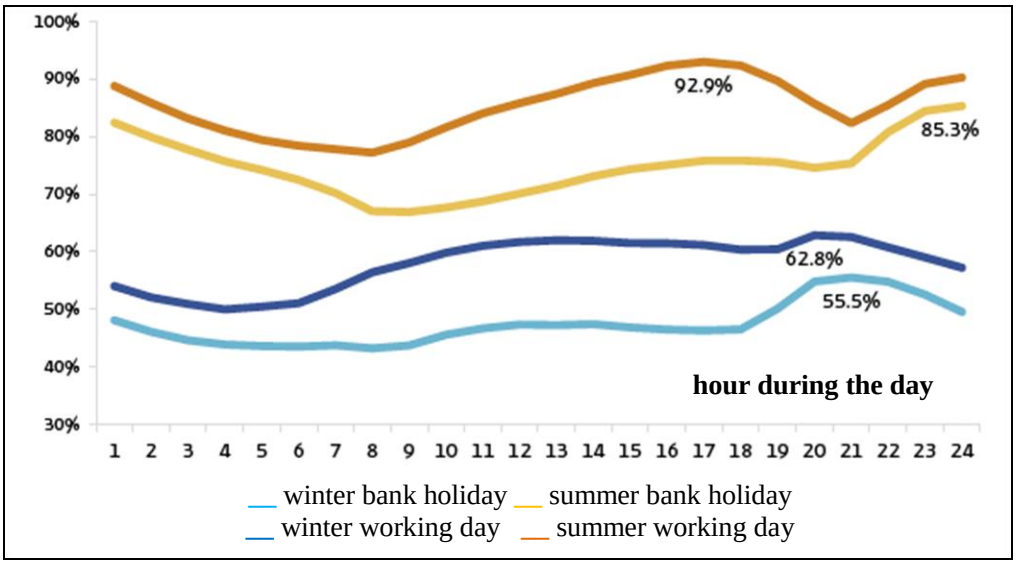

Figure 2.13. Variation of hourly electricity loads in the north of Mexico in summer and winter as well as for every season working and non-working days in 2011 (Mexican Ministry of Energy, 2012)

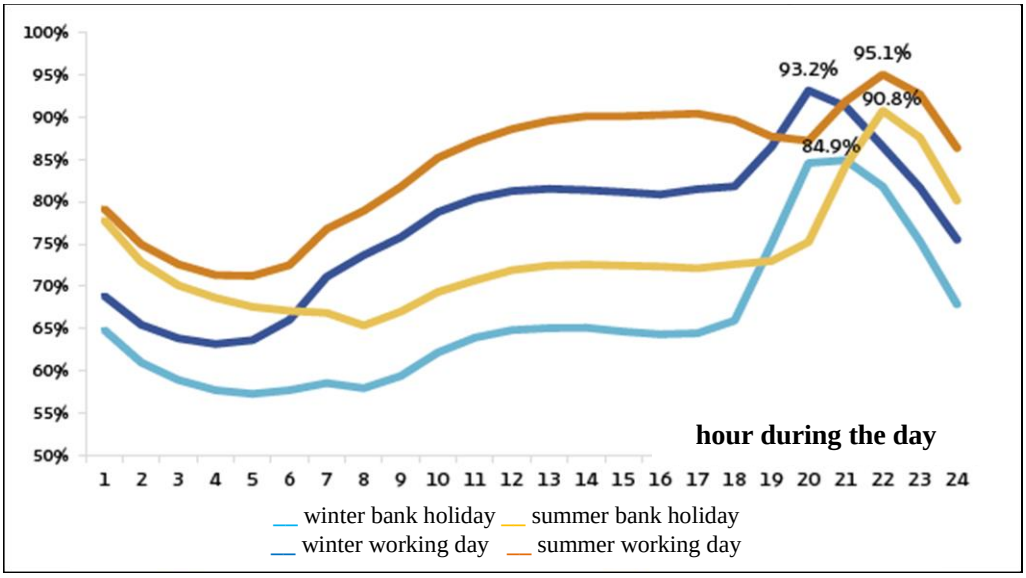

Figure 2.14. Variation of hourly electricity loads in the south of Mexico in summer and winter as well as for every season on working and non-working days (Mexican Ministry of Energy, 2012)

2.5 Conclusion

Natural gas is expected to be the dominant source of energy in Mexico beyond 2028 because of the shale gas reservoir in Mexico and North America and the cheap gas price. CCS in NGCC power plants will be needed due to the large share of this technology in power generation. New power plants are expected to emit around 50 million tonnes CO_2 / year.

It is expected that the oil industry will require large amounts of CO_2 for EOR in the oil fields located in the Gulf of Mexico region which is the largest emitters of CO_2. Geological storage sites for injecting CO_2 are close to the new power plants, less than 100 km away.

EOR is one on the main drivers of CCS in Mexico, as it provides a positive immediate economic benefit, as well as helping to mitigate long-term environmental impacts and create infrastructure and experience for CO_2 storage. Mexico will need to take advantage of the opportunities for CO_2 storage if it wishes to reach its mitigation target in 2050.

Based on experience around the world using amine solvent, Mexico is developing experience in this area according to Mexico's roadmap for CCUS, and it is expected to continue to do so in the future. The technology and alternatives suggested for Mexico should be focused on amine-based post-combustion CO_2 capture.

CCS-ready design for new power plants is important to complement the Mexican roadmap. It is important to include these, as they would avoid risks and allow greater flexibility for future power plants with CO_2 capture. In terms of operation of the future power plant combined cycle, because of the variations of electricity demand in Mexico, any novel alternative proposed in this thesis has to be evaluated at part-load.

3. Post-combustion capture in natural gas power plant

3.1 Introduction

This chapter is focused on post-combustion capture technology in natural gas combined cycles. Currently, it is the first commercialised technology for CO_2 capture from a power plant e.g. Boundary Dam project. It is the most commercially advanced method as a result of considerable industrial experience with similar processes in, for example, natural gas sweetening plants. It can be applied in an existing power plant (retrofit) without requiring excessive modifications as well as in a new power plant with substantial cost reduction (Herzog et al, 2009).

In short term, actions described in Mexico's CCUS roadmap are focused on solvent absorption technologies linked to natural gas combined cycle plants. A CCS pilot plant and a quasi-commercial post-combustion capture plant facility are planned to be built in 2016 in order to prepare for the introduction of CCS and to train people in the electricity sector (Mexican Ministry of Energy, 2014). Taking advantage of the knowledge gained during this process, it is important to focus on solvent absorption technologies in this thesis.

However, the incorporation of post-combustion carbon capture in a natural gas power plant has three main challenges when compared with coal power plants; these engineering challenges may have impacts on the capital and operational costs:

1. CO_2 concentration in the exhaust gases. A low concentration of CO_2 in the exhaust gases affects the electricity output penalty of capture because of the lower driving force for CO_2 absorption and the associated increase in the absorber size and the solvent energy of regeneration (e.g. Hellat and Hoffmann 2016; National Energy Technology Laboratory, 2013; Li, et al, 2012; Merkel et al., 2012; IEAGHG, 2012; Aboudheir and ElMoudir, 2009). Typical CO_2 concentrations in the exhaust gases are approximately 10-15% in a coal power plant and 3-4% in a gas turbine.
2. O_2 concentration: large amounts of excess air are necessary for gas turbine operation, typically 200% - 500%, which result in high O_2 concentration in gas turbine exhaust composition, around 15% v/v, increasing solvent oxidative degradation and operational costs (e.g. Goff and Rochelle, 2004).

3. Large exhaust gas volumes overall lead to higher capital costs. Gas turbines use large excess of air in order to maintain stable the temperature of the exhaust gas

In the next sections of this chapter an in-depth literature review related to alternatives to solve these three main challenges is given, including the main important parameters affected when these alternatives are applied in a NGCC. A comparison of alternatives including the novelty proposed in this thesis, "sequential supplementary firing", is analysed. After that, a literature review related to the design and operation at part-load conditions of the CO_2 capture plant and compressor system is included in this chapter in order to select the optimum alternative.

3.2 Literature review on novel alternatives in natural gas power plants to enhance CO_2 concentration, reduce O_2, and reduce exhaust gas volume

A typical NGCC integrated with carbon capture plant and compressor is described in Figure 3.1. The exhaust gas leaving the HRSG enters the capture plant. The CO_2 capture plant using monoethanolamine (MEA) includes an absorber and stripper. The combustion gases are cooled down before entering the absorber in the direct contact cooler (DCC) to around 40-45 °C. The chemical absorption process is exothermic, and as such the process favours as low a flue gas temperature as possible at the inlet to the absorber (IEAGHG, 2012). The solvent MEA, which is vaporised in the absorber and goes with the clean flue gas, is captured by water-wash section located in the top of the absorber and is sent back to the lower section of the absorber. The CO_2 is absorbed by the aqueous MEA solution. The purified gas passes up through the water wash section, and is then emitted to the atmosphere through the stack. The solvent enriched with CO_2 is pumped to a heat exchanger where it is preheated by the hot lean solution which has left the bottom of the stripper. The preheated rich solvent is then sent to the stripper where the CO_2 and MEA solution are separated using thermal energy added by condensing steam. The steam is typically extracted from the crossover pipe between the intermediate pressure (IP) and the low pressure (LP) turbines of the steam cycle. The saturated CO_2 leaves the top of the stripper and enters the condenser. The condensed water is then returned to the stripper and the CO_2 is sent to the compression system. It has been verified that the thermal energy input required in the reboiler to regenerate the solvent is sensitive to the CO_2 concentration of exhaust gas as shown in Figure 3.2 (Hellat and Hoffmann, 2016; National Energy Technology Laboratory, 2013; Li, et al, 2012; IEAGHG, 2012; Aboudheir and ElMoudir, 2009; Evulet et al, 2009).

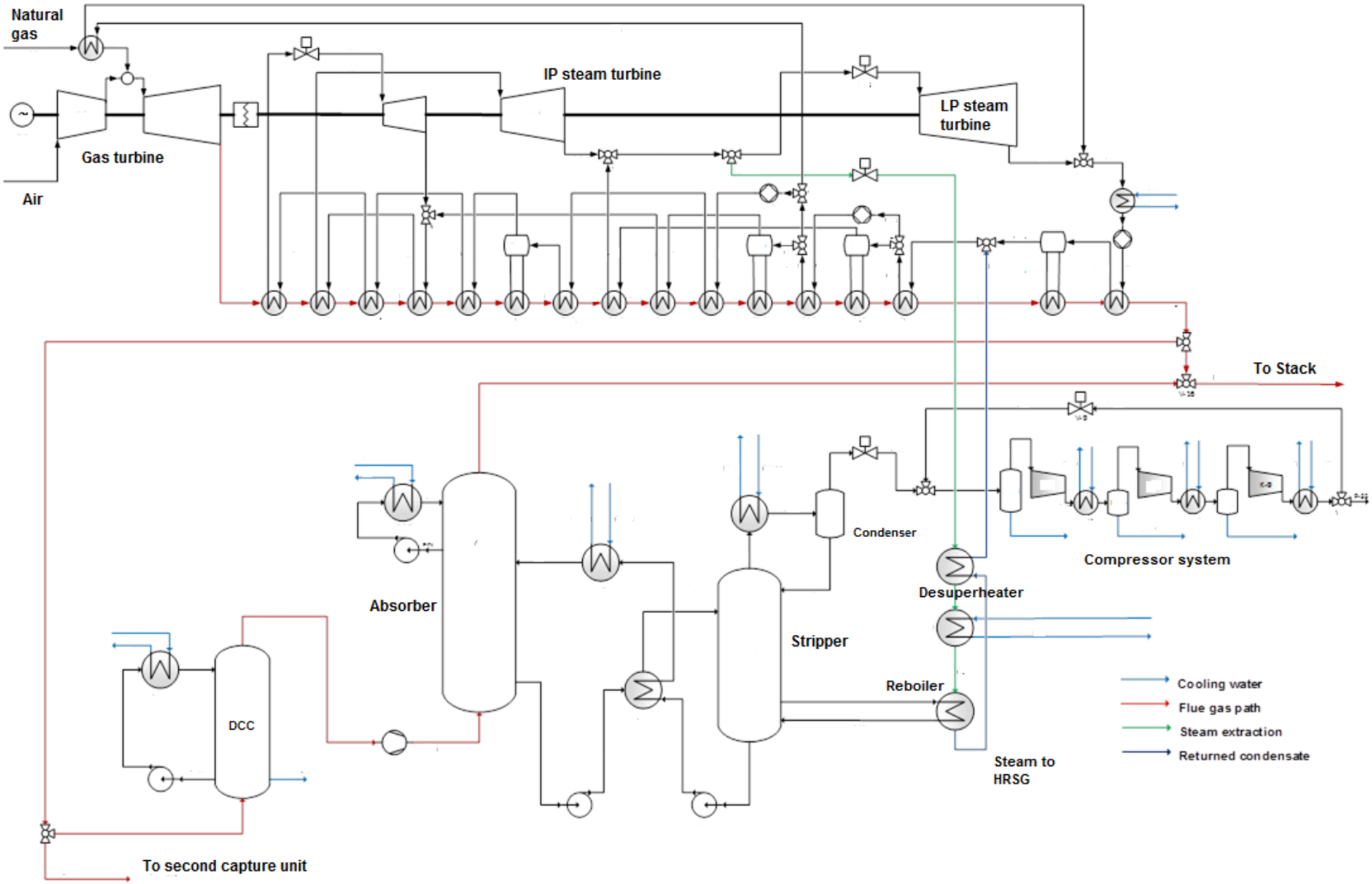

Figure 3.1. Natural gas combined cycle with CO_2 capture plant and compression unit (Sanchez-Fernandez, 2015)

Different concepts for NGCC power plants integrated with the CO_2 capture process have been investigated in order to enhance CO_2 concentration in exhaust gas and to reduce O_2 concentration such as:

1. NGCC with exhaust gas recirculation (EGR) (Hellat and Hoffmann, 2016; National Energy Technology Laboratory, 2013; IEAGHG, 2012; Merkel et al., 2012; Aboudheir and ElMoudir, 2009; Evulet et al, 2009; Bowman et al, 2008; ElKady, 2008; Bolland and Sæther, 1992; Bolland and Mathieu, 1998)
2. Selective exhaust gas recirculation: series and parallel membrane / solvent hybrid capture system (Voleno et al, 2014; Swisher and Bhown, 2014; Merkel et al., 2012)
3. Sequential gas turbine combustion (Asen and Eimer, 2008)
4. Humidification (Li et al, 2011; Li et al, 2009; Takahashi, 2007; Yari and Sarabch, 2005; Hatamiya et al, 2004; Hatamiya et al, 2003; Lindquist et al, 2002, Lindquist et al, 2000; Thern et al, 2003, Agren et al, 2000)
5. Supplementary firing (Biliyok and Yeung, 2013; Li et al., 2012; Kehlhofer, et al, 2009; Wylie, 2004)

In the first three alternatives the main modification occurs in the gas turbine; in the fourth, the gas and steam cycle are modified; and in the fifth only the HRSG.

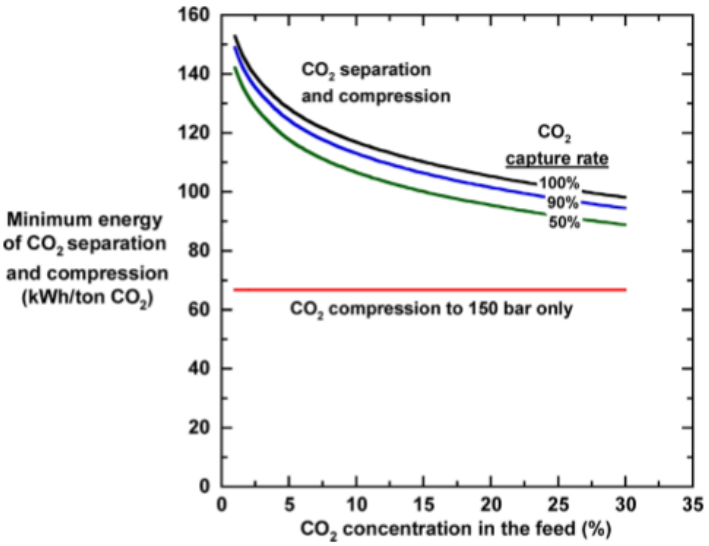

Figure 3.2. Minimum energy per ton of CO_2 captured as a function of CO_2 concentration in a flue gas stream (Merkel et al., 2012)

3.2.1 Natural gas combined cycle with exhaust gas recirculation (EGR)

EGR consists of returning a fraction of the flue gas to the inlet of the gas turbine air compressor and replacing some of the air going to the combustor. The main reason for

recirculating a fraction of the exhaust gas is to increase the concentration of CO_2 and reduce the volumetric flow (Markel and Wei, 1998; Li et al, 2012). However, the percentage of recirculation is limited by the combustor. There are important parameters in the design of combustors such the inlet temperature, velocity, turbulence, and resident time that are based on 21 mol% of O_2 (Li, et al, 2012 Ditaranto et al, 2009). In the situation of low concentration of O_2, these parameters are affected. With EGR, the concentration of O_2 in the combustion air is reduced. Experiments suggest that using a combustor designed at 21 mol% O_2, up to 16 mol% the flame is stable. Concentration of O_2 below 16 mol% would be possible with modifications of existing combustor. With EGR, the presence of CO_2 in the combustion air affects the combustion since it has higher heat specific capacity than the O_2. The specific heat capacity of O_2 at 650K is 1.017 kJ/kg K and of CO_2 at the same temperature is 1.102 kJ/kg K. Therefore, the CO_2 absorbers more heat resulting in lower combustion temperature which affects the efficiency of the power plant.

The exhaust gas is cooled before being put back into the gas turbine. A process diagram is shown in Figure 3.3.

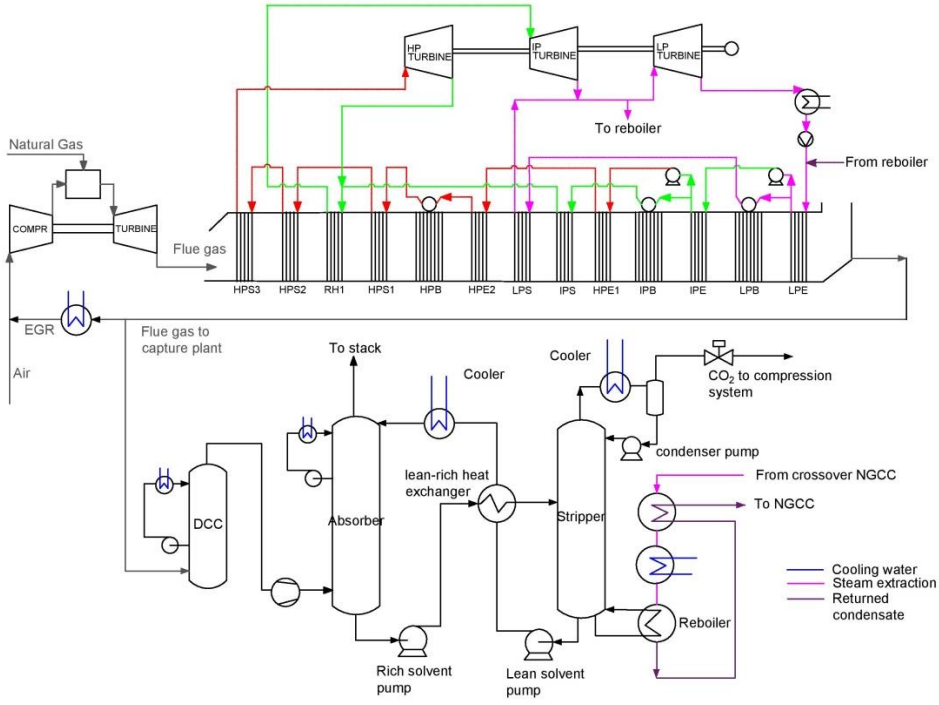

Figure 3.3. Schematic of a natural gas combined cycle with exhaust gas recirculation

Li et al. (2012) reported that with 50% EGR, the energy consumption in the reboiler could be reduced by 8.1% points increasing the efficiency of the cycle by 0.4% points. At that condition, the CAPEX for the absorber could also be reduced 21%. In addition, CO_2

concentration could increase from 3.8 mol% to 7.8 mol% (wet) and O_2 could reduce from 12.2 mol% to 4.8 %mol. Nonetheless, at 50% EGR the oxygen concentration after mixing with air and before entering the combustor is reduced from 21 mol% to 12.5 mol%.

Li et al (2012) concluded that 35% EGR would be the maximum to maintain 16 mol% of O_2 in the combustor. As shown in Figure 3.4.a, the CO_2 concentration in the flue gas increases as the EGR ratio increases. However, the O_2 concentration in the combustor is reduced as shown in Figure 3.4. b. At 35% EGR the O_2 after mixed with EGR is 16 mol%. Most of the combustors are design to use air, which contains 21 mol% O_2 for the combustion (Li, et al, 2012) and without the presence of CO_2.

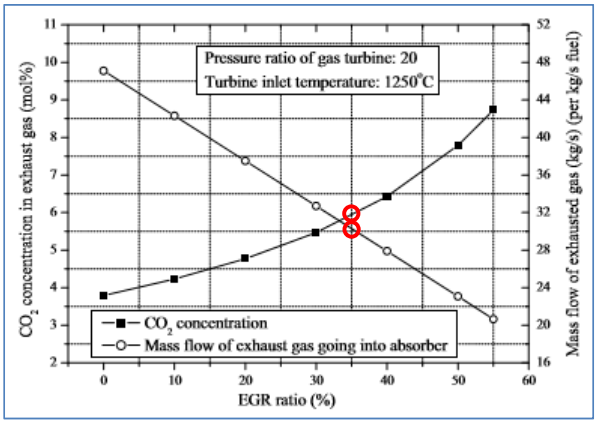

a) CO_2 concentration in exhaust gas

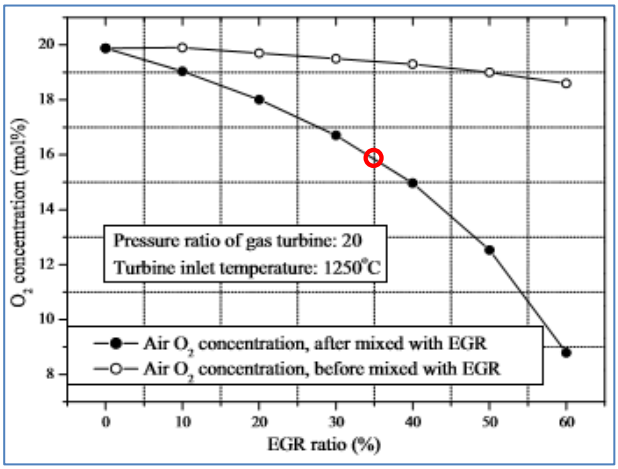

b) O_2 concentration in after mixed with EGR

Figure 3.4. CO_2 concentration and mass flow of the exhaust gas going into absorber at different EGR ratios and O_2 concentration before/after mixing with EGR at different EGR ratio (Li et al, 2011)

Experiments in a General Electric combustion turbine have confirmed that exhaust gas recycling up to 30% of the total flue gas is possible. Based on bench-scale testing, when the

O_2 concentration was reduced to 17.7 mol%, the flame was stable, suggesting this level could be achieved without any major modification of the combined cycle plant equipment (Evulet et al., 2009; Bolland and Saether, 1992).

National Energy Technology Laboratory (2010) concluded that post-combustion capture with amine absorption using 35% EGR was the lowest cost of CO_2 capture option when compared to:

1. Conventional NGCC with post-combustion capture using MEA
2. Natural gas reforming combined with pre-combustion CO_2 capture
3. Oxy-combustion of natural gas. In this alternative EGR was replaced with CO_2 recycle. O_2 from the ASU, CO_2 recycle, and natural gas enter to the combustor

National Energy Technology Laboratory (2013) reported that 35% EGR improves the efficiency by approximately 0.3 % and reduces the cost of electricity by 3 % compared with a conventional NGCC with capture. The CO_2 is enhanced from 4 mol% to 6.7 mol% and O_2 concentration reduced from 12.1 mol% to 8.3 mol% in the exhaust gas.

The IEAGHG (2012) developed a techno-economical study on CO_2 capture in gas fired power plants and five alternatives integrated with CO_2 capture were evaluated:

1. Conventional NGCC with post-combustion capture using MEA
2. Conventional NGCC with post-combustion capture using proprietary solvent
3. NGCC with 50% of EGR using MEA
4. Pre-combustion
5. Pre-combustion with H_2 storage

The first lowest cost of electricity was for conventional NGCC using proprietary solvent. The new solvent requires less energy for its regeneration. The cost reduction for saving energy in the reboiler is dominant over the additional operating cost for using new solvent. The second lowest cost of electricity was for a NGCC with 50% EGR. As it is mentioned before, higher that 35% EGR is possible with new design of gas turbine. The cost of electricity reduces by 3.2% and the reboiler energy consumption by 7.17% increasing the efficiency from 51.04% to 51.33% compared with a conventional NGCC using MEA. Combining a proprietary solvent with EGR, the cost of electricity of EGR could be lower than conventional NGCC with post-combustion capture using proprietary solvent. In this study, the CO_2 concentration in the exhaust gas increases from 4.46 mol% to 9.03 mol% and the O_2 reduces from 12.28 mol% to 4.4 mol%. However as mentioned previously, 50 % EGR is problematic for flame stability.

In conclusion, EGR is an option to increase the concentration of CO_2 in the flue gas and presents lower costs of electricity compared with conventional NGCC with CO_2 capture using MEA. According to the results presented by different sources, 35% EGR is reasonable and allowed in a GE gas turbine, but higher than this percentage the O_2 concentration in the combustor is reduced below 16 mol%. If EGR was higher than 35%, modifications in the design of the combustor would probably be needed.

It is expected that the resulting gas after mixing with EGR could not have a negative effect on compressors with lower margin surging than the compressor from GE. The reason is explained as follows:

Compressors are design to operate at certain surge margin depending of the property of the gas if it is heavy, medium or light gases shown in Figure 3.5. Compressors to compress air are design with surge margin for medium gas. The molar weight of the mixture of air with 35% EGR is 29.96 kmol/kg. It is almost similar to the air molar weight which is 28.97 kmol/kg. However, the final answer could be given after the evaluation of EGR in different industrial gas turbines.

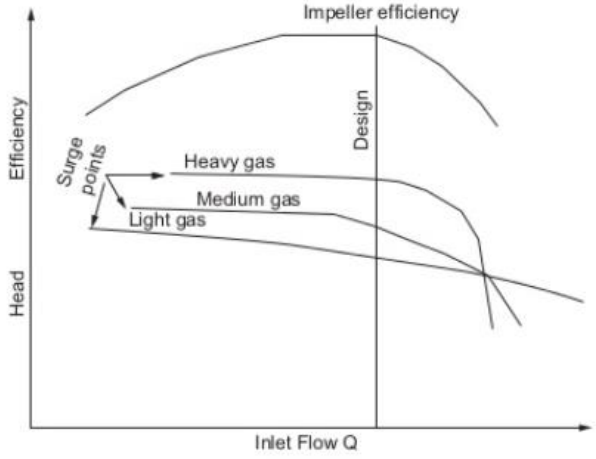

Figure 3.5. Effect of gas composition in a centrifugal compressor (Boyce, 2006)

A heavy gas has high molar weigh. Propane (molar weigh 44.097 kg / kmol), propylene (molar weigh 42.08 kg / kmol. The medium gas includes air (28.966 kg / kmol), natural gas (19 kg / kmol), and nitrogen (28.0134 kg / kmol). Light gases include gases such as Hydrogen-rich (around 2.016 kg / kmol) and gases found in hydrocarbon processing plants. Figure 3.5 shows the performance of an individual stage at a given speed for three levels of gas molecular weight (Boyce, 2006). It can be seen from Figure 3.5 that for a heavy gas:

1. The flow at surge is higher
2. The stage produces slightly more head than medium gas

3. The right-hand side of the curve turns downward more rapidly
4. The curve is flatter in the operating stage. This point often presents a problem to the designer of anti-surge control system

3.2.2 Selective exhaust gas recirculation (SEGR): Series and parallel membrane / solvent hybrid capture systems

Unlike EGR where a portion of exhaust gas is recycled; here only CO_2 is recirculated to the gas turbine in order to increase the CO_2 concentration in the exhaust gases and to keep the O_2 in the combustor up to 16 mol%. Recirculating only CO_2 is possible using a selective membrane.

The NGCC power plant integrated with CO_2 a separation membrane is proposed by Voleno et al, (2014) and Swisher and Bhown, (2014). The system is based on two membranes operating in series on the cooled flue gas from the HRSG. The first membrane consists with no sweep gas inlet on the permeate side, using a vacuum pump to keep a sub-atmospheric pressure of 0.2 bar in the permeate stream. CO_2 separated by this membrane is sent to storage after intercooled compression. The second membrane consists with a sweep gas inlet stream, flowing counter-currently, where fresh air for the gas turbine is used as sweep gas on the permeate side. This second membrane allows a selective CO_2 recycle in order to increase the CO_2 concentration of the flue gas. In the first membrane, separation of 90% of the CO_2 generated by the NGCC combustion is set.

The alternative proposed by Merkel et al, (2012) consists in a combination of two processes: the MEA-based CO_2 capture and a novel selective membrane reported by Merkel et al, (2012). In the membrane equipment, in one side, air is passed counter-currently to the flue gas on the other side of this membrane. As the membrane is selective for CO_2 over oxygen and nitrogen, CO_2 permeates into the air stream which enters the compressor. Therefore, the CO_2 concentration is increased in the exhaust gas, which has a positive effect in the MEA-based CO_2 capture unit. There are no compressors or vacuum pumps required for this membrane. The only energy required is for the fans or blowers that are used to push the exhaust gas to the membrane unit and to compensate the pressure drop (Merkel et al., 2012). Two configurations are possible: series and parallel membrane / solvent capture system. In the series membrane / solvent hybrid capture system shown in Figure 3.6, the total amount of the exhaust gas leaving the HRSG is first sent to the MEA-based CO_2 capture, which removes only a portion of CO_2. For example, only 50% of the CO_2 from the flue gas is captured in the absorber of the post-combustion plant using MEA which means a reduction

in the absorber size. Then, the exhaust gas that leaves the absorber is sent to the selective membrane equipment, which removes the rest of the CO_2 in order to achieve 90% overall removal (Merkel et al., 2012). With selective exhaust gas recirculation (SEGR) in series it is possible to increase CO_2 concentration in the flue gas from 4 mol% to 13.7 mol% approximately whilst maintaining oxygen at 16.3 mol% in the gas turbine combustor (Merkel et al, 2012). The O_2 concentration in the exhaust gas reduces from 12 mol% approximately to 8.17 mol%.

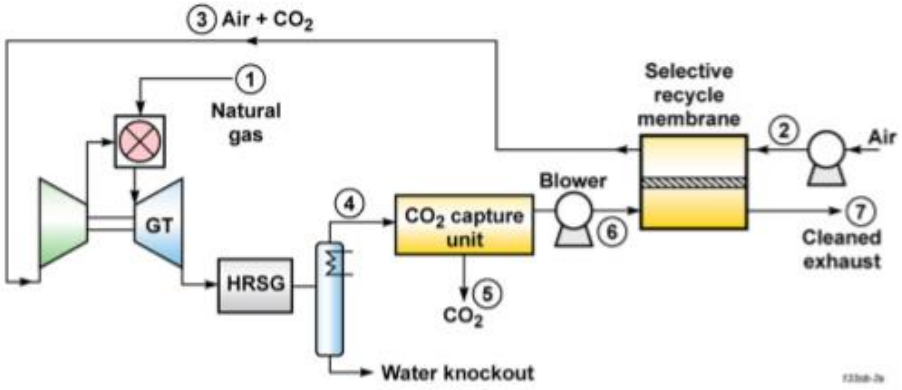

Figure 3.6. Schematic of the series membrane / solvent hybrid capture system (Merkel et al., 2012)

In parallel membrane / solvent hybrid capture system, shown in Figure 3.7, the flue gas is split into two portions. One portion of the exhaust gas leaving the HRSG is sent to the MEA-based CO_2 capture and the other to selective membranes. The proportion of the flue gas will depend on the economic analysis of the membrane and MEA-based CO_2.

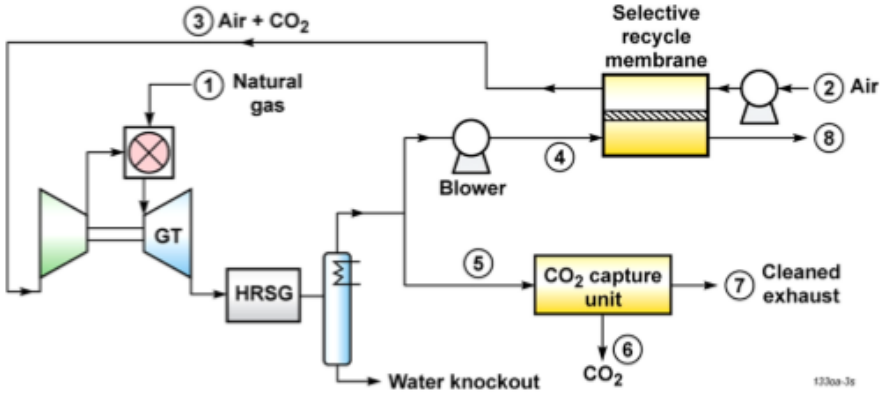

Figure 3.7. Schematic of parallel membrane / solvent hybrid capture system (Merkel, et al., 2012)

Sending 77% of exhaust gas to the membranes, with selective exhaust gas recirculation in parallel it is possible to increase CO_2 concentration in the flue gas from 4% to 18.6 %

approximately whilst maintaining oxygen at 16% in the gas turbine combustor (Merkel et al, 2012). O_2 concentration in the exhaust gas reduces from 12 mol% approximately to 7.58 mol%. In addition, only 23% of the volumetric flow is treated in the amine capture unit.

CO_2 recycling with this novel membrane in the NGCC gives more flexibility without approaching stoichiometric oxygen limits as happens with EGR (Merkel et al, 2012). High capital cost for the use of selective membranes could be a disadvantage for this alternative. In addition, this membrane is not mature technology and more research still is needed.

3.2.3 Supplementary firing natural gas combined cycle

In this process, additional fuel is fired in the supplementary burner located at the inlet duct burner of the HRSG, as shown in Figure 3.8. As a result, the oxygen is reduced and CO_2 is increased. Supplementary firing in NGCC power plant is typically used to increase power output by around 30% during times of peak demand of electricity (Kiameh, 2003). The maximum additional heat input in a single in-duct burner arrangement is, however, limited by the temperature constraint of the heat exchangers in the HRSG.

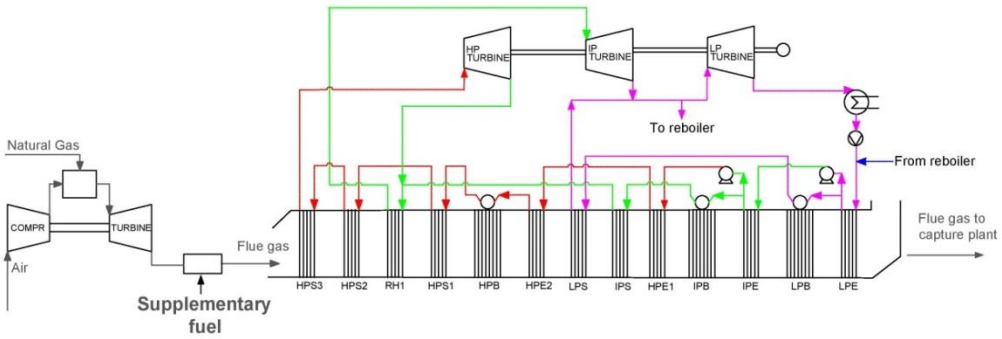

Figure 3.8. Schematic of the natural gas combined cycle with supplementary firing

Supplementary duct firing increases CO_2 concentration to levels similar to those achievable with the EGR method whilst avoiding modifications to the gas turbine. A study on supplementary firing performed by Li et al. (2012) reported an increment for CO_2 from 3.9 mol% to 8.4 mol% and O_2 concentration from around 12 mol% to 5.8 mol%. The temperature difference at the high pressure superheater header of the HRSG increases from 50ºC to 800ºC leading to a gas temperature of 1280ºC, compared to a gas temperature around 530ºC. In both cases, high pressure steam temperature is 480ºC; information related to the three levels of pressure generated in the HRSG is provided in Li et al, (2012) and are listed below:

HP steam temperature	°C	480
HP steam inlet pressure	bar	111

IP steam inlet pressure	bar	27
LP steam inlet pressure	bar	4

In the hypothetical case where fuel is burnt only in one step, the high temperature constraints on materials are not taken into account. The efficiency of the cycle drops with this alternative and the exhaust gas volume is not reduced; it increases for the additional fuel burned in the HRSG. An economic analysis is needed for new material because of increasing the temperature at these levels.

To improve this alternative, Li et al (2012) proposed three important modifications in the cycle:

1. Supplementary firing cycle integrated with exhaust gas reheating shown in Figure 3.9. The gas turbine is divided in two stages. The exhaust gas that leaves the first stage is reheated before going the second stage. This alternative could increase the CO_2 concentration and decrease the temperature difference in the HRSG.
2. Supplementary firing cycle integrated with exhaust gas recirculation (EGR) can efficiently increase the CO_2 concentration and reduce the mass flow of exhaust gas. However, with 40% EGR, the O_2 concentration in the combustor is reduced significantly; this could affect the flame stability.
3. Supplementary firing cycle integrated with a supercritical bottoming cycle can reduce the temperature difference in HRSG and increase the efficiency of the cycle

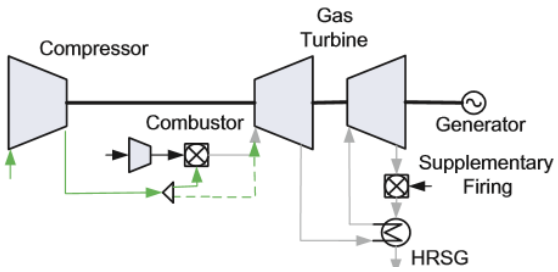

Figure 3.9. Scheme of supplementary firing with exhaust gas reheating (Li et al, 2012)

A combination of these three alternatives was estimated to raise CO_2 concentration in exhaust gas to 11.2 mol%. The gas/gas heat exchanger could result in additional capital cost that has to be quantified.

In conclusion, the main difficulty in using supplementary firing is that the temperature of the exhaust gas rises when additional fuel is used, whilst the maximum temperature is restricted by metallurgical constraints (Li et al., 2012). With this alternative it is possible to increase the amount of CO_2; and reduce the O_2 concentration in the exhaust gas but not the gas

volume of the exhaust gas. The alternative proposed by Li et al, (2012) shown in Figure 3.9 could solve the problem of the temperature constrain. In addition, the gas turbine would not require additional modification. However, economic analysis would be necessary to quantify the additional capital cost for the heat exchanger used to reheat the exhaust gas. The additional cost would depend on how much supplementary fuel is burnt and the resulting temperature of the exhaust gas.

3.2.4 Sequential gas turbine combustion

This concept is proposed by Asen and Eimer, (2008) in the patent US20080060346 A1, in order to increase the CO_2 concentration and reduce the volumetric flow of the flue gas.

The process is shown in Figure 3.10. The exhaust gas from a conventional NGCC is cooled down. Then, the flue gas enters the second conventional NGCC. The resulting hot exhaust gas is cooled again and after that it is sent to a CO_2 capture process using amine for capturing the CO_2. These methods can reduce the total amount of flue gas and increase the CO_2 concentration and reduce the O_2 concentration. As a result, the size of the absorber is reduced. However, the O_2 concentration in the flue gas that enters the second NGCC reduces and affects the combustion, which can lead to an incomplete unstable combustion and result in high CO emissions. According to the results, CO_2 increases from 4.25 mol% to 8.8 mol% and O_2 is reduced from 13.61 mol% to 6.02 mol% (wet base). The volume of the exhaust gas is reduced 50% as the same flue gas without adding additional air is used in the second NGCC.

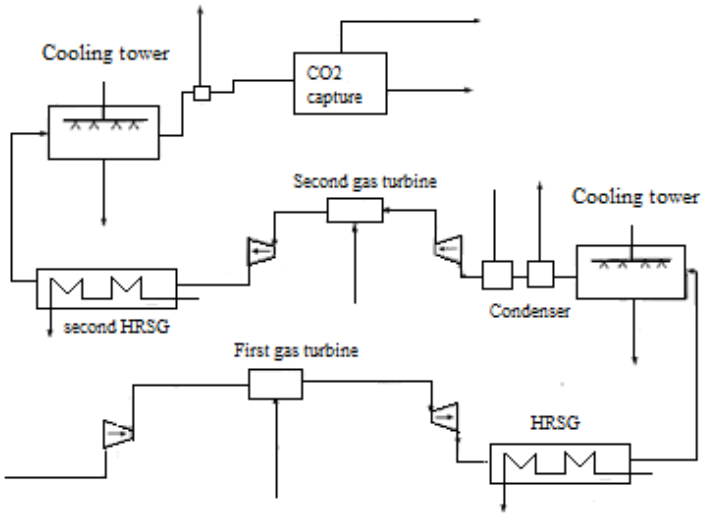

Figure 3.10. Sequential gas turbine combustion (Asen and Eimer, 2008)

As mentioned before, most of the combustors are design to use air which contains 21 mol% O_2. The O_2 concentration of the exhaust gas of a conventional NGCC is around 12 mol% and

4% of CO_2. This condition of the flue gas in the inlet of the second combustor would present a challenge for this alternative as a new design would be needed.

3.2.5 Gas turbine humidification

The gas turbine humidification or evaporative gas turbine cycle (EvGT) has been under research study for many years (Li et al, 2011; Li et al, 2009; Takahashi, 2007; Hatamiya et al 2004; Thern et al, 2003, Lindquist et al, 2002; Lindquist et al, 2000, Agren et al, 2000). The process is shown in Figure 3.11. The water is heated to saturated point before entering the humidification tower (column with packing) interchanging heat with the air that leaves the compressor. Then it enters the top of the humidification tower in contact counter-current with the compressed air which enters in the bottom of the tower. An amount of water is evaporated and leaves the tower together with the humidified compressed air. After that, the humidified air is preheated with the exhaust gas in order to increase the temperature to approximately the same temperature of the air at the outlet of the compressor, and then enters the combustor. The exhaust gas is sent to the CO_2 capture process. Before entering the absorber, the exhaust gas with an excess of steam passes to the condenser where the water is removed and as a result the CO_2 concentration in exhaust gas is increased. An EvGT pilot plant has been constructed and successfully operated in Lund Institute of Technology in Sweden (Thern et al, 2003, Lindquist et al, 2002; Lindquist et al, 2000, Agren et al, 2000).

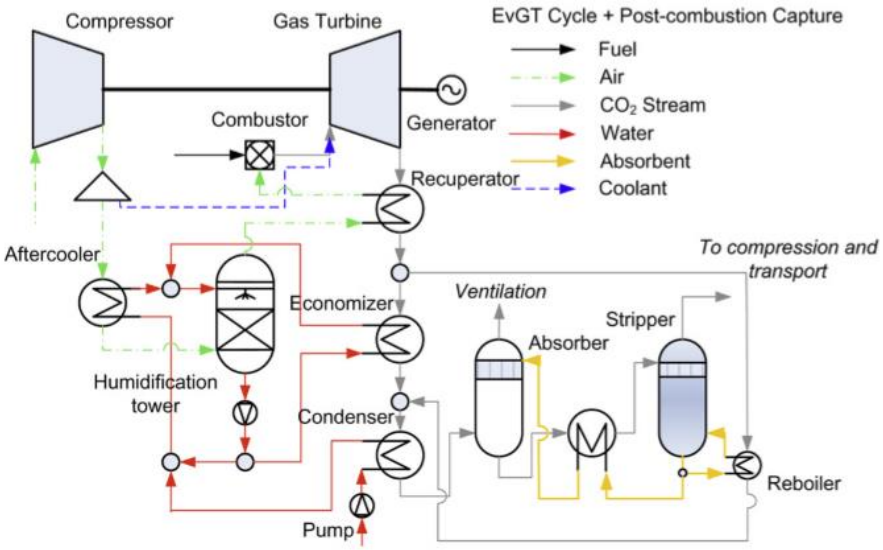

Figure 3.11. System of gas turbine humidification with amine-based CO_2 capture (Li, et al 2011; Li et al, 2009)

Li et al (2011) concluded that with this alternative it is possible to increase the CO_2 concentration from 3.9 mol% to 5 mol%. When this alternative was compared to EGR and

supplementary firing, humidification represented the lowest efficiency which is 41.6%. In term of investment cost, gas turbine humidification has the lowest capital cost as it does not have a steam cycle. As the air is replaced by water, this has the same effect as the EGR low O_2 concentration in the flue gas that goes to the combustor. The injection of the water in the gas turbine would cause a volumetric flow rate mismatch between the compressor and expander. The degree of mismatch, which depends on how much water is injected in the turbine, to accommodate the increased flow rate is under developed. Therefore, more than research is needed i.e. testing and experiments unit. As this work is focus on more mature technology, this technology is not selected because of this disadvantage.

3.3 Impact of the new alternatives on power plant and capture plant

This section describes the main parameters affected by the modifications to the natural gas combined cycle described in previous sections. These parameters such as O_2 CO_2, O_2, and NOx concentration at the combustor and before capture need special attention in order to understand the negative and the positive impacts on the power plant and CO_2 capture.

3.3.1 Effect of CO_2 concentration on NOx emission

The presence of the CO_2 in the flue gas that enters the combustor could be considered an important option for NO_X reduction (Lombardi, 2003).

At the flue gas temperatures faced during combustion of gas and light oil, one of the mechanisms for the NO_X formation is the thermal NO_X formation. The thermal NO_X formation results from high temperature dissociation and chain reaction of elemental nitrogen and oxygen from the air during combustion. It is highly dependent on the temperature, especially at temperatures above 1570 °C (Røkke, 2005 after Lefebvre, 1998) so the higher the temperature, the higher the NO formation.

NO_x formation are due to NO formed by the Thermal (Zeldovich reaction) described by the following reactions 3.1, 3.2 and 3.3 (Zeldovich et al, 1947):

$N_2 + O \rightarrow NO + N$ Reaction 3.1

$N + O_2 \rightarrow NO+O$ Reaction 3.2

$N + OH \rightarrow NO + H$ Reaction 3.3

In summary, with EGR in the gas turbine and selective EGR the reduction of NO_X formation are due to: The cooled recirculated flue gases acting as a heat sink from the flame and lowering peak flame temperatures

3.3.2 Effect of O_2 reduction in the combustor

The main difficulty with EGR is that O_2 concentration is reduced when a portion of air mass flow is replaced with exhaust gas. According to some authors, the reduction of O_2 in the gas that enters the combustor has negative effects on the combustor, especially in the flame stability. These are summarised in the following list:

1. The levels of unburned hydrocarbons and CO are very high at O_2 < 16 mol%. (Li, 2011). The present of hydrocarbon mean lower efficiency of the cycle.
2. The flame velocity reduces for some hydrocarbon fuels (Glassmann, 1996)
3. With EGR, combustion O_2 concentration should be kept between 16-18 mol% in order to maintain the flame stability (Bolland et al., 1997; Evulet et al, 2009)
4. EGR may induce loss of efficiency of the combustor because of the incomplete combustion of the fuel for the O_2 reduction (Evulet et al, 2009)
5. High levels of CO_2 in the system with EGR can provide a significant perturbation of the nominal reactant kinetics as CO_2 takes part in the combustion reaction (Lieuwen and Yang 2013).

3.3.3 Effect of O_2 concentration in exhaust gas on amine solvents degradation

Amine degradation at high concentration of O_2 occurs because it reacts with the amine forming salts and other components that are not regenerated with heat. In the case of MEA (C_2H_7NO), Goff and Rochelle (2004) reported the formation of various degradation products, and Figure 3.1 shows their stoichiometry.

Table 3.1. Oxygen stoichiometry for the formation of degradation products (Goff and Rochelle, 2004)

C_2H_7NO (MEA) + νO_2 ⟶ NH_3 + degradation products	
Product	**Stoichiometry (ν)**
Formaldehyde (CH_2O)	0.5
Acetic acid (CH_3COOH)	0.5
Hydroxyacetaldehyde ($C_2H_4O_2$)	0.5
Glycolic acid ($C_2H_4O_3$)	1.0
Formic acid (CH_2O_2)	1.5
Carbon monoxide (CO)	1.5
Oxalic acid ($C_2H_2O_4$)	2.0
CO_2	2.5

3.4 Comparison of results including the novel alternative proposed in the thesis

The most promising alternatives proposed in the literature review and the configurations proposed in this thesis "supercritical and subcritical sequential supplementary firing" are compared. Table 3.2 shows important information such as CO_2 and O_2 concentration in the exhaust gas, percentage of volumetric reduction, and the increment or reduction in the efficiency of the cycle. The alternative of EGR increases the CO_2 concentration mol% to 6.7mol%, and the efficiency of the cycle by 0.5 percentage points. In addition, it reduces the volumetric flow in the capture plant by 35%, which means a reduction in capital cost of the absorber. However, the O_2 concentration reduces from 12 mol% to 8.3 mol% which does not solve the problem with amine degradation. Selective EGR in parallel presents the highest increment of CO_2 in the exhaust gas from 4 mol% to 18.6 mol%. In series the CO_2 increases from 4 mol% to 13.7 mol%. It represents the greatest reduction of exhaust flue gas going to the absorber of 77.5 %. In addition, the efficiency increases 0.5 % points. Nevertheless, economic evaluation is needed as the main high cost comes from the membranes and the high pressure drop in the membrane has to be considered. In addition, the concentration of O_2 in the exhaust gas still remains high and options for separating CO_2 from the air (e.g. membranes) still do not exist in the market. Supplementary fuel in one step increases the CO_2 concentration from 3.9 mol% to 8.4 mol% and reduces the O_2 concentration from 12.4 mol% to 5.8 mol%. However, the efficiency penalty is 6.7 % and the volume of the exhaust gas does not reduce significantly because of the temperature restriction. What is more, economic analysis is needed because new material in the HRSG for high temperature would be necessary, thus it would increase the capital cost of the cycle. Supercritical and subcritical sequential supplementary firing increases the CO_2 concentration 4.2 mol% to 9.4 mol% and the volumetric flow is reduced 50% approximately. This alternative represents the highest reduction in the O_2 concentration from 11.9 mol% to 1.3 mol%. However, the efficiency penalty is 5.7 % for supercritical and 8.2 % for subcritical. There are two circumstances that have to be considered before proposing an alternative for CO_2 capture for Mexico: The cheap gas price and the high opportunity for developing EOR projects. The effect of the efficiency in the cost of the electricity is likely to have a reduced impact because of the low gas price. The positive impact on the post combustion capture plant size and energy requirements for solvent regeneration are attractive for markets with cheap natural gas, and where the emphasis on capital cost reduction is important. In chapter 4 a rigorous techno-economic analysis of supercritical and subcritical SSFCC is carried out.

Table 3.2. Comparison of alternatives for enhancing the CO_2 concentration (wet base); reduce the volume and O_2 concentration in the exhaust gas (Li et al, 2012; Merkel et al., 2012; IEAGHG, 2012; Aboudheir and ElMoudir, 2009) including the alternative proposed in this thesis

Alternatives	**NGCC with EGR**	**NGCC Selective EGR parallel**	**Selective EGR series**	**NGCC with supplementary firing**	**Supercritical SSFCC**	**Subcritical SSFCC**
Capture level %[1]	90	90	50	90	90	90
Main modification	Gas turbine	Gas turbine	Gas turbine	HRSG	Steam cycle	Steam cycle
mol % CO_2 exhaust gas	4 to 6.7	4 to 18.6	4 to 13.7	3.9 to 8.4	4.2 to 9.3	4.2 to 9.3
mol % O_2 exhaust gas	12.1 to 8.3	12 to 7.58	12 to 8.17	12.4 to 5.8	From 11.9 to 1	From 11.9 to 1
mol % O_2 exhaust gas before combustor	16	16	16.3	21	21	21
% reduction of volumetric flow to CO_2 capture	35	77.5	2.7 (height of the absorber is reduced)	0	50	50
ΔReduction or Δincrement in efficiency	0.5 >	0.5 >	0.5 >	6.7 <	4.8 <	7.3 <

[1]Capture level is related to the percentage of CO_2 captured from the flue gas that enters the absorber of the post-combustion plant using MEA

3.5 Literature review of capture plant and CO_2 compressors at design and part-load conditions

This section provides important information from the literature related to the design and operation of the capture plant and compressor unit used in this thesis. In addition, simulation results of the optimisation of the capture plant are given in the last section.

3.5.1 Design condition of CO_2 capture plant

This section focuses on the optimisation of conventional post-combustion capture process design, and on technical evaluation at part-load condition based on the state-of-art.

Firstly, it is necessary to determine the optimum design condition of the capture plant. There are some parameters that have to be evaluated and defined such as size of the absorber, lean and rich loading, temperature and pressure in the stripper

Effect of different lean solvent loading. The total energy required to regenerate a CO_2 loaded solvent can be expressed as follows, according by Chakma, (1997); Kim and Svendsen, (2007); and Mohammad, (2009):

Total Energy = Heat of Reaction + Sensible Heat to heat up the rich amine to the operating temperature of the reboiler + Latent Heat of Vaporization of the evaporated Water

The contributions of each of these parts are varied while changing the lean loading. The lean loading is defined as the ratio of moles of CO_2 to moles of amine in the regenerated amine solution exiting the regenerator or stripper bottom.

At constant CO_2 removal efficiency:

1. At different lean loading the heat of reaction remains almost constant
2. At lower lean loadings the latent heat of water evaporation to achieve the same CO_2 removal becomes dominant
3. At higher lean loadings a larger amount of solvent is needed to achieve the same CO_2 removal which means more sensible heat is required to raise the temperature of the solvent to the stripper temperature

Effect of the stripper pressure and temperature. At high temperature and pressure, the CO_2 mass transfer rate increases through the stripper column because of the high driving force that enhanced the vapour - liquid equilibrium for desorption. However, higher amine

degradation rates and corrosion problems occur at high pressure and temperature (Mohammad, 2009). The recommended temperature of the reboiler for MEA is 120 °C (Kohl and Nielsen, 1997; IEAGHG, 2010; Rochelle, 2009). It was verified to be optimal in the experimental results of Knudsen (2011) in a pilot plant with capacity to capture 1 t/h of CO_2 from the flue gas generated at the coal fired power plant operated by Dong in Esbjerg, Denmark (Sanchez-Fernandez et al, 2013 after Knudsen, 2011).

Diameter of the absorber. The column diameter is a function of the liquid and gas flow rates and their densities (Abu-Zahra et al, 2007; Rezazadeh, 2015). It is based on the flooding limitation, and pressure drop (depending on the packing). Although a diameter large enough is necessary to prevent flooding through the column, very large diameters are not recommended.There is a maximum volume flow rate of 300,000 m^3/h (292.5 tonne/h approximately) which could be treated in an absorber column due to economic limits to the size of the absorber based on pressure drop constraints to ensure a stable operating condition with proper liquid and gas distributions (Desideri and Paolucci, 1999; Yagi et al, 1992; Rezazadeh, 2015) also in terms of available column vendors. For systems that require the processing of a larger flow, a modular design with several trains operating in parallel is adopted. Rezazadeh et al (2015) after Reddy et al. (2003) reported that the maximum diameter for an absorber column under operation is 18.2 meters. According to Kvamsdal et al (2009), flooding is not a limitation at part-load operation as the liquid flow does not increase with the reduction in the gas flow.

Flooding. When the inlet gas flow rate is so high that it interferes with the downward flow of the solvent liquid, it may cause an upward flow of the liquid through the tower, the liquid is no longer able to flow downwards, and fills the entire column due to a high gas velocity and liquid flow. This phenomenon is known as flooding.

The rich loading. The rich loading is the solvent loading with CO_2 at the absorber outlet and is a good indication of the level of solvent saturation (Mohammad, 2009). As MEA is a primary amine, carbamate is predominant product in the equilibrium Reaction 3.4 (Sanchez Fernandez, 2013; Versteeg, et al 1996; Versteeg, et al 1988):

$$CO_2 + 2R\text{-}NH_2 \longleftrightarrow R - NHCOO^- + R\text{-}NH_3^+ \qquad \text{Reaction 3.4}$$

Carbamate

So the ideal maximum rich loading with MEA is close to 0.5 mol CO_2/mol MEA (Mohammad, 2009 after Kohl and Nielsen, 1997). It depends mainly on operating absorber

temperature (40-55 °C) and CO_2 partial pressure which depends strongly on the CO_2 concentration as shown in Equation 3.1:

$$P_{CO2} = X_{CO} P_T \quad \text{Equation 3.1}$$

Where:

P_{CO2} Partial pressure of the CO_2,

X_{CO2} CO_2 concentration in the flue gas,

P_T Total pressure of the system, which is close to atmospheric

3.5.2 Strategies to operate the capture plant

After defining the optimal design condition, the next step is to determine the optimal operating condition that is influenced by the design of the capture and power plant, and the operating strategy at part-load (Van der Wijk et al., 2014).

The operating condition of the CO_2 capture plant has a strong connection with the power plant through the steam extracted from the IP/LP crossover to supply thermal energy to the reboiler. The pressure in the crossover drops at part-load. Unless measures are taken to stop it, such as using a steam ejector, or the pressure may be higher than required at full load (Irons, 2013), the capture plant has to be adapted to the variation of the steam at part-load (Gibbins and Crane, 2004; Lucquiaud et al., 2009). Then it is important to understand the alternatives of operating strategy.

Two operating strategies for part-load operation of capture plants have been analysed by Van der Wijk et al., (2014) and Kvamsdal (2009):

1. **Constant L/G ratio**: this strategy is based on a constant L/G in the absorber approximately equal to the optimum at design condition, whilst maintaining a constant capture rate. This means that the liquid flow rate is decreased as the gas flow is reduced. The reduction in the liquid flow rate results in an increment of the rich loading which helps to reduce the thermal energy. Although this alternative is called constant L/G, results by Kvamsdal (2009) showed that L/G was reduced from 7.1 to 4.8 kg/kg in order to get the same capture level. This is because of the increase in the gas and liquid residence time in the absorber (Sanchez Fernandez et al, 2016).
2. **Constant solvent flow:** maintains a constant solvent flow rate through the capture unit. According to the simulation results by Kvamsdal (2009), as the load decreases, the L/G increases reducing the rich loading. This phenomenon is not beneficial to the reduction of the energy in the reboiler as higher rich loading acts as a driving force.

Both authors confirmed that this alternative represents less efficient operating strategy to operate the capture plant

In the two operating strategies above, stripper pressure was fixed, as well as the exchanger temperature approach 10 °C and amine concentration 30%, as they depend on the optimum design condition of a specific amine (Kvamsdal, 2009). With respect to the reboiler temperature, because of the reduction in the steam pressure in the cross-over (the saturated temperature of the steam in the reboiler reduces), the temperature of the solvent in the reboiler is lower than at design. This is linked to a less favourable vapour-liquid equilibrium for desorption, which reduces the extent of solvent regeneration and leads to higher CO_2 regenerated solvent (Sanchez Fernandez et al, 2016). Higher lean loading results in a large amount of steam (sensible Heat) demand to heat up the solvent.

In recent publication by Rezazadeh et al (2015), the operating mode at part load was: L/G slightly variable and pressure and temperature in the reboiler, and steam pressure were kept constant. However, it is possible to keep the temperature in the reboiler constant only if the heating steam pressure can be held constant at part-load keeping fixed pressure in the crossover.

Sanchez Fernandez et al (2016) proposed three part-load strategies:

1. **Constant Stripper pressure for load following:** This option consists in maintaining the stripper pressure at design value. The solvent flow to the absorber column is adjusted to maintain capture level, so the L/G increases.
2. **Constant L/G ratio in the absorber:** In this turn down strategy the solvent flow is adjusted at lower loads in order to keep a constant L/G ratio in the absorber. Unlike in the previous option, the solvent lean loading is maintained constant by releasing stripper pressure.
3. **A combination of releasing stripper pressure and increasing the L/G ratio in the absorber:** This strategy represents a maximum solvent regeneration, the capture level is kept at 90% for all loads and the maximum possible flow of rich solvent is regenerated. This strategy can be used when the pressure of the steam to regenerate the solvent is very low in order to reduce the amount of LP steam

In the first option the stripper pressure is kept at design value. Keeping the pressure in the stripper constant, the suction pressure at compressor inlet is maintained at its design value, reducing the power required for compression. On the other hand, maintaining the L/G ratio constant, the lean loading at part-load is kept at value, approximately equal to the design, by

releasing the stripper pressure in order to extend the regeneration degree of the solvent (Sanchez Fernandez, et al, 2016). Releasing the pressure makes it possible to reduce the sensible heat and increase the latent heat of water evaporation to achieve the same CO_2 removal. At lower pressures and temperatures in the stripper more energy per unit CO_2 is required to achieve the same degree of solvent regeneration as in the design case due to a less favourable CO_2 to steam ratio. Nevertheless, the latent heat of steam increases with decreasing condensing pressures and a final energy balance is achieved in the reboiler. This strategy has a negative impact on the downstream compressor operation. Sanchez Fernandez et al (2016) concluded that the most efficient strategy is to keep the stripper pressure constant.

3.5.3 Strategies to operate the CO_2 compressor

The CO_2 can be transported by pipeline in different phases: vapour, liquid or supercritical. In the United States several thousand kilometres of high pressure CO_2 pipeline have been used for more than 40 years, mainly for EOR purposes. The existing pipelines for CO_2 transport are operated in supercritical phase at ambient temperature and with pressures up to several hundred bars because of the large distances between the CO_2 sources and the injection locations. High pressures and high densities result in smaller pipelines and less recompression required at certain intervals in the pipeline (Vermeulen, 2011).

Siemens (2009) has presented three optimal scenarios to compress the CO_2 shown in Figure 3.12:

1. In scenario A: Compression to subcritical conditions, liquefaction and pumping. The CO_2 is compressed until 45 bar approximately, after which the CO_2 is condensing at approximately 0°C, and then a pump is used to get the desired pressure (Vermeulen, 2011)
2. In scenario B: Compression to supercritical conditions and pumping. The CO_2 is compressed until 100 bar approximately, after that the CO_2 is cooled to approximately 20°C (Vermeulen, 2011). As in option A, a pump is used to get the desire pressure
3. In scenario C: Compression to supercritical conditions. The CO_2 is not condensed and a compressor is used to get the desired pressure

Although the option A is characterized by the lowest compression power for CO_2, the condensation of CO_2 at low temperature 0°C, refrigeration has to be used in warm countries

such as Mexico, probably most for at least part of the year. Therefore, it will represent an increment in capital and operating cost.

The selection between scenario B and C mainly depends on the final pressure required. For high discharge pressures the final compression stages can be replaced by a pump to reduce power consumption i.e. offshore pipeline. Very high discharge pressure is required when long pipelines are used because it reduces the number of intermediate re-pressurisation locations in the pipeline. In this thesis, the onshore pipeline collection network, less than 100 kilometres is required as discussed in Chapter 2 section 2.2.4., which consists of relatively short pipelines without recompression. For that reason, path C is selected in this thesis. The log P-H diagram of pure CO_2 is presented in Figure 3.13, with an overlay of the different phases. The distinction between liquid, supercritical and vapour phase is set by the critical pressure and temperature of CO_2 (Vermeulen, 2011).

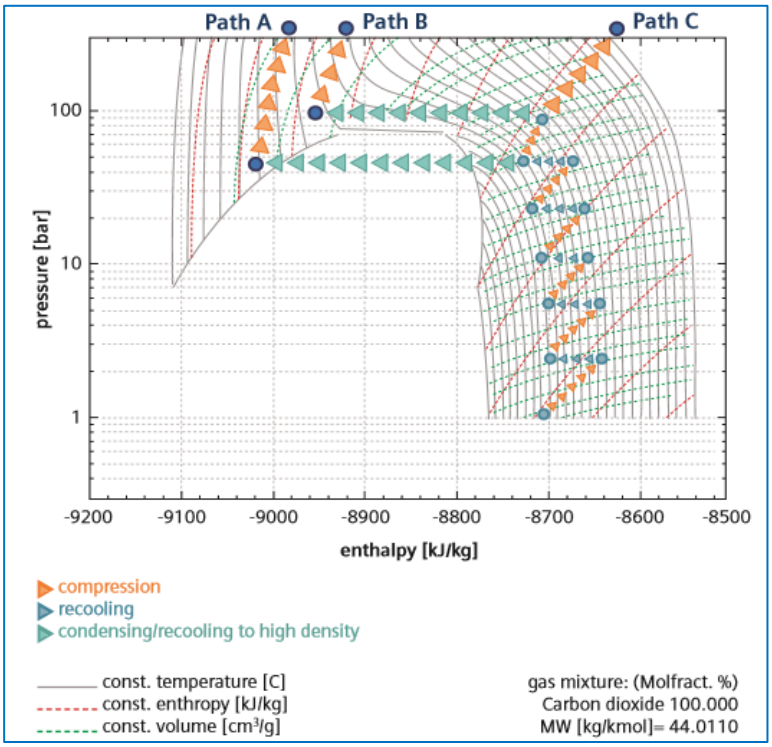

Figure 3.12 Illustration of possible compression paths for a CO_2 capture process (Ogink, 2015, after Siemens, 2009)

The scenario C consists of an integrally gear-type centrifugal compressor with several stages to compress the CO_2 stream is suggested by Jockenhövel (2009) and Siemens (2009). It may be equipped with up to 4 stages, with a maximum of 8 stages. The number of stages depends on the pressure ratio. To compress CO_2 from 2 bar to 110 bar, for which pressure ratio is 55, six stages are needed (Liebenthal and Kather, 2011). For pressure ratios higher than 55 more

compressor stages might be necessary. Inter-coolers are used to cool the gas at 40°C after each compression stage to condense the water and reduce the volume in the next stage of the compressor. The reason for cooling to 40°C is to keep the supercritical condition (supercritical condition of CO_2 is 31.10 °C and 73.9 bar). Reducing the volume leads to reducing power consumption and the size of the compressor stage (Liebenthal and Kather, 2011). Re-cooling the fluid after every stage is easily feasible and shows the lowest specific power duty and cooling duty (Jockenhövel el at, 2009; Liebenthal and Kather, 2011). Knock-out drums and dehydrators are used for removing stream impurities.

For large flow rates and the operational discharge pressure range, centrifugal compressors are more attractive such as single shaft and integrally geared compressors (Vermeulen, 2011). They present lower capital and operational cost, due to a lower number of impellers, smaller size of impellers and high achievable impeller efficiencies. Integrally geared compressors can easily be adjusted for specific operation modes and inter-stage activities, like flow and pressure control are possible, but also inter-stage dehydration is also easily implemented (Vermeulen, 2011).

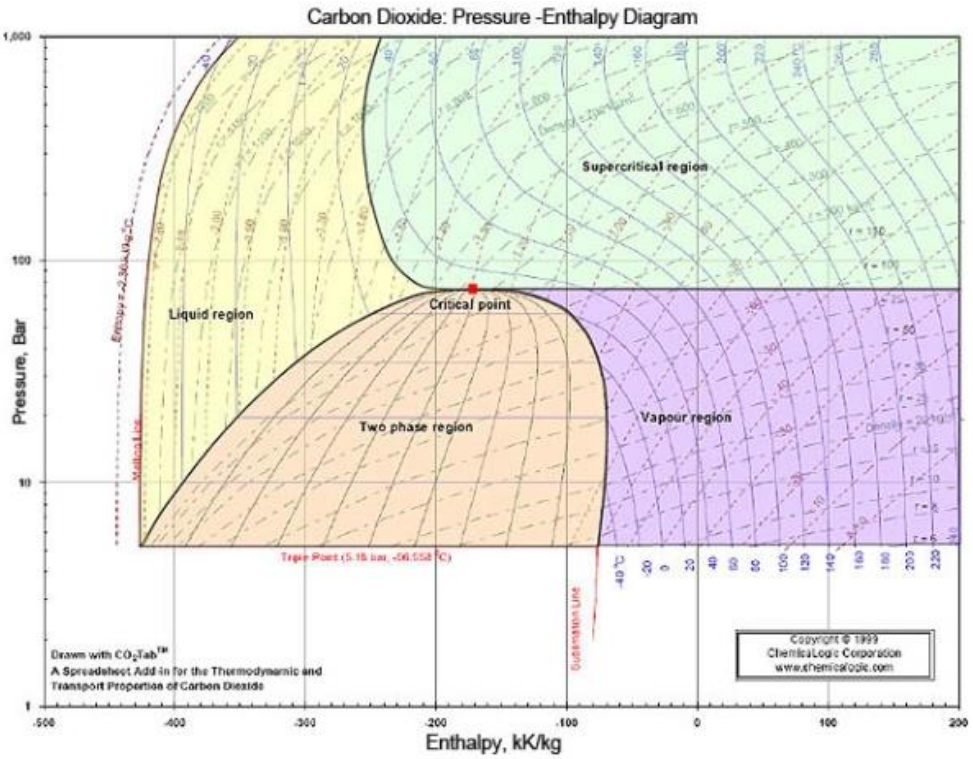

Figure 3.13. Log P-H diagram of CO_2 (Vermeulen, 2011)

After selecting the configuration of the CO_2 compressor and the operating condition, compressor control is the next aspect to be considered. Compressor control is very important to maintain a compressor in its stable operating range out of the surge line and the capacity limit when it is operating at off-design. Surge phenomena cause vibrations that result in high stresses on the compressor components that damage the equipment (Kiameh, 2013). There are several control methods to prevent surge (Liebenthal and Kather, 2011 after LÜDTKE, 2004) at off-design which are described below:

Variable Speed. The shaft speed is linearly varied with changing inlet volume flow. It represents the most efficient method at off-design condition (Liebenthal and Kather, 2011). However, from the mechanical perspective, variable speed drive compressors may have issues with vibrations (Sanchez Fernandez et al., 2015).

Suction throttling. A throttle valve is used in the suction line as an integral part of the compressor. In part-load operation this throttle is activated to decrease the suction pressure (pressure ratio is increased because the pressure of the CO_2 downstream of the compressor does not fall quickly enough) and thus increase the inlet volume flow. This alternative represents the lowest efficiency as a result of the use of the throttle valve.

Recycle valve. This control alternative consists of using a recycle valve in the suction side of the compressor. When mass-flow is reduced at part-load, part of the compressed gas from the discharge of the compressor is recycled at the inlet of the compressor in order to work at the same volumetric flow and its corresponding pressure out of the surge line. As a result, the efficiency decreases. Although it causes a high efficiency penalty, it gives the highest working range of operation (Liebenthal and Kather, 2011; Ogink, 2015).

Adjustable Inlet Guide Vanes. Inlet Guide Vane (IGV) control is based on the possibility of changing the guide vanes orientation in order to control the angle at which the flow enters the compressor. IGV is used to reduce the mass-flow and the pressure ratio in the compressor. Although at part-load the efficiency drops when closing the IGV, this alternative is more efficient than using recycling and throttling valves (Sanchez Fernandez et al, 2016). For that reason, this alternative is selected in this thesis.

Liebenthal and Kather (2011) presented the resulting performance map of a gear-type centrifugal compressor with 6 stages using IGV at part-load shown in Figure 3.14. Although the compressor is control adjusting the IGV, for a constant suction and discharge pressure, the operation at 70% for the related volume flow (V/Vn) part of the CO_2 will be recycled automatically in order to prevent surge region.

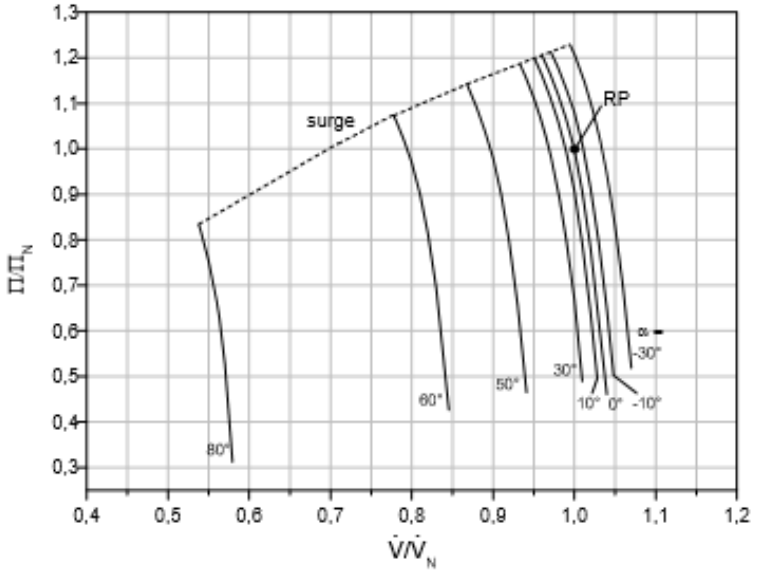

Figure 3.14. Resulting performance map of the complete compressor including 6 stages (Liebenthal and Kather, 2011)

The polytropic efficiency and the pressure ratio for each stage are estimated using the performance map shown in Figure 3.15. The pressure ratio for each stage is calculated using Equation 3.2.

$$y_p = RZ_m T_1 \frac{n_v}{n_v - 1}\left[\pi^{\frac{n_{v-1}}{n_v}} - 1\right] \qquad \text{Equation 3.2}$$

Where

y_p Polytropic head shown in Figure 3.15

π Pressure ratio

R The ideal gas constant

Z_m The real gas factor (average between the inlet and outlet)

T_1 Inlet temperature in the stage (40 °C)

n_v Polytrophic exponent (average between the inlet and outlet)

The polytropic exponent is calculated using Equation 3.3

$$\eta_p = \frac{\frac{k-1}{k}}{\frac{n_v - 1}{n_v}} \qquad \text{Equation 3.3}$$

Where

η_p Polytropic efficiency estimated with the performance shown in Figure 3.15

k Average $\frac{C_p}{C_v}$ at the inlet and outlet of the stage

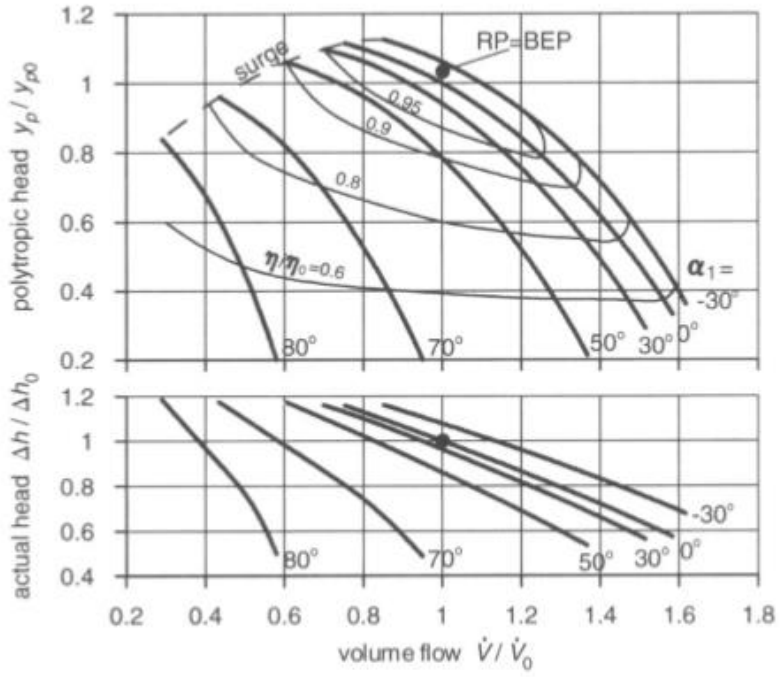

Figure 3.15. Typical single-stage performance map for adjustable inlet guide vane control (Liebenthal and Kather, 2011)

3.6 Simulation of the capture plant and compression

In order to illustrate the effect of the CO_2 concentration on the rich loading and the height of the absorber; and the stripper pressure and the lean loading on the thermal energy consumption, a standard CO_2 capture plant using 30% MEA, shown in Figure 3.16, is simulated in Aspen plus® using a rate-based approach. The capture plant was validated by several authors based on various data sets from different pilot plants (Razi et al. 2013; Sanchez Fernandez et al. 2014).

The rate-based model provides excellent predictions for the overall performance of the CO_2 capture system, including CO_2 removal percentage, CO_2 loading, reboiler duty, etc. while the equilibrium-stage model cannot predict these key performance variables reliably. The rate-based model is a very useful simulation and optimization tool to study sensitivities of various CO_2 capture process variables, including liquid/gas ratio, CO_2 concentration in the feed stream, CO_2 loading and MEA concentration in the lean amine stream, operating pressure, packing height and type, etc. (Zhang and Cheng, 2011).

The basic information for one train of the capture plant such as the absorber pressure drop packing characteristics is provided in Table 3.3. This information is recommended from the literature based on experimental experience: the flue gas inlet absorber at 44 °C and 1.13 bar;

40 °C the temperature in the stripper condenser; 10°C approach temperature is assumed in the reboiler to ensure reliable operation and avoid thermal degradation of the solvent (Rezazadeh et al, 2015); and lean/rich stream heat exchanger approach temperature 10°C (Sanchez Fernandez, et al, 2013). 70% of the maximum gas velocity is selected in this work. Experience based rules of thumb suggests to design absorbers to operate at no more than 70% of the maximum gas velocity that can cause flooding (Aguilar, 2007).

The flue gas comes from a NGCC for which information and configuration were taken from IEAGHG, (2012).

Table 3.3. Basic information of the simulation of the capture plant

	Unit	Absorber	Stripper
Column pressure drop[1]	bar	0.015	0.03
Number of stages		20	8
Simulation		Rate-based approach	Equilibrium
Packing characteristics		Sulzer standard 250Y	Tray sieve
Rich loading inlet	°C		115
Temperature reboiler	°C		120
Temperature condenser	°C		40
Flue gas flow rate	kg/s	337	
Pressure flue gas inlet	bar	1.13	
Flue gas temperature inlet	°C	44	1
Lean/rich heat exchanger approach[1]	°C	10	

[1]Sanchez Fernández et al, (2013), Rezazadeh et al, (2015)

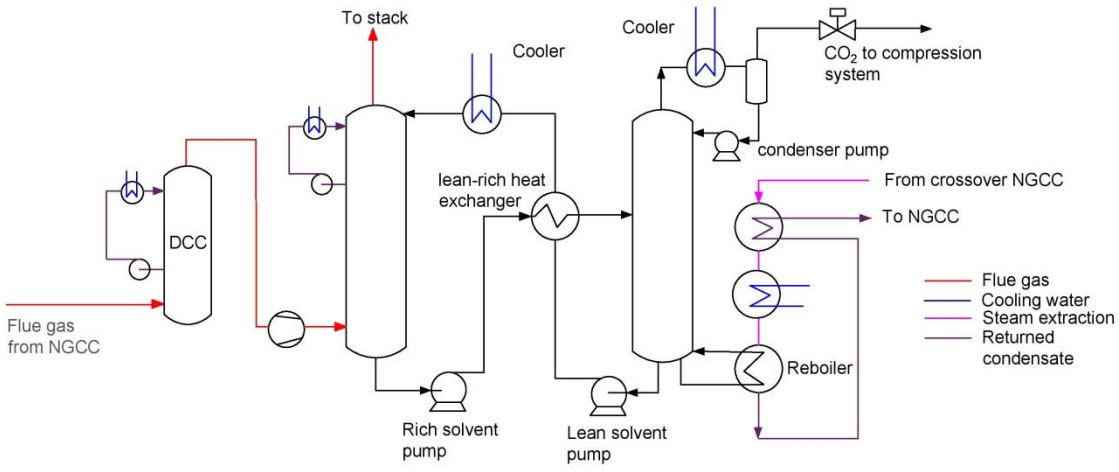

Figure 3.16. Figure Schematic of CO_2 capture plant simulated in Aspen plus@

The effect of the CO_2 concentration and the height of the absorber on the rich loading are shown in Figure 3.17. The calculation of rich loading is without any optimisation. At lower absorber height a higher solvent flow rate is required to reach the same percentage of

capture. It is necessary to adjust the liquid to gas ratio (L/G) to maintain the same capture rate. The diagram shows that the higher the CO_2 concentration in the flue gas, the higher the rich loading. At absorber heights greater than 16 meters, the rich loading does not change significantly.

Figure 3.18 shows the results of simulation of the whole capture plant. The reboiler pressure was varied from 2 to 1.8 bar in order to find an optimum combination of pressure, lean loading, and solvent flow rate that minimises the reboiler duty. The lean loading that minimises the specific reboiler energy is found at 0.269 mol CO_2/mol MEA that corresponds to a reboiler pressure of 1.9 bar. Lower lean loadings, below 1.9 bar, result in high energy to vaporise the water. The generation of stripping steam is higher than at pressure up to 1.9 bar, resulting in a high water to CO_2 molar ratio at the top of the stripper column. This requires relatively high reboiler energy per unit of CO_2 desorbed. For pressures higher than 1.9 bar the lean loading increases and solvent capacity is reduced. Therefore, the lean solvent flow increases in order to maintain the CO_2 removal rate at 90%. As a consequence, the specific reboiler energy increases because the sensible heat to heat up the solvent to the stripper temperature increases. The optimum reboiler duty is 3.562 MJ/tonne CO_2 that corresponds to a pressure of 1.9 bar. Figure 3.19 shows the variation of the rich loading and the regeneration energy at different height of the absorber after the optimisation. As the rich loading increases the energy required in the reboiler reduces.

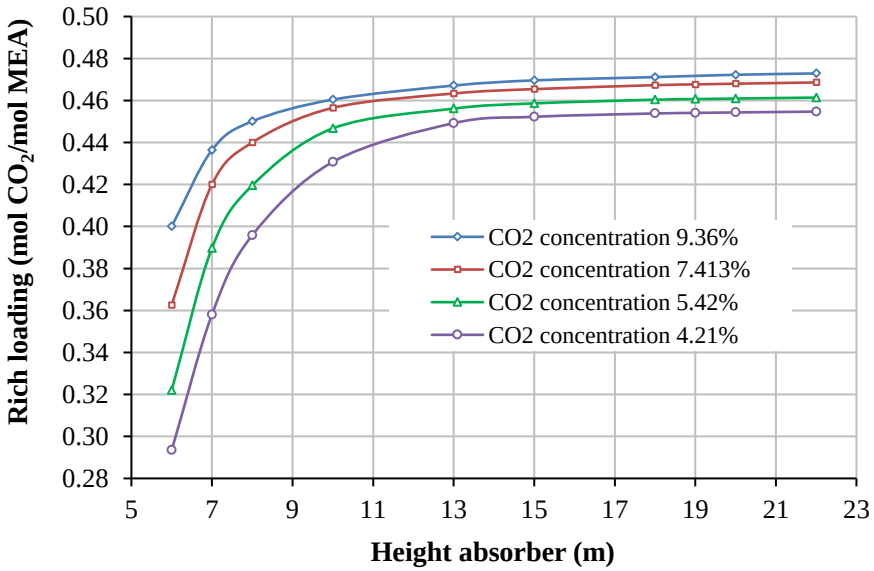

Figure 3.17. Variation of rich loading mol CO_2/mol MEA at different CO_2 concentration and height of the absorber. Lean loading 0.27 mol CO_2/mol MEA; 30% MEA concentration; 90% capture, temperature 120°C and 1.9 bar

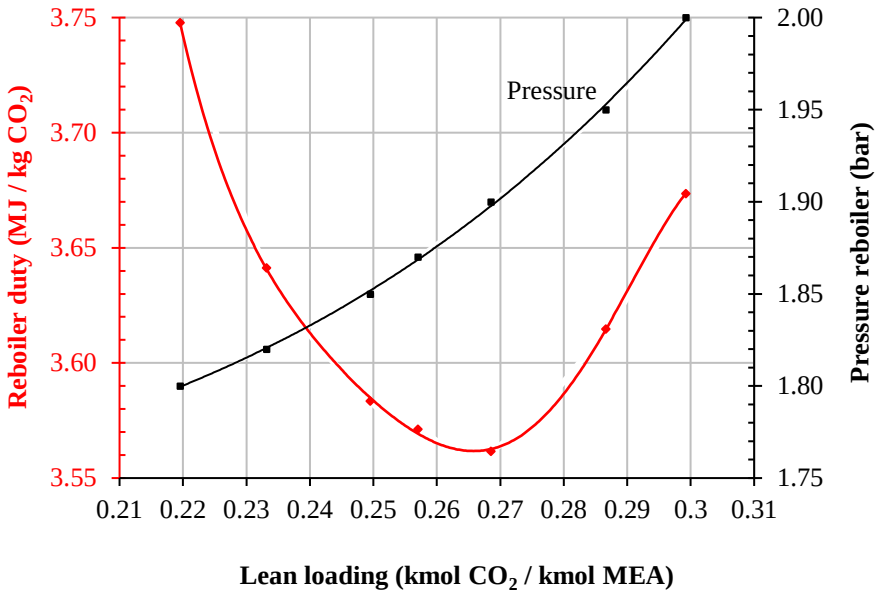

Figure 3.18. Optimisation of the energy in the reboiler for a natural gas combined cycle (NGCC) as a function of solvent lean loading, with CO_2 removal rate of 90% and stripper temperature of 120ºC. The CO_2 concentration in the flue gas is 4.2 mol% and the pressure is 1.9 bar

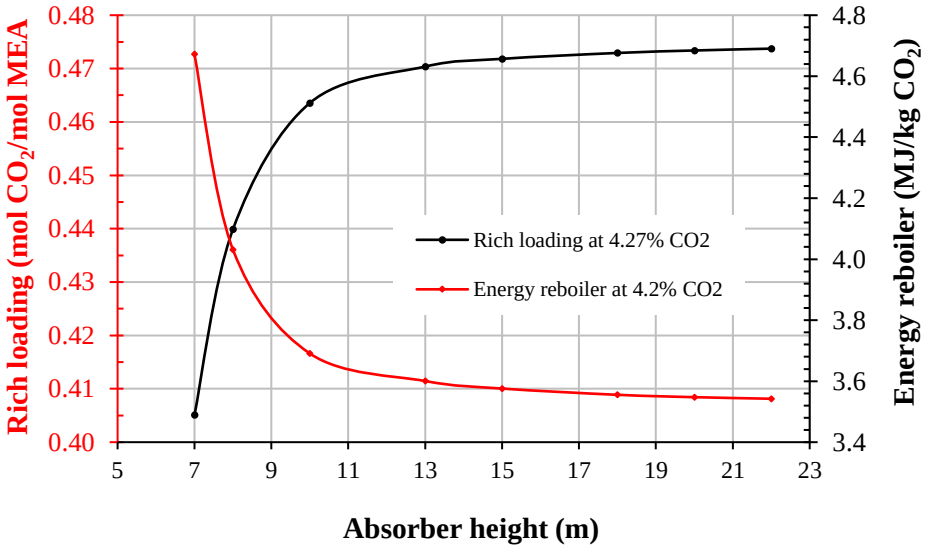

Figure 3.19. Specific reboiler duty and the rich solvent loading are calculated and plotted as a function of height of the absorber for a constant CO_2 removal rate of 90% and constant stripper temperature of 120ºC and pressure 1.9 bar, CO_2 concentration in the flue gas 4.2 mol%, lean loading 0.269 mol CO_2/mol

At part-load, the operation strategy is: constant pressure and variable L/G. Based on the conclusion of Sanchez Fernandez, et al. (2016), this represent the most efficient alternative at part-load operation. This is mainly because the reboiler temperature achievable at constant pressure is higher than at constant L/G, which helps the generation of the solvent. In addition, constant pressure reduces compression work.

With respect to the compressor configurations proposed by Siemens, (2009), "compression to supercritical conditions, without CO_2 condensation, using a compressor to get the desire pressure instead of a pump" is selected. The main reason of that is because short distant is required in this study i.e. onshore, less than 100 km from the power plants to the oil fields in the Gulf of Mexico. The number of stages of a gear-type centrifugal compressor is selected based on the advice from the Liebenthal and Kather, (2011). They suggest that to compress CO_2 from 2 bar to 100 bar, which correspond to a pressure ratio of 55, 6 stages are needed. For higher pressure ratio than 55, more stages might need. In this thesis, the CO_2 is compressed from around 2 bar to 150 bar for the purpose of EOR (DOE/NETL, 2012). The pressure ratio is around 80, therefore one more stage is needed.

Based on the state-of-art, the configuration of the compressor selected in this thesis is two trains of a gear-type centrifugal compressor with 7 stages and intercooling after each stage as shown in Figure 3.20. The compression plant is divided into two identical parallel trains in order to avoid recycling CO_2 as much as possible. It is designed for a nominal pressure ratio 80 and a CO_2 temperature of 40 °C after the intercoolers. The compressor is simulated in Aspen plus® and the performance map stage by stage is calculated using equations 3.2 and 3.3 and the performance map presented in Figure 3.15. The result is given in Appendix D.

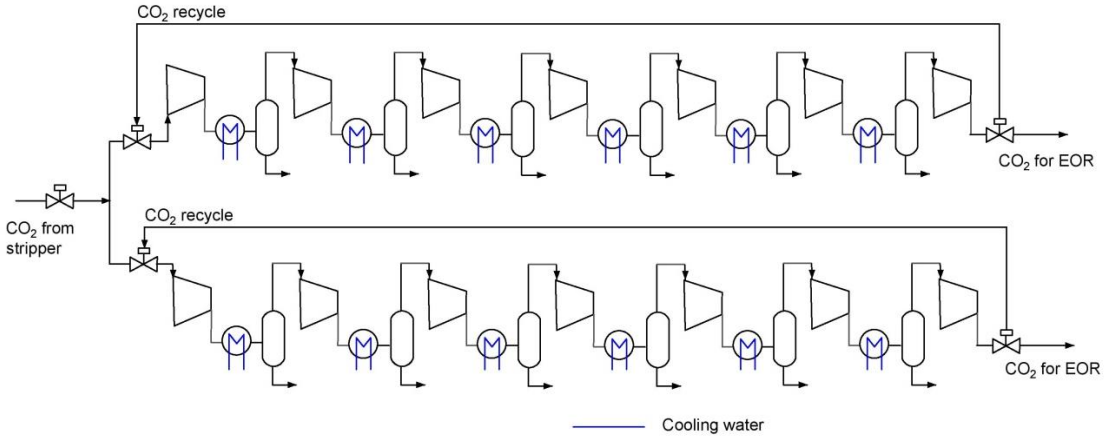

Figure 3.20. Schematic of CO_2 compressor trains with inlet guide vanes in the first stage and intercooling after each stage simulated in Aspen plus@

Table 3.4 presents a summary of the operation mode for CO_2 capture plant and compressor unit used in this thesis, as well as the design conditions for both units and the final configuration of the compressor system.

Table 3.4. Optimun operating strategy for capture plant and CO_2 compressor

Design configuration	**CO_2 compressor configuration**
Pressure 1.87 bar, temperature 120°C	A gear-type centrifugal compressor with 7 stages with intercoolings to cool the CO_2 at 40°C after each stage
CO_2 capture plant at part-load	**CO_2 compressor at part-load**
L/G variable and pressure constant	IGV, constant pressure ratio, and constant temperature at inlet of each compressor stage

Simulation results at base load and at part-load are compared with Rezazadeh et al (2015) shown in Table 3.5. With the difference in the steam pressure, Rezazadeh et al (2015) considered constant steam pressure 2.5 bar at part-load, in this study 3 bar at full load is considered, and it varies at part-load because of the pressure drop in the crossover pressure. Shadow rows show the simulation results from Aspen plus@.

Table 3.5. Comparison of simulation results from Aspen Plus of the capture plant at part-load and Rezazadeh et al, (2015)

			load %					
Reference	**Concept**	**Unit**	**100**	**90**	**80**	**70**	**60**	**50**
Rezazadeh, et al, 2015	lean loading		0.21	0.21	0.21	0.21	0.21	
This work	lean loading		0.269		0.275	0.273		0.272
Rezazadeh, et al, 2015	Temperature reboiler	°C	117.2	117.2	117.2	117.2	117.2	
This work	Temperature reboiler	°C	120		120	119.5		118
Rezazadeh, et al, 2015	steam pressure	bar	2.5	2.5	2.5	2.5	2.5	
This work	steam pressure	bar	3		3	2.9		2.51
Rezazadeh, et al, 2015	L/G	mass	1	0.985	0.98	0.972	0.963	
This work	L/G	mol	1.470		1.530	1.500		1.6
Rezazadeh, et al, 2015	Rich loading		0.4761	0.4764	0.4766	0.477	0.4773	
This work	Rich loading		0.4721		0.4725	0.4725		0.4721
Rezazadeh, et al, 2015	Reboiler duty	MW/tCO_2	3.64	3.65	3.66	3.70	3.70	
This work	Reboiler duty	MW/tCO_2	3.56		3.58	3.60		3.65

3.7 Conclusion

A post-combustion capture plant is the most commercially flexible alternative to be applied in a new power plant or in an existing one. The incorporation of the CO_2 capture plant in a NGCC has three main challenges compared with a coal power plant: the high concentration of O_2, the low concentration of CO_2 and the high amount of exhaust gas. Different alternatives have been proposed in order to solve these three main challenges i.e. EGR, selective EGR, humidification, and supplementary firing.

At higher CO_2 concentrations the partial pressure increases, which means a higher driving force for absorption that helps to reduce the energy to regenerate the solvent.

There is a maximum volume flow rate (300,000 m^3/h) which can be treated in an absorber column due to economic limits on the size of the absorber. For systems that require the processing of a larger flow, a modular design with several trains operating in parallel is adopted.

The best operating strategy to operate the CO_2 capture plant at part-load is at variable L/G and constant pressure in the reboiler. Temperature of the reboiler at part-load reduces as a consequence of the pressure drop of the steam extraction in the crossover to regenerate the solvent. As a result, the lean loading increases.

The configuration selected to compress the CO_2 is a gear-type centrifugal compressor with 7 stages and intercooling after each stage and control by adjusted IGV of the CO_2 compressor at part-load, which is the optimum based on the efficiency.

4. Sequential supplementary firing in natural gas combined cycle with carbon capture and CO_2 enhanced oil recovery

4.1 Introduction

Electricity production in Mexico is expected to grow from 62 GW in 2009 to 113.7 GW in 2028, with natural gas being the dominant energy source in 2027 (Federal commission of electricity, 2014), as described in Chapter 2, section 2.2.1. In this context of rapid electrification dominated by natural gas power plants, Mexico intends in parallel to reduce "its greenhouse gas (GHG) emissions by 50% below 2000 levels by 2050" (CTF/TFC, 2009). One of the strategies proposed to reach this objective is the application of Carbon Capture and Storage (CCS) on fossil fuel power plants for the purpose of EOR in the oil industry, which relies on the availability of large amounts of CO_2 (Mexican Ministry of Energy, 2012) between 2020 and 2050.

The triple challenge of rapid electrification through natural gas, reducing CO_2 emissions in power generation and rolling out Enhanced Oil Recovery at national level requires an important R&D effort to develop nationally relevant CCS technology options. The outcome could then be implemented in the current technology roadmap for the design of new build CCS-EOR ready NGCC power plants, to facilitate incorporating CO_2 capture technologies and EOR into the future energy mix.

This chapter presents the results from a techno-economic study of power plant configurations dedicated to address this triple challenge. It involves the sequential supplementary firing of natural gas in the heat recovery steam generator of a natural gas combined cycle power plant, followed by the removal of carbon dioxide in a post-combustion scrubbing amine-based capture unit to supply CO_2 for EOR. This capture technology has, at the time of writing, been deployed at commercial scale at the Boundary Dam power plant in Canada (Herzog et al, 2009). It is particularly relevant in the context of a technology roadmap for CCS released by the Mexican Ministry of Energy, recommending actions at national level until 2024 with a particular focus on developing solvent absorption technologies linked to natural gas combined cycle plants (Mexican Ministry of Energy, 2014).

In the first section, the methodology for the optimisation of subcritical SSFCC and capture plant is described. After that the economic study for subcritical SSFCC is developed. Results are compared with a conventional NGCC. Finally, tech-economic results for supercritical SSFCC are compared with subcritical SSFCC.

4.2 Supplementary firing with carbon capture

4.2.1 Introduction to the concept

Non- sequential, single stage, supplementary firing is typically used in Natural Gas Combined Cycle (NGCC) power plants to increase power output by around 30% during times of peak demand of electricity and high electricity selling prices (Kiameh, 2003). Li et al (2012) proposed to implement supplementary firing in gas-fired power plants with carbon capture. They reported a concentration of O_2 of 5.6% v/v in the exhaust gas, compared to 12.4% v/v without supplementary firing. The temperature difference at the high pressure superheater header of the heat recovery steam generator (HRSG) increases from 50ºC to 800ºC leading to a gas temperature of 1280ºC and large heat transfer irreversibilities, compared to a gas temperature around 530ºC. In both cases, high pressure steam temperature is 480ºC. Single stage supplementary firing requires advanced alloys to cope with the maximum temperature achievable, which then restricts the amount of supplementary fuel that can be used. Modifications to the HRSG design to withstand higher temperatures are, however, compensated by higher CO_2 concentrations at the capture unit inlet.

Sequential combustion effectively makes use of the excess oxygen necessary for gas turbine combustion to generate additional CO_2 and allows to keep temperature around 800-900°C, an achievable range within a heat recovery steam generator with supplementary firing (Kehlhofer et al., 2009). The last stage of supplementary firing brings oxygen close to stoichiometric limits (1% v/v). This corresponds to an excess air around 5 % v/v.

Gas and oil fired boilers used in utility and industrial steam generation applications typically operate with an excess air in the range of 5-10% v/v, resulting in oxygen levels in the combustion gas of the order of 1-2% v/v (Steam its generation and use, 2005). In the context of sequential combustion in HRSG at low excess oxygen, this suggests complete combustion with oxygen levels as low as 1% v/v may be practically achievable with good air/fuel mixing with appropriate burner design.

The resulting flue gas of sequential combustion is then more comparable to the flue gas of a coal plant, which facilitates the incorporation of post-combustion CO_2 capture by addressing

three specific challenges associated with natural gas flue gas described in chapter 3, section 3.1:

1. CO_2 concentrations in the exhaust gas are typically 10-15% v/v in a coal power plant and 3-4% v/v in a gas turbine. They increase to 9.4% v/v with the configuration with five stages of sequential supplementary firing which is described in the next section of this chapter.
2. With five stages of supplementary firing, the overall flue gas flow rate entering the capture plant is around 50% of the flow rate of a standard NGCC plant with post-combustion capture with the same power output.
3. With five stages of sequential supplementary firing, the O_2 concentration is around 1.3% v/v at the inlet of the absorber

Burning supplementary fuel in consecutive stages increases the heat available in the HRSG and leads to a larger combined cycle power output and a reduction of the number of the GT trains, at constant power output. This also has a positive impact on the number of absorbers and the capital costs of the post combustion capture plant by reducing the total volume of flue gas by half on a normalised basis with respect to a conventional NGCC with CO_2 capture. It decreases marginally the energy requirements for solvent regeneration and marginally reduces amine degradation.

In practice, the overall thermal efficiency of a SSFCC plant is lower than that of a standard NGCC. One useful metric is the marginal thermal efficiency of the additional natural gas combustion, as given in Equation 4.1. This is defined as the ratio of the increment in power output to the added fuel input in the HRSG:

$$\eta_{marg} = \left[\frac{W_{SF} - W_0}{M_{SF} LHV}\right] \qquad \text{Equation 4.1}$$

Where

η_{marg}	Marginal efficiency (%)
W_0	Power output of steam turbine of conventional NGCC plant (MW)
W_{SF}	Power output of the steam turbine of a plant with sequential supplementary firing (MW)
M_{SF}	Mass flow of supplementary fuel in the HRSG (kg/s)
LHV	Fuel low heat value (MJ / kg)

Equation 4.1 can be used to compare power plants without and with capture.

4.2.2 Steam cycle and heat recovery design with sequential supplementary firing

A configuration with two stages of supplementary firing with subcritical steam cycle is presented in Kehlhofer et al. (2009) shown in Figure 4.1. Natural gas fired is burnt at two locations in the primary heat exchange section. Information related to the values of final CO_2 and O_2 concentration in the flue gas is not provided. The flue gas temperature is increased after the gas turbine via a first stage of firing to a maximum temperature around 750 °C and enters a superheater heat exchanger. Natural gas is then fired again in a second stage followed by an evaporator.

The power plant configurations proposed in this thesis are based on existing patents, manufacturer data and are, to an extent, analogous to the concept proposed by Kehlhofer (2009) and to a concept for supplementary firing with supercritical steam conditions, proposed by Wylie (2004) shown in Figure 4.2, with the exception that carbon capture is not included as this alternative is proposed to increase the power output during time of peak demand of electricity. Wylie proposed to fire supplementary fuel in three stages through a single pressure HRSG with a supercritical steam turbine to improve the efficiency of the cycle. Natural gas fired is fired at three points in the primary heat exchange section in order to mitigate high peak temperatures in the HRSG when generating supplementary power. The peak temperature reached is 760 °C, however, the values of final CO_2 and O_2 concentration in the flue gas are not provided.

On the other hand, Ganapathy (1996) suggests that higher maximum temperatures are possible by introducing other modifications in the HRSG. For instance, a temperature of 927 °C is achievable with the use of insulated casings and up to 1316 °C when equipped with water-cooled furnaces. In order to avoid including advanced alloys, boiler design consisting of water-cooled furnaces and excessive capital expenditure, exhaust gas temperatures should be kept at a maximum of 820°C, a typical temperature in a conventional NGCC with supplementary firing (Thermoflow, 2013). Both the subcritical and supercritical configurations proposed here are based on this concept.

Two steam cycle configurations are possible with sequential supplementary firing: Supercritical steam conditions: 630ºC, 295 bar (McCauley, et al, 2012; Salazar-Pereyra, et al, 2011; Satyanarayana, et al, 2011, Cziesla et al, 2009) and subcritical steam conditions: 601.7ºC, 172.5 bar (IEAGHG, 2012). In both cases, the maximum design temperature is a critical parameter for the design of the HRSG.

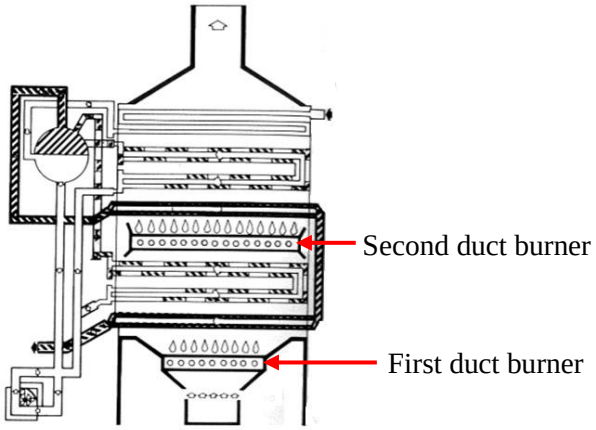

Figure 4.1. Heat recovery steam generator with two stage supplementary firing (Kehlhofer, et al, 2009)

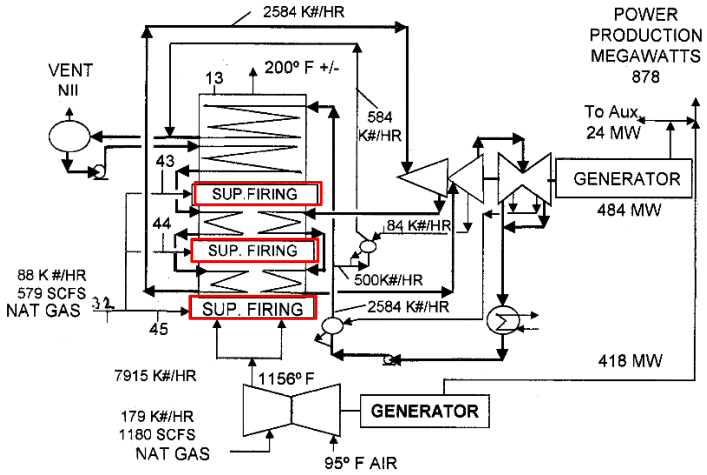

Figure 4.2. Heat recovery steam generator with three stages (Wylie, 2004)

4.3 Sequential supplementary firing with a subcritical combined cycle

Power plants configurations are simulated using Aspen HYSYS®. Aspen HYSYS is process simulation software for the optimization of conceptual design and operations. With this software it is possible to calculate the mass and energy balances of the power plant in steady state at full load. A techno-economic study of a subcritical combined cycle configuration is first compared to a reference plant consisting of a new-build NGCC plant with post-combustion capture in this section. The next section of the chapter examines the benefits of a supercritical combined cycle over a subcritical configuration. Both configurations examined here are equipped with a conventional HRSG, where the maximum temperature achievable is 820ºC. A model of the power cycle integrated with the capture plant is used to optimise performance and provide the basis for the techno-economic study.

4.3.1 Modelling and optimisation of subcritical SSFCC cycle alternative

In a real process there are energetic and exergetic losses. Energetic losses occur by radiation and convection. Exergetic losses are related to internal losses caused by irreversible processes according to the second law of thermodynamics (Kehlhofer, et al, 2009). The optimization of the SSFCC in this study is focused on reducing exergetic losses in order to improve the power plant efficiency. The parameters involved in the optimisation of the overall thermal efficiency and the marginal thermal efficiency of the additional natural gas combustion in the HRSG are:

1. The number of additional firing stages
2. The amount of fuel burnt
3. The pinch point temperature
4. Number of pressure levels in the HRSG (single, double, and triple pressure)
5. The steam condition: subcritical and supercritical
6. The stack temperature

The number of additional firing stages and the amount of fuel. Setting the maximum HRSG temperature achievable allows for a given number of stages of supplementary firing with a minimum level of excess O_2 content in the flue gas for complete combustion. After the final firing stage, the oxygen content in the flue gas is 1%v/v (Steam its generation and use, 2005, pp 11.4), which is sufficient to achieve complete combustion.

The pinch point temperature. Important parameter in the optimisation of the steam cycle is the pinch point, which affects the amount of the steam generated and the efficiency of the steam cycle. This parameter is more important in system with single pressure. When there is more than one pressure level, if the pinch point of the HP steam is not the optimum, the heat that is not utilised is recovered in the low pressure evaporator (Kehlhofer, et al, 2009).

The number of pressure levels. Different pressure levels can be generated in a HRSG: triple, double and single pressure (Jonshagen et al, 2011).

1. HRSG with triple pressure consists of three evaporators: LP, IP, and HP evaporators, designed for parallel flow operation; LP, IP, and HP economisers; LP, IP, and HP superheaters, as shown in Figure 4.3
2. HRSG with double pressure consists of two evaporators: LP and HP evaporators, designed for parallel flow operation; LP and HP economisers; LP and HP superheaters
3. HRSG with single pressure consists of one HP evaporator; HP economiser; and HP superheater

The main reason for multiple-pressure levels in a conventional NGCC is to reach the maximum efficiency. A single pressure has a stack temperature around 100-110°C while with a triple pressure the stack temperature is reduced in the range of 70-80°C, both at the same pinch point (Sipocz et al, 2011). However, when supplementary fuel is burnt in a single pressure boiler the temperature raises, more heat is recovered and more steam is generated reducing the stack temperature. Stack constrained heat recovery is most likely to be encountered in boilers designed with supplementary firing. Pinch point constrained heat recovery is more common in conventional NGCC without supplementary fuel. As a result, there is no difference in the efficiency between the single and double pressure.

Minimum stack temperature. The exhaust gas leaving the boiler needs to be hot enough so it can rise higher into the atmosphere and mixes with the air, to avoid causing high levels of pollutant concentrations in the vicinity of the plant. Pollutant dispersion is not a problem in NGCC as it burns natural gas which is sulphur-free and has low NO_x. Beside the pollutant dispersion issue, the condensation of water vapour in the flue gas produces as unsightly plume that may be disliked by the populace. Hotter flue gas discharge reduces the extent of the condensation plume. The temperature could be in the range of 80-95 °C (Elmasri, 2002). In this thesis the stack temperature is fixed at 8 °C in all case studies.

The optimisation in Aspen HYSYS consists of maximising marginal efficiency and reducing heat transfer irreversibilities as much as possible by analysing different pressure levels of steam produced in the HRSG (triple, double or single pressure). The integration between the combined cycle and the capture plant consists of solvent regeneration steam being extracted from the crossover pipe between the intermediate pressure (IP) and the low pressure (LP) turbines of the steam cycle at a pressure 3 bar in order to allow optimum solvent regeneration of a 30%wt MEA solvent. Table 4.1 lists the ambient conditions at standard conditions, and information for the compressor and turbine from the gas turbine. Table 4.2 lists the parameters of the steam turbines used in the modelling of the power plants for all case studies.

The information of the temperature and pressure, temperatures, and the efficiencies of steam turbines for a NGCC and subcritical SSFCC are taken from IEAGHG, (2012) and (Franco et al, 2011); and for supercritical steam turbine is based from several authors (Cziesla et al, 2009; McCauley, et al, 2012; Salazar-Pereyra, et al, 2011; Satyanarayana, et al, 2011). Information given in theses publication is based on industrial and existing steam turbines. The steam turbine operating conditions are not part of the optimisation of SSFCC as the main modifications occur in the HRSG of the NGCC power plant with this alternative.

Table 4.1. Ambient conditions and modelling basis for all case studies

Concept	Unit	Value
Ambient temperature	°C	15
Ambient pressure	bar	1.013
Relative humidify	%	60
Cooling water temperature	°C	25
Cooling water maximum temperature rise	°C	10
Fuel calorific value (LHV)	kJ/kg	46510
Pressure ratio compressor		19.5
Pressure in condenser	bar	4.38
Adiabatic / polytrophic efficiency compressor	%	82/87.4
Adiabatic / polytrophic efficiency gas turbine	%	88/83.2

Table 4.2. Input data for all case studies for steam turbines

Concept	Unit	NGCC	SSFCC Supercritical	SSFCC subcritical
Inlet pressure SC steam turbine	bar	NA	295.0	NA
Inlet temperature SC steam turbine	°C	NA	630.0	NA
Inlet pressure HP steam turbine	bar	172.5	80.0	172.5
Inlet temperature HP steam turbine	°C	601.7	601.0	601.0
Inlet pressure IP steam turbine	bar	41.4	42.6	42.6
Inlet temperature IP steam turbine	°C	601.5	601.0	601.0
Inlet pressure LP steam turbine	bar	3.0	3.0	3.0
Inlet temperature LP steam turbine	°C	292.4	229.5	229.5
Isentropic efficiency SC steam turbine[1]	%	NA	92.0	NA
Isentropic efficiency HP steam turbine	%	86.0	86.0	86.0
Isentropic efficiency IP steam turbine	%	90.0	90.0	90.0
Isentropic efficiency LP steam turbine	%	87.6	87.6	87.6

4.3.2 Modelling and optimisation of the CO_2 capture plant and compressor unit

All case studies have been integrated with a standard CO_2 capture plant shown in Figure 3.16 using 30% wt MEA, and with a compressor system shown in Figure 3.20. The CO_2 capture plant is simulated in Aspen plus® using a rate-based approach. Basic information for the capture plant for all cases is given in Table 3.3, section 3.6, chapter 3.

The performance of the absorber is estimated to find the optimum parameters such as lean loading, rich loading, absorber and stripper packing height, heat transfer area, and energy removed from the condenser, and the electricity output penalty (*EOP*) to achieve 90% CO_2 capture rate based on the methodology described in chapter 3, section 3.5.1.

The EOP can be calculated using Equation 4.2.

$$EOP = \frac{MW_{without/capture} - MW_{with/capture}}{CO_2 captured} \quad \text{Equation 4.2}$$

Where

EOP	Electricity Output Penalty (kWh / tonne CO_2)
$MW_{without/capture}$	Net power output without capture (kW)
$MW_{with/capture}$	Net power output with CO_2 capture and compressor unit (kW)
$CO_2 captured$	Amount of CO_2 capture (tonne / h)

The lean solvent loading of the MEA is varied to find the minimum *EOP* for a given CO_2 concentration in the flue gases. While studying the effect of different lean loading on the capture process, the stripper reboiler pressure is varied to change the values of the lean loading and the temperature is kept constant at 120 °C (Kohl and Nielsen, 1997; IEAGHG, 2010; Rochelle, 2009).

For each lean loading specified, the height of the absorber is then varied. At a given absorber height, the absorption solvent circulation rate is varied to achieve the same CO_2 removal capacity (90%). The flue gas inlet absorber at 44 °C and 1.13 bar; 40 °C the temperature in the stripper condenser, and lean/rich stream heat exchanger approach temperature 10°C (Sanchez Fernandez E., et al, 2013), and 30% MEA are kept constant.

4.3.3 Conventional natural gas combined cycle configuration

The conventional case is a NGCC plant integrated with MEA-based CO_2 capture. The configuration and operating parameters for the conventional case has been taken from Parsons Brinckerhoff (IEAGHG, 2012). The configuration of the NGCC consists of two gas turbines and three steam turbines. Each train comprises of one GE 937 IFB gas turbine with flue gas exiting into a HRSG. The total steam generated in both HRSG's supply steam to a subcritical triple pressure steam cycle comprising of three steam turbines, as shown in Figure 4.3.

The pinch diagram for the hot gas turbine exhaust and the steam cycle water/steam flow rates for the conventional case is shown in Figure 4.4. The pinch temperature in the evaporator is 10°C for the standard reference plant (Kehlhofer, et al, 2009).

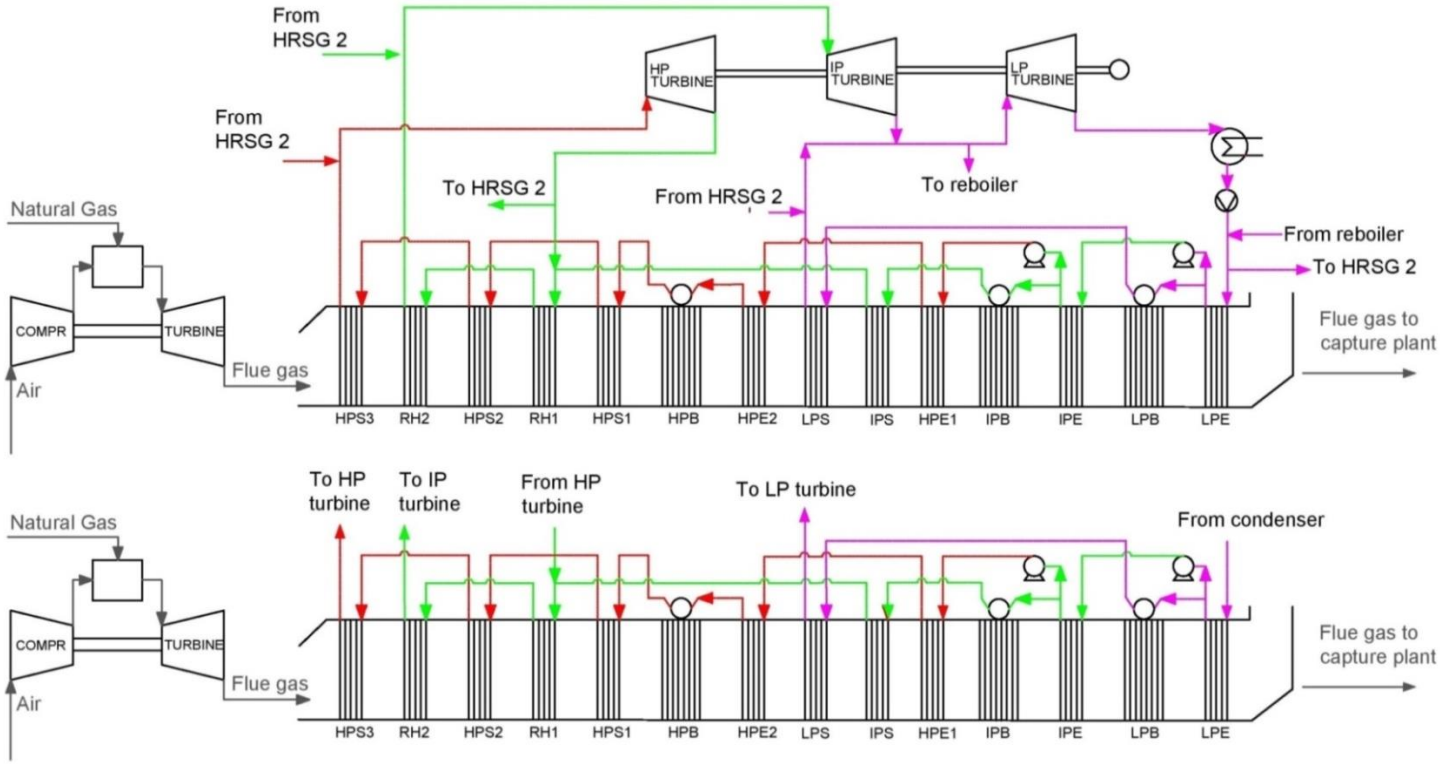

Figure 4.3. Schematic process flow diagram of the conventional natural gas combined cycle configuration with two GE 937 IFB gas turbines, two triple pressure HRSGs and one subcritical steam turbine simulated in Aspen Hysys[@]

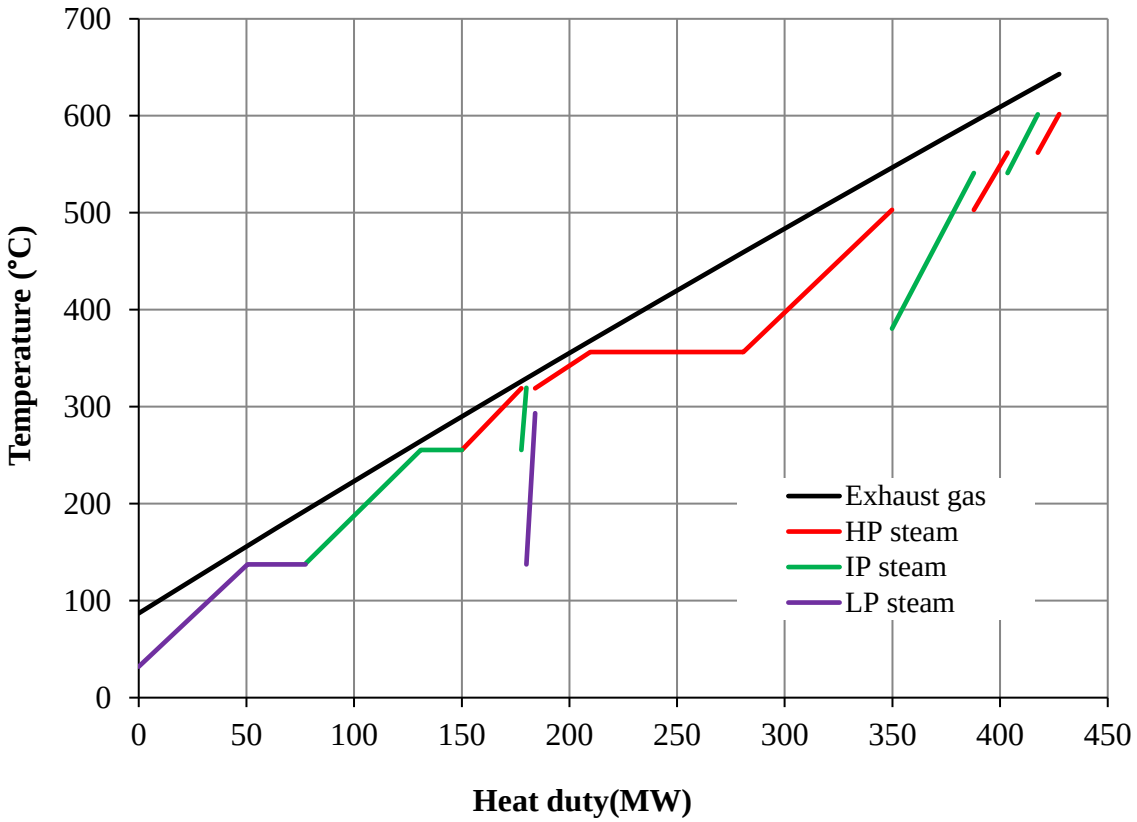

Figure 4.4. Temperature/heat diagram for the Heat Recovery Steam Generator of the Natural Gas Combined Cycle plant (Figure 4.3) with subcritical steam conditions (601.7°C, 601.5°C, 172.5 bar)

4.3.4 Subcritical SSFCC power plant case

This section starts with the analysis of the implication on the new design of the HRSG such as the pinch diagrams for triple, double, and single pressure configuration.

Figure 4.5 shows the pinch diagram for a configuration where the total amount of supplementary fuel is burnt using a single duct burner to reach 1% v/v O_2 in the flue gas. The temperature rises up to 1700 °C, with this temperature the boiler has to be equipped with water-cooled which mean an excessive capital expenditure. With sequential supplementary firing, the total amount of natural gas is divided into five stages through the HRSG. As a result, the peak temperature is dropped to around 820°C as shown in Figure 4.6. The total amount of natural gas burned in five stages in the HRSG is 22.3 kg/s. This corresponds to 57% of the total fuel input of the gas turbine and the HRSG referred to Figure 4.9.

Subcritical SSFCC at different pressure levels of steam triple, double, and single pressure produced in the HRSG have been analysed. The efficiencies calculated without capture are 50.1%, 50.28%, and 50.44%, respectively; assuming 80°C as the minimum stack temperature. The pinch points are 83°C for triple pressure shown in Figure 4.6, 82 °C double pressure shown in Figure 4.7, and 70°C for single pressure shown in Figure 4.8. Single pressure represents the optimum alternative for subcritical SSFCC configuration.

Results show that when a SSFCC subcritical boiler is designed to produce steam at given condition from feed-water at specific condition and at given stack temperature as the constraint, triple and double boilers do not have any beneficial. In a single pressure, higher exhaust gas temperature produces higher steam flow, so the resulting increase in water flow through the economisers cools the gas at the stack limit. Then it is not necessary to increase the number of pressure levels in the sequential supplementary firing HRSG to reduce the stack temperature. The temperature profile of the vapour and the number of sections of the HRSG have been optimised to reduce heat transfer irreversibilities by adjusting the heat transfer area available for each heat exchanger. For example, there is a change of slope in the superheater section as well as in the economiser of the single pressure HRSG in order to reduce the difference in temperatures.

The schematic process flow diagram shown in Figure 4.9 is the optimum subcritical SSFCC configuration and consists of a single GE 937 IFB gas turbine followed by a single HRSG unit. The HRSG operates with a single pressure and provides steam to a single reheat steam cycle. Similar materials to that of a conventional HRSG (stainless steel 304) can be used.

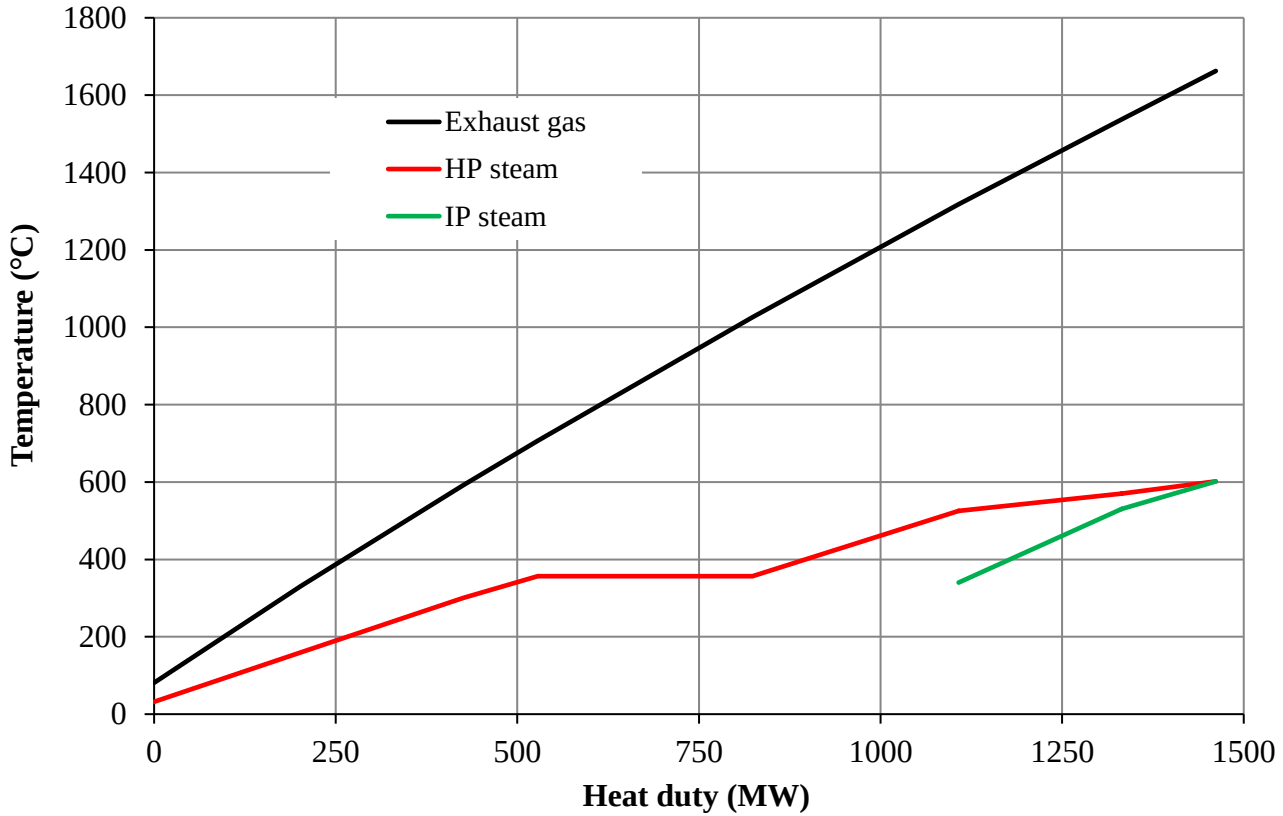

Figure 4.5. Temperature/heat diagram of the Heat Recovery Steam Generator with supplementary firing in a single stage, and with subcritical steam conditions (601.7°C, 601.5°C, 172.5 bar)

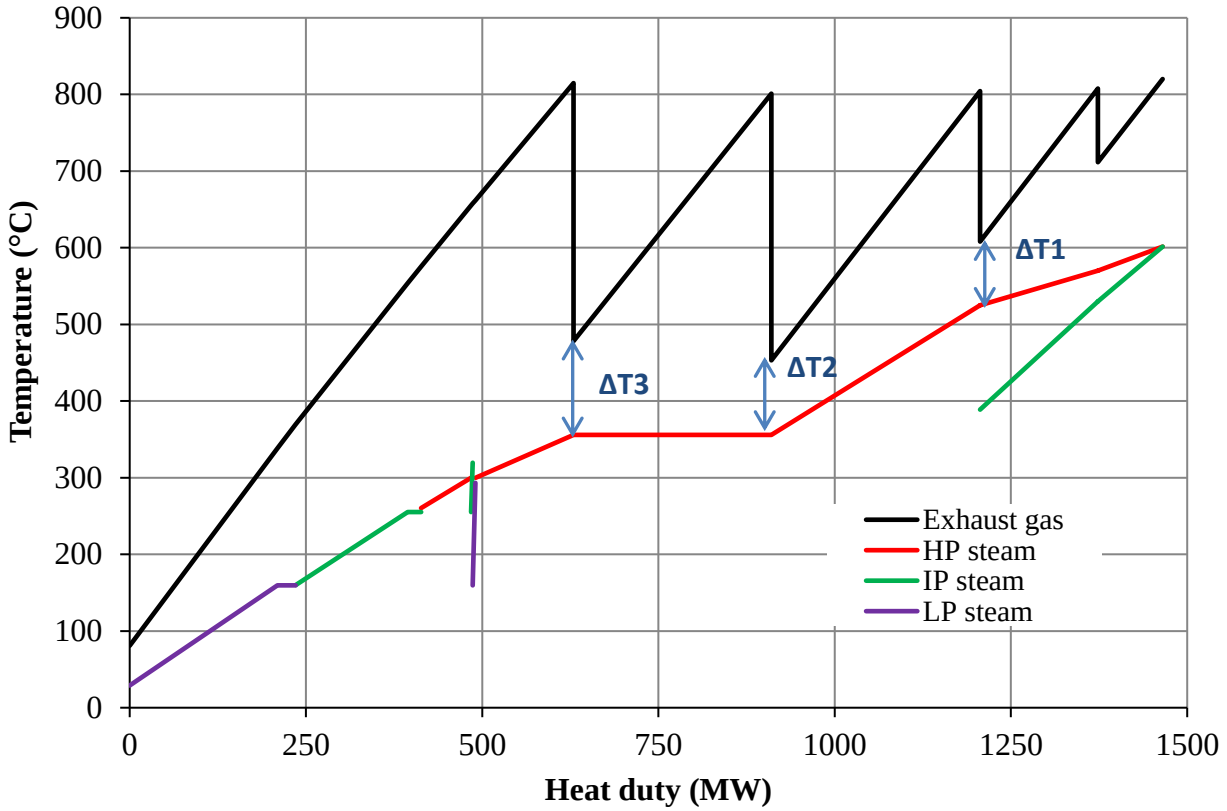

Figure 4.6. Temperature/heat diagram of the Heat Recovery Steam Generator of a five stage sequential supplementary firing configuration with a triple pressure HRSG, with a single reheat combined cycle and subcritical steam conditions (601.7°C, 601.5°C, 172.5 bar). The three pinch temperatures ΔT1, ΔT2, ΔT3 are respectively 83ºC, 97ºC, 122ºC

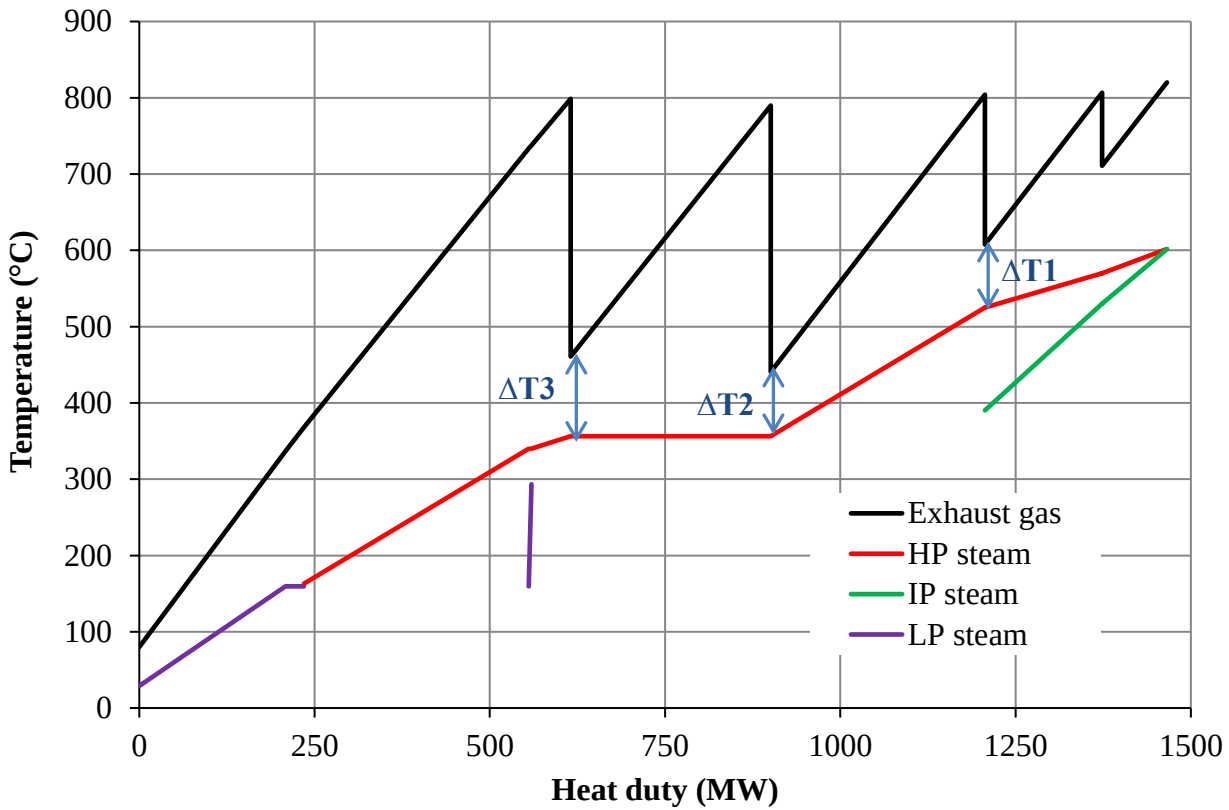

Figure 4.7. Temperature/heat diagram of the Heat Recovery Steam Generator of a five stage sequential supplementary firing configuration with a double pressure HRSG, with a single reheat combined cycle and subcritical steam conditions (601.7°C, 601.5°C, 172.5 bar). The three pinch temperatures ΔT1, ΔT2, ΔT3 are respectively 82ºC, 84ºC, 82ºC

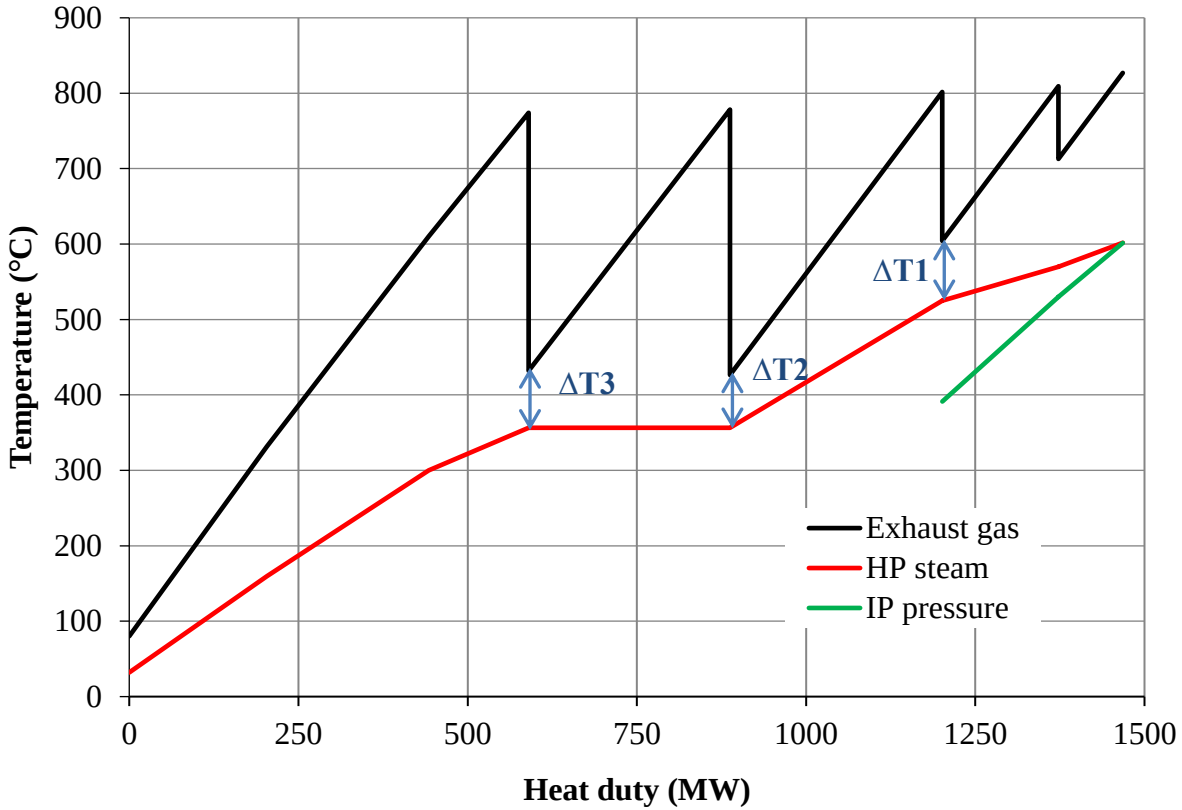

Figure 4.8. Temperature/heat diagram of the Heat Recovery Steam Generator of a five stage sequential supplementary firing configuration with a single pressure HRSG, with a single reheat combined cycle and subcritical steam conditions (601.7°C, 601.5°C, 172.5 bar). The three pinch temperatures ΔT1, ΔT2, ΔT3 are respectively 79ºC, 70ºC, 76ºC

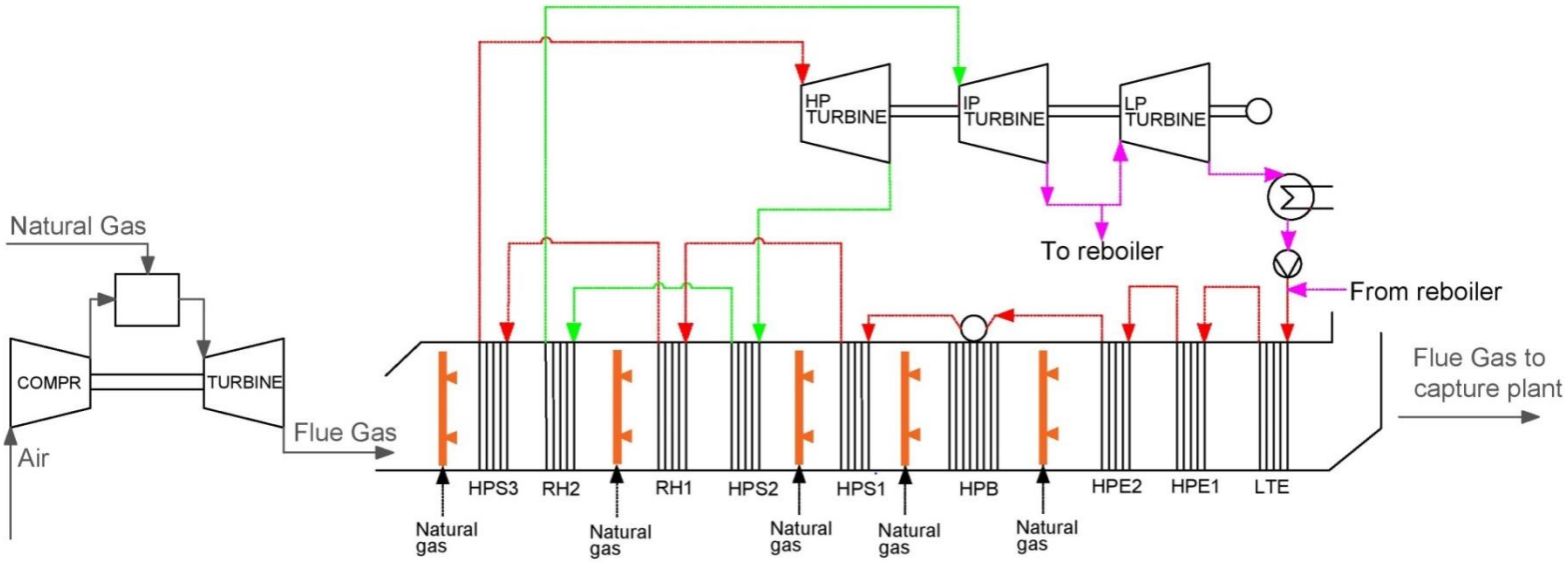

Figure 4.9. Schematic process flow diagram of a subcritical sequential supplementary firing configuration with one GE 937 IFB / single pressure HRSG train combined with a single reheat steam cycle simulated in Aspen Hysys[@]

Table 4.3 shows the inlet and outlet temperature, and the O_2 and CO_2 concentration in each duct burner for the optimum configuration of subcritical SSFCC single pressure. The inlet temperature, velocity, turbulence of the exhaust gas, and the burner configuration can lead to increasing the efficiency of combustion in a situation of low concentration of oxygen (Ditaranto, et al, 2009). The main challenge may lay in the design of the last two duct burners (4^{th} and 5^{th} duct burners) where lower levels of oxygen compared to the first three burners are present. High temperature can compensate for the low levels of oxygen and the combustion can be stabilised with simple burner ramps (Li, et al, 2012). It is also worth reiterating that gas and oil fired boilers used in utility and industrial steam generation applications typically operate with an excess air in the range of 5-10% v/v (Steam its generation and use, 2005), comparable to the 6% v/v of equivalent excess air at the inlet of the last burner. Although the specific design of duct burners to operate within this range is outside the scope of this study, it is worth noting that the presence of higher levels of CO_2 compared to conventional gas and oil boilers requires further investigation of combustion stability and efficiency. If satisfactory combustion proved to be challenging in the final duct burner, this could lead to removing the burner and optimise the configuration to operating with one fewer burner, with possible higher outlet temperature to maximise natural gas usage.

Table 4.3. Temperature, O_2 concentration, CO_2 concentration at the inlet of each duct burner for subcritical sequential supplementary firing power plant

	Temperature	**O_2 concentration**	**CO_2 concentration**	**Equivalent exit excess of Air**
Unit	**°C**	**%**	**%**	**%**
Duct burner 1	643	11.9	4.2	100
Duct burner 2	712	10.2	5.01	69
Duct burner 3	608	8.0	5.45	39
Duct burner 4	453	5.8	6.33	26
Duct burner 5	480	4.0	7.85	6

4.3.5 Impact of the sequential supplementary firing on the power plant with CO_2 capture

Key parameters for the conventional NGCC configuration and subcritical SSFCC without and with CO_2 capture are described in Table 4.4 and Table 4.5, respectively. When supplementary fuel is burnt sequentially in a single HRSG attached to a gas turbine, the capacity of the steam cycle increases. The corresponding total net power with CO_2 capture of the SSFCC is 781 MW, similar to the conventional NGCC configuration with 794 MW. As

in SSFCC only one gas turbine is used, the total volume of the exhaust gases is reduced by half. This has a positive impact on the number of direct contact coolers (DCC) and absorbers of the capture plants. Total net power of NGCC and subcritical SSFCC with and without capture are not equal because design for SSFCC is based on burning additional fuel to get 1 mol% of O_2 concentration in the flue gas.

Although the efficiency of the subcritical SSFCC configuration is of the order of 43.1% LHV, compared to 51.3% LHV for a standard NGCC plant with capture, there are significant capital cost implications for the gas turbine, the heat recovery steam generator, the steam cycle, the absorber trains and the stripper/compression part of the capture plant and the potential for additional revenue from EOR:

1. The SSFCC configuration makes use of a single gas turbine/HRSG train compared to two gas turbine/HRSG trains for a standard configuration
2. The number of absorber trains is reduced from four to two, as previously discussed
3. The capacity of the stripper and the compression train is increased by around 17.7%

The concentration of the CO_2 presented in Table 4.5 after the direct contact cooler is higher than in the HRSG because of the condensation of a fraction of the water contained in the flue gas.

Table 4.4. Results for the conventional natural gas combined cycle and sequential supplementary firing combined cycle with a single pressure HRSG and double reheat subcritical steam conditions (601.7°C, 601.5°C, 172.5 bar) without capture

Concept	**Unit**	**NGCC[1]**	**SSFCC subcritical**
LHV gross electric efficiency	%	60.4	51.4
LHV net electric efficiency	%	58.85	49.8
Gas turbine power output GT	MW	590	295
Steam cycle power output	MW	343	635
Total LHV gross power output	MW	936	930
Total LHV net power output (including ancillaries)	MW	910	902
Mass flow rate of natural gas to gas turbine	kg/s	33.2	16.6
Total mass flow rate of natural gas for supplementary firing	kg/s	NA	22.2

[1]Power generated and fuel mass flow include the total for two trains

Table 4.5. Summary of key parameters of a SSFCC with single pressure subcritical steam cycle with (Saturated vapour at 3 bar is used in the reboiler) with CO_2 capture

Concept	Unit	NGCC	SSFCC subcritical
LHV gross electric efficiency	%	55.17	46.38
LHV net electric efficiency (including CO_2 compression and other ancillaries)	%	51.3	43.1
Gas turbine power output GT	MW	590	295.5
Steam cycle power output	MW	245	544.7
Total LHV gross power output	MW	835	840
Total LHV net power output (including CO_2 compression and other ancillaries)	MW	794	781
Marginal efficiency of natural gas fired in HRSG (LHV)	%	NA	36
Marginal efficiency of natural gas fired in HRSG (LHV) without post-combustion capture (for comparative purposes only)	%	NA	44.7
Electricity output penalty (*EOP*)	$kWh_e/tonne CO_2$	408	362
Carbon intensity of electricity generation	$kgCO_2/MWh$	39.8	47.5
Flue gas mass flow rate	kg/s	1347	696
CO_2 mass flow to pipeline	kg/s	79	93
Capture level	%	90	90
Solvent energy of regeneration	$GJ/tonne CO_2$	3.56	3.42
Steam mass flow to solvent reboiler	kg/s	145	146
Number of absorber trains		4	2
Diameter	m	15.5	15.5
Absorber height	m	21	21
Flue gas mass flow rate at each absorber inlet	kg/s	337	348
Volume of packing used for CO_2 capture (not including water wash sections)	m^3	16260	8130
Flue gas composition in the HRSG			
Water (H_2O)	% vol	8.84	17.57
Carbon dioxide (CO_2)	% vol	4.20	9.36
Oxygen (O_2)	% vol	11.88	1.32
Nitrogen (N_2)	% vol	75.07	71.94
Flue gas composition after direct contact cooler			
Water (H_2O)	% vol	4.29	4.29
Carbon dioxide (CO_2)	% vol	4.37	10.87
Oxygen (O_2)	% vol	12.52	1.31
Nitrogen (N_2)	% vol	78.79	83.52

[1]LHV net electric efficiency includes CO_2 compression and parasitic losses and transformed losses

4.3.6 Effect of increased CO_2 concentration on solvent energy of regeneration and absorber column design

The combustion of additional natural gas in the HRSG increases the CO_2 concentration in the flue gas from 4.2% v/v to 9.36% v/v, whilst reducing the excess oxygen to 1.3% v/v. The optimum lean loading for a NGCC configuration with capture reaches 0.27 mol CO_2/mol MEA and 0.26 mol CO_2/mol MEA for a SSFCC configuration. The higher rich loading achieved with higher CO_2 concentration leads to an increase in solvent capacity and the specific reboiler duty decreases from 3.56 to 3.42 GJ/tonne CO_2 for a configuration with 21 meters of structured packing height in the absorber columns. This is illustrated in Figure 4.10 where the optimisation of the overall electricity output penalty with solvent lean loading is reported.

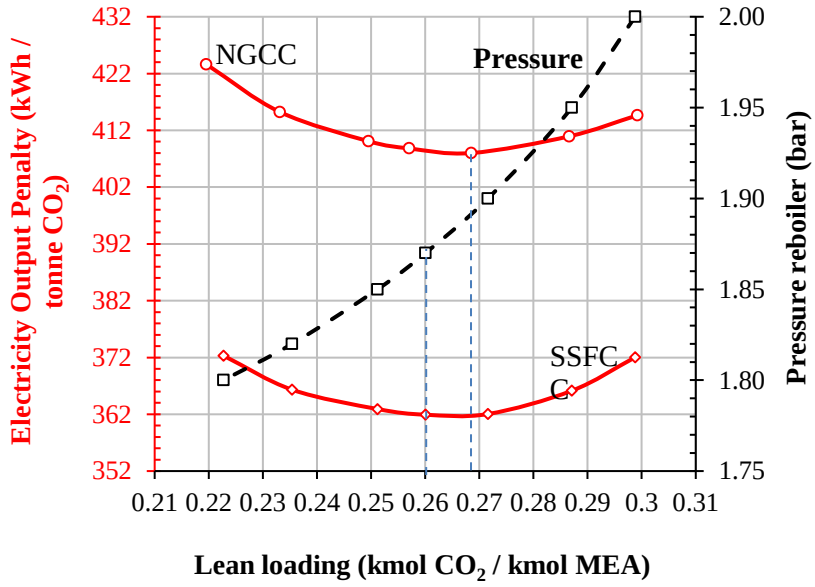

Figure 4.10. Optimisation of electricity output penalty for a natural gas combined cycle and for sequential supplementary firing combined cycle as a function of solvent lean loading, with a CO_2 removal rate of 90% and stripper temperature of 120ºC. The CO_2 concentration in the flue gas is, respectively, 4.2 mol% and 9.4% for a NGCC and a SSFCC configuration. The blue dotted lines indicate the optimum solvent lean loading

In subcritical SSFCC, the total flue gas flow rate is 696 kg/s containing 93 kg/s of CO_2 compared with a conventional NGCC where total flue gas flow rate is 1347 kg/s which contain 79 kg/s that can be seen in Table 4.5. Then based on the argument described previously in chapter 3 section 3.5.1 related to the maximum capacity of the absorber, the flue gas flow rate of one train of SSFCC is 348 kg/s which contain 46.5 kg/s of CO_2 and the flue gas flow rate of one train of the NGCC is 336.8 kg/s which contain 19.75 kg/s. The final

configuration of SSFCC is: two DCC and two absorbers; and two stripper columns and two rich/lean heat exchangers. For NGCC: four DCC and four absorbers; and two stripper columns and two rich/lean heat exchangers. The reduction by approximately 50% of the overall gas flow rates has a positive impact on the capital costs of the DCC and absorber columns which are reduced from four to two columns. The height of the absorber for SSFCC and the NGCC are optimised, based on the reduction of the reboiler duty, for the CO_2 content in flue gas and 90% capture and both cases arrive at the same height of 21 m of packing in each absorber column as shown in Figure 4.11.

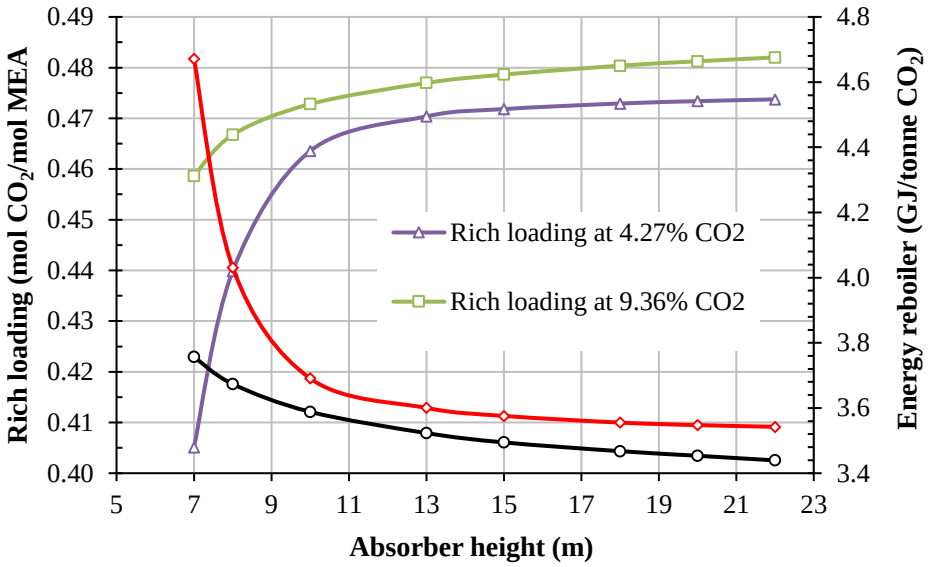

Figure 4.11. Effect of CO_2 concentration in the flue gas on solvent energy of regeneration for a range of absorber column heights. The capture rate is 90%. The lean loading and pressure in the reboiler for NGCC is 4.21% and 1.9 bar respectively and for SSFCC 9.36% and 1.87 bar

4.3.7 Comparison of cost of electricity

The main objective of this economic study is to compare the expected cost of electricity, taking into account revenues from EOR, of a SSFCC configuration with a conventional NGCC. There are important differences between both configurations, such as thermal efficiency, size of critical pieces of equipment, operational costs. In this study, the direct comparison of the expected costs of sequential supplementary firing with a conventional configuration, using consistent sources of information ensures that error and inaccuracies in capital costs are mitigated. A sensitivity analysis is also provided to examine the robustness of the findings over a range of capital cost estimates to account for the associated estimate uncertainties.

4.3.7.1 Capital cost

Cost estimation for all configurations is based on a methodology proposed in Rubin et al (2013). The sources of information are given in Table 4.6

Table 4.6. References of capital cost for power and CO_2 capture, CO_2 compressor plants

Equipment	Reference
Gas turbine, generator and auxiliaries 9F 5-series model	Gas turbine handbook (2013)
HRSG, steam turbine, and balance of plant BOP	Franco et al (2011)
In duct firing	Thermoflow (2013)
Supercritical steam turbine	DOE/NETL (2013)
Capture plant	IEAGHG (2012)
CO_2 compressor	Hendriks et al (2003)
CO_2 transport	DOE/NETL (2013)

The Chemical Engineering Plant Cost Index 2013 is used to update the cost of equipment to 2013 and a currency exchange of 0.8 EUR/USD in 2014 is used. The Chemical Engineering Plant Cost Index is dimensionless numbers used to adjust process plant construction costs from one period to another. The updated cost at 2013 is calculated using the equation 4.3.

$$Cost\ (cost\ at\ 2013) = Cost\ (past\ date)\left[\frac{Index\ at\ 2013}{Index\ (past\ date)}\right] \qquad \text{Equation 4.3}$$

Where

$Cost\ (past\ date)$ For the HRSG, the final cost is calculated using the equation reported by Franco et al (2011); for the capture plant by IEAGHG (2012); and for the compressor by Hendriks et al (2003)

$Index\ (past\ date)$ For the HRSG at 2011 is 525.4; capture plant at 2012 is 581.7; and compressor at 2003 is 402

$Index\ at\ 2013$ The dimensionless number is 567 for all cases

The estimation of the capital costs is calculated as follow:

1. The gas turbine handbook 2013 reported the cost of the 9F 5-series gas turbine of 298 MW, which is the same gas turbine size used in this thesis of 295.5 MW.
2. As the main modification occurs on the HRSG, it is necessary to describe it in more detail. The cost of the HRSG for all cases is calculated using Equation 4.4 proposed by Franco et al (2011):

$$C = C_0\left[\frac{UA}{U_0A_0}\right]^f \qquad \text{Equation 4.4}$$

Where

C_0 Reference erected cost component 32.6 (M€)

UA Scaling parameter (MW/K), U heat transfer coefficient and A is the heat transfer area. The information to calculate UA is taken from the simulation $UA = Q/\Delta T_{lm}$, where Q is the heat transfer (MW/s) and ΔT_{lm} is logarithmic temperature difference (°C)

U_0A_0 Reference size component (12.9 MW/K)

f Scale factor (-)

Details for the HRSG of a NGCC, subcritical and supercritical SSFCC are provided in Appendix A. Equation 4.5 is used to estimate the capital cost of the steam turbine (Franco et al, 2011) which can be applied for any size of steam turbine.

$$C = C_0 \left[\frac{ST_{gross\ power}}{ST_{gross\ power0}}\right]^f \quad \text{Equation 4.5}$$

Where

C_0 Reference erected cost component 33.7 (M€)

$ST_{gross\ power}$ Scaling parameters, gross power steam turbine (MW)

$ST_{gross\ power0}$ Reference component size, gross power steam turbine (291 MW)

f Scale factor (-)

3. Duct burners cost to deal with the same flue gas capacity required in this thesis were estimated from PEACE/GT-PRO (Thermoflow, 2013)
4. Capital costs of the MEA-based CO_2 capture for NGCC are not calculated and are based on the estimation given by IEAGHG (IEAGHG, 2012), the information of the based case of this thesis is based on this report. In that report, the cost is given for different sections of the plant, which makes it possible to determine the cost of capture plant for a SSFCC configuration. The cost is converted from EUR to American dollar. The total volume of packing of the absorber and the stripper and the area of heat exchangers are used to analyse the implications on the required capital expenditure (CAPEX).
5. Investment costs of the compressor are estimated using equation 4.6 that can be applied for any size

$$I = \left[C_1F^{C2} + C_3LN\left[\frac{P_{outlet}}{P_{inlet}}\right]F^{C4}\right]F \quad \text{Equation 4.6}$$

Where

I	Total investment cost (M€)
F	Flow of CO_2 (kg/s)
C_1	Constant = 0.1 x 10^6 (€/(kg/s))
C_2	Constant = -0.71
C_1	Constant = 1.1 x 10^6 (€/(kg/s))
C_1	Constant = -0.60
P_{outlet}	*Outlet pressure CO_2 (Pa)*
P_{inlet}	*Inlet pressure (Pa)*

The sum of all equipment costs, together with the balance of plant (BOP), cooling water system, and installation costs is, as it is described by Rubin et al (2013), the bare erected cost (BEC). Following the methodology, the BEC including indirect costs, engineering procurement and construction (EPC) costs, contingencies, and owner's costs gives the total capital requirement (TCR) for the power plant as well as for capture plant and compression system.

The specific investments of the conventional NGCC and subcritical SSFCC cases have been evaluated and are reported in Table 4.7. The net specific investment estimated for the NGCC case is 773 $/kW, which increases to 1698 $/kW when the CO_2 capture unit is incorporated. Table 4.7 shows a reduction in total specific investment for the subcritical SSFCC with CO_2 capture configuration of 15.32%, from 1698 $/kW to 1438 $/kW. This is due to a reduction in the cost of the absorption part of the capture unit and also a reduction in the cost of the HRSG caused by a reduction in the total volume of exhaust gas. The reduction of the volumetric flow leads a reduction in cross sectional area of the HRSG. Also, the complexity and the number of heat exchangers are smaller as the HRSG is a single pressure system instead of a triple pressure system. The contribution of the gas turbine to the overall power output is much lower than in the NGCC. Effectively, the number of gas turbine trains is reduced from 2 to 1. The additional investments in the steam cycle are compensated by the removal of a gas turbine train, leading to 11% lower power plant specific investment than NGCC with capture. The investment in the steam part of the power cycle (steam turbines, cooling system and BOP) increases to generate more power from the heat recovered in SSFCC.

In all the cases, as the power plants are designed to operate with CO_2 capture, the LP steam turbine size is smaller than if it would operate without capture. The results of the NGCC power plant are in good agreement with other published sources (Gas Turbine Handbook,

2013; IEAGHG, 2012; Franco et al, 2011), and with the predictions of the commercial software PEACE/GT-PRO (Thermoflow, 2013) as shown in Table 4.8.

Table 4.7. Estimated specific investment for the natural gas combined cycle with and without capture and subcritical sequential supplementary firing combined cycle with capture

Plant component	Unit	NGCC	NGCC w/capture	Subcritical SSFCC w/capture
Gross power output	MW	928	835	839.7
Net power output	MW	909	794	781
Power plant main items				
Gas turbine, generator and auxiliaries	M$	137	137	68
HRSG, ducting and stack	M$	65	65	33
Duct burner	M$	0	0	2
Steam turbine generator and auxiliaries	M$	66	55	88
Cooling system and miscellaneous, Balance of Plant (BOP) system	M$	69	36	68
Subtotal	M$	**336**	**293**	**260**
Total Installation cost[a]	M$	163	142	126
Bare Erected Cost (BEC)	**M$**	**499**	**434**	**386**
Indirect cost[b]	M$	70	61	54
Engineering Procurement and Construction (EPC)	M$	569	495	440
Contingencies, owner's costs[c]	M$	134	116	103
Total Capital Requirement (TCR) power plant	**M$**	**703**	**611**	**544**
Capture plant main items				
Flue gas cooling	M$	NA	21	11
CO_2 absorber & flue gas re-heater	M$	NA	110	55
Rich/ lean amine circulation	M$	NA	6	6
Stripping section	M$	NA	139	139
Ancillaries	M$	NA	5	5
Suporting facilities & labor (direct and indict)[d]	M$	NA	61	47
Subtotal	M$	NA	342	262
Installation cost[e]	M$	NA	128	98
BEC	M$	NA	470	361
EPC, Contingencies and owner's costs[f]	M$	NA	216	166
Total Capital Requirement (TCR) capture plant	**M$**	**NA**	**687**	**527**
Total Capital Requirement (TCR) CO_2 compression[g]	**M$**	**NA**	**49**	**53**
Specific investment – Gross	**$/kW**	**757**	**1614**	**1337**
Specific investment – Net	**$/kW**	**773**	**1698**	**1438**

[a] 49.8% of subtotal cost (IEAHGH, 2012)
[b] 14% of BEC (cost Franco et al, 2012)
[c] 23.5% of EPC (IEAHGH, 2012)
[d] 2.7 % of the total equipment cost (IEAHGH, 2012)
[e] 37.5% of subtotal cost (IEAHGH, 2012)
[f] 46% of BEC (IEAHGH, 2012)
[g] Hendriks et al (2003), includes installation, indirect costs, contingencies and owner's costs

Table 4.8. Comparison of the estimated cost in this study with other published sources

Reference	Size of NGCC (MW) without capture	Estimated cost ($/kW)	Size of NGCC (MW) with capture	Estimated cost (M$) with capture
Gas Turbine Handbook, 2013[1]	913	757	---	---
Franco et al, 2011[2]	830	737.29	710	1134
GHGT-12, 2012[2]	910	749.64	786	1662
Thermoflow, 2013	850	785.8	---	---
In this study	909	773	794	1698

[1]The cost reported in Gas Turbine handbook of 538 $/kW includes only BOP and construction so to be comparative with this study, additional 40% of that cost was included.
[2]The Chemical Engineering Plant Cost Index (2013) is used to update the cost of equipment from 969.9 €/kW reported by Franco et al, (2011) and the cost reported in GHGT-12 (2012) to 2013; and a currency exchange of 0.8 EUR/USD in 2014 is used

4.3.7.2 Operation and maintenances cost O&M

Information for the operation and maintenance fixed and variable costs (O&M) for case studies for the power plant section are provided by Costs and benchmarks for the development of investment projects in the Mexican electricity sector (COPAR, 2013), which gives information for Mexico regarding new power plant projects in Mexican Federal commission of electricity. The estimation includes the expenses for consumables and chemical solvent make-ups (variable) as well as costs for maintenance and labour.

Variable O&M costs for CO_2 capture plant studies are calculated and considered make up of water and chemicals such as soda ash, corrosion inhibitor, activated carbon, molecular sieve, and diatomaceous. The variation of these chemicals varies according to the amount of MEA make up reported in DOE/NETL (2007). Solvent make up is estimated as 2.4 kg MEA/t CO_2 for the NGCC case with 13% v/v O_2 in the flue gas (Gorset, 2014) and 1.5 kg MEA/t CO_2 for the SSFCC cases for O_2 concentrations similar to coal flue gas (below 4% v/v) (Rubin and Rao, 2002; DOE, 2007).

The O&M for NGCC and subcritical SSFCC are provided in Table 4.9. The operating costs of a conventional NGCC configuration increase by 70.2%, from 30.9 to 52.6 M$ (million dollar), when capture is added. The variable operating costs of the capture unit decrease for the SSFCC configuration compared to the NGCC with CO_2 capture. Mainly this reflects the benefits of having lower solvent degradation with lower oxygen concentrations in the flue gas.

Table 4.9. Operating and maintenance cost (O&M) of the power plant and CO_2 capture plant for the natural gas combined cycle and subcritical sequential supplementary firing combined cycle

	Unit	NGCC	NGCC with capture	Subcritical SSFCC
Power plant	M$		M$	M$
Fixed O&M costs[a]	M$	13.3	11.6	11.4
Variable cost[a]	M$	17.6	15.4	15.2
CO_2 capture and compression				
Fixed O&M costs[b]	M$	NA	14.7	11.6
Variable cost[c]	M$	NA	10.9	7.4
Total	M$	30.9	52.6	45.5
Total O&M – net	$/kWh	4.85	9.46	8.32

[a]COPAR (2013)
[b]2% TCR CO_2 capture plant including compression (IEAGHG, 2011)
[c]Solvent make up is estimated as 2.4 kg MEA/t CO_2 for the NGCC case with 13% v/v O_2 in the flue gas (Gorset, 2014) and 1.5 kg MEA / t CO_2 for the SSFCC cases for O_2 concentrations similar to coal flue gas (below 4% v/v) (Rubin and Rao, 2002; DOE, 2007)

4.3.7.3 CO_2 Transport cost

The total cost of CO_2 transport is provided in Table 4.10. The cost of geological storage is not included as the CO_2 produced is considered for EOR. Only transport considering 100 km approximately from the power plant and the oil field as indicated in the DOE study. The CO_2 conditions considered in this study are at a pressure of 150 bar and 95% CO_2 purity for the purpose of EOR projects (DOE/NETL, 2012). The economic evaluation of EOR project is not evaluated in this work as it is assumed that this work finishes when the CO_2 is given and sold to the oil company. However, the CO_2 price is analysed in a sensitivity analysis in order to evaluate its implication in the cost of electricity.

Table 4.10. Total cost of CO_2 transport for the natural gas combined cycle and subcritical sequential supplementary firing combined cycle

	Unit	NGCC	NGCC with capture	Subcritical SSFCC
CO_2 transport[a]	M$	NA	7.0	8.2
	$/kW	NA	8.9	10.5

[a] 3.65 $/t$CO_2$ in 2011 dollar (DOE/NETL, 2013) 3.51 $/t$CO_2$ in 2013 dollar (Chemical Engineering index 2013)

4.3.7.4 Levelised cost of electricity

The levelised cost of electricity (LCOE) is calculated by annualizing the total capital cost and the total operating and maintenance costs and variable costs in $/MWh. The net electricity produced and sold, the operating, maintenance and fuel cost are considered constant over the life of the plant based on constant dollar. Carbon prices are not included in this analysis. Then, the simplified equation for these conditions is expressed by Equation 4.7 reported by Rubin et al (2013). All assumption for estimating the levelised cost of electricity is shown in Table 4.11.

$$LCOE = \frac{(TCR)(FCF) + FOM}{(Net\ power\ output)(CF)(8760)} + VOM + (HR)(FC) + \mathrm{TC}O_2 \qquad \text{Equation 4.7}$$

$$FCF = \frac{r(1+r)^T}{(1+r)^T - 1} \qquad \text{Equation 4.8}$$

Where

TCR	Total capital requirement ($)
FCF	Fixed charge factor
FOM	Fixed operating and maintenance (*O&M)* costs ($)
Net power output	Net power output (MW)
CF	Capacity factor (-)
VOM	Variable operating and maintenance *O&M* costs ($ / MWh)
HR	Net power heat rate (MMBTU/MWh)
FC	Fuel cost per unit of energy ($/MMBTU)
r	Interest rate (-)
T	Economic life of the plant (30 years in this study)
TCO_2	CO_2 transport cost ($/MWh)

Table 4.11. Summary of key assumptions for estimating cost

Capture level for post-combustion capture plant	%	90
Power plant fixed cost (COPAR 2012)	$/MW-year	14,594
Power plant variable cost (COPAR 2012)	$/MWh	2.77
Annual fixed capture plant related to CAPEX	%	2.0
Interest rate or discount rate	%	10
Plant life (COPAR 2012)	years	30
Load factor for new plant, assumed to be all at full output (COPAR, 2012)	%	80
Running hours per year for retrofit load factor	hrs/yr	7008
Variable costs for new plant, before capture basis	$/MWh	2
CO_2 emission price	$/t$CO_2$	0

4.3.8 Total revenue requirement sensibility and decision diagram

The values provided in Tables 4.7, 4.9, 4.10, and 4.11 are used to estimate the levelised cost of electricity (*LCOE*) using the Equation 4.7 and then calculate the total revenue requirement (*TRR*). The *TRR* is defined as the total revenue necessary for the project to break even. It is quantified at different CO_2 selling prices using Equation 4.9.

$$TRR = LCOE - EOR\ revenue \qquad \text{Equation 4.9}$$

Where

TRR Total revenue requirement ($/MWh)

LCOE Levelised cost of electricity ($/MWh)

EOR revenue Revenue for selling CO_2 in $/MWh is calculated using the Equation 4.10

$$EOR\ revenue = \frac{CO_2\ selling\ price \times levelised\ flow\ of\ CO_2 captured}{net\ power\ output} \qquad \text{Equation 4.10}$$

Where

CO_2 selling price CO_2 price ($/tonne$CO_2$)

Net power output Net power generated in power plant with CO_2 capture (MW)

$levelised\ flow\ of\ CO_2 captured$ is in (tonne/h)

The following underlying assumptions are used in this analysis:

1. There is no carbon price associated with the residual carbon emissions
2. It is financially worth building a new NGCC plant with capture in the electricity market where all the possible configurations of plants would operate
3. Therefore, the electricity selling price averaged over the life of a plant is at least higher than the LCOE of the NGCC plant with capture.

The cost impacts of CO_2-EOR sales are investigated, with a sensitivity analysis of the capital of the SSFCC configuration, in Figure 4.12 the subcritical SSFCC configuration is more sensitive to variation of the CO_2 selling price mainly because of the additional revenue from selling CO_2 for EOR, normalised per unit of energy. With respect to the price of crude oil, the commercial CO_2 price decreased within the range from 25 to 65 $/tonne when the crude oil price is $100/barrel to 45 $/tonne$CO_2$ at oil price of 70 $/barrel (Zhai and Rubin, 2013; National Energy Technology Laboratory, 2012 and 2010). In this analysis, the CO_2 sale price covers a range from 0 to $50/tonne$CO_2$ and the gas price from 2 to 6 $/MMBTU, indicating that:

- For a gas price of 6 $/MMBTU (5.69 $/GJ), the total revenue requirement lines of the subcritical SSFCC configuration intersect with the total revenue requirement line of the NGCC configuration at a breakeven CO_2 selling price of 37 $/tonne CO_2, as shown in Figure 4.12. With a relative reduction of capital cost of 10% of the SSFCC configuration, the lines intersect at 7.5 $/tonne CO_2.For a CO_2 selling price above the breakeven value in the intersection, the subcritical SSFCC plant with CO_2-EOR has a smaller TRR than the NGCC plant and would generate additional revenues if both configurations receive the same electricity selling price.
- For a gas price of 4 $/MMBTU (3.79 $/GJ), the two total revenue requirement lines intersect at a breakeven CO_2 selling price of 2.5 and 33.5 $/tonne CO_2 for variations of the capital costs of the SSFCC configurations of 0 and 10%.
- For a gas price of 2 $/MMBTU (1.896 $/GJ) in Mexico, the current price at the time of writing this thesis (Regulatory Commission of Energy, 2016), the subcritical SSFCC configuration presents the lowest total revenue requirement for all CO_2 selling price and for capital costs varying from -20% to 10%. At an increment of 20% relative, the lines intersect at a breakeven CO_2 selling price of 30 $/tonne CO_2.

This analysis is summarised in a decision diagram in Figure 4.13 for a difference range of capital cost estimates for the subcritical SSFCC configuration and a range of gas prices.

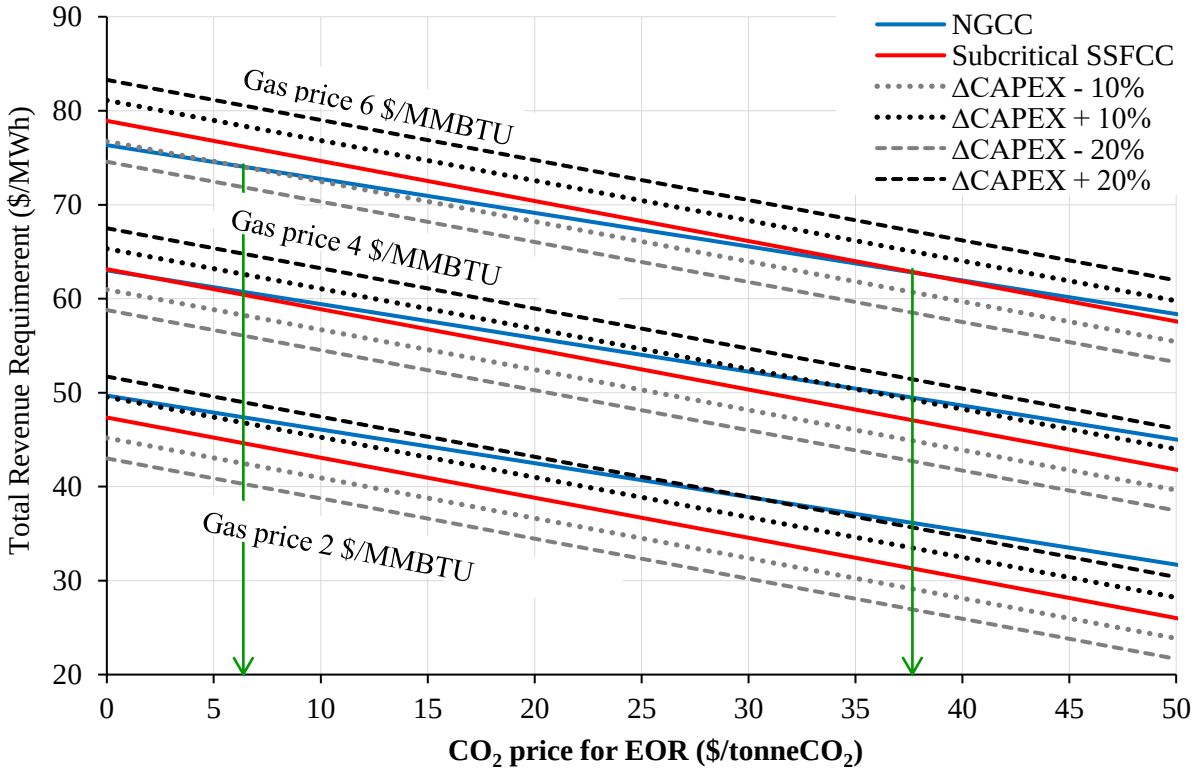

Figure 4.12. Total revenue requirement for a subcritical sequential supplementary firing configuration and a conventional natural gas combined cycle configuration for a range of representative CO_2 price for EOR and fuel prices. The relative variation in capital costs of the subcritical sequential supplementary firing configuration (ΔCAPEX) ranges from -20% to 20%. The vertical lines indicate the breakeven CO_2 price of equal total revenue requirements

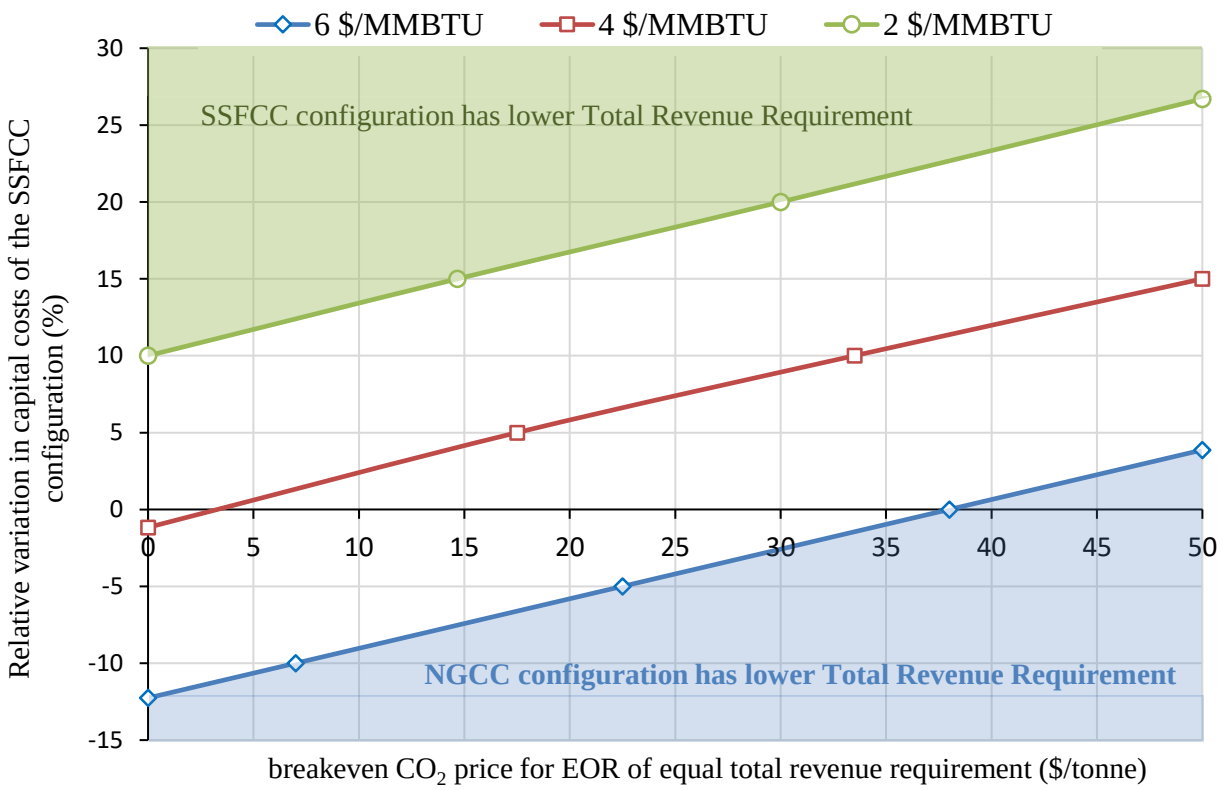

Figure 4.13. Decision diagram for a range of capital cost estimates and gas prices

4.4 Sequential supplementary firing with a supercritical combined cycle

4.4.1 Performance assessment

This second configuration is a supercritical SSFCC configuration and consists of one train of GE 937 IFB gas turbine, the HRSG is a single pressure Once Through Steam Generator type supplying heat to a double reheat combined cycle with four steam turbines, as shown in Figure 4.14. An HRSG design for supercritical steam conditions is a once-through steam generator with the main advantages of size reduction, a simplified control system, and fast start up (Innovative Steam Technologies Company, 2012). Nevertheless, advanced alloys, such as Incoloy Alloy 800 & 825, a nickel and iron-chromium enriched alloy with additions of molybdenum and copper, are required compared to a conventional HRSG, with Stainless Steel 304 (Innovative Steam Technologies Company, 2012).

The gas turbine is identical to the gas turbine of the conventional NGCC and of the subcritical SSFCC configurations. The capacity of the combined cycle is higher than the subcritical configuration since there is an increment in the marginal thermal efficiency of the additional gas usage with supercritical steam conditions. The configuration of the steam turbines is adapted from a configuration described by Kjaer (1993) for a pulverised coal power plant. As in the subcritical SSFCC configuration, supplementary gas is burned in 5 stages throughout the HRSG to reduce the excess O_2 down to a concentration of 1 % v/v.

With sequential supplementary firing, supercritical steam conditions of 630 °C, 601.5 °C, 290 bar (McCauley, et al, 2012; Salazar-Pereyra, et al, 2011; Satyanarayana, et al, 2011, Cziesla et al, 2009) increase the average temperature of heat addition to the steam cycle. The absence of phase change between the evaporator to the superheater allows for a reduction in heat transfer irreversibilities with lower temperature difference between the flue gas and the turbine working fluid. The pinch point of the HRSG is reduced with supercritical conditions from 70 °C to 27 °C seen in Figure 4.15 and the marginal thermal efficiency of natural gas usage is increased from 36.0% to 40.2% shown in Table 4.12.

Table 4.12 presents the performance assessment of the supercritical SSFCC configurations and compares it to the equivalent subcritical configuration. With additional fuel being burnt in one HRSG with supercritical steam conditions, the capacity of the steam turbine increases from 245 MW to 589 MW compared to the conventional NGCC configuration.

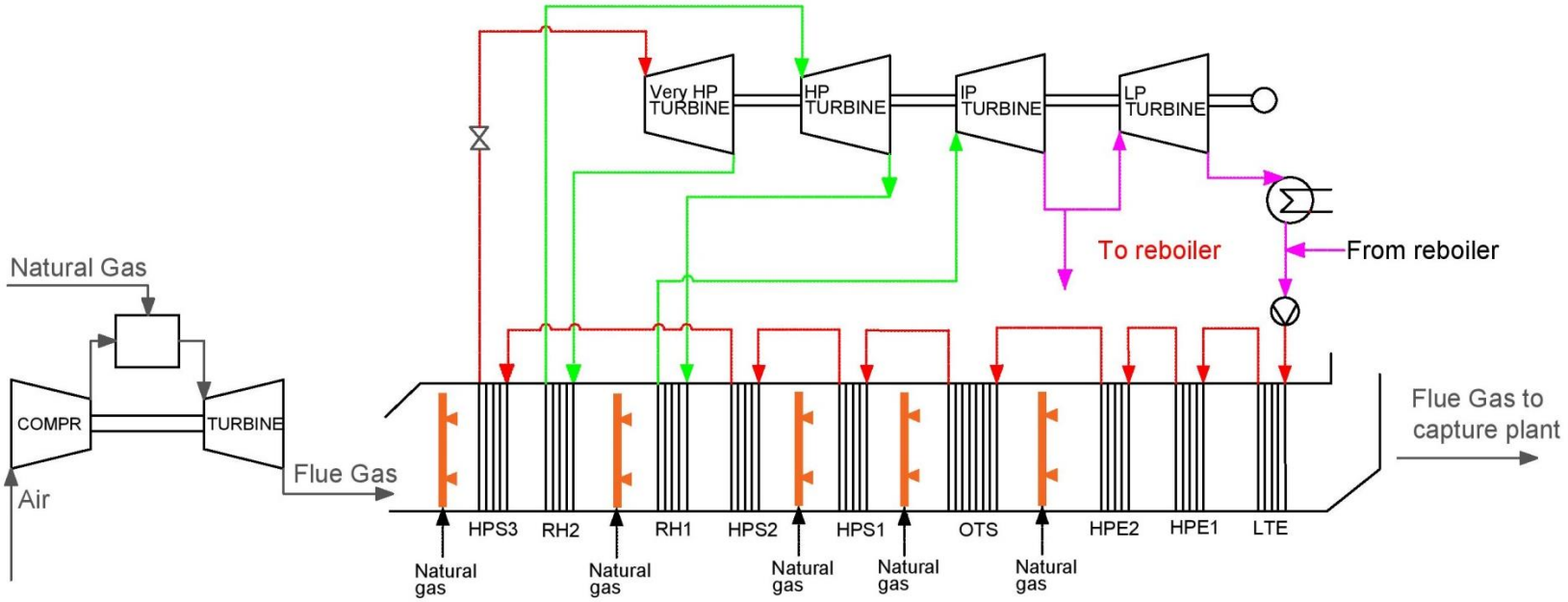

Figure 4.14. Schematic process flow diagram of a supercritical sequential supplementary firing configuration with one GE 937 IFB/single pressure HRSG train combined cycle with a double reheat steam cycle simulated in Aspen Hysys[@]

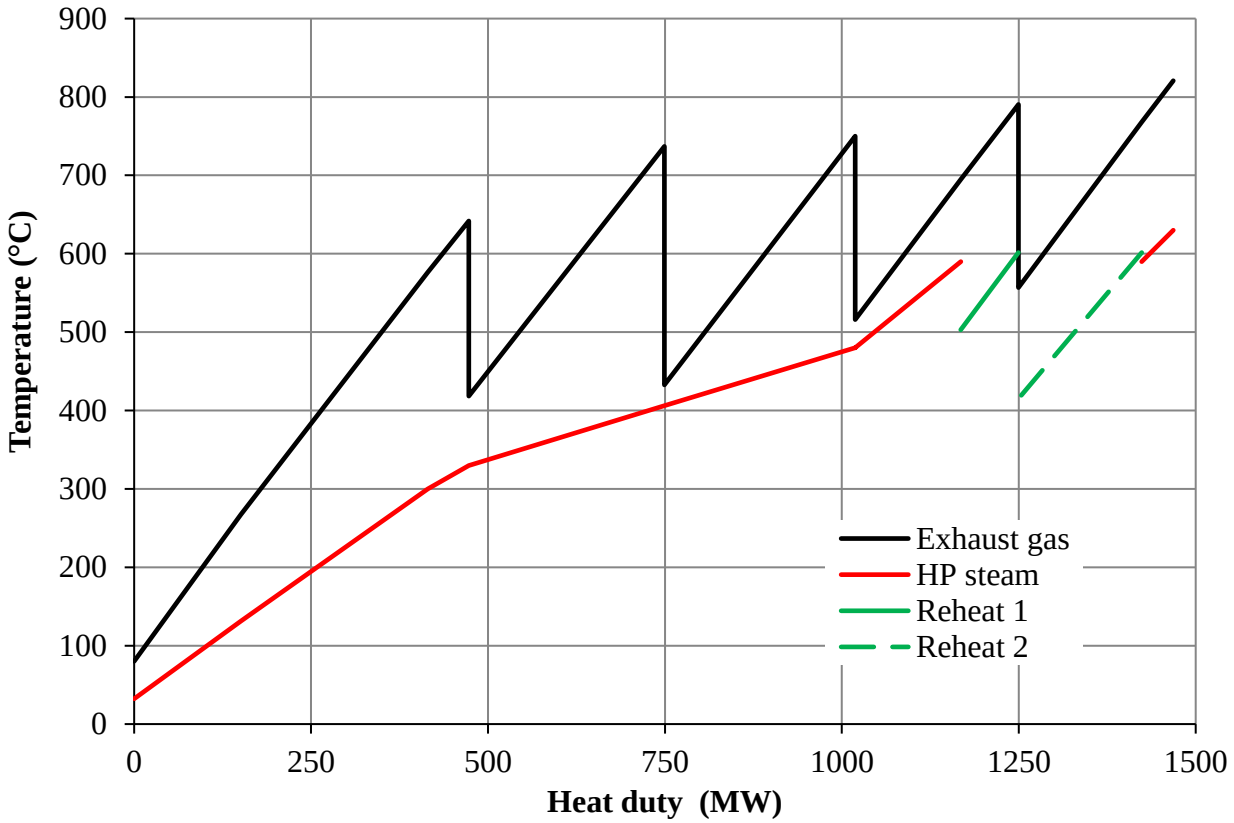

Figure 4.15. Temperature/heat diagram for the Heat Recovery Steam Generator of a five stage sequential supplementary firing configuration, with a double reheat combined cycle and supercritical steam conditions (630 °C, 601.5 °C, 295 bar). The two pinch temperatures ΔT1, ΔT2 are respectively 27ºC, 36ºC

In power plant with single reheating the cold reheat temperature will get lower and lower when the live steam pressure is increased, and from a thermodynamic point of view this is disadvantageous. The temperature drops at 300 °C with a live pressure of 300 bar in coal power plant (Kjaer, 1993). Then the steam flowing to the reheater is not much warner than the feedwater. Therefore, reheating does not contribute much to raising the temperature level of the boiler's heat supply. For that reason, as the live steam pressure is increased it will be necessary to introduce double reheating. Double reheat is recommended by steam suppliers for a live steam pressure of 300 bar (Kjaer, 1993). Figure 4.16 shows the expansion lines of the supercritical double reheat combined cycle and the subcritical single reheat combined cycle on an enthalpy-entropy diagram, data is taken from the Aspen Hysys@ simulation. In the supercritical Rankine cycle with double reheat, steam is expanded from 295 bar to 80 bar in the Very High Pressure (VHP) turbine and sent back to the HRSG where it is reheated in Reheater RH2 of Figure 4.14. Steam then expands in the HP steam turbine down to around 42 bar and is sent back to the HRSG where it is reheated in Reheater RH1. The steam temperature rises to 601°C before it is expanded in the IP steam turbine.

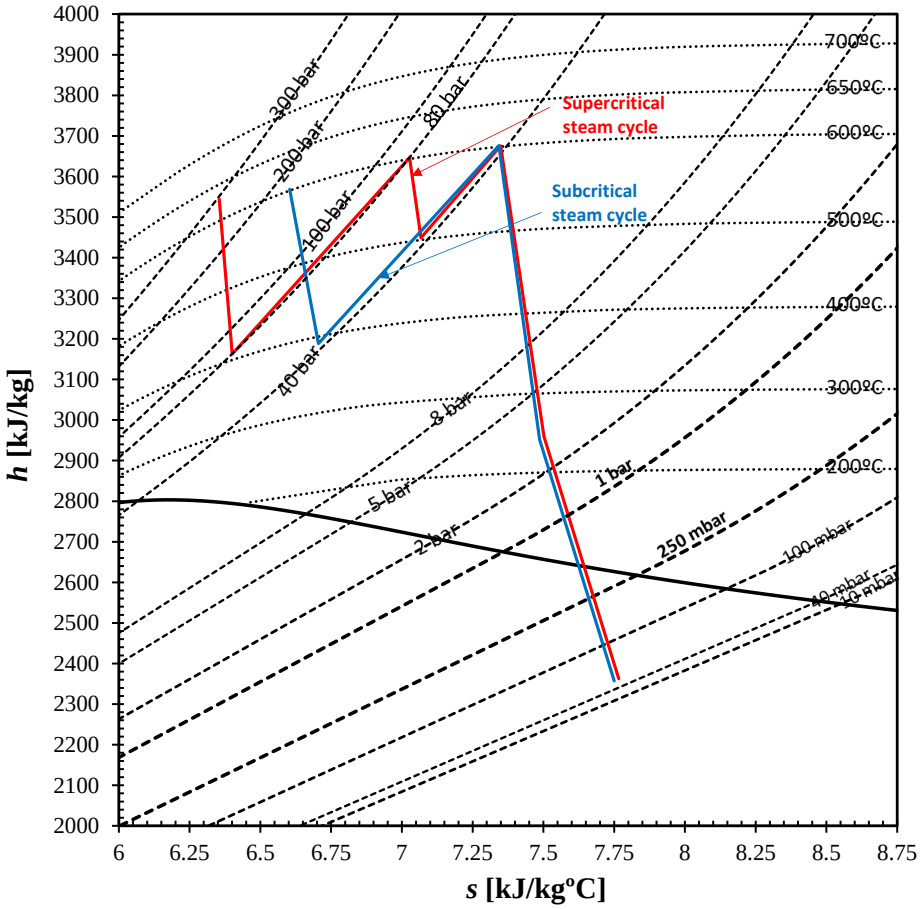

Figure 4.16. Enthalpy-entropy diagram of the supercritical Rankine cycle with double reheat and the subcritical Rankine cycle with single reheat. Results from Aspen Hysys@ simulation

The total net power of the supercritical SSFCC configuration is 824 MW, compared to 794 MW with a NGCC and 781 MW with subcritical SSFCC. The thermal efficiency of the supercritical SSFCC configuration with post-combustion capture is 45.6 % LHV, compared to 43.1% for a subcritical SSFCC, as shown in Table 4.12. However, there are cost implications: The HP part of the combined cycle, including the HP steam turbine, valves, pipework, and the HP requires being of supercritical design which means additional capital cost.

Table 4.12. Summary of key parameters of a sequential supplementary firing with single pressure HRSG and a double reheat supercritical steam cycle with CO_2 capture (steam condition for the reboiler T=138 ºC, 3 bar)

Concept	**Unit**	**Supercritical SSFCC**	**Subcritical SSFCC**
LHV net electric efficiency[1]	%	45.6	43.1
Gas turbine power output	MW	296	296
Steam cycle power output	MW	589	545
Total LHV gross power output	MW	884	840
Total LHV net power output (including CO_2 compression and other archillaries)	MW	824	781
Mass flow rate of natural gas to gas turbine	kg/s	16.6	16.6
Mass flow rate of natural gas for supplementary firing	kg/s	22.2	22.2
Marginal efficiency of natural gas fired in HRSG (LHV)	%	40.2	36
Marginal efficiency of natural gas fired in HRSG (LHV) without post-combustion capture (for comparative purposes only)	%	49.1	44.7
Electricity output penalty	$kWh_e/tonne CO_2$	350	362
Carbon intensity of electricity generation	$kgCO_2/MWh$	45.0	47.5
Flue gas mass flow rate	kg/s	696	696
Flue gas composition after direct contact cooler			
Water (H_2O)	% vol	4.29	4.29
Carbon dioxide (CO_2)	% vol	10.87	10.87
Oxygen (O_2)	% vol	1.312	1.312
Nitrogen (N_2)	% vol	83.52	83.52
CO_2 mass flow to pipeline	kg/s	93	93
Capture level	%	90	90
Solvent energy of regeneration	$GJ/tonne CO_2$	3.42	3.42
Steam mass flow to solvent reboiler	kg/s	157	145.6
Number of absorber trains		2	2
Diameter	m	15.5	15.5
Absorber height	m	21	21
Volume of packing used for CO_2 capture (not including water wash sections)	m^3	8130	8130

[1]LHV net electric efficiency includes CO_2 compression and parasitic losses and transformed losses are included

4.4.2 Cost estimation of supercritical SSFCC

The methodology used to estimate the cost of the supercritical SSFCC configuration is identical to the subcritical one described in section 4.3.7. For supercritical steam conditions, the cost estimate of the HRSG in sections with high temperature is based on Equation 4.5, where a factor *N*=3.3 (World steel prices, 2013) is used to account for the use of more expensive alloys to support supercritical conditions. The specific investment of supercritical SSFCC is reported in Table 4.13.

$$C = C_0 \left[\frac{UA}{U_0 A_0}\right]^f \mathrm{N} \qquad \text{Equation 4.5}$$

Table 4.13. Estimated specific investment for the supercritical sequential supplementary firing combined cycle with capture

Plant component	Unit	Supercritical SSFCC w/capture
Gross power output	MW	884
Net power output	MW	824
Power plant main items		
Gas turbine, generator and auxiliaries	M$	68
HRSG, ducting and stack	M$	88
Duct burner	M$	2
Steam turbine generator and auxiliaries	M$	108
Cooling system and miscellaneous, BOP system	M$	64
Subtotal	**M$**	**331**
Total Installation cost[a]	M$	161
BEC	**M$**	**492**
Indirect cost[b]	M$	69
EPC	M$	561
Contingencies, owner's costs[c]	M$	132
TCR power plant	**M$**	**693**
Capture plant main items		
Flue gas cooling	M$	11
CO_2 absorber & flue gas re-heater	M$	55
Rich/ lean amine circulation	M$	6
Stripping section	M$	139
Ancillaries	M$	5
Suporting facilities & labor (direct and indict)[d]	M$	47
Subtotal	**M$**	**262**
Installation cost[e]	M$	98
BEC	**M$**	**361**
EPC, Contingencies and owner's costs[f]	M$	166
TCR capture plant	**M$**	**527**
TCR CO_2 compression[g]	**M$**	**53**
Specific investment – Gross	**$/kW**	**1,439**
Specific investment – Net	**$/kW**	**1,544**

[a]49.8% of subtotal cost (IEAHGH, 2012); [b]14% of BEC cost (Franco et al, 2012); [c] 23.5% of EPC (IEAHGH, 2012); [d]2.7 % of the total equipment cost (IEAHGH, 2012); [e]37.5% of subtotal cost (IEAHGH, 2012); [f]46% of BEC (IEAHGH, 2012); [g]Hendriks et al (2003), includes installation, indirect costs, contingencies and owner's costs

When compared with the conventional NGCC configuration, there is a reduction in the total specific investment of 9.1%, equivalent to 75 M$, lower than for the subcritical configuration with 15.32% and 264 M$ respectively. The O&M are provided in Table 4.14. Since the fuel thermal input is the same for both configurations with sequential firing, the amount of CO_2 generated is the same. Total cost of CO_2 transport is provided in Table 4.10.

Table 4.14. Operating and maintenance cost (O&M) of the power plant and CO_2 capture plant for the supercritical sequential supplementary firing combined cycle

	Unit	Subcritical SSFCC
Power plant	M$	M$
Fixed O&M costs[a]	M$	12.0
Variable cost[a]	M$	16.0
CO_2 capture and compression		
Fixed O&M costs[b]	M$	11.6
Variable cost[c]	M$	7.4
Total	M$	47.0
Total O&M - net	$/kWh	8.14

[a]COPAR (2013); [b]2% TCR CO_2 capture plant including compression (IEAGHG, 2011)
[c]Solvent make up is estimated as 2.4 kg MEA/t CO_2 for the NGCC case with 13% v/v O_2 in the flue gas (Gorset, 2014) and 1.5 kg MEA / t CO_2 for the SSFCC cases for O_2 concentrations similar to coal flue gas (below 4% v/v) (Rubin and Rao, 2002; DOE, 2007)

4.4.3 Total revenue requirement and sensitivity to gas price and CO_2 selling price of supercritical SSFCC

The TRR of the supercritical configuration is evaluated and then compared with the corresponding subcritical configuration. Figure 4.17 (Figure 4.18 shows the absolute TRR) shows a reduction of the total revenue requirement of supercritical with respect to subcritical SSFCC at 0-50 $/tonne CO_2 selling price and gas price in a range from 2-6 $/MMBTU. The supercritical SSFCC configuration presents overall a lower TRR than a subcritical configuration. This is due to an improvement in efficiency associated with supercritical steam conditions and the fact that revenue from CO_2 sales is identical to the subcritical configuration. If both configurations of CCS power plants were receiving the same electricity price and the same CO_2 price, the supercritical configuration would receive higher revenue over the economic life chosen for this analysis. It can be concluded that a supercritical combined cycle is an improvement to a subcritical combined cycle in this context, as it presents consistently a lower TRR in a range of gas price from 6 to 2 $/MMBTU and when the CO_2 captured is utilized for EOR at commercial prices from zero to 50 $/tonne$CO_2$. However, supercritical combined cycles have not been rolled out commercially yet, compared with subcritical SSFCC that uses existing off-the-shelf solutions.

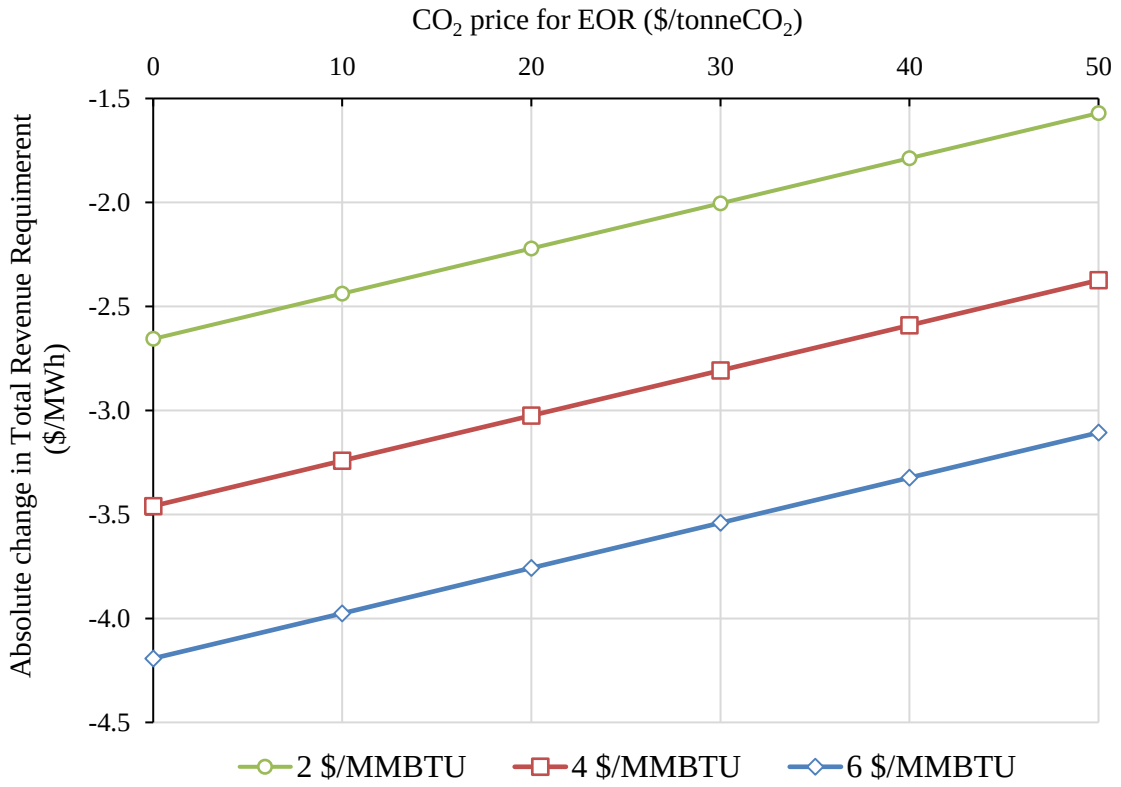

Figure 4.17. Reduction in total revenue requirement for sequential supplementary firing combined cycle plant with supercritical steam conditions compared to a subcritical configuration, for a range of representative CO_2 price for EOR and fuel prices

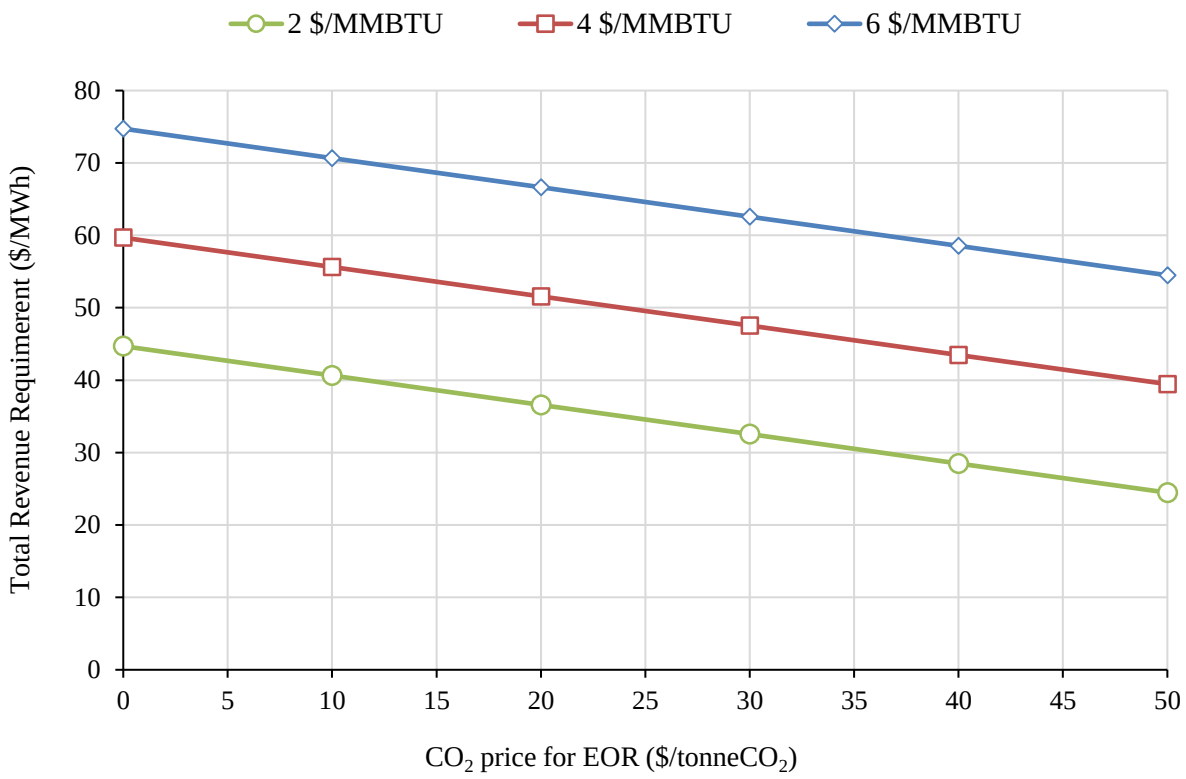

Figure 4.18. Total revenue requirement for supercritical sequential supplementary firing combined cycle plant with supercritical steam conditions, for a range of representative CO_2 price for EOR and fuel prices

4.5 Conclusions

The integration of sequential supplementary firing combined cycle plants is examined in the context of deploying CCS with Enhanced Oil Recovery in Mexico. A new design of heat recovery steam generator is proposed where additional fuel is combusted to increase the volumes of carbon dioxide available for EOR. The maximum amount of CO_2 is produced by reducing excess oxygen levels as low as practically possible (of the order of 1% v/v).

The total power output of a sequential supplementary firing configuration with CO_2 capture, consisting of a single gas turbine and heat recovery steam generator train, is 824 MW with a supercritical combined cycle, 781 MW with a subcritical combined cycle, compared to 794 MW for a conventional NGCC configuration with capture with two gas turbines and two HRSGs. The difference in the power output is due to the design of the heat recovery steam generator where additional fuel burnt increases heat available for steam generation in the combined cycle. This allows a reduction by half of the number of GT/HRSG trains and of the total volume of flue gas. This has a positive impact on the number of direct contact cooler and absorbers required in the post combustion capture plant. The reduction of overall capital costs is, respectively, 9.1 % relative and 15.3% relative for the supercritical and the subcritical configurations compared to the conventional configuration with capture. Both sequential supplementary firing configurations also present a reduction in the electricity output penalty compared to a conventional NGCC plant with capture.

The sensitivity of total revenue requirements for low-carbon electricity generation, a metric combining levelised cost of electricity and revenue from EOR, to CO_2 prices and fuel prices is used to compare configurations. Since capital cost estimates are bound to include large biases and uncertainties, I perform a sensitivity analysis showing that our conclusions are robust over a range of gas prices and CO_2 prices for EOR, and that sequential supplementary firing is advantageous in the context of North American gas prices. A comparison between subcritical and supercritical SSFCC configurations shows that improvements in power plant efficiency with supercritical steam conditions consistently result in a lower TRR. At gas prices ranging from 2 to 6 $/MMBTU, supercritical SSFCC may receive additional revenues ranging from 1.5 to 4$/MWh for CO_2 prices ranging from 0 to 50$/tonne CO_2 compared to subcritical configurations. Further work is needed to include site specific considerations and detailed capital estimates beyond the work included in this study, which is effectively a very first attempt at assessing the feasibility and validity of the concept in the context of CCS in Mexico, with access to affordable natural gas prices and likely revenues from Enhanced Oil Recovery.

5. Part-load operation of sequential supplementary firing combined cycle power plant with CO_2 capture

5.1 Introduction

Power plants operate at part-load due to variations in electricity demand caused by weather conditions, seasonal, daily and hourly changes in demand, e.g. there is a difference between week days and weekend days (Mexican Ministry of Energy, 2012). In the future, the electricity demand will be influenced by the introduction of intermittent renewable energy. It is expected that the installed wind power capacity will increase from 1.8 % in 2014 to 10.9% in 2028 (Federal Commission of Electricity, 2014). One characteristic of NGCC power plants is their flexibility to change power output according to electricity demand (IEAGHG, 2012). Therefore, it is necessary to evaluate and to ensure the continuity of flexibility in the operation of new alternatives proposed to decarbonise the electricity market. Any novel alternative with carbon capture should not impose a constraint to this need for flexibility.

The part-load performance of NGCC plants with carbon capture has been evaluated by Rezazadeh et al, (2015) and Karimi et al, (2012). Rezazadeh et al, (2015) concluded that a NGCC with CO_2 capture is viable to operate at part-load down to 60% of the nominal load of the gas turbine but with penalty in the power output and efficiency. Kehlhofer, et al, (2009) and Elmasri, et al (2002) suggest that the optimum way to operate a NGCC is using the variable inlet guide vanes (IGV) at off-design operation. To change the load of a NGCC, the fuel and air mass flows must be reduced simultaneously. The air flow rate is regulated using the variable IGV. The inlet guide vanes are also known as stators, and are located in front of the first stage of the compressor of a gas turbine engine. The compressor of the gas turbine can have fixed or variable IGVs.

Karimi et al, (2012) investigated two operation strategies for the gas turbine: variable IGV (reducing the air and the fuel) and fixed IGV (reducing only the fuel of the GT combustor); and two alternatives of integration for extracting steam from the cross-over: with and without a throttling valve at the inlet of the LP turbine. Results show that the net efficiency of the variable IGV gas turbine is about 6.2% points higher than the efficiency with constant IGVs gas turbine at 50% of the nominal load. In addition, a power plant with a throttled valve configuration for steam extraction has a better performance than the sliding configuration.

The reason for this is that at full load in sliding pressure, the pressure is 5 bar; and in fixed pressure it is kept constant at 4 bar at different loads of the NGCC. Rezazadeh et al, (2015) only evaluated the use of variable IGV and purely sliding steam extraction.

Three important aspects are of critical importance to be analysed at part-load operation of a power plant integrated with CO_2 capture and the compression system:

1. Power plant part-load operation strategy
2. Operating strategy of the CO_2 capture and compression system
3. The integration of the power plant and capture and compressor unit

This chapter focuses on evaluating and defining the power plant operating strategy of a supercritical and a subcritical SSFCC configuration integrated with MEA-based CO_2 capture. This is a novel contribution of this thesis, where the objective is to maximise power for any given fuel input and revenues from electricity and CO_2 production. The operating strategy and the integration of the capture and compression system are based on the state of the art. The operating strategy of the power plant is novel, since supplementary firing adds a level of permutation not encountered in conventional configurations. Unlike conventional configuration, in SSFCC the fuel input can be adjusted in the GT or in the HRSG. This is an additional degree of freedom.

For the purpose of part-load study, a different version of the gas turbine 9FB has been used because more details were available to validate the model of the conventional NGCC in Aspen plus®. The main difference between the gas turbine from the previous sections lies in the compressor which has lower efficiency. However, both have similar capacity. The gas turbine 9FB and the HRSG of the NGCC have been modelled in Thermoflow (2013) by Alcaraz, (2015), and the date has then correlated the results, which are used in this thesis. The performance of the gas turbine 9FB from Alcaraz, (2015) is validated with information from a thermal test of the 9FB published by Ol'khovskii, et al, (2013). Thermoflow is a suite of software which includes GT PRO, GT MASTER and Thermoflex programmes. GT PRO is a leading gas turbine and combined cycle modelling programme that utilises a database of gas turbines with mapped performance curves. GT master enables the performance of off-design scenarios to be modelled i.e. at part-load (IEAGHG, 2012; Karimi et al, 2012).

The configuration and operating parameters for the HRSG of the conventional NGCC configuration at design condition have been taken from Thermoflow data. At part-load, the model for the HRSG and steam turbines of the NGCC is based on typical modelling principles, such as Stodola ellipse low for steam turbines, heat transfer fundamentals in the

HRSG, and relevant pressure drop equations that are described with details in the next sections. In order to solve the equation system, the number of equations must be equal to the number of variables. The equation system is solved in Aspen Plus® to estimate the steady state performance at design and part-load conditions using an equation-oriented approach. The efficiency of SSFCC power plant configuration at part-load is an important parameter and the criteria to decide the mode of operation of the plant.

The results at part-load in the integrated Aspen Plus® model are in good agreement with Thermoflow data, which allow the use of the same assumptions and equations for SSFCC. Start-up/shut-down and variation of the performance with environmental conditions are outside the scope of this study.

In the first section of this chapter, operating strategies are defined for all case studies. Then, the thermodynamic model for the gas turbine, HRSG, and steam turbine of the power plants at part-load are described in detail. Finally concluding remarks are given in the last section.

5.2 Operating strategy at part-load

5.2.1 Gas turbine

A gas turbine in a combined cycle configuration operates at part-load with varying airflow rates using the IGV. As the gas turbine changes its load, the steam turbine output adjusts automatically. The overall efficiency depends on the efficiency of the gas turbine. The optimum mode to operate a NGCC plant is using variable IGV from 40% to 100% load of the gas turbine (Kehlhofer, et al, 2009). When a power plant combined cycle has supplementary firing, the steam cycle is controlled independently of the gas turbine, and the power demand is regulated by the amount of fuel burnt in the duct burners as in a conventional boiler (Kehlhofer, et al, 2009).

5.2.2 Boiler and steam cycle

There are two common ways to operate a steam cycle and boiler: sliding and fixed pressure control modes.

Sliding pressure control: In this case, inlet turbine areas remain constant, and the live steam pressures will naturally result, function of the live steam flows (turbine loads) (Darie et al, 2007). Pressure is reduced by controlling the discharge pressure of feed pumps. In a NGCC, the steam cycle functions most economically using sliding pressure from 100% to 50% load, shown in Figure 5.1, allowing for fast start-up. This alternative offers greater flexibility.

Fixed pressure control: In constant live steam pressure operation mode, the pressure of the steam is maintained constant in the boiler, controlling admission to the steam turbine using a throttle valve. Throttle-controlled turbines at constant pressure suffer in efficiency at part loads. This is characterised by exegetic losses (Darie et al, 2007). Nozzle-controlled turbines also operate with the boiler at constant pressure and have nearly the same efficiency as at sliding pressure (Vitalis, 2006). They are not commonly used in combined cycle plant.

A supercritical conventional power plant is able to operate with sliding pressure as load is varied. However, the boiler must be designed to accommodate both single and two-phase flow, resulting in additional capital cost but also higher efficiency at part-load. Alternatively, it must be operated at fixed pressure in order to maintain a single phase with supercritical steam conditions at off-design. This results in a drop in efficiency but provides a fast dynamic response (Vitalis, 2006).

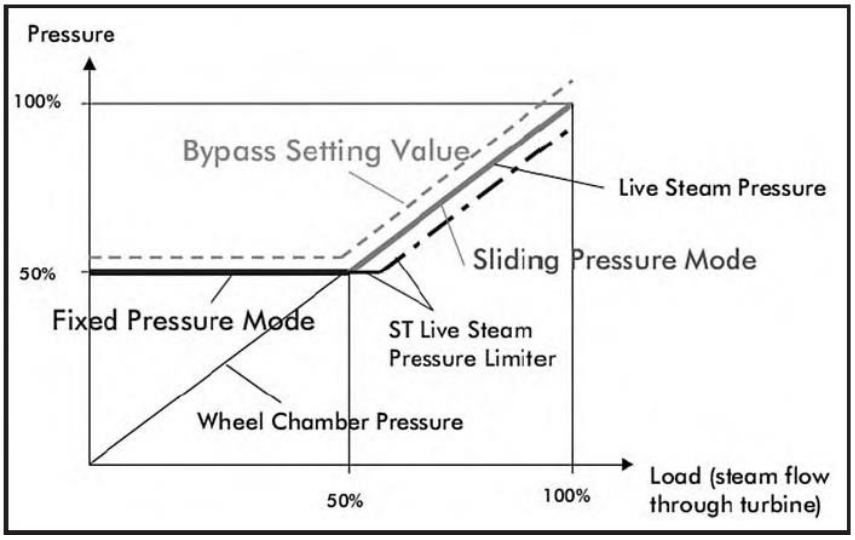

Figure 5.1. Sliding pressure operations up to 50% load in a natural gas combined cycle (Kehlhofer, et al, 2009)

The minumun reduction of aceptable part-load of a conventional NGCC is appoximately 50% and it is based on the following reasons (Kehlhofer, et al, 2009):

1. Below 80% load of the gas turbine, the inlet temperature must be reduced, which results in a fast reduction of the gas turbine effciency.
2. Below 45% load of the NGCC, the temperature of the exhaust gas decreases drastically as shown in Figure 5.2. from 590°C to 500°C affecting the temperature of the steam turbine which reduces from 567°C to 490°C

3. The steam turbine is operating with sliding pressure down to about 50% load (steam flow through turbine) as shown in Figure 5.1. Below 50% load, the live-steam pressure is held constant in the HRSG in order to increase the utilisation of the exhaust gas and is then controlled by the steam turbine inlet valve. This results in throttling losses and increasing stack loases

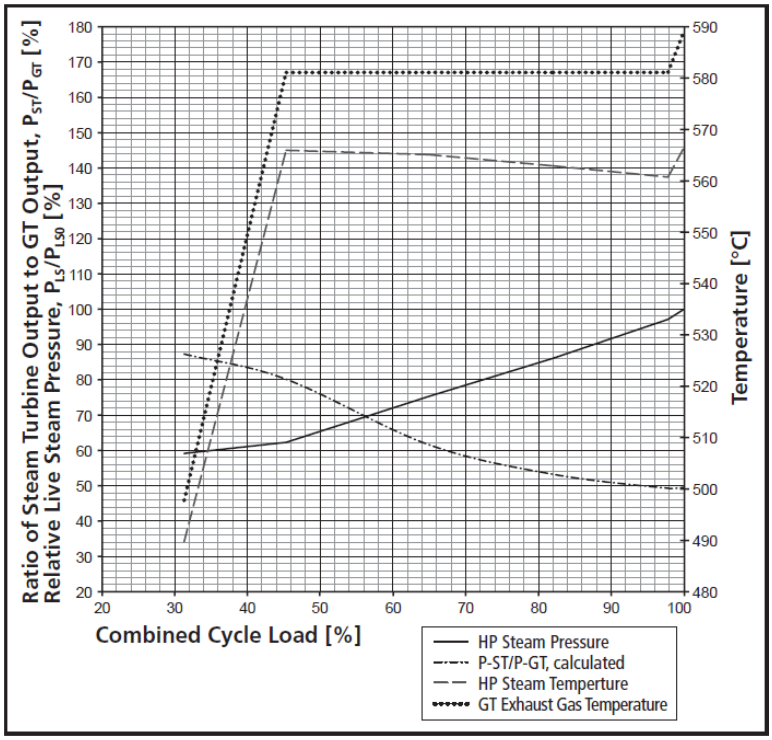

Figure 5.2. Ratio of steam turbine and gas turbine output and live-steam data of a combined cycle plant at part-load (Kehlhofer, et al, 2009)

The pressure and temperature of the main steam of a steam turbine at design conditions are based on information data from Thermoflow (2013), which utilises a database of gas and steam turbines with mapped performance curves provided by manufactures and supplies.

The reason of that is to ensure that available steam turbines are used in this study. High temperature of the main live steam improves thermodynamics of the water/steam cycle and steam turbine efficiency due to the wetness in the low pressure section. However, too high a live steam temperature can also cause an increase in power plant cost since great amount of expensive material is necessary to deal with this high temperature. The exhaust gas is another limit for the live steam temperature level (Kehlhofer, et al, 2009).

5.2.3 Operating mode of sequential supplementary firing combined cycle

Based on this state- of- the- art analysis of NGCC, the operation strategy of supercritical and subcritical SSFCC power plants is defined. As the steam cycle becomes independent from the gas turbine when supplementary firing is incorporated, there are two alternatives when varying load: fixed IGV where the gas turbine operates at full load and the desired load of the power cycle is reached by varying the amount of the supplementary fuel in the duct burners in the HRSG; and variable IGV where the desired load is reached by a combination of closing the IGV in the gas turbine and varying the amount of fuel in the duct burners in the HRSG. Sliding and fixed pressure in the steam cycle are evaluated for supercritical SSFCC and for subcritical SSFCC only at sliding pressure, which is the optimum way to operate at part-load. In the last case, as it is subcritical, it is not necessary to operate at fixed pressure using a throttle-controlled turbine affecting the efficiency at part loads.

The different combinations of operating strategies under consideration for SSFCC power plants are summarised as follow:

Supercritical SSFCC

a. Gas turbine with fixed IGV and fixed pressure in HRSG
b. Variable IGV and fixed pressure in HRSG
c. Gas turbine with fixed IGV and sliding pressure in the HRSG

Subcritical SSFCC

a. Gas turbine with fixed IGV and sliding pressure in the HRSG
b. Variable IGV and sliding pressure in the HRSG

Only one case study for sliding pressure control in the HRSG is evaluated for supercritical SSFCC: with fixed IGV. It is included in order to illustrate the effect of the fixed and sliding pressure in the efficiency of the SSFCC power plant. The reason for this is: supercritical boilers can be operated in dual mode fixed and sliding pressure at expense of additional capital cost (Vitalis, 2006). It is necessary to evaluate the effect of the additional capital cost at part-load that is outside the scope of this study. In addition, the effect of variable IGV is a detrimental effect to the gas turbine isentropic efficiency. The efficiency of the gas turbine reduces at variable IGV, as mentioned previously in section 3.2.2, because below 80% load of the gas turbine, the inlet temperature must be reduced, in order to control the exhaust

temperature, which results in a fast reduction of the gas turbine effciency (Kehlhofer, et al, 2009).

The selected configuration and operation strategy of CO_2 capture and compressor units are based on Sanchez-Fernandez et al, (2016); Van der Wijk et al., (2014); Liebenthal and Kather, (2011); and Kvamsdal, (2009) described in chapter 3.

5.2.4 Integration of the power plant and CO_2 capture and compressor unit

One important issue at part load of a power plant with capture is the reduction of steam extraction pressure for solvent regeneration. Lower steam generation in the HRSG reduces flow rate across the combined cycle and all operating steam pressures. This affects the operation of the capture plant because of the change in steam conditions to regenerate the amine. Irons, (2013) suggests three alternatives for capture plant integration:

1. Modification to IP/LP-Turbine overflow with throttle valves to maintain steam extraction pressure as high as possible at part load (Lucquiaud and Gibbins, 2009, 2011). The philosophy of this strategy consists of setting the IP/LP crossover pressure at the desired value for a specific solvent regeneration temperature at full load, and then control pressure with a throttling valve upstream of the LP turbine to maintain pressure and, by extension, solvent regeneration temperature as high as possible when the IP turbine outlet pressure drops with load.
2. IP/LP cross-over at full load and auxiliary header (9 bar) in part load
3. IP/LP cross-over at full load and use “steam jet booster” at part load shown in Figure 5.3

The last two alternatives for integration proposed by Irons, (2013) are of special interest. Nonetheless, they have not been compared and evaluated with other alternatives already evaluated e.g. Sanchez Fernandez et al, (2016). As mentioned in the introduction of this chapter, this work is focussed on evaluating the operating strategy only for SSFCC power plant at part-load. The evaluation of the integration strategy is outside the scope of this study and is based on the state of the art.

Sanchez Fernandez et al, (2016) evaluated two capture plant integrations:

1. Controlled by throttling LP steam or fixed crossover pressure
2. Floating IP/LP crossover pressure or uncontrolled extraction: the extraction pressure is determined by the amount of steam extracted. The initial IP/LP crossover pressure

is set so that, when the predicted amount of steam is extracted for solvent regeneration, its pressure falls or 'floats' to the desired value

According to her results, uncontrolled steam extraction (or floating pressure integration) provides better full and part load performance when compared to control by throttling (fixed pressure). Therefore, the strategy selected in this study is floating IP/LP crossover pressure (uncontrolled extraction). In this thesis the power plant is designed to operate with the CO_2 capture unit so the desire pressure in the cross over is set up considering the steam extraction. The desired pressure in the crossover used in different sources for MEA is: 4 bar using a throttle valve and 5 using uncontrolled extraction (Karimi et al, 2012); 3 bar (Jordal et al, 2012); and 3.37 bar Rezazadeh et al, (2015). All the combinations of integrated model: the power plant with capture plant and the compression unit cases are listed in Table 5.1.

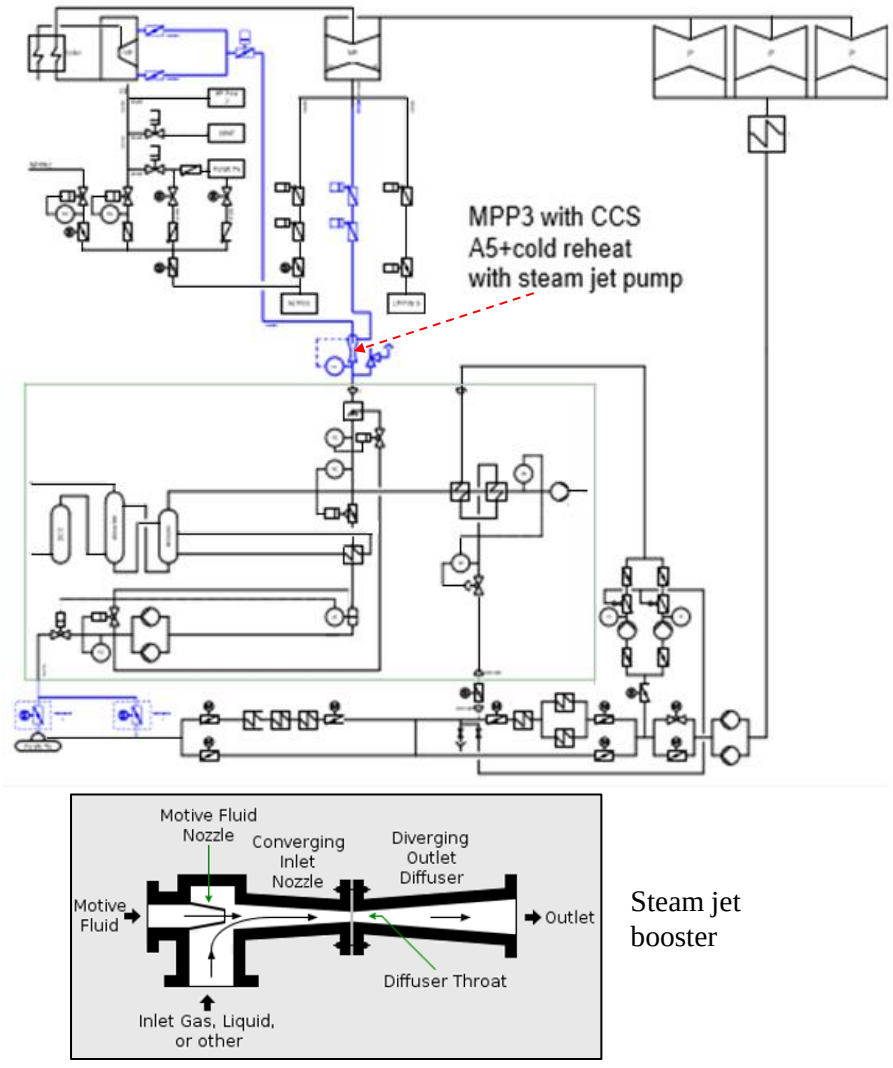

Figure 5.3. Schematic diagram of the integration alternative: IP/LP cross-over at full load and use "steam jet booster" at part load (Irons, 2013)

Table 5.1. Lists of option for part-load operation for the power plant, CO_2 capture, and compressor unit

Power plant case	**NGCC**	**Supercritical SSFCC**			**Subcritical SSFCC**	
Gas turbine control	Variable IGV	Fixed IGV	Fixed IGV	Variable IGV	Fixed IGV	Variable IGV
HRSG	No supplementary firing	Sequential supplementary firing	Sequential supplementary firing	Sequential supplementary firing	Sequential supplementary firing	Sequential supplementary firing
Steam cycle (Pressure and temperature)	Subcritical	Supercritical	Supercritical from 85-100% and subcritical from 50-85%	Supercritical	Subcritical	Subcritical
Steam cycle control	Sliding pressure	Fixed pressure and throttling steam	Sliding pressure	Fixed pressure and throttling steam	Sliding pressure	Sliding pressure
Steam extraction	Uncontrolled extraction	Uncontrolled extraction	Uncontrolled extraction	Uncontrolled extraction	Uncontrolled extraction	Uncontrolled extraction
Capture plant	*Constant* stripper pressure, *variable* Temperature and L/G for all cases					
CO_2 compressor	IGV with CO_2 recycle valve and constant pressure ratio (P_{inlet} and P_{outlet} constant)					

IGV = Inlet Guide Vanes; HRSG = Heat Recovery Steam Generation; L/G = Liquid to gas ratio in the absorber; NGCC= Natural Gas Combine Cycle; SSFCC= Sequential Supplementary Firing Combined Cycle

5.3 Part-load thermodynamic modelling of power plant

The part-load modelling of the NGCC and SSFCC power plants has three main units: the gas turbine, the HRSG and the steam cycle. This section describes the thermodynamic model of the power plant for the gas turbine and steam cycle with details.

5.3.1 Gas Turbine

Compressor

The inlet guide vanes are typically located only in the first stage of the compressor due to the complexity of the adjusting mechanism and physical dimensional limitations. The positive effect of the IGV is diluted in other stages downstream of the first (Boyce, 2006). The IGV at the compressor inlet regulates the incoming air at the compressor suction and the compression ratio is reduced (Kamire, et al, 2012; Elmasri, 2002). The air regulates the air/fuel ratio of the gas turbine to control the load and the temperature of the exhaust gas. The reduction of the pressure ratio is necessary when the volumetric flow is reduced in order to avoid surge condition. A surging phenomenon is associated with a sudden pressure drop and with violent aerodynamic pulsations that are transmitted throughout the machine causing high oscillations in mass-flow and pressure. Oscillation produces vibrations that result in high stresses on the compressor components and must be avoided.

The air enters the rotor as shown in Figure 5.4 with an absolute velocity (V) and an angle α_1, which combines vectorially with the tangential velocity of the blades (U) to produce the resultant relative velocity W_1 at an angle α_2. Air flowing through the passages formed by the rotor blades gives a relative velocity W_2 at angle α_4, which is less than α_2 because of the blades. The IGV is adjusted to control the axial velocity into the first stage of the compressor varying the angle as shown in Figure 5.4, where the new trajectory is shown by red lines once the IGVs are actuated. The effect of varying the angle is:

1. Change the absolute velocity V_1 that affects W_1
2. Reduce the effective throat area, which affects the mass flow
3. Lower the pressure at the inlet which affects the pressure downstream of the pressure ratio of each stage

Change of delta in relative velocity reduces work input. It is explained by the Euler turbine equation shown in Equation 5.1 assuming that the blade speeds at the inlet and exit of the compressor are the same.

$$H = \frac{U}{g_c}(V_{Z1}tan\alpha_2 - V_{z2}tan\alpha_3)$$ Equation 5.1

Where

H Energy head

U Tangential velocity of the blade

V_{Z1} Absolute axial velocity for the rotor

V_{Z2} Absolute axial velocity for the stator

g_c Gravitational acceleration

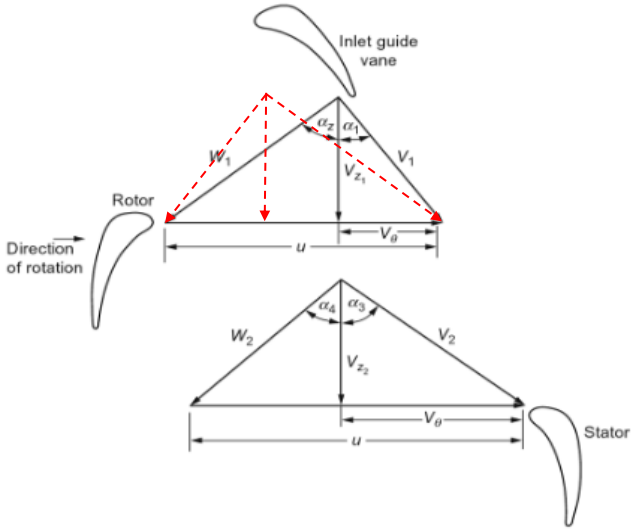

Figure 5.4. Typical velocity triangles for an axial-flow compressor (Boyce, 2006)

The behavior of compressor and gas turbine is given by performance maps. A particular performance map of a gas turbine can be adimensionalised with values of unity at design conditions for normalised flow, efficiency, and pressure ratio to create a generic performance map that can be used for any compressor. In this study, the compressor map of the gas turbine 9FB is based on Thermoflow data (Alcaraz, 2015) and validated by real information published by Ol'khovskii, (2013) as shown in Figures 5.5 and 5.6. It should be more accurate than a generic map. The pressure ratio and the efficiency of the compressor required in Equation 5.2 is provided by the performance map shown in Figure 5.5 and Figure 5.6.

$$\eta_{co} = \left[\frac{P_R^{\frac{k-1}{k}} - 1}{\frac{T_{out}}{T_{in}} - 1}\right]$$ Equation 5.2

Where

η_{CO} is the efficiency of the compressor (%)

P_R is the pressure ratio

T_{out} is the temperature at the outlet if the compressor (K)

T_{in} is the temperature at the inlet if the compressor in (K)

k is the isentropic exponent $\frac{C_p}{C_v}$

Figure 5.5 shows the variation of the pressure ratio at different mass flow for the gas turbine 9FB from two sources. There is a difference between the two curves. The details of the difference in the pressure ratio are given in Ol'khovskii, (2013). The reason for this difference is because the information of the compressor 9FB given in Ol'khovskii, (2013) is an upgraded version by General Electric used in chapter 4, this has higher compressor efficiency. Most new gas turbines are conservatively rated when introduced and are then periodically upgraded by their manufactures by retrofitting new design technology (Gas turbine handbook, 2013). In the 9FB GTU the pressure ratio has been increased at the same air flow rate from 16.5 to 18 with the compressor efficiency simultaneously increased from 88.5 to 90-90.5 %.

In this work, information from Alcaraz, (2015) is used. The reason for that is because, unlike the information from Ol'khovskii, (2013) where only the gas turbine information is available, in Alcaraz (2015) complete information of the NGCC is available, which is useful to validate the conventional NGCC model.

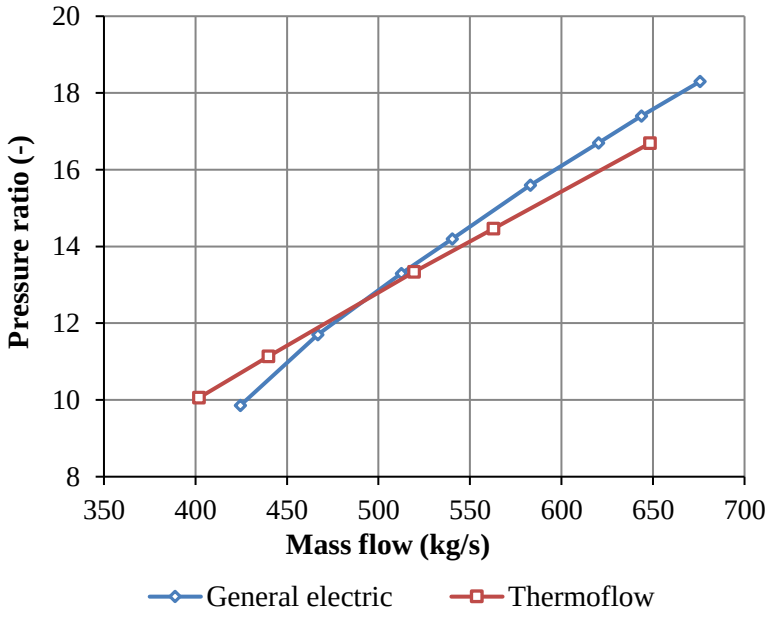

Figure 5.5. Variation of the pressure ratio at different mass flow for 9FB gas turbine compressor (Ol'khovskii, 2013; Alcaraz, 2015). Pressure ratio performance used in the simulation developed in Aspen Plus@ as an input data

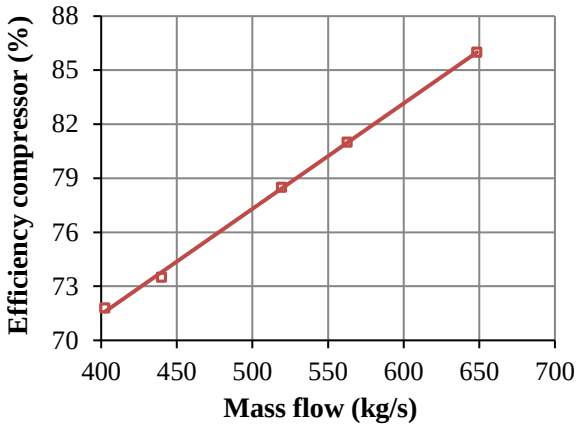

Figure 5.6. Variation of the efficiency at different mass flow for 9FB gas turbine compressor (Alcaraz, 2015). Efficiency performance used in the simulation as an input data

Combustor

The air / fuel ratio at part-load is taken from Alcaraz (2015) as shown in Figure 5.7 and 5.8 and validated with information published by Ol'khovskii, (2013) shown in Figure 5.9. The information from both sources is in good agreement. To control the inlet and outlet temperature of the turbine, it is necessary to adjust both the air flow and the fuel flow in the combustor (Elmasri, 2002). The optimum exhaust temperature of the gas turbine at partial load is different for each gas turbine from the different manufacturers. The resulting air/fuel ratio at different load for the gas turbine 9FB is shown in Figure 5.10.

The model for the combustion chamber is a simple heat and mass balance, taking into account the difference in enthalpy of formation of the reactants and the combustion products. It is calculated using a Gibbs reactor in Aspen plus@. The combustion was assumed to be complete. A simplified equation to calculate the temperature at the outlet of the combustor is given by Equation 5.3 and 5.4. These equations and assumptions are also used for supplementary firing in the HRSG. These equations give a good approximation when compared with Thermoflow data that is enough for the purpose of this study.

The heat balance:

$$\left[m_{gas} h_{gas}\right]_{out} = \left[\mathrm{m}_{air}\ \mathrm{h}_{air}\right]_{in} + \left[\mathrm{m}_{fuel}\ \mathrm{h}_{fuel}\right]_{in} + \mathrm{m}_{fuel}\mathrm{LHV}_{\mathrm{fuel}} \qquad \text{Equation 5.3}$$

Mass balance:

$$\left[m_{gas}\right]_{out} = \left[\mathrm{m}_{air}\ \right]_{in} + \left[\mathrm{m}_{fuel}\ \right]_{in} \qquad \text{Equation 5.4}$$

Where

m_{gas} Mass flow of combustion gases at the outlet of the combustor (m/s)

h_{gas}	Enthalpy of combustion gases at the outlet of the combustor (m/s)
m_{air}	Mass flow of air that enters in the combustor (m/s)
h_{air}	Enthalpy of air that enters in the combustor (kJ/kg)
m_{fuel}	Mass flow of fuel that enters in the combustor (m/s)
h_{fuel}	Enthalpy of fuel that enters in the combustor (kJ/kg)
LHV_{fuel}	Low heat value of the fuel (kJ/kg)

The composition of the combustion gas is calculated by the combustion reaction

$$aCH_4 + bC_2H_6 + cC_3H_8 + dC_4H_{10} + eCO_2 + fN_2 + gH_2O + h(O_2+3.76N_2) \leftrightarrow wCO_2 + xH_2O + yN_2 + zO_2$$

Where a, b, c, d, e, f, and g are the natural gas composition; h the air; and w, x, y, and z the product (combustion gas). The reaction for each product is given for the follow molar balances:

O_2 balance

$$z = \frac{2e + g + 2h - 2w - x}{2}$$

CO_2 balance

$$w = a + 2b + 3c + 4d + e$$

H_2O balance

$$x = g + nH_2$$

$$nH_2 = \frac{4a + 6b + 8c + 10d}{2}$$

N_2 balance

$$y = 3.76h + f$$

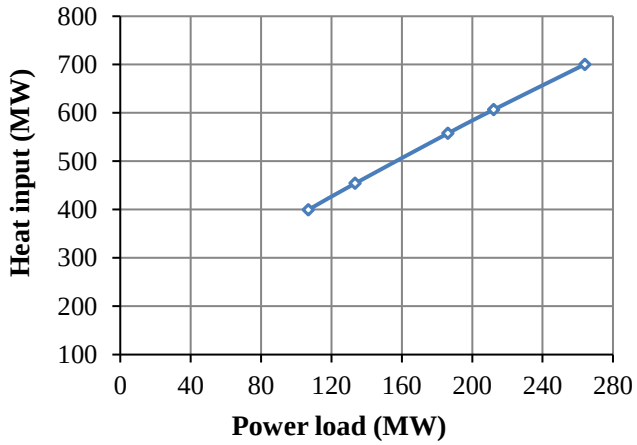

Figure 5.7. Dependence of heat input and the electric load (Alcaraz, 2015). Heat input (natural gas mass flow) performance used in the simulation as an input data

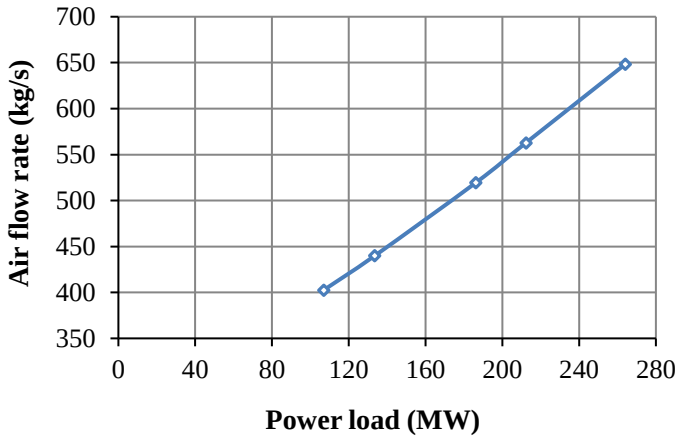

Figure 5.8. Dependence of air flowrate and the electric load (Alcaraz, 2015). Air flow rate performance from Thermoflow used in the simulation as an input data

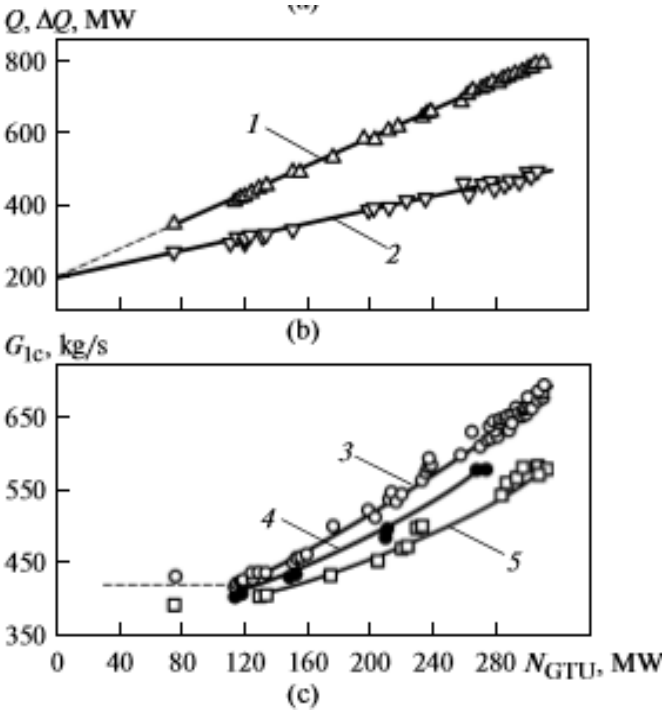

Figure 5.9. Variation of air flow rate G_{1C}, heat input Q, depending on the position of the IGV position on the electric load GTU, (b) heat inputs, and (c) air flowrate and IGV position. (1) Heat input to the combustion chamber, MW; (2) enthalpy of spent gases, MW; (3) air flow rate, kg/s; and (4) and (5) IGV position in summer and in winter (Ol'khovskii, 2013)

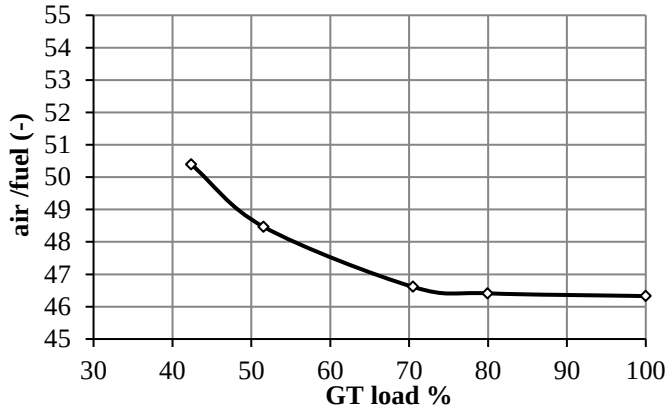

Figure 5.10. Variation of the air /fuel ratio on the electrical load for the gas turbine 9FB (Alcaraz, 2015). Air / fuel performance from Thermoflow is used in the simulation developed in Aspen Plus@ as an input data

Gas turbine

The assumption of a constant efficiency at part-load is made in the model. Kehlhofer indicates "At constant rotational speed, the efficiency depends only upon the enthalpy drop. In part-load no important changes occur in that drop except in the last stages. A big portion of the machine is operating at a constant efficiency" (Kehlhofer, 2009, p.367). The same gas turbine methodology is applied for the NGCC configuration and both supercritical and subcritical SSFCC part-load with variable IGV. The main differences occur in the HRSG in all case studies.

The gas turbine power output calculated in Aspen plus was validated with Thermoflow data as shown in Figure 5.11

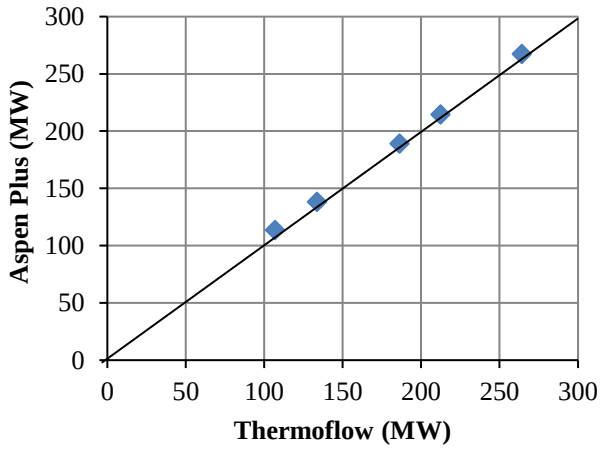

Figure 5.11. Comparison of gas turbine power output calculated with Aspen plus vs Thermoflow

5.3.2 Heat recovery steam generator (HRSG) and steam turbine cycle

The HRSG transfers heat from the gas turbine exhaust gas to the steam cycle. A subcritical boiler, it consists of three sections for each pressure level: an economizer, an evaporator or boiler, and a super-heater section as shown in Figure 5.23. In the economizer the subcooled water is heated up to saturated liquid temperature, although, in practice, a small degree of subcooling is applied to avoid a two phase operation; in the evaporator the marginally subcooled liquid is converted to saturated vapour and finally in the super-heater the saturated vapour is converted to superheated steam. The sections are integrated with a set of tubes that can be modelled as a generic heat exchanger. The main parameters at part-load are pressure, temperature, and mass flow.

Attemperation or de-superheating

At part-load operation the temperature of the live steam at the outlet of the superheater increases because of the increment in the temperature of the exhaust gas. The exhaust gas temperature increases due to reduction in the efficiency of the gas turbine section (Kehlhofer, et al, 2009). High steam temperature can be problematic for steam turbine operation over the maximum designed temperature of the main steam so it is necessary to keep it constant by using attemperation. The water used for attemperation comes from high pressure pumps as shown in Figure 5.23 in order to act as a spray with a uniform distribution through the steam to be cooled (Kehlhofer, et al, 2009). The live-steam temperature control loop in the drum-type HRSG limits the peak temperature during part-load and hot ambient temperature. For that reason, the attemperation is located after the superheater and not between two portions of the superheater as in conventional steam generator (Shown in Figure 5.23).

By burning supplementary fuel in the HRSG, the total amount of heat generated for steam generation becomes independent from the gas turbine and the HRSG behaves more as a conventional boiler. The additional combustion effectively adds a degree of freedom in the operation and optimization of the plant at part-load. The flue gas temperature after supplementary fuel and the steam temperature are higher than in HRSG without supplementary fuel. They rise further at part-load because the amount of steam is reduced in the heat exchanger and the temperature of the exhaust gas increases at part-load, more details is given in chapter 6 where results are described. In a conventional boiler, due to the higher temperature of the flue gas, the attemperation is located between sections of superheaters (primary and secondary superheaters) (Elmasri, 2002). Based on this argument, in this study the attemperation for supercritical and subcritical SSFCC of the main steam is located

between two sections as shown in Figure 5.24 and Figure 5.25. The equation needed to calculate the mass flow rate of the attemperation to maintain the temperature of the vapour constant at the inlet of HP and IP steam turbines is given in the Equation 5.5.

$$m_{SH}h_{SH} + m_{attemp}h_{attemp} = (m_{SH} + m_{attemp})h_{turbine} \quad \text{Equation 5.5}$$

Where

m_{SH}	Mass flow of vapour from superheater (kg/s)
h_{SH}	Enthalpy of vapour from superheater (kJ/kg)
m_{attemp}	Mass flow of water to temper the vapor from superheater (kg/s)
h_{SH}	Enthalpy of water to temper the vapor from superheater (kJ/kg)
$h_{turbine}$	Enthalpy of live steam before entering the turbine (the temperature at this point is constant at part-load) (kJ/kg)

The second step is to determine the pressure of the pumps and the pressure drop in each heat exchanger through the HRSG.

Pressure drop

The pressure drop for each heat exchanger is estimated from a simple flow – pressure drop relationship given by Equation 5.6, where the equipment parameter is the loss coefficient *k*. At design condition the constant *k* for a conventional NGCC is calculated using the pressure, temperature, and mass flow provided by Thermoflow data and for subcritical and supercritical SSFCC is calculated using the pressure, temperature, and mass flow at full load after the optimisation. At part-load, k is keeping constant and now the variable calculated is the pressure at the outlet of the heat exchanger.

This equation is used to estimate the pressure drop from the cross-over pipe where steam is extracted for solvent regeneration to the solvent reboiler of the capture plant, which includes the pressure drop through the pipeline and de-superheating. This equation was programmed in Aspen plus using a Fortran subroutine. The de-superheater is a heat exchanger to convert the steam going to the reboiler into saturation conditions.

$$\Delta p = P_{in} - P_{out} = km^2 \frac{\frac{1}{\rho_{in}} + \frac{1}{\rho_{out}}}{2} \quad \text{Equation 5.6}$$

Where

Δp	Pressure drop of steam through the heat exchanger (Pa)
m	Mass flow rate (kg/s)
ρ_{in} and ρ_{out}	Density at the inlet and outlet respectively (kg/m^3)

k A constant (1/m^4)

Pressure required at the inlet of the steam turbines

Most steam turbines in combined cycle plants operate by sliding pressure operation and generally have no control stage with a nozzle group (Kehlhofer, et al, 2009). A portion of the steam turbine with no extraction is defined by Equation 5.7 for its absorption capacity using the Law of Cones.

$$\frac{\dot{m}_S}{\dot{m}_{S0}} = \frac{\bar{V} x p_a}{\overline{V_D} x p_{a0}} \sqrt{\frac{p_{a0} x v_{a0}}{p_a x v_a}} \sqrt{\frac{1 - \left|\frac{p_w}{p_a}\right|^{\frac{n+1}{n}}}{1 - \left|\frac{p_{w0}}{p_{a0}}\right|^{\frac{n+1}{n}}}} \qquad \text{Equation 5.7}$$

Where

$\dot{m}_S$ Steam mass flow (kg/s)

p Pressure (bar)

v Specific volume (m^3/kg)

$\bar{V}$ Average swallowing capacity

n Polytrophic exponent

The suffix 0 is the design point, a inlet and w outlet of the steam turbine

In steam turbines, the absolute difference between the inlet and the outlet pressure is large so that the pressure ratio Pw/Pa is small and the ratio of the absorption capacity is close to 1. Equation 5.7 can then be simplified to Equation 5.8.

$$\frac{\dot{m}_S}{\dot{m}_{S0}} = \sqrt{\frac{p_{a0} x v_{a0}}{p_a x v_a}} \qquad \text{Equation 5.8}$$

At part-load operation, the mass flow of steam generated is reduced and this equation is used to calculate the pressure across the turbine, and by extension the pump heads. This equation was programmed in Aspen plus using a Fortran subroutine.

For a supercritical combined cycle operated at part-load with a fixed boiler pressure using a throttle valve, Equation 5.8 is used to calculate the pressure at the inlet of the supercritical steam turbine, therefore the pressure drops in the valve.

Overall heat-transfer coefficient

Two equations are needed to predict the behavior of all heat exchangers in the HRSG and the condenser (Rovira et al, 2010). The first one is the energy balance between the streams,

considering heat loss by radiation, convection, and conduction from the HRSG representing by Equations 5.9 and 5.10. The second equation is the heat transfer across the heat exchanger surface given by Equation 5.11 (Valdes et al. 2004; and Gonzalez et al, 2007).

$$Q = m_v (h_{vout} - h_{vin})$$ Equation 5.9

$$Q = m_g (h_{gout} - h_{gin})$$ Equation 5.10

If a counter-flow exchanger is used, the heat transfer equation allows calculating the product of the overall heat-transfer coefficient *U* and the exchange surface A by means of a logarithmic mean temperature difference, as in Equation 5.11. U_DA is calculated at design condition and the new *UA* at part-load is calculated using the correlation shown in Equation 5.12. Additional information is provided in Appendix C. The same set of equations can be used for a once through heat recovery boiler (supercritical condition).

$$Q = UA \frac{(T_{gin} - T_{vout}) - (T_{gout} - T_{vin})}{ln\left(\frac{T_{gin} - T_{vout}}{T_{gout} - T_{vin}}\right)}$$ Equation 5.11

For economizers and evaporators

$$\frac{U_{op}A}{U_DA} = \left(\frac{m_{gop}}{m_{gD}}\right)^m$$ Equation 5.12

For superheaters, Equation 5.12 is

$$\frac{U_{op}A}{U_DA} = \left(\frac{m_{gop}}{m_{gD}}\right)^m \left(\frac{m_{vop}}{m_{vD}}\right)^n$$

Where

Q	Heat transfer (kW)
T_g	Temperature gas side (K)
T_v	Temperature vapour side (K)
h_g	Enthalpy gas side (kJ / s)
h_v	Enthalpy vapour side (kg/s)
m_g	Mass flow of the gas (kg /s)
m_v	Mass flow of the steam (kg /s)
U_D	Overall heat-transfer coefficient at design condition (kW /m^2 K)
Uop	Overall heat-transfer coefficient at part-load (kW /m^2 K)

Suffix *in* and *out* denote inlet and outlet of the heat exchange, and suffix D is design and suffix op operation at part-load condition

The empirical coefficients *m* (gas side) and *n* (vapour side) depend on the geometry and the heat transfer mechanism as shown in the Equation 5.13-5.15, and are dependent on the Nussel number. The coefficient *n* for subcritical vapour is 0.8 and for exhaust gas is 0.6 is estimated based on correlations of the Nussel number shown in Equation 5.13 and Equation 5.14 (Steam its generation and use, 2005).

In a supercritical region, thermophysical properties, such as thermal conductivity, viscosity, density, and specific heat, important to estimate heat transfer, experience radical changes as the temperature approaches and exceeds the critical temperature, as shown in Figure 5.12. The temperature at which the specific heat reaches a peak is known as the *pseudocritical temperature* T_{pc} around 374°C (705 °F). Because of the significant changes in thermophysical properties near the pseudo- critical temperature, a modified approach to evaluating convective heat transfer is needed (Steam its generation and use, 2005). The correlation developed by Swenson et al (Swenson et al, 1965; Shiralkar and Grifftith, 1968; Steam its generation and use, 2005) is given by Equation 5.15 which is a representative relationship for smooth bore tubes, where n is 0.923.

$$\frac{h_v D_i}{k_v} = 0.023 \left[\frac{D_i G_v}{\mu_v}\right]^{0.8} Pr_v^{0.33} \qquad \text{Equation 5.13}$$

$$\frac{h_g D}{k_g} = 0.4 \left[\frac{D G_g}{\mu_g}\right]^{0.6} Pr_g^{0.33} \qquad \text{Equation 5.14}$$

$$\frac{h_v D_i}{k_v} = 0.00459 \left[\frac{D_i G_v}{\mu_v}\right]^{0.923} \left[\frac{H_v - H_b}{T_v - T_b}\right] \left[\frac{\mu_w}{k_w}\right]^{0.613} \left[\frac{v_b}{v_v}\right]^{0.231} \qquad \text{Equation 5.15}$$

Where

h_v Heat transfer coefficient of the steam, (W/m^{2}K)

h_g Heat transfer coefficient of the gas, (W/m^{2}K)

G_v Steam mass flux, (kg/m^{2}s)

G_g Gas mass flux, (kg/m^{2}s)

D_i Diameter inside the tube (m)

D Tube diameter (m)

k_v Thermal conductivity of the steam W/mK)

k_g Thermal conductivity of the gas (W/mK)

μ_v Viscosity of the steam (kg/ms)

μ_g Viscosity of the gas (kg/ms)

Pr_v Prandtl number steam side

Pr_g Prandtl number gas side

H_v Entalphy at wall temperature (J/kg)

H_b Entalphy vapour at bulk fluid temperature (J/kg)

v_v Specific volume at wall temperature (m^3/kg)

v_b Specific volume at bulk fluid temperature (m^3/kg)

T_v Wall temperature (C)

T_b Bulk fluid temperature (C)

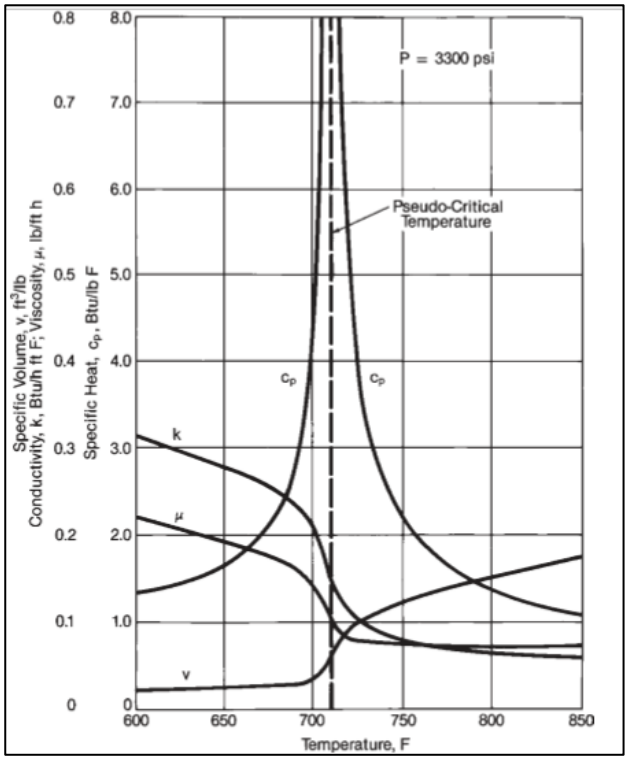

Figure 5.12. Thermophysical properties of water at supercritical condition (Steam its generation and use, 2005)

When supplementary fuel is burnt in the HRSG, the gas temperature increases compared to a standard HRSG. Yet the main contribution to heat transfer remains as convection, for different reasons. The contribution of radiative heat transfer does increase. However, in the case of sequential supplementary firing, radiative heat transfer continues to play a secondary role because the gas temperature only increases to 820°C. This is significantly lower than the typical temperature of around 1500 °C encountered in a conventional boiler. Secondly, natural gas radiation is lower compared to coal or oil (Dumont and Heyen, 2004; Kehlhofer, et al, 2009). The radiation produced by a flame depends on how luminous it is. An oil flame can radiate 3 to 4 times more than a gas flame mainly because of the soot production in the flame which makes it luminescent. A gas flame could produce soot under certain conditions

of mixing, but the amount of radiation attained is still significantly lower than an oil and coal flame (Sáez, 2010). The tube spacing is short in an HRSG compared to tubes in a conventional boiler because minimum soot is generated.

Steam generation in the evaporators

In the evaporator, a phase transition from water to steam occurs, which means that the Equation 5.9 must be replaced by Equation 5.16.

$$Q = m_v \left(\Delta h_{evaporation}\right) \qquad \text{Equation 5.16}$$

Where

$\Delta h_{evaporation}$ Evaporation enthalpy (kW)

The $\Delta h_{evaporation}$ depends on the saturation pressure. The steam mass flow rate in the HRSG of the NGCC and subcritical SSFCC configurations at part-load is calculated taking into account the capacity of the evaporators to convert the water from saturated liquid to saturated vapour and the fact that the separation between the gas and the liquid phase in evaporators occurs through gravity. The steam mass flow rate in the HRSG of the NGCC and subcritical SSFCC at part-load is calculated considering the capacity of the size of the evaporators to convert the water from saturated liquid to saturated vapour. This is possible considering an additional assumption in the system: dryness fraction **x = 1** at the outlet of HP, IP, and LP boilers in the NGCC as shown in Figure 5.23 and at the outlet of the HP boiler in subcritical SSFCC Figure 5.24.

Steam generation in the supercritical evaporator once through boiler (OTB)

The liquid single phase and vapour single phase conditions are easily identified from temperature and pressure data. As we can see in Figure 5.13, there is no different between supercritical and subcritical heat transfer coefficients for liquid from -73°C to 377°C. The difference between supercritical and subcritical heat transfer coefficients for vapour is not too different from 527°C, as shown in Figure 5.14. The supercritical HRSG of SSFCC includes a supercritical evaporator arranged to supply steam to a superheater between the supercritical evaporator and the economisers of the HRSG. In this section, the separation of liquid and steam is not so clear. Unlike in the evaporator of a conventional HRSG of NGCC where the amount of steam generated depends on the evaporator capacity, in a supercritical SSFCC, the amount of steam generated in the HRSG would depend on the capacity of the economiser to rise the temperature to supercritical temperature where the unstable condition of the steam and water starts. In that section, the heat transfer from 377°C to 527°C occurs in

the evaporator OTB and the heat transfer coefficient used, as is mentioned before, is shown in Equation 5.15.

A rigorous mathematical model is proposed by Rovira et al, (2010) to calculate the heat in the section of evaporator OTB. His model consists of discretising the heat as he considered that it is not constant, the heat is calculated as integration function. Here the heat transfer for evaporator OTB is calculated using Equation 5.9, 5.10, 5.11 and 5.12.

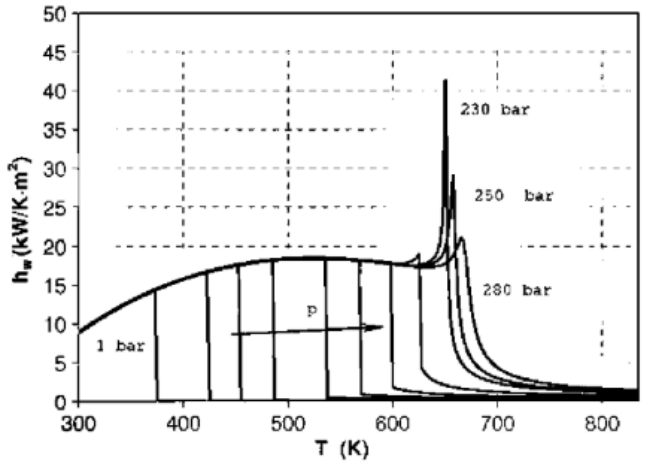

Figure 5.13. Usual convective heat transfer coefficient of liquid water at different pressure (Rovira et al, 2010)

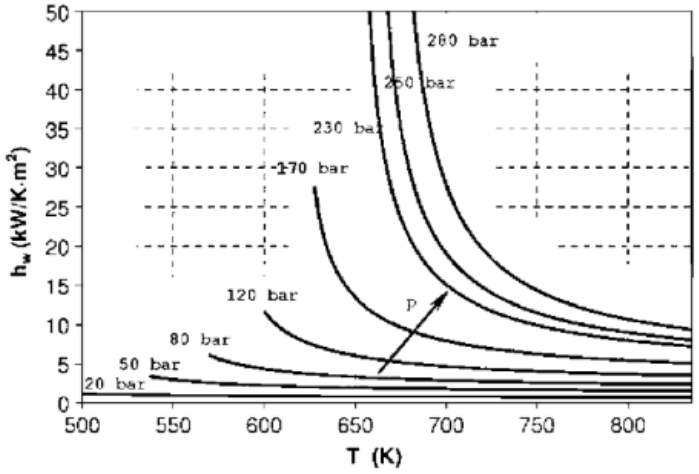

Figure 5.14. Convective heat transfer coefficient of steam at different pressure (Rovira et al, 2010)

Condenser

One option for off-design modelling of the condenser is to fix the cooling water circulation rate, regardless of the reduced load. In that way, the cooling water pumps are running at an almost constant speed (Halvorsen, 2012). As the gas turbine load is reduced, the steam generation in the HRSG is reduced and less steam needs to be condensed in the condenser

for a given condenser pressure. In this thesis the total amount of cooling water is calculated at full load to condense the saturated mixture of steam and water leaving the LP steam turbine and is kept constant at part-load. If the cooling water flow is maintained constant at part load, the vacuum is reduced even further due to a smaller pinch point in the condenser. It is also possible to regulate the cooling water flow by a regulation in the pump capacity or by shut-off one or more pumps, dependent of the number of pumps in the system (Halvorsen, 2012). Although the mechanical energy in the pump is reduced, the pressure in the condenser is higher compared to the case where the pumps are running at full capacity (Halvorsen, 2012).

Throttling valve

Throttling is used at the inlet of the HP steam turbine in the supercritical combined cycle operated at "fixed boiler pressure" in order to control the pressure at the inlet of the steam turbine. In this method steam is passed through a restricted passage thereby reducing its pressure across the governing valve. The flow rate is controlled using a partially opened steam control valve.

Comparison of simulation results of the steam cycle of a conventional NGCC is shown in Figures 5.15 to 5.22. The simulation carried out using Aspen plus is compared with Thermoflow data. The performance of steam turbine power output, steam mass flow of HP steam turbine, steam mass flow of IP steam turbine, steam mass flow of BP steam turbine, inlet pressure of HP steam, outlet pressure of HP steam, inlet pressure of IP steam, inlet pressure of LP steam is compared with information provided in Appendix B.

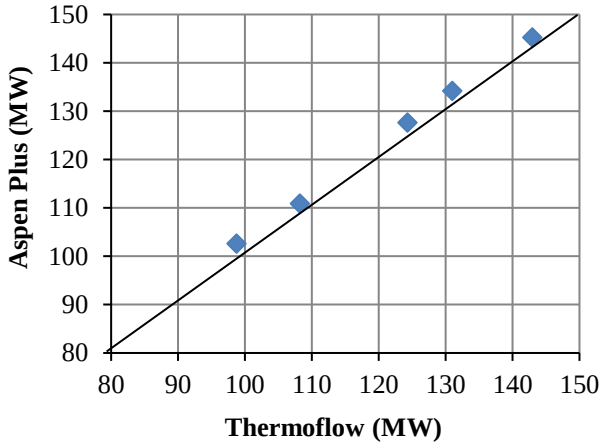

Figure 5.15. Comparison of steam turbine power output calculated with Aspen plus and Thermoflow

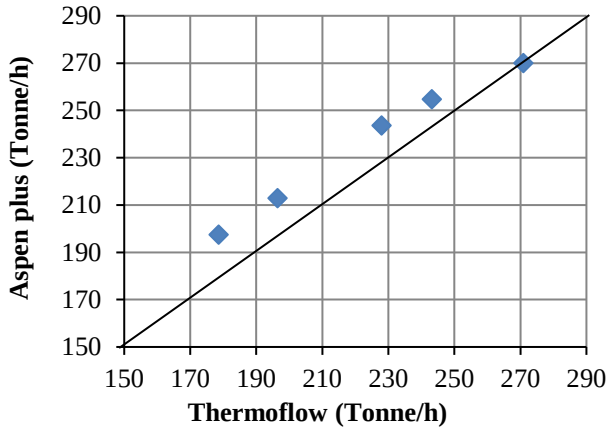

Figure 5.16. Comparison of steam mass flow of HP steam turbine calculated with Aspen plus and Thermoflow

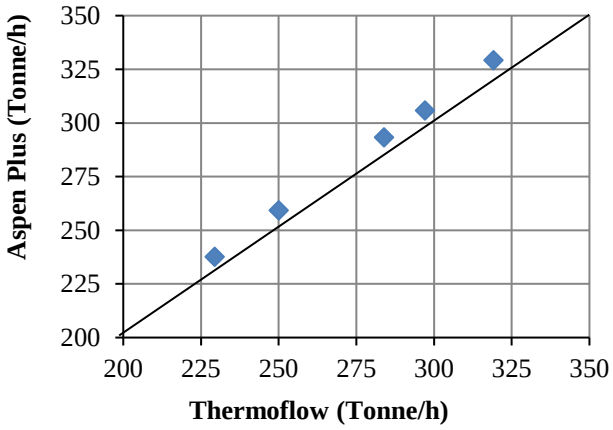

Figure 5.17. Comparison of steam mass flow of IP steam turbine calculated with Aspen plus and Thermoflow

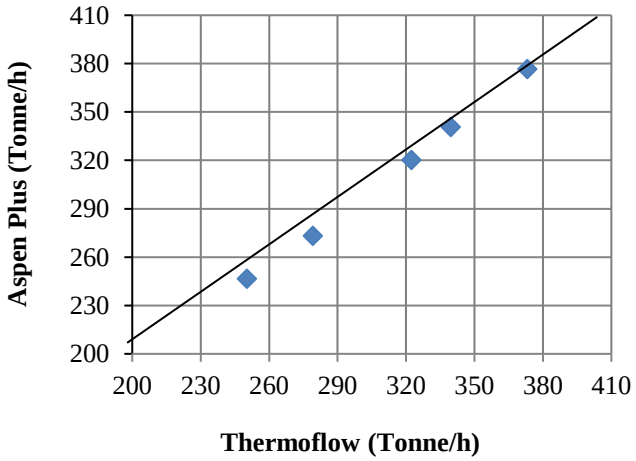

Figure 5.18. Comparison of steam mass flow of LP steam turbine calculated with Aspen plus and Thermoflow

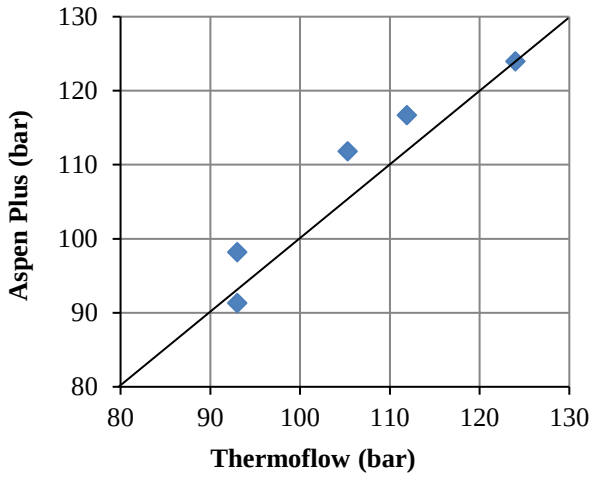

Figure 5.19. Comparison of inlet pressure of HP steam (HP steam turbine) calculated with Aspen plus and Thermoflow

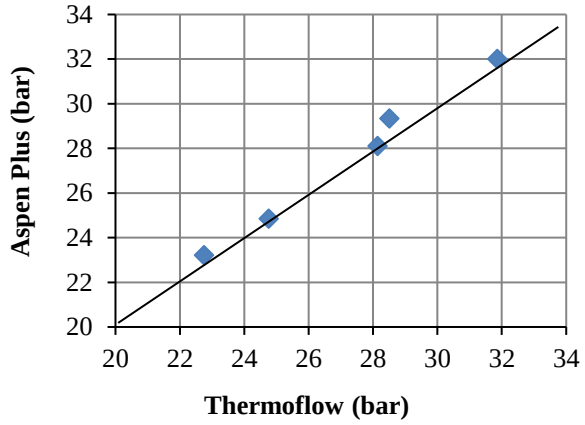

Figure 5.20. Comparison of outlet pressure of HP steam (HP steam turbine) calculated with Aspen plus and Thermoflow

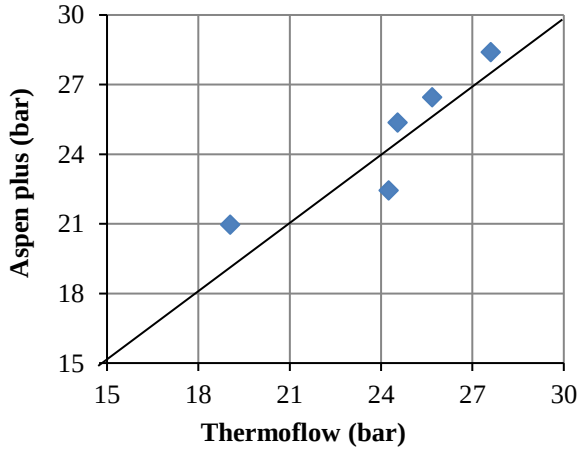

Figure 5.21. Comparison of inlet pressure of IP steam (IP steam turbine) calculated with Aspen plus and Thermoflow

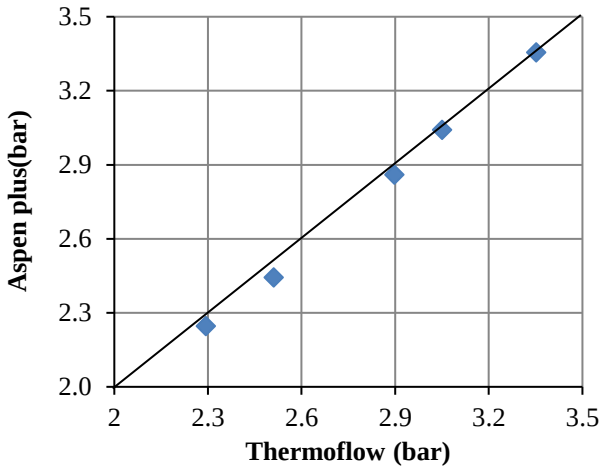

Figure 5.22. Comparison of inlet pressure of LP steam (LP steam turbine) calculated with Aspen plus and Thermoflow

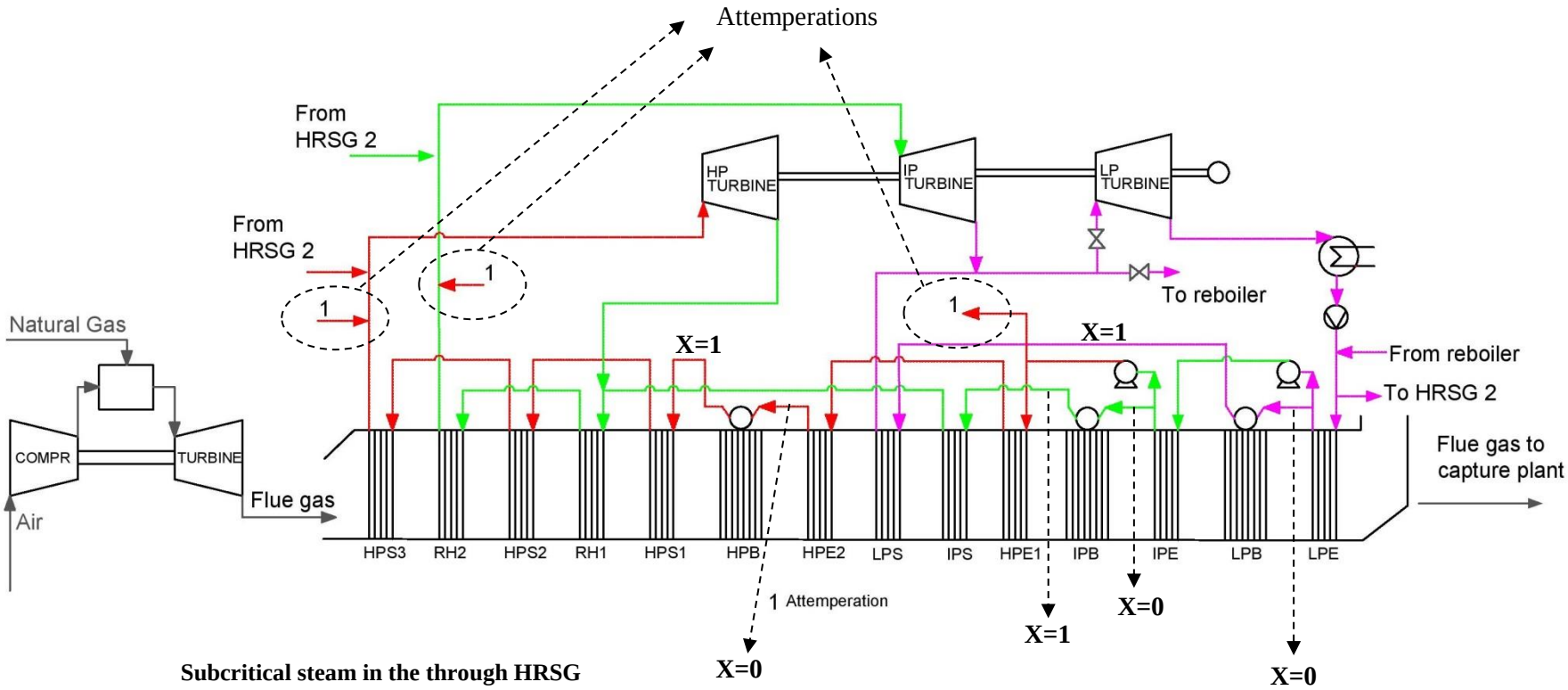

Subcritical steam in the through HRSG

$$\frac{h_v D_i}{k_v} = 0.023 \left[\frac{D_i G_v}{\mu_v}\right]^{0.8} Pr_v^{0.33}$$

Figure 5.23. Schematic process flow diagram of the conventional natural gas combined cycle configuration with two GE 937 IFB gas turbines, two triple pressure HRSGs and one subcritical steam turbine Natural gas combined cycle simulated in Aspen Plus@ using equation oriented tool

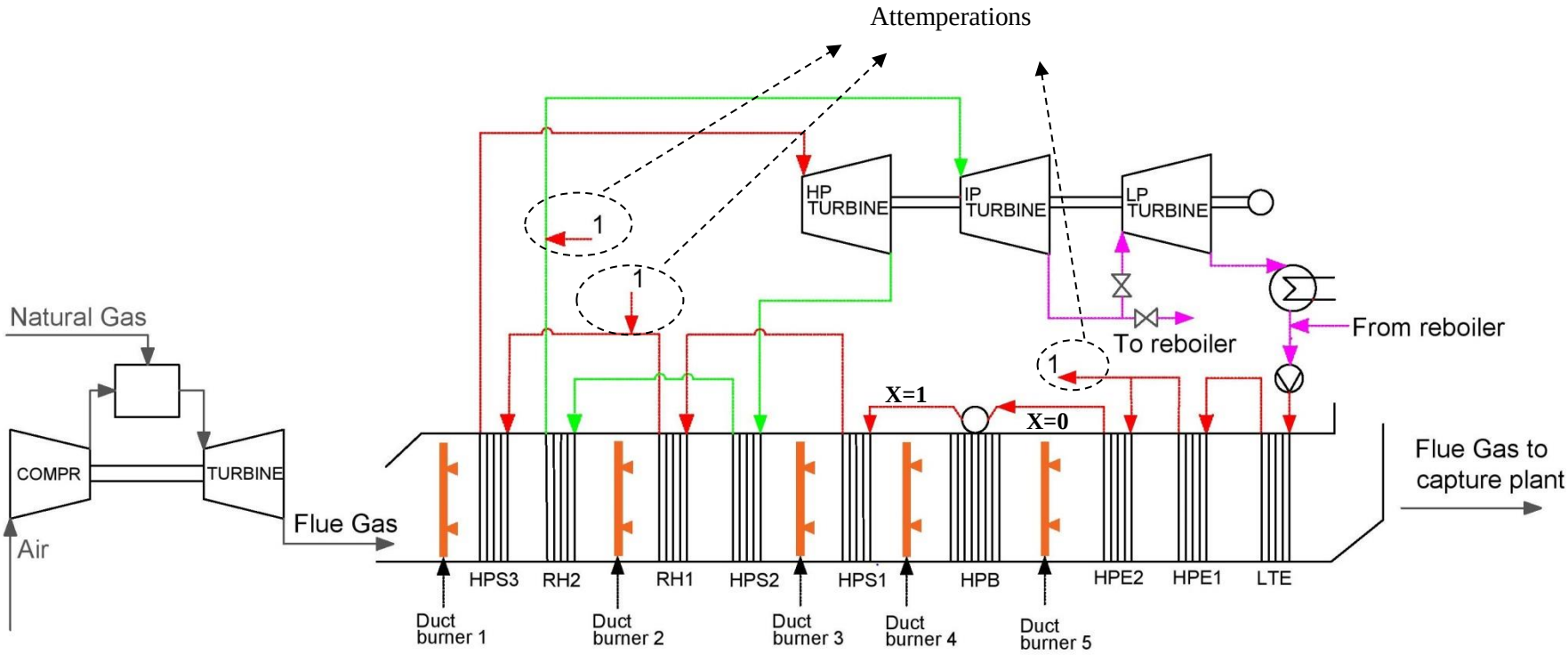

Subcritical steam in the HRSG

$$\frac{h_v D_i}{k_v} = 0.023 \left[\frac{D_i G_v}{\mu_v}\right]^{0.8} Pr_v^{0.33}$$

Figure 5.24. Schematic process flow diagram of a subcritical sequential supplementary firing configuration with one GE 937 IFB / single pressure HRSG train combined with a single reheat steam cycle simulated in Aspen Plus@ using equation oriented tool

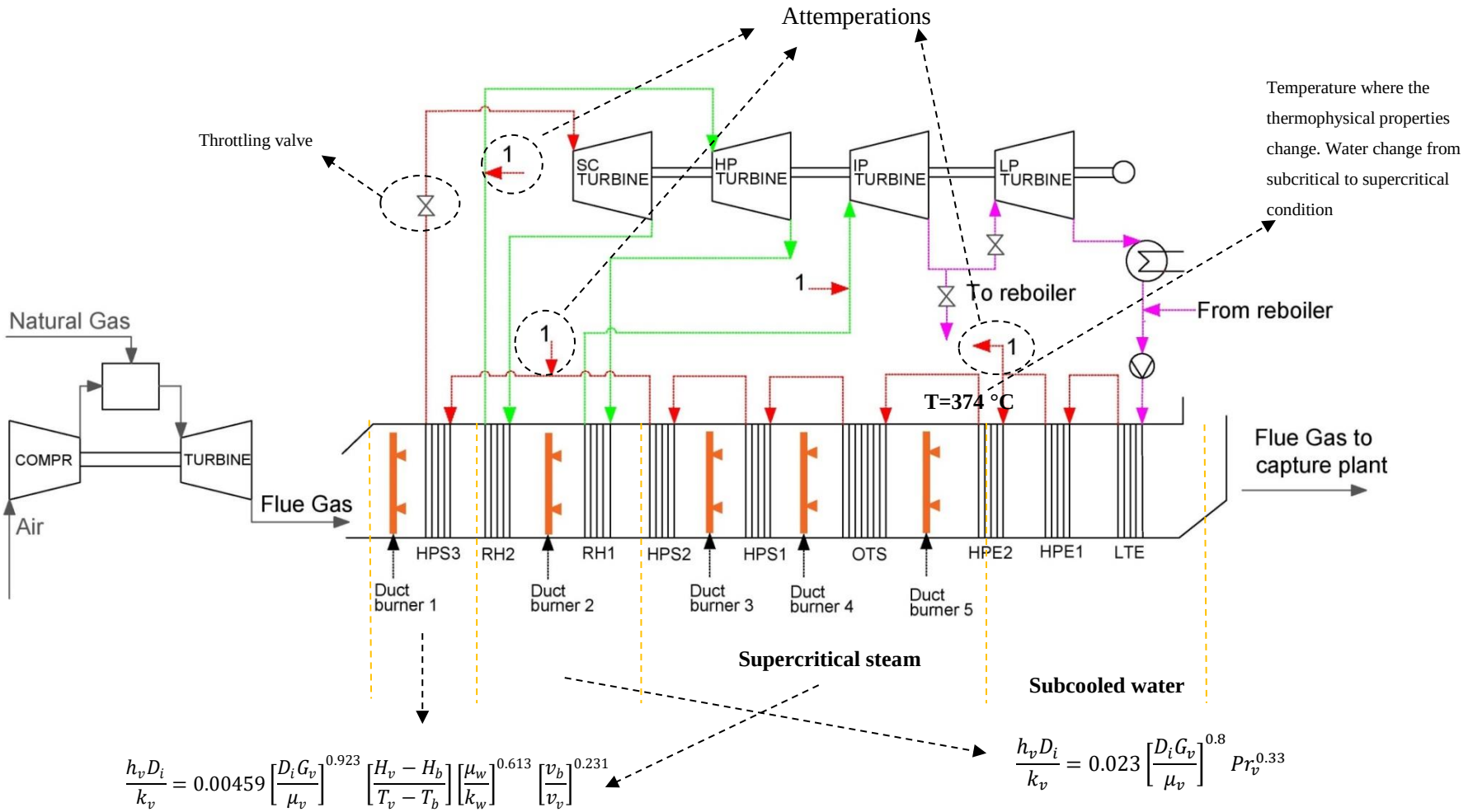

Figure 5.25. Schematic process flow diagram of a supercritical sequential supplementary firing configuration with one GE 937 IFB/single pressure HRSG train combined cycle with a double reheat steam cycle simulated in Aspen Plus@ using equation oriented tool

5.4 Part-load operating strategies for sequential firing in the HRSG

Each stage of sequential supplementary firing in the HRSG effectively adds degrees of freedom to the power plant operator to optimise part-load operation. In this work, the principle for part-load operation is to maximise power output for any given fuel input, including additional fuel firing in the HRSG. The underlying thermodynamic principle is to maximise the average temperature of heat addition to the steam cycle by adjusting the rate of firing of each duct burner, which, in returns, increases the efficiency of the corresponding Carnot cycle.

The methodology followed to adjust the natural gas mass flow in each duct burners is described as follow

1. Fuel reduction is prioritized in the 5th and 4th duct burners where the steam temperature, and by extension the 'local' average temperature of heat addition to the steam cycle is lower than in the first duct burner. The latter is located immediately before the HP superheater and HP and IP reheaters where steam temperature is at its highest.
2. When steam flow rate is reduced across the HRSG to reduce the power output of the steam cycle, the mass flow of natural gas firing in each duct burner needs to be adjusted, if necessary, to maintain flue gas temperatures of below 820°C
3. This principally causes a reduction of firing in the 1st and 2nd duct burners. It is more pronounced at very low load with very low steam mass flow rates absorbing less heat.
4. With a subcritical HRSG and with a supercritical HRSG operated with sliding pressure, an evaporator is located is located between the 4th and 5th duct burners. When steam pressure is below the critical pressure, the latent heat necessary for phase change from saturated liquid to saturated vapour must be overcome with additional gas firing. This does not apply to supercritical configuration with fixed pressure operation of the HSRG.
5. The 3rd burner is then typically adjusted to ensure that the total net steam production across the HRSG matches the power output.

5.5 Conclusion

Power plants in Mexico operate at part-load due to variations in electricity demand. The variability of electricity supply from other energy sources will largely be influenced by the introduction of the intermittent renewable energy, which is expected to increase in 2028, as indicated in (Mexican Ministry of Energy, 2012).

The main characteristic of NGCC power plants is good operating flexibility, which enables power output to be changed according to the electricity demand. It is necessary to evaluate and to ensure the continuity of flexibility in the operation of new alternatives proposed to decarbonise the electricity market.

This chapter focuses on the methodology used to evaluate and define operating strategy modes for supercritical and subcritical SSFCC configurations, with the objective of maximising power and revenue form electricity and CO_2 sales for a given fuel input.

In a conventional NGCC configuration, as the gas turbine changes its load, the steam turbines will automatically adjust their output.

When a power plant combined cycle has supplementary firing, the steam cycle is controlled independently of the gas turbine and the power output is regulated with an additional degree of freedom by adjusting the amount of fuel burnt in the duct burners.

Steam turbines function most economically at part-load using sliding pressure up to 50% and the minimum load for natural gas combined cycle is 50% because of a drastic efficiency drop.

The selected operating modes for evaluating the gas turbine for supercritical and subcritical SSFCC are fixed and variable IGV, and sliding and fixed pressure in the steam cycle

Three thermodynamic models are developed in order to evaluate different operating strategies for a NGCC, supercritical and subcritical SSFCC integrated with CO_2 capture and compression. The model of a NGCC at design condition is based and validated at part-load from information from Thermoflow data (Alcaraz, 2013) and by (Ol'khovskii, et al, 2013). This action aims to validate the equations and assumptions used in the NGCC in order to use them in the novel proposal SSFCC.

6. Performance of supercritical and subcritical sequential supplementary firing power plants with CO_2 capture at part-load operation

6.1 Introduction

This chapter examines the results of the simulation of supercritical and subcritical SSFCC power plants and compares their performance with a conventional NGCC at part-load operation integrated with MEA-based CO_2 capture. Details of the performance of the power plant configurations in different operating modes are provided. The operating modes of the power plants that have been evaluated are summarised in Table 6.1.

The load of the SSFCC can be reduced, as described in chapter 5, in two ways:

1. By using inlet guide vanes and reducing the supplementary fuel in the duct burners
2. By reducing the supplementary fuel in the duct burners with the gas turbine at full load (fixed IGV)

The performance analysis in this chapter begins by describing part-load operation with variable IGV for the gas turbine compressor, and how this method impacts the exhaust gas temperature of the gas turbine and the air / fuel ratio. Subsequently, part-load operation achieved by reducing the amount of supplementary fuel is described and analysed. Then, the results for the part-load operating strategies proposed are presented in two steps:

1. First the thermal efficiency of a conventional NGCC configuration, a subcritical and a supercritical SSFCC without capture are shown. This information is useful to select the most efficient operating strategy so that the variation of thermal efficiency over different load with CO_2 capture and compression system can be introduced
2. Then, the variation of the efficiency at part-load operation with integrated CO_2 capture and compressor unit is presented

Table 6.1. Summary of options for part-load operation of the power plant configurations

Power plant case	**NGCC**	**Supercritical SSFCC**			**Subcritical SSFCC**	
Gas turbine control	Variable Inlet Guide Vanes	Fixed Inlet Guide Vanes	Variable Inlet Guide Vanes	Variable Inlet Guide Vanes	Fixed Inlet Guide Vanes	Variable Inlet Guide Vanes
HRSG	No supplementary firing	Adjust sequential supplementary firing	Adjust sequential supplementary firing	Adjust sequential supplementary firing	Adjust sequential supplementary firing	Adjust sequential supplementary firing
Steam cycle Pressure and temperature	Subcritical	Supercritical	Transition from supercritical to subcritical	Supercritical	Subcritical	Subcritical
Steam cycle control	Heat recovery steam generator sliding pressure	Fixed pressure in the heat recovery steam generator	Heat recovery steam generator sliding pressure	Fixed pressure in the heat recovery steam generator	Heat recovery steam generator sliding pressure	Heat recovery steam generator sliding pressure

6.2 Limitations to part-load operation of sequential supplementary firing combined cycle

By varying the IGV of the compressor, the load of gas turbines can be controlled. As a result, the power output of the gas turbine changes as well as the amount of exhaust gas. Consequently, the total net power output of the NGCC can be reduced by controlling the IGV and by burning less fuel in the duct burners.

6.2.1 Variable inlet guide vanes

The air/fuel ratio of the gas turbine has an important role not only for controlling the load, but also for controlling the temperature of the exhaust gas (TET). It is possible to change the air / fuel ratio by closing or opening the IGV. An elevated exhaust temperature compared to the design temperature is problematic for the last uncooled turbine stages, and the maximum permissible TET is attained 50°C above nominal ISO base load exhaust temperature (600°C in this case) (Elmasri, M., 2002; Kehlhofer R., et al, 2009). Figure 6.1 shows the path followed by the air / fuel ratio when the load of the gas turbine is changed from 100% to 40% and how it controls the variation of the temperature. The simulation results of the inlet temperature (TIT) in the gas turbine and of the air/fuel ratio at different loads are shown in

Figure 6.2. The air / fuel ratio is kept relatively constant around 46.4 (-) between 100% - 80% of the gas turbine load in order to keep the turbine inlet temperature constant. Then, the exhaust gas temperature starts increasing with decreasing load because of the reduction in the efficiency of the gas turbine shown in Figure 6.3. Below 80% low the air / fuel ratio increases in order to avoid a dramatic increment of the TET. Figure 6.1 shown that at approximately 50% load, the increment over the design TET is 45°C, it is in good agreement with the data published sources (Elmasri, M., 2002; Kehlhofer R., et al, 2009), which the maximum permissible is 50° above nominal ISO. The TET is reduced at expense of reducing the TIT, which results in a reduction of the efficiency of the gas turbine.

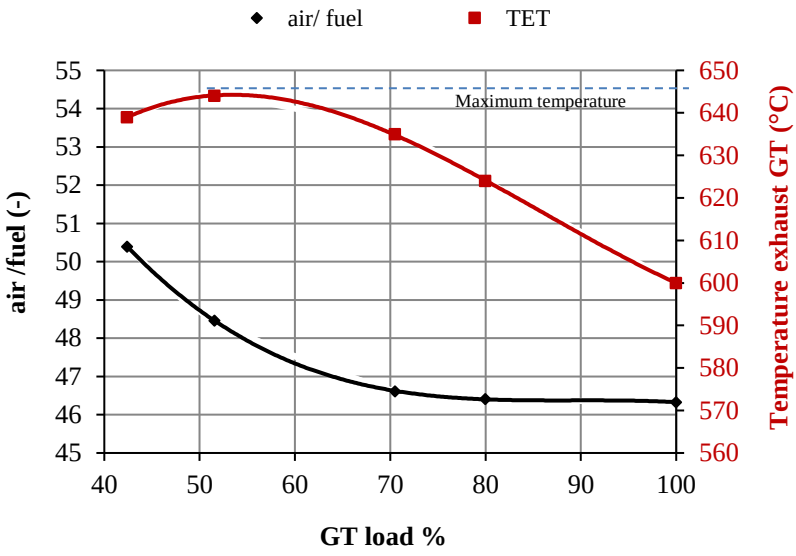

Figure 6.1. Performance of the gas turbine using a variable inlet guide vanes (IGV) Exhaust gas temperature and the load of the gas turbine vary with changes in the air/fuel ratio

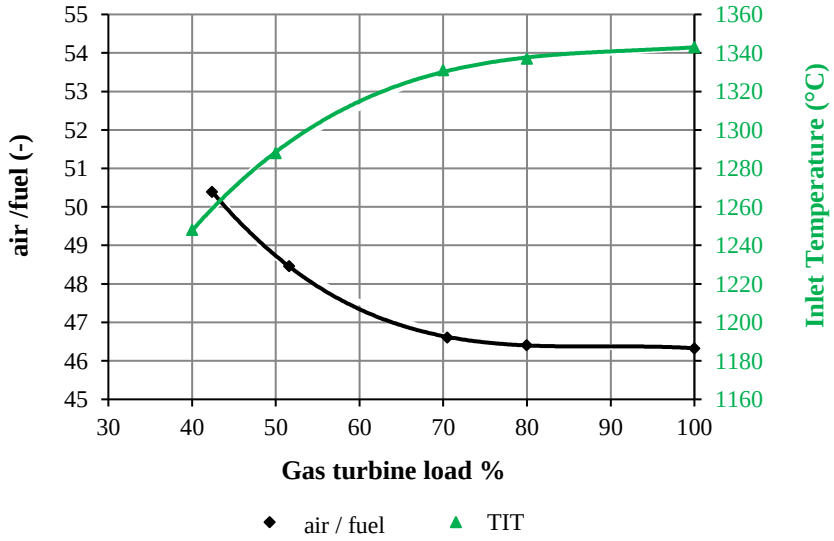

Figure 6.2. Performance of the gas turbine using variable inlet guide vanes (IGV). Inlet gas temperature and the load of the gas turbine vary with changes in the air/fuel ratio

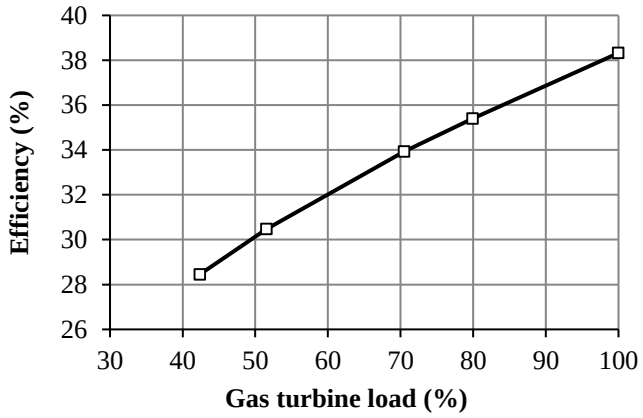

Figure 6.3. Part-load efficiency of the gas turbine

6.2.2 Minimum load generation with variable inlet guide vanes and sequential supplementary firing

As explained in chapter 5, the minimum load of a conventional NGCC is 45% because of the drastically drop in the efficiency and sudden decrement of the temperature of the exhaust gas after attaining the maximum permissible TET of 50°C above nominal ISO. The drop in the exhaust temperature results in a reduction of the steam generated in the HRSG and the efficiency of the cycle.

With sequential supplementary firing, the limitation on minimum load is not the temperature of the exhaust gas because it is controlled by supplementary firing. Table 6.2 shows that, at 42% of total net power output of a supercritical SSFCC with CO_2 capture, the mass flow entering the LP steam turbine cycle is 15% of the design value, indicated in bold number. Reducing the minimum load at which a steam turbine can reliably operate is one way to optimise revenue for marginal base-load units during periods of low electrical demand. For this reason, although it is not unusual to operate power plants at load levels below the typical 25% with respect to full-load limits, steam turbines may experience undesirable damage for a number of reasons (Cotton, 1994). Under severe low flow conditions, the LP stages will subtract net power due to windage and freewheeling causing a significant temperature rise of the materials of the rotating and stationary components. Information of the allowable minimum steam flow steam turbine is commercial in confidence and is not provided by manufacturers in the public domain. Mitsubishi, (2007) indicates that operation of the LP steam turbine above 20% is acceptable. In order to avoid severe damage in the last blades of the LP steam turbine, the minimum load for this configuration of SSFCC is defined as 49% in this thesis in order to keep LP steam turbine flow above 25% indicated in shaded lines.

Table 6.2. Variation of load and steam of supercritical SSFCC with variable IGV, fixed pressure in the HRSG and throttling steam, with CO_2 capture

Load of power plant	%	100	76	58	49	42
Load of gas turbine	%	100	80	75	71	61
Load of steam turbine	%	100	74	51	42	34
Power output SC steam turbine	MW	138	90	54	37	33
Load of supercritical steam turbine	%	100	65	39	27	24
Supercritical steam mass flow	t/h	1292	884	563	413	363
Power output HP steam turbine	MW	69	50	32	22	20
Load of HP steam turbine	%	100	72	46	32	28
HP steam mass flow	t/h	1291	957	654	508	429
Power output IP steam turbine	MW	233	184	134	109	94
Load of IP steam turbine	%	100	79	58	47	40
IP steam mass flow	t/h	1291	1008	736	615	515
Power output LP steam turbine	MW	142	104	62	37	22
Load of LP steam turbine	%	100	73	43	26	**15**
LP steam mass flow	t/h	794	592	376	255	155
LP steam mass flow	%	100	75	47	32	**20**

The numbers in bold indicate the main constrain for the LP steam turbine related to the steam mass flow and the power that are below the acceptable of 20%, and the reason why this percentage of load is not selected. Shaded line indicates the minimum load selected in this study in order to avoid severe damage in the LP steam turbine

6.3 Part-load operation with variable sequential supplementary fuel input in the duct burners

Sequential supplementary firing adds degrees of freedom in terms of part-load operation. One strategy to maximize power output at part-load with sequential supplementary firing is to operate the gas turbine at full load to maintain high efficiency and adjust the total net power output by varying the amount of fuel input in the duct burners. Since the marginal change in thermal efficiency of a steam cycle at part-load is smaller than that of a gas turbine, this section demonstrates that this is the most thermally efficient way to operate a SSFCC plant.

6.3.1 Supercritical combined cycle with fixed inlet guide vanes and with fixed pressure in the heat recovery steam generator

Firstly, the minimum load for sequential supplementary firing with fixed IGV is defined based on the simulation results. In this configuration, the load is reduced by varying the amount of fuel in the duct burners. As a result, the load of the steam cycle is reduced even further compared with a conventional NGCC and supercritical SSFCC with variable IGV. At 52% of the total net power output, the LP steam turbine operates with 17% of the steam mass

flow as shown in Table 6.3 in bold number. Considering 25% as a minumum in the steam, 57% of the total power output is defined as the minimum for this configuration which is indicated in Table 6.3 in shaded line.

Table 6.3. Variation of load and steam of supercritical SSFCC with fixed IGV, fixed pressure in the HRSG and throttling steam, and CO_2 capture

Load of power plant	%	100	84	74	57	52
Load of gas turbine	%	100	100	100	100	100
Load of steam turbine	%	100	77	62	37	30
Power output supercritical steam turbine	MW	139	99	76	43	40
Load of supercritical steam turbine	%	100	71	54	31	29
Supercritical steam mass flow	t/h	1292	951	756	462	410
Power output HP steam turbine	MW	69	53	44	28	25
Load of HP steam turbine	%	100	77	63	40	35
HP steam mass flow	t/h	1292	1009	837	549	468
Power output IP steam turbine	MW	235	188	159	110	90
Load of IP steam turbine	%	100	80	68	47	38
IP steam mass flow	t/h	1292	1039	876	549	468
Power output LP steam turbine	MW	144	109	89	37	18
Load of LP steam turbine	%	100	76	62	26	**13**
LP steam mass flow	t/h	795	624	516	242	134
LP steam mass flow	%	100	79	65	30	**17**

The numbers in bold indicate the main constrain for the LP steam turbine related to the steam mass flow and the power that are below the acceptable of 20%, and the reason why this percentage of load is not selected. Shaded line indicates the minimum load selected in this study in order to avoid severe damage in the LP steam turbine

Figure 6.4 shows the performance of the duct burners for a supercritical SSFCC power plant configuration with fixed IGV, fixed pressure in the HRSG with throttling immediately after the last HP superheater as shown in Figure 5.25. Flue gas temperature in each duct-burner varies with changes in the load, caused by the variation of the natural gas mass flow in the duct burners. At part-load the temperature of each duct burner reduces below the design value of 820 °C at 100% load. At 100% of total power output, the natural gas mass flow rate in the first duct burners is lower than in 4th duct burner because they are limited by the maximum temperature of 820°C, as shown in Figure 6.4. Since the exhaust gas leaving the gas turbine is at 600°C, i.e. higher than the temperature of 557°C at the inlet of the 4th duct burner, less natural gas is required than in the last duct burners to reach the temperature of 820°C.

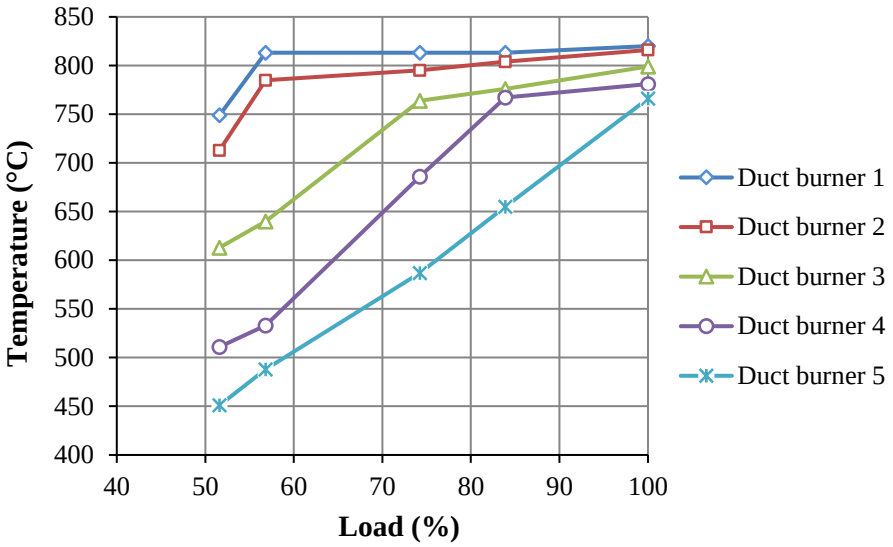

Figure 6.4. Flue gas temperature across the HRSG at part-load for a supercritical SSFCC power plant with fixed IGV and fixed pressure in the HRSG. The flue gas temperature in each duct-burner varies with the changes in load of the power plant, caused by variations of the natural gas mass flow and subsequent reductions of steam flow

The temperature of the last three duct burners decreases significantly more than the temperature of the first two duct burners as a consequence of reducing the fuel mass flow rate, as shown in Figure 6.5. Fuel reduction is prioritized in the last three duct burners. The main reason for this is because the first duct burner is located immediately before superheater 3 (HPSP3) and reheat 2 (RH2) as shown in Figure 5.25, which adds heat to the main steam entering the supercritical steam turbine, and the reheat steam that enters to the HP steam turbine to raise to 630 °C and 600 °C, respectively. The 2nd duct burner is located before reheat 1 (RH1) and superheater 2 (HPSP2) in Figure 5.25, which adds heat to IP steam to raise its temperature to 600 °C.

The air / fuel ratio of the last three duct burners increases drastically when the amount of fuel is reduced from approximately 75% to 50% load, as shown in Figure 6.6. Steam generation in the lower pressure sections of the HRSG is reduced significantly to maximize efficiency, since the average heat-addition temperature is lower than in the high pressure sections. The amount of fuel in the fifth duct burner is reduced to zero at loads below 85%. As less fuel is burnt in the duct burners at part-load, the concentration of O_2 increases and the concentration of CO_2 reduces, as shown in Figure 6.7 and Figure 6.8.

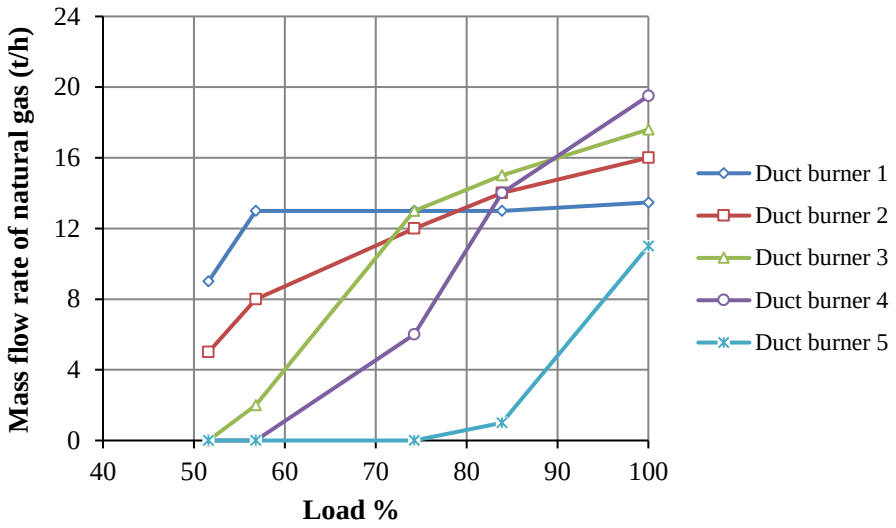

Figure 6.5. Variation of the natural gas mass flow across the HRSG at part-load of a supercritical SSFCC power plant with fixed IGV and fixed pressure in the HRSG

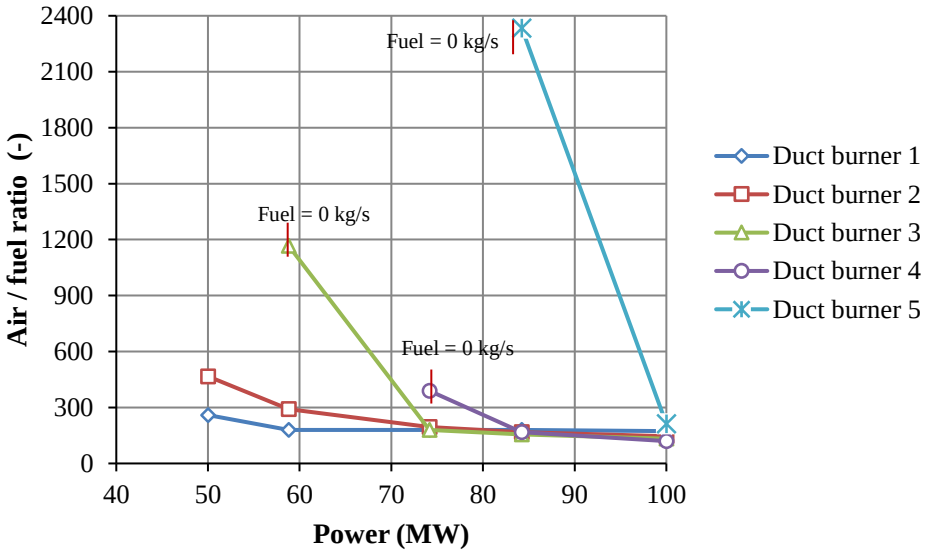

Figure 6.6. air / fuel ratio in each duct-burner at part-load for a supercritical SSFCC power plant with fixed IGV and fixed pressure. The variations are caused by a reduction of the natural gas mass flow to accommodate subsequent reductions of steam production

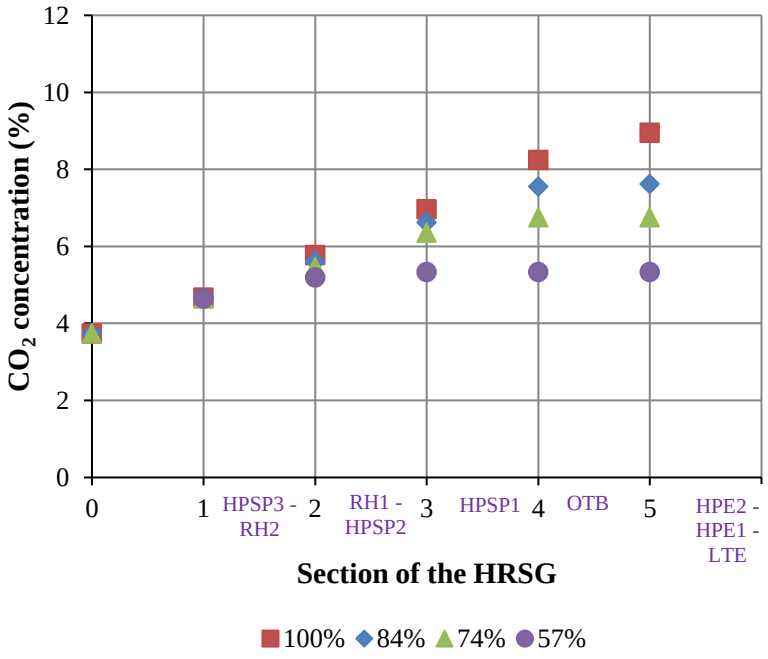

Figure 6.7. Variation of CO_2 concentrations across each section of the HRSG at different loads for a supercritical SSFCC with fixed IGV and fixed pressure in the HRSG. The acronyms used to refer to Figure 5.25

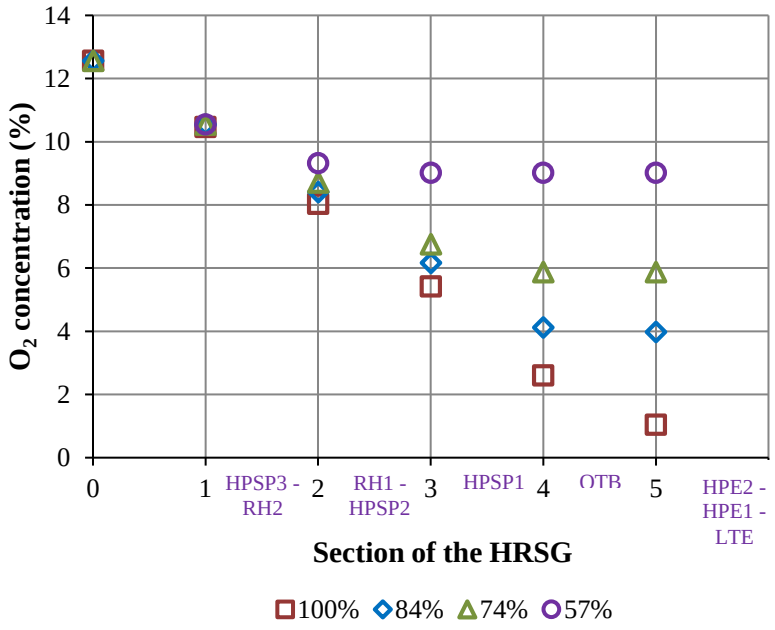

Figure 6.8. Variation of O_2 concentrations across each section of the HRSG at different loads for a supercritical SSFCC with fixed IGV and fixed pressure in the HRSG. The acronyms used to refer to Figure 5.25

6.3.2 Supercritical combined cycle with fixed inlet guide vanes and sliding pressure operation of the heat recovery steam generator

The minimum load determined for supercritical SSFCC with fixed IGV and sliding pressure operation in the HRSG is 57%. This is based on the LP steam turbine operating at 28 of its capacity when the total load is reduced to 57% %, indicated in shaded line, compared with 14% of its capacity, indicated in bold, at 51% of total power output, as shown in Table 6.4.

It is worth noting that the mode of operation of the steam cycle/HRSG, sliding pressure or fixed pressure, has a limited effect on the minimum load achievable. The minimum load of sliding pressure operation is very similar to that of fixed pressure operation of the HRSG as both steam cycles have similar capacity, both produce the same amount of steam. The only difference is on the efficiency of the cycle, fixed pressure has lower efficiency causes by the throttle valve, as explained in the next section 6.5.

Table 6.4. Variation of load and steam flows of supercritical SSFCC with fixed IGV, sliding pressure in the HRSG, and CO_2 capture

Load of power plant	%	100	84	75	57	51
Load of gas turbine	%	100	100	100	100	100
Load of steam turbine	%	100	76	63	37	29
Power output supercritical steam turbine	MW	139	100	82	51	43
Load of supercritical steam turbine	%	100	72	59	36	31
Supercritical steam mass flow	t/h	1292	942	766	473	397
Power output HP steam turbine	MW	69	53	44	28	24
Load of HP steam turbine	%	100	76	64	40	34
HP steam mass flow	t/h	1292	1002	838	543	453
Power output IP steam turbine	MW	235	187	158	106	87
Load of IP steam turbine	%	100	80	67	45	37
IP steam mass flow	t/h	1292	1033	868	543	453
Power output LP steam turbine	MW	144	108	87	34	15
Load of LP steam turbine	%	100	75	60	23	**11**
LP steam mass flow	t/h	795	618	508	223	114
LP steam mass flow	%	100	78	64	28	**14**

The numbers in bold indicate the main constrain for the LP steam turbine related to the steam mass flow and the power that are below the acceptable of 20%, and the reason why this percentage of load is not selected. Shaded line indicates the minimum load selected in this study in order to avoid severe damage in the LP steam turbine

Figure 6.9 and Figure 6.10 show the variation of temperature and mass flow rate in each duct burner for supercritical SSFCC configuration with fixed IGV and sliding pressure in the

HRSG. Sliding pressure operation in the HRSG is the main difference with respect to the configuration described in section 6.3.1. At loads below 85%, the pressure in the steam cycle falls below the supercritical pressure of water and the heat exchanger replacing the evaporator needs to operate with two-phase flow on the water/steam side. The main difference with respect to the previous option lies within duct burners 3 and 4, particularly from 85% to 50% load, where the pressure reduces and two phases exist.

Less fuel is needed in duct burner 3 when the pressure is reduced from 75% to 50% load compared with fixed pressure. This happens because the capacity of steam to absorb heat decreases as pressure decreases. This can be seen in Figure 6.9, where the temperature is the same as in the SSFCC at fixed pressure, but the natural gas mass flow rate is lower. In the 4th duct burner, where the 'evaporator-like' heat exchanger is located, more heat is needed to change the phase from saturated liquid to saturated vapor. Although more fuel is used at 75% and at 50% load, the temperature is lower than in SSFCC at fixed pressure in the boiler.

The air / fuel ratio is shown in Figure 6.11. The main difference of the air / fuel ratio with respect to the fixed pressure HRSG configuration is a consequence of the apparition of two phases below 85%, where the pressure is subcritical, as explained previously. Also the mass flow of the 4th duct burner reduces to zero here, unlike in the previous configuration, the variation in CO_2 and O_2 concentration for this configuration is shown in Figure 6.12 and Figure 6.13.

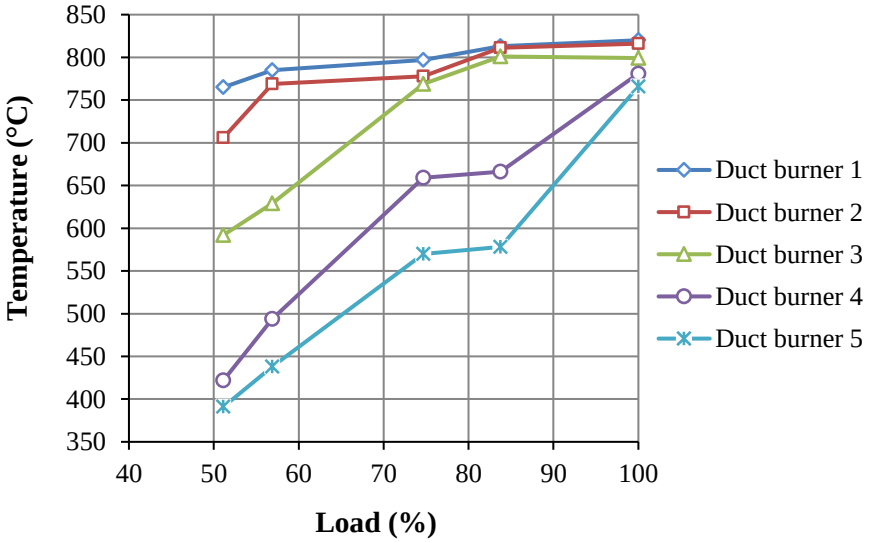

Figure 6.9. Flue gas temperature across the HRSG at part-load for a supercritical SSFCC power plant with fixed IGV and sliding pressure in the HRSG. The flue gas temperature in each duct-burner varies with the changes in load of the power plant, caused by variations of the natural gas mass flow and subsequent reductions of steam flow

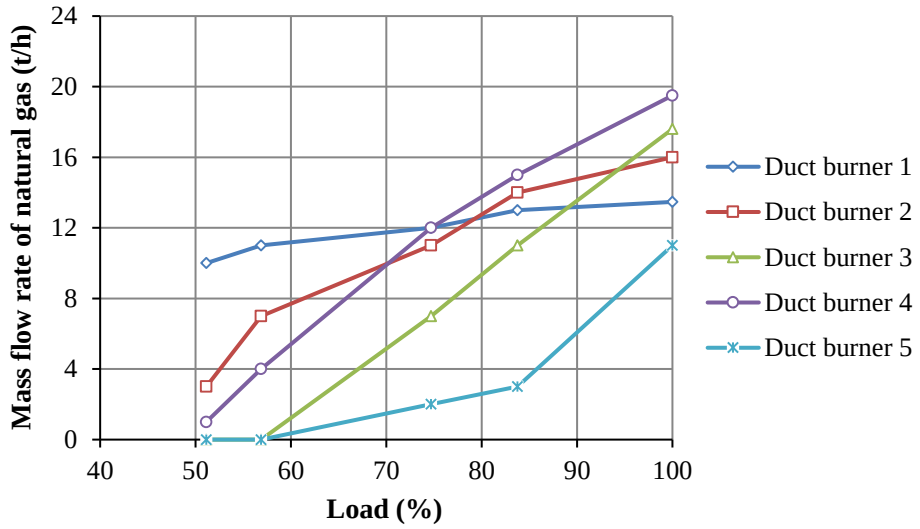

Figure 6.10. Variation of the natural gas mass flow across the HRSG at part-load of a supercritical SSFCC power plant with fixed IGV and sliding pressure in the HRSG

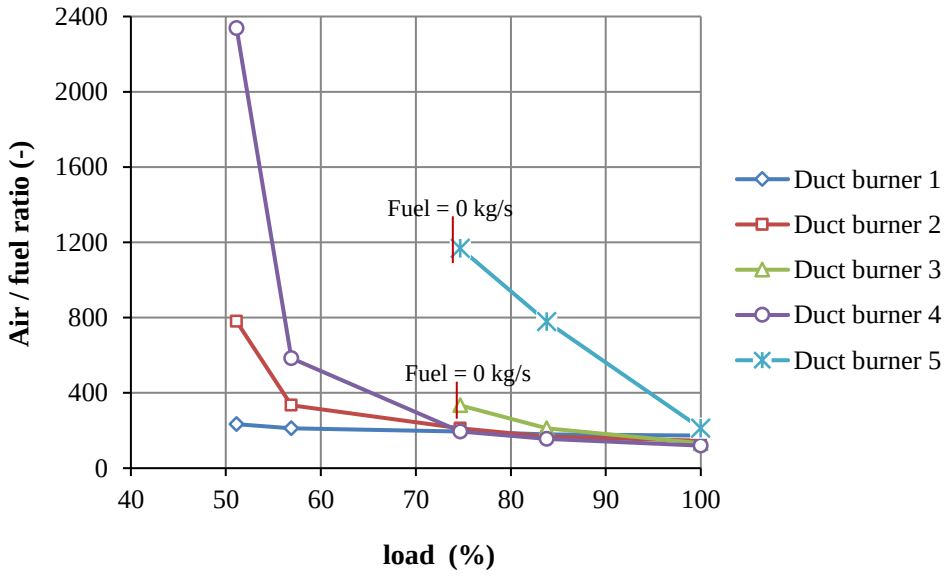

Figure 6.11. air / fuel ratio in each duct-burner at part-load for a supercritical SSFCC power plant with fixed IGV and sliding pressure. The variations are caused by a reduction of the natural gas mass flow to accommodate subsequent reductions of steam production

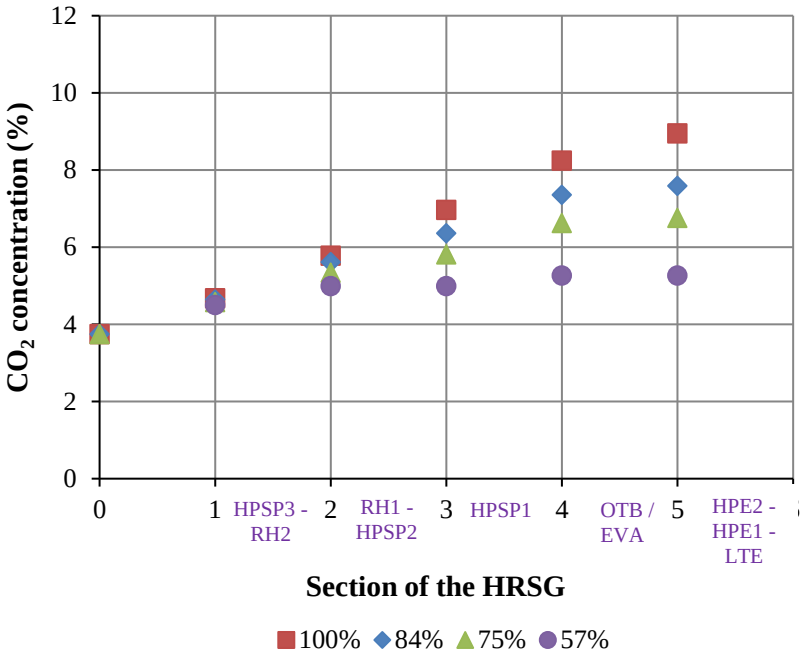

Figure 6.12. Variation of CO_2 concentrations across each section of the HRSG at different loads for a supercritical SSFCC with fixed IGV and sliding pressure in the HRSG. The acronyms used to refer to Figure 5.25

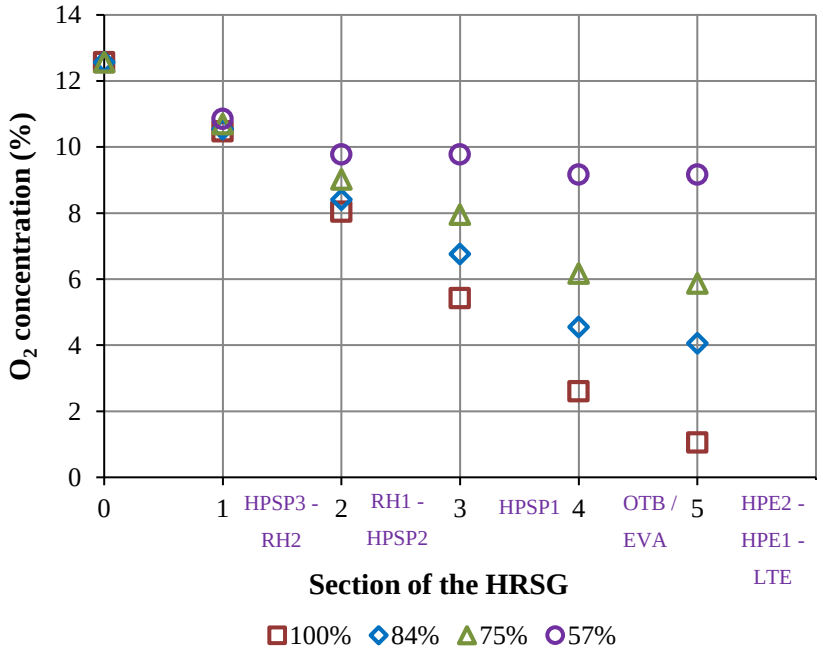

Figure 6.13. Variation of O_2 concentrations across each section of the HRSG at different loads for a supercritical SSFCC with fixed IGV and sliding pressure in the HRSG. The acronyms used to refer to Figure 5.25

This section is summarised as follow:

- The variation of the flue gas temperature of the 1st and 2nd duct burners for supercritical SSFCC with fixed and sliding pressure in the HRSG configuration are similar, especially from 100% to 85% load.
- The main difference laid in the 4th and 5th for supercritical SSFCC sliding pressure where the evaporator is located between 85% and 75% load, more heat is needed to change the phase from saturated liquid to saturated vapor. It can be seen in Figures 6.4 and 6.5; although the natural gas flow is higher the temperature is lower compared with Figures 6.9 and 6.10.

6.3.3 Subcritical combined cycle with fixed inlet guide vanes and sliding pressure operation of the heat recovery steam generator

Table 6.5 shows the variation of the percentage of the power capacity for each steam turbine. In this study, the minimum load for this configuration is 57% in order to be consistent with the other configurations, because the LP steam turbine is operating at 28% of its capacity, indicated in shaded line. The numbers in bold show that at 46% of load, the LP steam turbine does not have vapour and it is not generated power.

Table 6.5. Variation of load and steam of subcritical SSFCC with fixed IGV, sliding pressure in the HRSG and CO_2 capture

Load of power plant	%	100	85	75	57	46
Load of gas turbine	%	100	100	100	100	100
Load of steam turbine	%	100	78	63	38	19
Power output HP steam turbine	MW	142	112	93	63	39
Load of HP steam turbine	%	100	79	66	44	28
HP steam mass flow	t/h	1350	1040	859	568	348
Power output IP steam turbine	MW	241	190	157	105	65
Load of IP steam turbine	%	100	79	65	44	27
IP steam mass flow	t/h	1350	1073	881	684	359
Power output LP steam turbine	MW	156	118	90	37	0
Load of LP steam turbine	%	100	75	58	23	**0**
LP steam mass flow	t/h	855	658	521	236	0
LP steam mass flow	%	100	77	61	28	**0**

The numbers in bold indicate the main constrain for the LP steam turbine related to the steam mass flow and the power that are below the acceptable of 20%, and the reason why this percentage of load is not selected. Shaded line indicates the minimum load selected in this study in order to avoid severe damage in the LP steam turbine

In the case of subcritical steam conditions, the temperature in all duct burners reduces almost linearly with power as shown in Figure 6.14. Steam temperature at the inlet of the HP turbine is 601°C, lower than the 630°C under supercritical conditions.

In the third duct burner, less fuel is needed from 100% to 75% load compared with the other two configurations, as can be seen in Figure 6.15. The natural gas mass flow rate is lower, but the temperature is higher. The main reason is because the reduction of the capacity of lower pressure steam to absorb heat. From 75% to 50% load, in 3rd and 4th duct burners, the temperature and natural gas mass flow rate behave similarly to SSFCC with fixed pressure and sliding pressure in the HRSG. The main fuel demand is in the last duct burner where the evaporator is located. A large amount of heat is needed to change the phase from saturated liquid to saturated vapor.

The air / fuel ratio is shown in Figure 6.16 and the percentage of O_2 and CO_2 for all duct burners at part-load is shown Figure 6.17 and Figure 6.18.

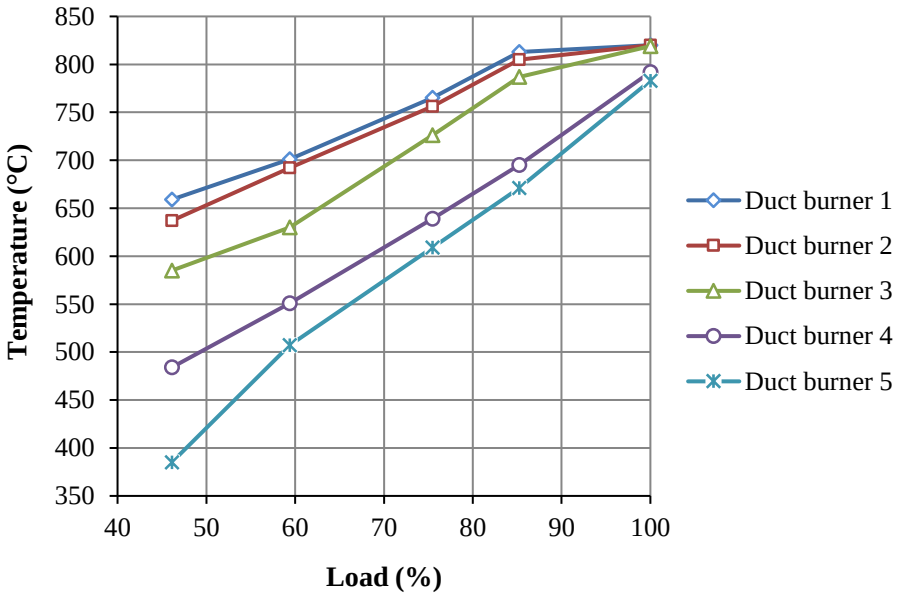

Figure 6.14. Flue gas temperature across the HRSG at part-load for a subcritical SSFCC power plant with fixed IGV and sliding pressure in the HRSG. The flue gas temperature in each duct-burner varies with the changes in load of the power plant, caused by variations of the natural gas mass flow and subsequent reductions of steam flow

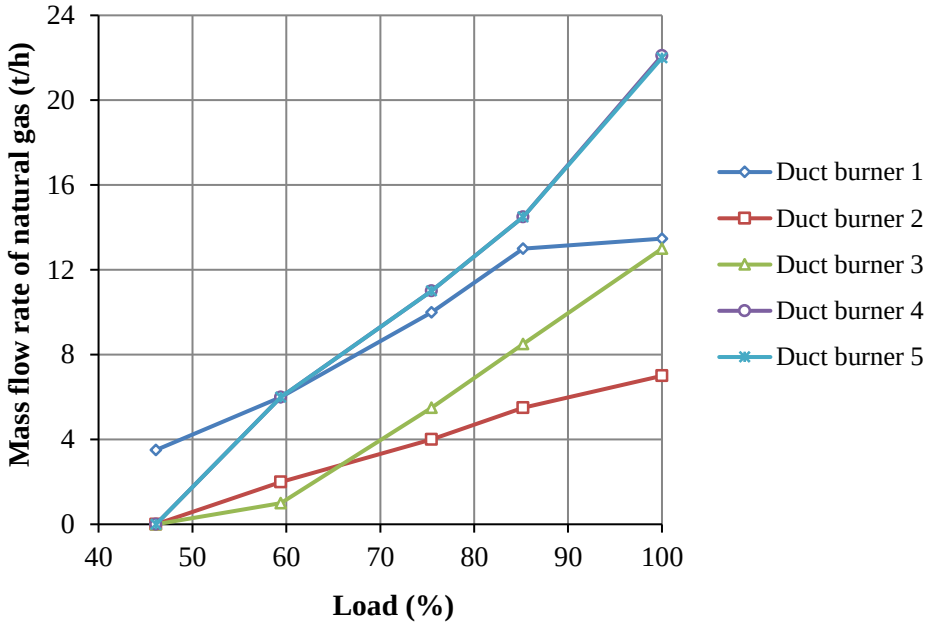

Figure 6.15. Variation of the natural gas mass flow across the HRSG at part-load of a subcritical SSFCC power plant with fixed IGV and sliding pressure in the HRSG

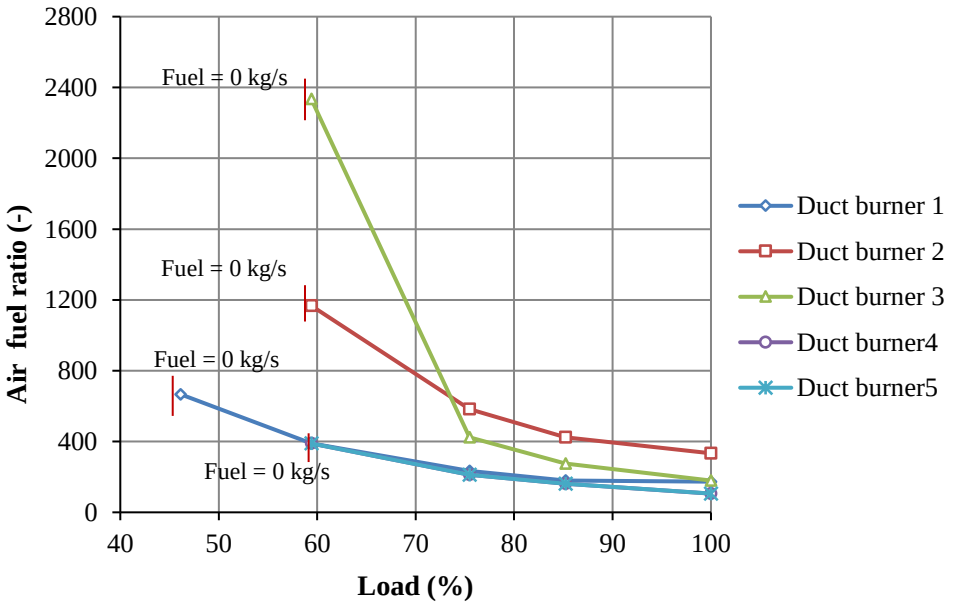

Figure 6.16. air / fuel ratio in each duct-burner at part-load for a subcritical SSFCC power plant with fixed IGV and sliding pressure. The variations are caused by a reduction of the natural gas mass flow to accommodate subsequent reductions of steam production

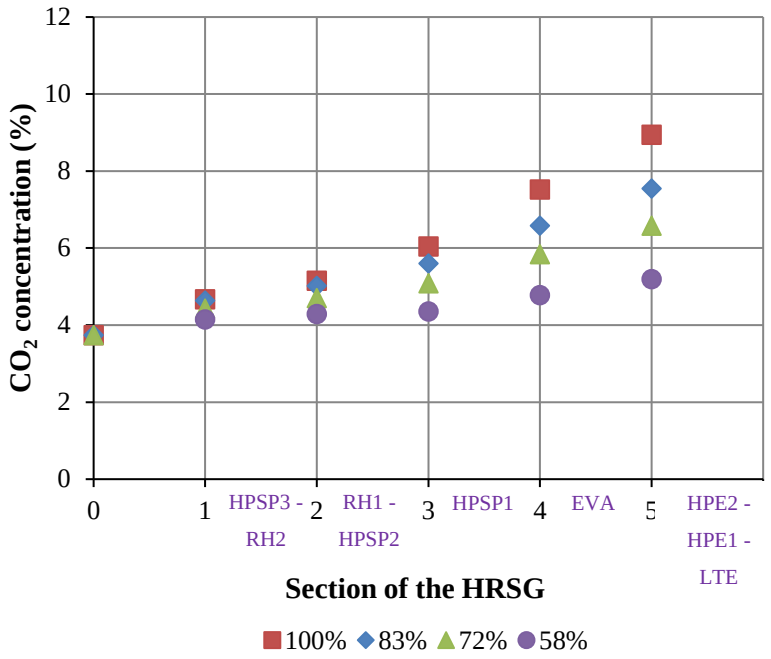

Figure 6.17. Variation of CO_2 concentrations across each section of the HRSG at different loads for a subcritical SSFCC with fixed IGV and sliding pressure in the HRSG. The acronyms used to refer to Figure 5.24

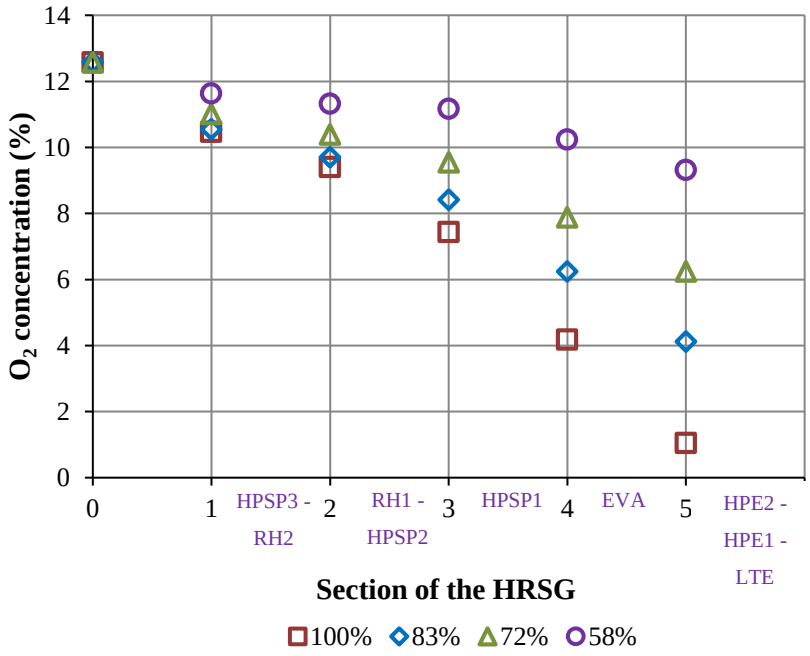

Figure 6.18. Variation of O_2 concentrations across each section of the HRSG at different loads for a subcritical SSFCC with fixed IGV and sliding pressure in the HRSG. The acronyms used to refer to Figure 5.24

The mass flow of the 3rd duct burner reduces more than in the other configurations here. It is worth highlighting that the reason for this, as mentioned previously, is the effect of the reduction of the steam flow pressure.

6.3.4 Summary

Supercritical SSFCC with fixed pressure in the HRSG absorbs more heat in the first than in the last duct burners so more natural gas is burnt which maximises the average temperature of heat addition. In addition, the higher the temperature of the main steam entering the supercritical steam turbine, the higher temperature of the flue gas is across the HRSG.

After the first duct burner, additional natural gas combustion for the additional steam production, the concentration of the CO_2 is higher and the O_2 is lower than with subcritical SSFCC configuration.

In subcritical SSFCC configuration, more heat is required in the last two duct burners where the evaporator is located than in the first. The heat is needed to change the phase from saturated liquid to saturated vapor. Although less natural gas is burnt in the first duct burners, more fuel is needed in the last duct burners. So at the end, the final CO_2 and O_2 in these three configurations are the same.

Although the temperature of the flue gas after the last duct burner is similar to the supercritical SSFCC configuration, the average temperature of heat addition to the steam cycle is lower at part-load than in supercritical configurations, as illustrated in Figure 6.19. This has the effect of lowering the thermal efficiency of the steam cycle, as discussed further in Section 6.7. The behaviour of the temperature, natural mass flow, CO_2 and O_2 concentration, and the air fuel ratio in the duct burners of supercritical SSFCC with sliding pressure is a combination of both supercritical SSFCC fixed pressure and subcritical SSFCC sliding pressure. From 100% to 85% load, these parameters in the last duct burner behave like in supercritical SSFCC fixed pressure. From loads below 85%, under subcritical pressure, these parameters in the last duct burner behave more like in subcritical SSFCC sliding pressure configuration.

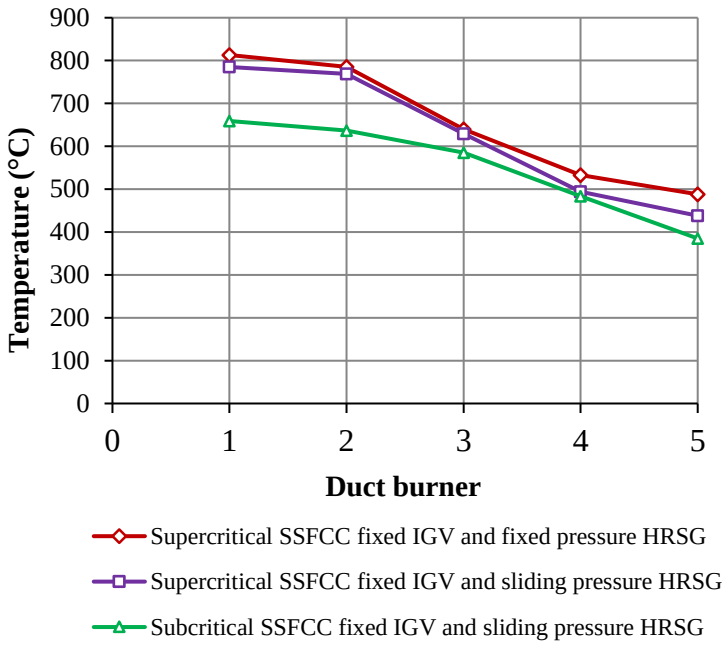

Figure 6.19. Average temperature of heat addition of the five duct burners for all configurations at 58% load

6.4 Part-load behaviour of the HRSG and implications for steam generation

The pressure of the main live steam is an important parameter to control at part-load. It affects the boiler, the steam turbine operation, and the efficiency of the power plant. Figure 6.20 shows the variation of the pressure of the main steam across a range of loads. The inlet pressure of the HP turbine of the conventional NGCC configuration reduces from 123.7 bar at 100% load to 89.6 bar at 51% load of the power plant (100% to 40% gas turbine load). The pressure varies significantly when compared with subcritical SSFCC which varies in the range from 172.5 bar to 64.9 bar when reducing load from 100% to 50%. In the conventional NGCC, the load is reduced by decreasing the power output of the gas turbine as well as the power output of the steam cycle. In the case of subcritical SSFCC with fixed IGV and sliding pressure configuration as was mentioned before, the power output is reduced by lowering the steam cycle output by reducing the sequential supplementary fuel input in the HRSG, increasing the charge in pressure ratio across the steam turbines and thus lowering steam turbine part-load efficiency.

Two alternatives are evaluated for supercritical steam generation: fixed and sliding pressure. As mentioned in chapter 5, supercritical boilers can operate at fixed pressure or dual mode fixed and sliding pressure at expense of additional capital cost. At fixed pressure, the

pressure across the HRSG and the pressure of the main steam remain constant as shown in Figure 6.20, around 298 bar, when load is reduced from 100% to 50%. But the pressure at the inlet of the steam turbine is not constant. At the inlet of the steam turbine, a throttle valve is necessary. The effect of pressure drop is useful in throttle valves for reducing load as it is a restriction on the turbine. On the other hand, in sliding pressure control, the pressure varies from 299 bar at 100% load to 96.4 bar at 50% load. When the load of the NGCC power plant is 50%, the load of the gas turbine is 77% and the steam cycle is 52% as shown in Figure 6.21. On the other hand, when the load of SSFCC power plant with fixed IGV is 50%, the load of the steam cycle is 40%.

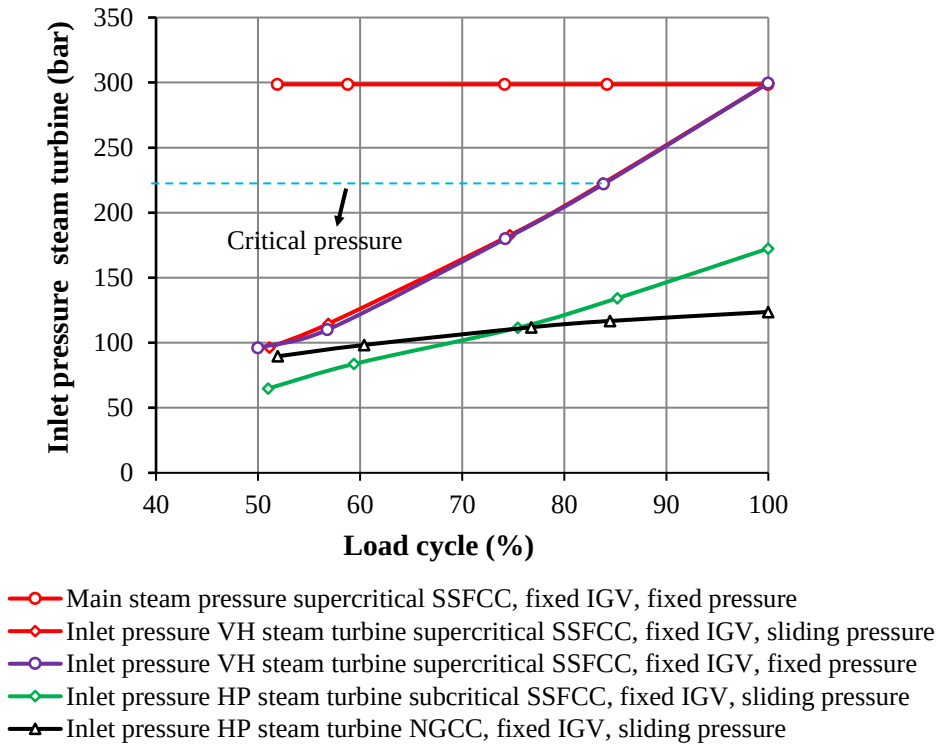

Figure 6.20. Variation of the inlet pressure of the steam turbine with changes in load of the power plants, for four case studies

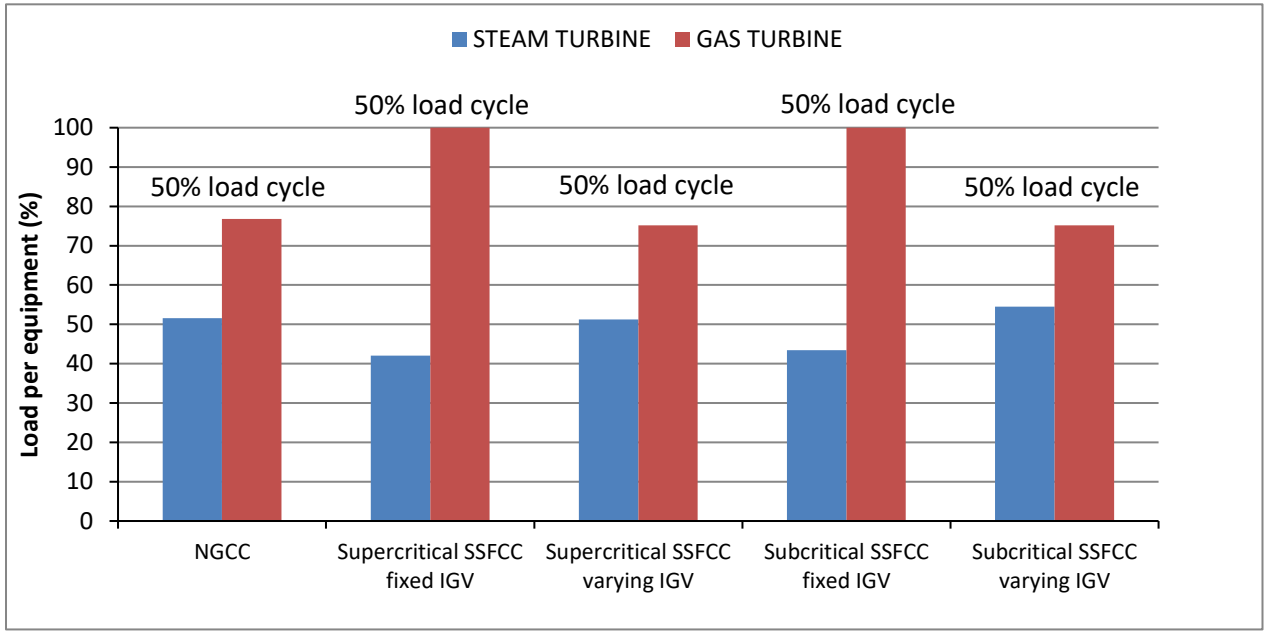

Figure 6.21. Comparison of the load of the power plant cycle, at the same load of the steam cycle for each configuration without capture

6.5 Part-load efficiency without capture

In order to evaluate the implications of each operating mode on the efficiency of the power plant, the part-load performance of the six case studies outlined in Table 6.1 are first evaluated in this section without the capture process and compressor unit.

1. Conventional NGCC configuration with IGV and sliding pressure
2. Supercritical SSFCC with fixed IGV, and fixed steam pressure
3. Supercritical SSFCC with fixed IGV, and sliding steam pressure
4. Supercritical SSFCC with variable IGV, and fixed steam pressure
5. Subcritical SSFCC with fixed IGV, and sliding steam pressure
6. Subcritical SSFCC with variable IGV, and sliding steam pressure

The efficiencies for the outlined case studies are shown in Figure 6.22. The efficiency of the NGCC configuration without capture decreases from 59% to 51% when the load is reduced from 100% to 41%. The efficiency drops mainly because the efficiency of the gas turbine reduces by using the IGV at part-load.

In the case of the subcritical SSFCC configuration with variable IGV, the efficiency increases from 50.1% to 52.3% when the load is reduced from 100% to 50%. The reason for this opposite behaviour compared to the NGCC configuration is that less fuel is burnt in the duct burners and the marginal thermal efficiency of natural gas firing increases (**positive effect in the efficiency**) as is explained in chapter 4, section 4.2.1. Although the marginal efficiency of the steam cycle of the SSFCC configuration increases when less fuel is burnt in the HRSG, the use of the variable IGV (**negative effect in the efficiency**), makes the efficiency of this alternative increase only 2.2% compared to 5.8% increase for the subcritical SSFCC with fixed IGV configuration where efficiency increases from 50.3% to 56.0% when the load is reduced from 100% to 50%.

Supercritical SSFCC with variable IGV and fixed pressure in the HRSG configuration has an additional drawback: **a throttle valve**. The negative effect of the IGV and the throttle valve dominates in this configuration. As a result, the efficiency decreases from 52% to 49.7% when the load is reduced from 100% to 50%.

On the other hand, the efficiency of the supercritical SSFCC with fixed IGV and fixed pressure configuration increases from 52% to 53.91% when the load is reduced from 100% to 50%. The efficiency increases because the effect of the IGV is eliminated. However, when compared to subcritical SSFCC at fixed IGV, the efficiency of supercritical SSFCC with

fixed IGV, and fixed pressure in the HRSG configuration is higher at load levels between 100% and 72%. For loads below 72%, the efficiency of subcritical SSFCC with fixed IGV becomes higher. The main reason for this is the loss of energy for the throttle valve.

Irrespective of the mode of steam generation (i.e. subcritical or supercritical), it can be seen that the used of variable IGV is detrimental to efficiency. This is the main reason why the more efficient part-load strategy is to run the gas turbine at full load and thus maximize work output per unit of fuel in the gas turbine and achieve part-load by reducing supplementary firing fuel input.

For both modes of steam generation, a sliding pressure achieves better efficiency than fixed pressure operation strategy. This is because the irreversibilites caused by the throttling valve at the inlet of the HP turbine are avoided and the pressure ratios across the turbines are larger, resulting in a detrimental effect to the turbine isentropic efficiency.

As the throttling valve causes inefficiencies at part-load, another further configuration is evaluated: supercritical SSFCC with fixed IGV, and sliding pressure control in the boiler configuration. This alternative represents the highest efficiency and the optimum alternative at part-load. The efficiency increases from 52.03% at 100% load to 56.04% at 50% load of the overall cycle. However, additional capital cost would be necessary for enabling the boiler to operate at supercritical sliding pressure.

Based on these results for the evaluated configurations without capture, it is clear that the operation with IGV has a negative effect on the efficiency on the overall power plant and can be disregarded. The difference between capture and with capture is the steam extraction for the reboiler which affects mainly the LP steam turbine. The power of the LP steam turbine is lower; therefore, the total efficiency of the cycle is reduced.

Three strategies for part-load operation of SSFCC are selected in the section:

1. A supercritical SSFCC with constant IGV, and sliding pressure operation in the HRSG
2. A supercritical SSFCC with constant IGV, fixed pressure operation in the HRSG
3. Subcritical SSFCC with fixed pressure, and sliding pressure operation in the HRSG

For supercritical steam cycle, both sliding pressure and fixed pressure operation of the HRSG are examined in this section (without capture) and in section 6.7 (with capture) since there is a trade-off between efficiency and additional capital cost. Subcritical steam generation is the lowest capital cost option, with more practical experience.

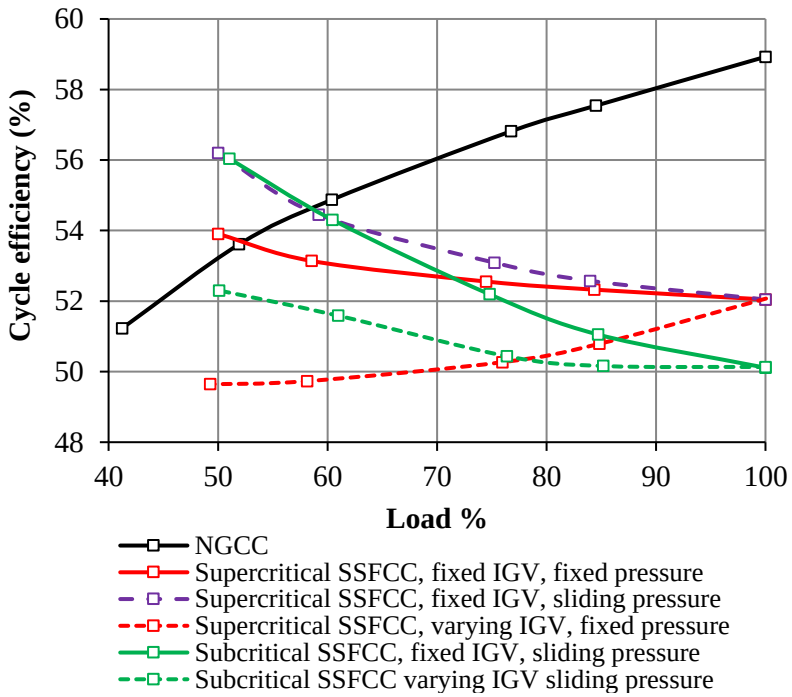

Figure 6.22. Variation of the efficiency of the power plant without CO_2 capture at part-load operation for six case studies

6.6 Steam extraction pressure for solvent regeneration at part-load

Operating pressures of the steam turbines decrease at part-load as a consequence of the reduction of the steam mass flow rate. With sliding pressure, the pressure ratios across the HP and IP turbines are kept constant as much as practically possible to maintain turbine efficiency. As shown in Figure 6.23, the crossover pressure declines as a function of load. Here the pressure at full load in the crossover is at 4 bar in order to have a margin to overcome the pressure drop from the crossover to the desuperheater. The pressure of steam extraction for solvent regeneration has a large impact on performance at part-load. A floating crossover pressure is the operating strategy used in this thesis. This is the optimum strategy for maximising the part-load performance, as demonstrated in Sanchez Fernandez et al, (2016) for coal-fired power plants with post-combustion capture. Although the study was applied for coal power plant, it could be applied to a NGCC because the integration strategy (steam extraction) links to the efficiency of the cycle through the IP and LP steam turbines which are affected by the pressure in the crossover and the amount of steam required in the reboiler, and the boiler or HRSG is not affected. It allows operating with a higher crossover pressure at part-load, compared to the alternative where a throttling valve at the inlet of the LP turbine is used to increase the crossover pressure. This results in higher steam

temperature in the reboiler, a higher stripper pressure in the capture process and lower compression work

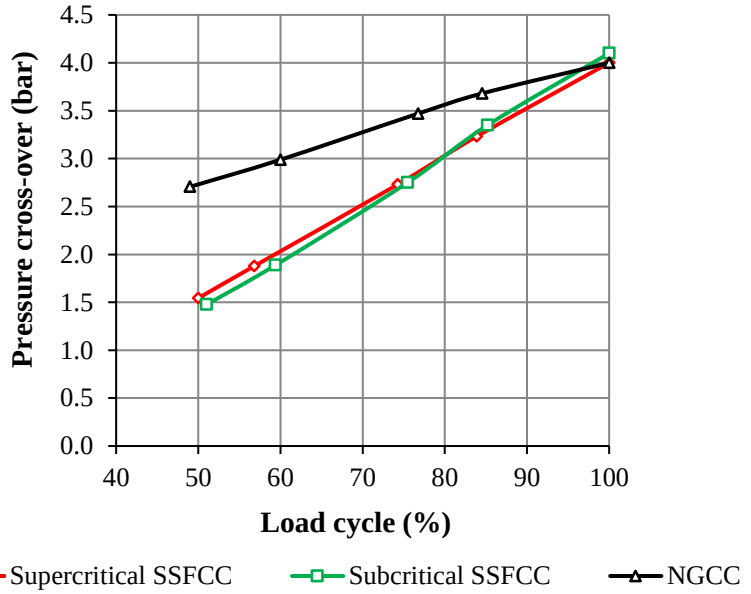

Figure 6.23. Reduction of cross-over pressure for supercritical and subcritical sequential supplementary firing, and the conventional natural gas combined cycle with CO_2 capture and compressor unit. Cross-over pressure at design conditions is 4 bar

6.6.1 Performance of the capture plant at part-load operation

As mentioned in chapter 5, Table 5.1, the part-load operating strategy of the capture plant unit used in this thesis is to maintain stripper pressure as high as possible at part-load and adjust the solvent recirculation low rate as proposed in Sanchez Fernandez et al (2016). Sanchez Fernandez et al (2016) and Mechleri et al., (2014) explain the basic controls to maintain these conditions in the capture plant:

1. The pressure is controlled by a valve downstream of the condenser following the stripper
2. The capture level of 90% is controlled by adjusting the solvent flow rate
3. The temperature in the stripper is kept at 120ºC at full load by adjusting the steam extraction flow. However, at part-load the temperature reduces below 120ºC as a consequence of the reduction of pressure drop at the outlet of the IP turbine and in the crossover
4. A summary of relevant parameters for the part-load operation of a conventional NGCC plant with capture are shown in Table 6.6. The small reduction of the temperature in the reboiler is not favourable to the vapour-liquid equilibrium in the

stripper because the extent of solvent regeneration is reduced and leads to higher CO_2 lean loading, as explained in chapter 3, sections 3.5.1 and 3.5.2. The lean loading increases from 0.269 to 0.272 as indicated in Table 6.6 and the specific reboiler duty increases marginally from 3.56 to 3.65 GJ/tonneCO_2. At higher lean loadings, a larger L/G is needed to achieve the same 90% of CO_2 removal. The L/G is adjusted at each load to get 90% of CO_2 capture. It is increased from 1.47 to 1.6 when reducing load from 100% to 58%. This leads to providing more energy to compensate for the increase contribution of the sensible heat of the solvent to raise the temperature of the solvent to the stripper temperature.

When a conventional NGCC configuration operates at part-load, the mass flow rate of flue gas that goes to the capture unit decreases which has a positive effect in the absorber as it increases the residence time (Sanchez Fernandez et al, 2016). In contrast, when a SSFCC plant operates at part-load, the mass flow rate of the flue gas treated in the capture plant remains almost constant, but with a higher concentration of O_2 and a lower concentration of CO_2 compared at full load.

The capture plant of subcritical and supercritical SSFCC at fixed and sliding pressure configurations have similar behaviours to the capture plant of a conventional NGCC when operating between 100% and 75% load. However, at 58% load, as the pressure in the crossover reduces significantly, the strategy proposed by Sanchez Fernandez et al (2016) is adopted, which is "A combination of releasing stripper pressure and increasing the L/G ratio in the absorber". At 58% load the crossover pressure in the SSFCC is 2 bar, which is lower than in the conventional NGCC (3 bar) at similar condition.

Table 6.6. Capture plant process simulation at part-load of conventional natural gas combined cycle

Load of power plant	**%**	**100**	**84**	**75**	**58**
Capture level	%	90	90	90	90
CO_2 captured	kg/s	69.2	60	55	45.6
Specific reboiler duty	GJ/tonneCO_2	3.56	3.58	3.60	3.65
Lean loading	kmolCO_2/ kmolMEA	0.269	0.2752	0.273	0.272
Rich loading	kmolCO_2/ kmolMEA	0.4721	0.4725	0.4725	0.4721
Liquid to gas molar ratio (L/G)	-	1.47	1.53	1.5	1.6
Solvent circulation rate	kmol/s	65.6	59.3	53.5	48.6
Solvent side reboiler temperature	°C	120	120	119.5	118
Pressure in the reboiler	bar	1.9	1.9	1.9	1.9
Total steam extraction from crossover	kg/s	111.2	106	98.08	96
LP turbine steam flow rate	kg/s	77.6	71.9	54.6	42.1
Fraction of steam extraction	kg/s	0.59	0.596	0.642	0.695

Figures 6.24 and 6.25 show the reduction of the crossover pressure causing lower operating temperatures in the reboiler and increasing the reboiler duty for supercritical and subcritical SSFCC. Both configurations have similar a behavior, at 58% load, their stripper pressures are released from 1.87 bar to 1.63 bar. The difference of 0.24 bar is because the pressure of the main steam for supercritical SSFCC is higher than subcritical SSFCC at full load. Releasing the pressure of the stripper for SSFCC was not expected as it does not happen in a conventional NGCC. The NGCC operates at part-load using the IGV, in this case, both the gas turbine and the steam cycle reduce the power generation. But in SSFCC at fixed IGV, the load is reduced only reducing the supplementary fuel in the HRSG. Therefore, the power is reduced only using the steam cycle which leads to lower pressure in the crossover compared with a NGCC. As a result, in order to reduce the amount of steam and to increase the solvent capacity as explained in chapter 3 section 3.5.2, the stripper pressure should be released.

The reboiler duty for supercritical and subcritical SSFCC increases from 3.44 MJ/tonne CO_2 to 3.88 MJ/tonne CO_2. The difference is because of the pressure in the crossover 1.87 bar to 1.63 bar for supercritical and subcritical, respectively.

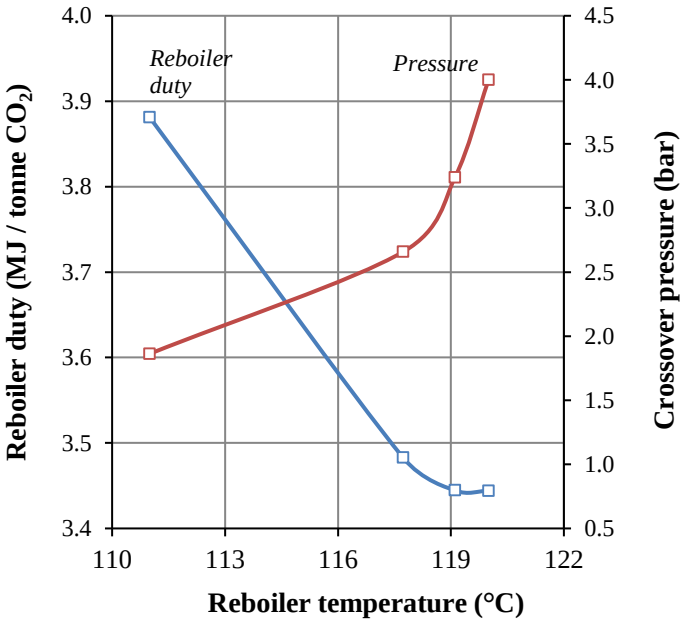

Figure 6.24. Performance of the capture unit with constant operating pressure in the stripper column. Reboiler duty and reboiler solvent temperature vary with changes in crossover pressure, caused by a reduction of steam cycle flow at part-load between 100% and 60% load, with 90% capture in the supercritical SSFCC with fixed IGV

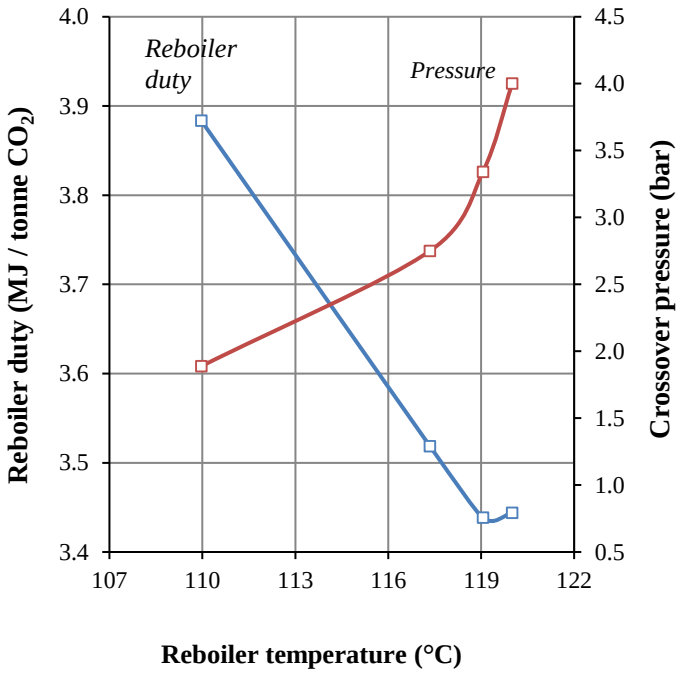

Figure 6.25. Reboiler duty and reboiler solvent temperature vary with changes in crossover pressure, caused by a reduction of steam cycle flow at part-load between 100% and 60% load, with 90% capture in the subcritical SSFCC with fixed IGV

Table 6.7 and 6.8 show the most important results of the capture plant for supercritical and subcritical SSFCC operated at part-load. Although the amount of supplementary firing in each duct burner is different, the total amount of fuel is the same. As a result, the amount of CO_2 capture is the same for subcritical and supercritical SSFCC configuration at part-load.

Table 6.7. Capture plant process simulation at part-load of supercritical SSFCC fixed and sliding pressure boiler

Load of power plant	**%**	**100**	**82.5**	**72**	**58**
CO_2 captured	kg/s	87.7	73.7	63.450	50.3
Capture level	%	90	90	90	90
Specific reboiler duty	GJ/tonneCO_2	3.44	3.44	3.48	3.88
Lean loading	kmolCO_2/ kmolMEA	0.2821	0.282	0.303	0.3537
Rich loading	kmolCO_2/ kmolMEA	0.4806	0.4787	0.47507	0.4477
Liquid to gas molar ratio (L/G)	-	4.03	3.73	3.71	5.6
Solvent circulation rate	kmol/s	76	72	74	104
Solvent side reboiler temperature	°C	120	119	118	111
Pressure in the reboiler	bar	1.87	1.87	1.87	1.63
Total steam extraction from IP/LP crossover to capture plant	kg/s	138.2	115.4	99.86	100
LP turbine steam flow rate	kg/s	221	173	143	67
Fraction of steam extraction	kg/s	0.38	0.40	0.41	0.60

Table 6.8. Capture plant process simulation at part-load of subcritical SSFCC sliding pressure boiler

Load of power plant	**%**	**100**	**85**	**75**	**58**
CO_2 captured	kg/s	87.7	73.7	63.4	50.3
Capture level	%	90	90	90	90
Specific reboiler duty	GJ/tonneCO_2	3.44	3.44	3.52	3.88
Lean loading	kmolCO_2/kmol MEA	0.2821	0.284	0.3137	0.3623
Rich loading	kmolCO_2/kmol MEA	0.4806	0.4785	0.4727	0.449
Liquid to gas molar ratio (L/G)	-	4.03	3.73	3.89	5.43
Solvent circulation rate	kmol/s	76.8	72.8	76.8	109.4
Solvent side reboiler temperature	°C	120	119.0	117.3	110
Pressure in the reboiler	bar	1.87	1.87	1.87	1.64
Total steam extraction from IP/LP crossover to capture plant	kg/s	138	115	100	100
LP turbine steam flow rate	kg/s	237.6	182.8	144.6	67.7
Fraction of steam extraction	kg/s	0.37	0.39	0.41	0.60

6.6.2 CO_2 compressor at part-load operation

Two trains with a similar gear-type centrifugal compressor with seven stages and intercooling after each stage are used in all configurations to compress the produced CO_2 to 150 bar for EOR purposes. The inlet and outlet pressures in each stage of the compressor are constant at part-load for the conventional NGCC and for both the subcritical and the supercritical SSFCC between 100% and 75%. However, for SSFCC configuration at 58% load, as the pressure in the stripper is released, the inlet pressure of the first stage of the compressor reduces. As described in chapter 3, section 3.5.3, below 75% load, a fraction of the compressed CO_2 must be recycled in order to avoid surge and prevent damage to the compressor. Recycling compressed CO_2 increases the auxiliary electricity consumption.

Table 6.9 summarises the auxiliary power consumption of the CO_2 compression unit at various load. The performance stage by stage of the compressor for the NGCC and SSFCC is provided in Appendix D.

Table 6.9. Auxiliary power consumption of the CO_2 compressor unit at part-load operation

Load of power plant	**%**	**100**	**85**	**75**	**58**
NGCC	MW	22.38	21.31	20.00	19.8
Supercritical SSFCC	MW	31.57	31.67	23.30	23.00
Subcritical SSFCC	MW	31.57	31.67	23.32	23.30

6.7 Variation of the efficiency at part-load operation with integrated CO_2 capture and compressor unit

The CO_2 capture and the compressor units in operation reduce the efficiency of the power plants because of the steam extraction and the power for compressing the CO_2. Recycling compressed CO_2 at loads below 75% penalise even further the efficiency of the NGCC and SSFCC power plant configurations.

Figure 6.26 shows the efficiency over load for the three evaluated power plant configurations selected in section 6.5 integrated with CO_2 capture, which are: supercritical SSFCC with constant IGV, and with two modes of operation in the boiler: fixed pressure and sliding pressure in the HRSG; and subcritical SSFCC with constant IGV and sliding pressure control in the HRSG. All cases are compared with a conventional NGCC.

The efficiency of the NGCC decreases from 51.1% at 100% load to 44.5% at 58% load. This result is in good agreement with the publication of Rezazadeh et al, (2015) as shown in Table

B1 in appendix B. Her part-load work including CO_2 capture considers load from 100% to 60% of the GT (68% load of total power output). The reason for this limit is that although the minimum stable generation load of a NGCC is around 40-50% of the design capacity (IEAGHG, 2012; Rezazadeh et al., 2015; McManus et al., 2007), Rezazadeh et al, (2015) said that the impact on the cost of electricity at load below 60% of GT integrated with CO_2 capture is more pronounced. CO_2 capture leads to a significantly decreased efficiency and the steam for the IP and LP steam turbines is reduced drastically at part-load (IEAGHG, 2012).

For SSFCC configurations, the minimum load at part-load with CO_2 capture unit is 58% load of the cycle (40% load of steam cycle). This is lower than the load proposed by Rezazadeh et al, (2015).

The efficiency of the subcritical SSFCC with fixed IGV, and sliding pressure control with CO_2 capture increases from 43.15% to 45.79% with load decreasing from 100% to 58%. It is almost the same as supercritical SSFCC with fixed IGV and fixed steam pressure in the HRSG.

The efficiency of the supercritical SSFCC with fixed IGV, and fixed pressure in the HRSG with CO_2 capture is lower than supercritical SSFCC with fixed IGV, and sliding pressure in the HRSG. This is due to the throttle valve causing irreversibilities as explained in a previous section. The negative effect of the throttle valve in the supercritical SSFCC is higher than the

improvements of the efficiency when operating at supercritical steam conditions between 100% and 85% load. Below 85% load, the efficiency starts increasing because the amount of supplementary firing is reduced.

Supercritical SSFCC with fixed IGV and sliding pressure is the most efficient system at part-load when operating between 100% and 58% load of the total power output.

The efficiency increases from 45.6% to 47% when the load of the cycle is reduced from 100% to 58%. The efficiency is 1.1% percentage points higher than supercritical SSFCC with constant IGV and fixed pressure at 58% load.

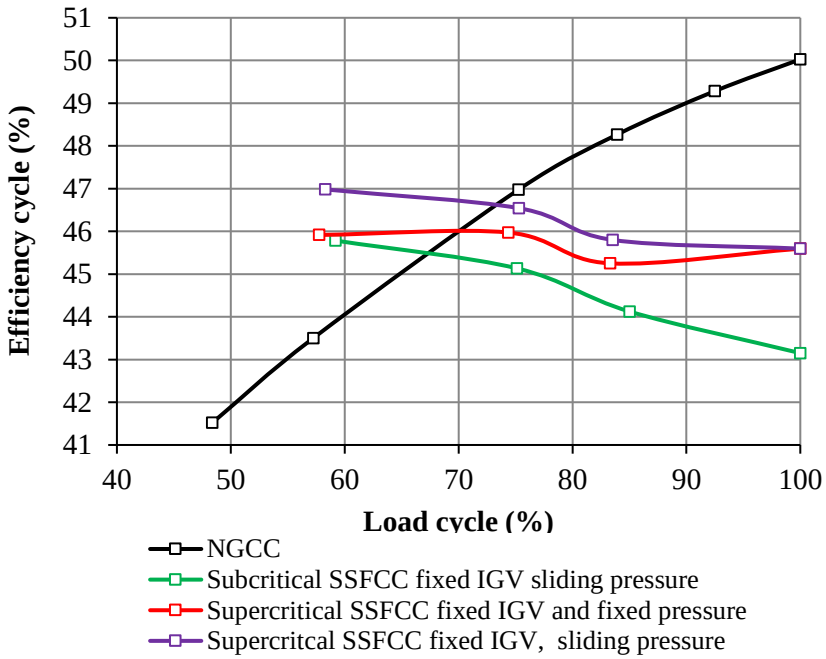

Figure 6.26. Efficiency at part-load operation for four case studies with CO_2 capture and compressor unit

The Electricity Output Penalty is calculated as using the Equation 6.1.

For the conventional NGCC plant

$$EOP = \frac{MW_{without/capture} - MW_{with/capture}}{CO_2 captured} \qquad \text{Equation 6.1}$$

Where

EOP	Electricity Output Penalty (kWh / tonne CO_2)
$MW_{without/capture}$	Net power output without capture (kW)
$MW_{with/capture}$	Net power output with CO_2 capture and compressor unit (kW)
$CO_2 captured$	Amount of CO_2 capture (tonne / h)

For the SSFCC plant

The equation 6.1 is expressed as follow

$$EOP = \frac{MW\ of\ a\ \ NGCC\ _{without/capture}\ with\ the\ same\ fuel\ input\ as\ SSFCC\ - MW\ of\ a\ \ SSFCC\ _{w/capture}}{CO_2 captured}$$

Equation 6.2

Figure 6.27 shows the electricity output penalty of the power plant configuration with CO_2 capture over the load. It ilustrates the contribution of the capture plant and compressor power to the electricity output penalty. As indiacted in Figure 6.26, while the load of the conventional NGCC decreases from 100% to 90%, the EOP reduces. Finally, with further load decreases from 90% to 58% the EOP increases because of the negative effect of CO_2 and of recycling CO_2.

The EOP of the subcritical SSFCC at fixed IGV and sliding pressure in the HRSG reduces between 100% ando 58% load.

The EOP of supercritical SSFCC with fixed IGV and fixed pressure reduces with decreasing the load from 100% to 58% load.

The energy required for the compressor power and the reduction of the amount of supplementary firing have a strong impact on the EOP at part-load

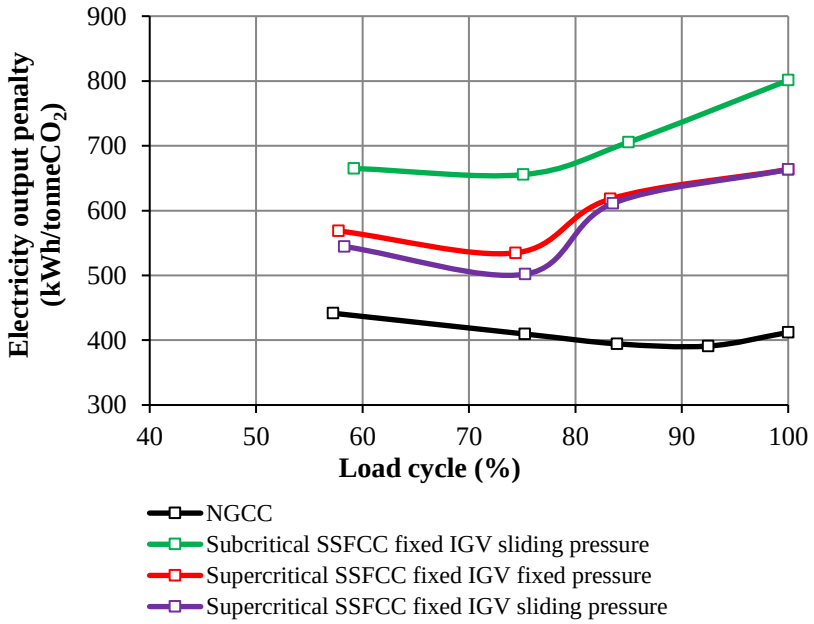

Figure 6.27. Electricity output penalty at part-load operation for four case studies with CO_2 capture and compressor unit

When operated at part-load, these configurations show greater operational flexibility by utilising the additional degree of freedom associated with the combustion of natural gas in the HRSG to change power output according to electricity demand and to ensure continuity of CO_2 supply when exposed to variations in electricity prices. The optimisation of steady state part-load performance shows that reducing output by adjusting supplementary fuel keeps the gas turbine operating at full load and at its maximum efficiency when the net power plant output is reduced from 100% to 50%.

For both subcritical and supercritical combined cycles, the thermal efficiency at part-load is optimised, in terms of efficiency (as shown in Figure 6.22 where the less efficient configuration is discarded and the configurations with higher efficiency are selected) with sliding pressure control in the HRSG. Fixed pressure operation is proposed as an alternative for supercritical combined cycles to minimise capital costs and provide fast response rates with acceptable performance levels.

One part-load strategy to maximise efficiency consists of maintaining the GT at 100% load. The disadvantage is that it increases minimum stable generation to around 60%. This is because the steam cycle is oversized compared to a conventional configuration and that the steam cycle contributes to the totality of the load reduction.

6.8 Concluding remarks

The operating strategy proposed for part-load operation of SSFCC plant configurations maximises part-load efficiency by shifting all of the output reduction to the combined cycle and keeping the amount of work generated in the gas turbine to a maximum.

The temperature in each duct burner decreases at part-load because of the reduction of the mass flow of the fuel. The reduction of the mass flow of natural gas in duct burners increases the efficiency of SSFCC.

The optimisation of steady state part-load performance shows that reducing the power output by adjusting supplementary fuel keeps the gas turbine operating at full load and at maximum efficiency when the net power plant output is reduced from 100% to 58%.

The thermal efficiency of subcritical and supercritical SSFCC at part-load is optimised, in terms of efficiency, with sliding pressure control in the heat recovery steam generator. The capital cost of the supercritical boiler would increase as it needs to be able to operate in two different ways: at supercritical conditions, where there is only one phase, and at subcritical condition where two phases exist.

Fixed pressure operation is proposed as an alternative for supercritical combined cycles to minimise capital costs and provide fast response rates with acceptable performance levels.

In a conventional NGCC, the amount of exhaust gas reduces as the load is reduced; this has a positive effect in the capture unit due to higher residence times of the solvent in the absorber column. In SSFCC with fixed IGV, the amount of exhaust gas is almost constant at part-load and the CO_2 concentration reduces due to the lower amount of fuel firing burnt. This gives a negative effect to the capture plant.

Steam extraction in the crossover at 4 bar is used in this study in order to account for the additional pressure drop from the crossover to the desuperheater in the capture plant.

The lower pressure of steam extraction at part-load in SSFCC compared with a conventional NGCC configuration, at 58% load, implies that the stripper pressure needs to be released.

Results confirm that the net thermal efficiency increases at part-load with SSFCC compared with to a conventional NGCC configuration where efficiency reduces at part-load operation.

When operated at part-load, these configurations show greater operational flexibility by utilising the additional degree of freedom associated with the combustion of natural gas in the HRSG to change power output according to electricity demand and to ensure continuity of CO_2 supply when exposed to variation in electricity prices.

Alternatively, it is possible to lower minimum stable generation, at the expense of efficiency, by altering the load of the GT and the load of the steam cycle. This is currently not included in the thesis because as discussed in section 6.5, the used of variable IGV is detrimental to efficiency and in this work the optimisation is based on selecting configurations of SSFCC with the highest efficiency and would consist of additional modelling work. The additional work would be worthy for Part-load optimisation where the aim is to maximize revenue considering selling CO_2 for EOR. This is included as future work in chapter 7 section 7.2.4.

United State and Canada were identified as countries where supplementary firing could be attractive because of cheap gas price and where supply CO_2 for EOR is important. The optimum operating strategy of SSFCC defined in this study could be applicable in these countries too where the introduction of intermittent renewable energy is growing exponentially. In addition, the extreme variation in temperature in winter makes to change the power output. The optimum way to operate SSFCC at part-load could be applicable to other alternatives such as sequential gas turbine combustion described in section 3.2.4 and combined cycle with additional arcillary boiler.

7. Conclusion and future work

7.1 Conclusion

A series of new gas-fired new power stations in Mexico with a total capacity of 8 GW is currently planned to be constructed less than 100 km away from significant geological CO_2 storage capacity in the form of hydrocarbon reservoirs where CO_2 would be injected for enhanced oil recovery. Based on the extensive experience around the world using amine solvents, Mexico is developing experience in this area, as proposed in Mexico's roadmap for CCUS, and will continue to do so in the future. This indicates that the technology and alternatives suggested for Mexico will continue to be focused on amine-based post-combustion CO_2 capture. The first main contribution and novelty of this work is to propose the priority CCS project in Mexico. It is proposed that the next steps for four power plants located in the inclusion zone: Noreste, Monterrey, Tamazunchale, Oriental I, II, III, IV, IX, and X is a technical feasibility study to assess whether they could be built as CCUS- ready or whether they could be cost-effectively retrofitted with CCUS. These power plants would supply CO_2 for the purpose of Enhanced Oil Recovery and could be considered as priority CCS project in Mexico. Overall, new gas-fired power stations built in the period 2014-2028 are expected to result in emissions of up to 50 million tonnes CO_2/year. Based on the distance and location from the oil field, 19.8 million tonnes/year out of 50 could be connected to EOR projects. As a result, they could supply a large fraction of the demand of CO_2 for EOR, estimated to be 50 $MtCO_2$ / year in Mexico (Lacy et al, 2013).

Sequential supplementary firing in the Heat Recovery Steam Generator (HRSG) of NGCC plants is evaluated in this thesis, and compared to a conventional NGCC plants with CO_2 capture for EOR, which is the main major thesis contribution and novelty. The technology is evaluated in the context of NGCC plants becoming the dominant source of electricity generation in Mexico, affordable natural gas prices in North America, and the opportunity for additional revenues to electricity sales with connection to an EOR project. Although the study was applied for Mexico, it is concluded that it can be applied in countries with similar characteristic to Mexico e.g. cheap gas price and opportunities for EOR projects.

A heat recovery steam generator is proposed where additional fuel is combusted to increase the volumes of carbon dioxide available for EOR. The maximum amount of CO_2 is produced by reducing excess oxygen levels as low as practically possible (of the order of 1% v/v). The

total power output of an illustrative sequential supplementary firing configuration with CO_2 capture, consisting of a single gas turbine and heat recovery steam generator train, is 824 MW with a supercritical combined cycle, 781 MW with a subcritical combined cycle, compared to 794 MW for a conventional NGCC configuration with capture with two gas turbines and two HRSGs. The difference in the power output is due to the design of the heat recovery steam generator where additional fuel burnt increases heat available for steam generation in the combined cycle. This allows a reduction by half of the number of GT/HRSG trains and of the total volume of flue gas. The reduction of overall capital costs is, respectively, 9.1 % relative and 15.3% relative for the supercritical and the subcritical configurations compared to the conventional configuration with capture. Both subcritical and supercritical sequential supplementary firing configurations also present a reduction in the electricity output penalty compared to a conventional NGCC plant with capture.

The sensitivity of Total Revenue Requirements (TRR) for low-carbon electricity generation, a metric combining levelised cost of electricity and revenue from EOR, to CO_2 prices and fuel prices, is used to compare configurations. Since capital cost estimates are bound to include large biases and uncertainties, a sensitivity analysis is performed showing that conclusions are robust over a range of gas prices and CO_2 prices for EOR, and that sequential supplementary firing is advantageous in the context of North American gas prices.

A comparison between a subcritical and a supercritical SSFCC configuration shows that improvements in power plant efficiency with supercritical steam conditions consistently result in a lower TRR. At gas prices ranging from 2 to 6 $/MMBTU, supercritical SSFCC may receive additional revenues ranging from 1.5 to 4$/MWh for CO_2 prices ranging from 0 to 50$/tonne CO_2 compared to subcritical configurations.

Power plants in Mexico are expected to increasingly operate at part-load in the future due to the variation in electricity demand according to the variations in weather conditions, day and hour, and working and non-working days (Mexican Ministry of Energy, 2012). The electricity demand will be influenced by the introduction of variable, non-dispatchable renewable energy. Therefore, the work developed in this thesis extends to examining the operational flexibility of SSFCC power plants to change power output according to electricity demand, and ensure continuity of CO_2 supply when exposed to variations in electricity prices; this is the third main contribution and novelty of this thesis. It evaluates the efficiency of SSFCC at part-load in order to define the power plant strategy modes that maximise power output over a range of fuel input.

Operating strategies for sequential supplementary firing power plant configurations are examined and compared:

1. Supercritical with variable IGV and fixed pressure
2. Supercritical with fixed IGV with fixed in the HRSG
3. Supercritical with fixed IGV with sliding pressure in the HRSG
4. Subcritical with variable IGV with sliding pressure in the HRSG
5. Subcritical with fixed IGV with sliding pressure in the HRSG

The results of these operating modes are compared with a conventional NGCC with capture at part-load where efficiency decreases from 51.1% at 100% load to 44.5% at 58% of load of the cycle.

The optimisation of steady state part-load performance shows that reducing the power output by adjusting supplementary fuel keeps the gas turbine operating at full load and at maximum efficiency when the net power plant output is reduced from 100% to 58%.

The efficiency of the supercritical SSFCC with fixed IGV and sliding pressure in the HRSG configurations increases from 45.6% at 100% load to 46.98% at 58% load because of the increment of marginal efficiency for burning less fuel in the HRSG. The efficiency for supercritical SSFCC with fixed IGV and fixed pressure in the HRSG configurations increases from 45.6% at 100% load to 46% at 58%. Finally, the efficiency for subcritical SSFCC with fixed IGV and sliding pressure in the HRSG configurations increases from 43.15% at 100% load to 45.92% at 58%. In terms of operating flexibility, the operation of the gas turbine at constant inlet guide vanes combined with a reduction of sequential supplementary fuel makes SSFCC configuration more flexible than a conventional NGCC. Fixed pressure operation is proposed as an alternative for supercritical combined cycles to minimise capital costs and provide fast response rates with acceptable performance levels.

7.2 Future works and recommendations

The author recommends the following actions as a future work listed in the next sections.

7.2.1 Sequential supplementary firing combined cycle in cogeneration system

Supplementary firing is an alternative to be used for cogeneration of heat and power because it makes it possible to control the electricity and thermal output separately (Kehlhofer et al.,

2009), as discussed in Chapter 5. The Mexican ministry of Energy launched the new future prospective of the electricity sector 2015-2029 where cogeneration systems are included for the first time. Its participation in electricity generation would be 6.8% in 2029 (Mexican Ministry of Energy, 2015). The limited time available during this Ph.D. thesis after the Mexican ministry of Energy launched the new future prospective of the electricity sector 2015-2029, meant that the potential of sequential supplementary firing combined in a cogeneration system for industrial applications e.g. refineries and petrochemical industries has not been undertaken.

In a cogeneration system, electricity and steam for the process are important. With the incorporation of the capture unit, steam production becomes more important as it would be necessary to supply steam for the capture unit and for the process.

Future assessments of sequential supplementary firing combined cycle recommended by the author are:

1. Evaluate the potential of a cogeneration system in the refineries in Mexico which would include an assessment of the current installed capacity and the future capacity of cogeneration systems
2. Evaluate the capacity for LP steam production for post-combustion capture and for the integration of the refinery process with sequential supplementary firing combined cycle
3. Evaluate sequential supplementary firing combined cycle for two categories:
   - Power station to supply steam to refinery plants at different pressure levels. Here, the power is the first product and steam is secondary
   - Refineries to supply power to the electricity sector. Here the main product is the steam and the electricity is secondary
4. Evaluate the performance of supplementary firing in cogeneration systems with CO_2 capture

7.2.2 Capture readiness for sequential supplementary firing combined cycle

A capture ready power plant is one that has been designed and built for incorporation with CCS technology in future (IEAGHG, 2007). It is very important to prepare future power plants in Mexico ready to capture, especially for power plant that would be built in 2023-2028 as described in chapter 2. This action leads to a reduction of the capital cost when CCS is incorporated in a power plant in the future, as well as the operating cost and a reduction in the

energy penalty. In addition, earlier research outcomes could be used to create a technology roadmap for the design of new built NGCC power plants and how they will have to operate for EOR and reduce CO_2 emissions.

Capture readiness is suggested by the author for new installed gas-fired capacity in planning of 14,795 MW in 2016-2022 and 26,955 MW in 2023-2028 to be built in Mexico, as discussed in chapter 2, section 2.2.4., as well as capture readiness in cogeneration systems. Capture-ready design options incorporating sequential supplementary firing are relevant strategies in this context, as well as capture ready design options in cogeneration systems integrated with refinery processes.

Modification in the number of duct burners. The main difference between a conventional NGCC and sequential supplementary firing consists of necessary modifications to the HRSG to accommodate several stages of duct burners and of changes to the steam turbine configurations. In the HRSG of a NGCC plant, the temperature of the flue gas is lower than in a coal power plant boiler. Therefore, the main contribution to the heat transfer coefficient is due to convection (Dumont and Heyen, 2012).

This is one of the reasons for the short spacing of the tubes. If a NGCC plant were built to be made 'sequential supplementary firing' ready, without the sequential duct burners initial, as shown in Figure 7.1, enough space would be necessary to incorporate the duct burners later. This would affect convective heat transfer, and as a result, additional heat loss would occur during the operation of the plant without duct firing. These additional losses can be expected to be small and a recommendation for future work is to examine the performance of 'sequential supplementary firing' ready unit without duct firing and without capture.

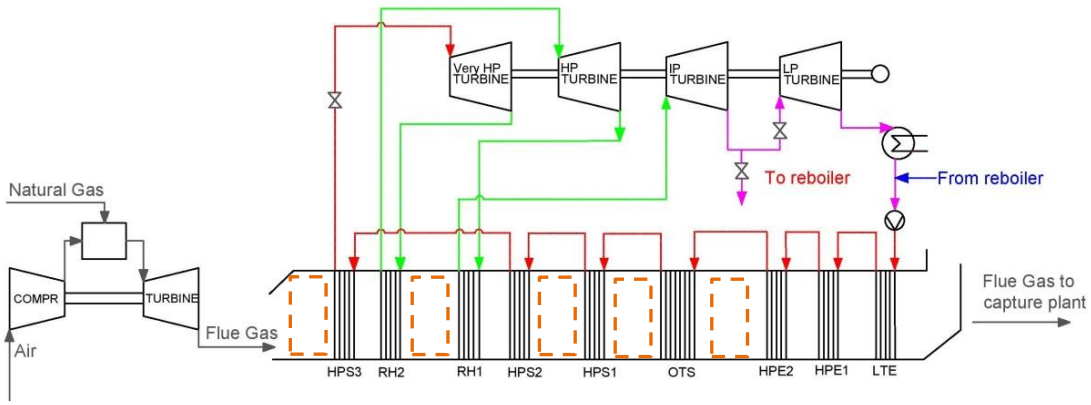

Figure 7.1. Supercritical SSFCC without duct burners

7.2.3 A detailed capital estimation

Further work is needed to include site specific considerations and detailed capital estimates at basic and detailed engineering stage beyond this conceptual work included in this thesis.

7.2.4 Part-load optimisation where the aim is to maximize revenue

Further work is needed for evaluating part-load optimisation where the aim is to maximize revenue, not power output using the additional degrees of freedom of supplementary firing to

- Optimise ratio of CO_2 to electricity to maximise revenue
- Establish ways to maintain a minimum CO_2 flow for EOR when the plant is at minimum stable generation

7.2.5 The use of steam jet booster and

The additional work will consist in evaluate the alternative of integration "the use of steam jet booster at part-load" and to compare with other alternatives in order to analyse the benefit over other alternatives of integration.

7.2.6 Economic implication of supercritical SSFCC operated in dual mode fixed and sliding pressure

This study is important in order to decide if it is worthy to invest additional capital cost to operate at sliding pressure in a supercritical HRSG to increase the efficiency at part-load.

References

Abbd-Alla, G.H., et al., 2001. Effects of diluent admissions and intake air temperature in exhaust gas recirculation on the emissions of an indirect injection dual fuel engine. Energy Convers Manage. 42, 1033-1045.

Abu-Zahra, M.R.M., Schneiders, L.H.J., Niederer, J.P.M., Feron, P.H.M., Versteeg, G.F., 2007. CO_2 capturefrompowerplantsPartI.Aparametricstudyofthetechnical performance based on monoethanolamine. Int. J. Greenh. Gas Control 1, 37–46.

Aboudheir, A., ElMoudir, W., 2009. Performance of Formulated Solvent in Handling of Enriched CO_2 Flue Gas Stream. Energy Procedia 1 (2009) 195–204.

Aburto, J. L., and Valdovinos, M. A. 2014. Visión de CFE sobre la captura y confinamiento de CO_2, Gas networking meeting UKCCRC, Cuernavaca, Morelos, Mexico, February, 2014.

Agren, N., Westermark, M., Bartlett, M., and Lindquist, T., 2000. First experiments on an evaporative gas turbine pilot power plant: water circuit chemistry and humidification evaluation. ASME paper No. 2000-GT168. Proceedings of ASME International Gas Turbine and Aeroengine Congress and Exhibition, Munich, Germany, 8–11 May 2000.

Aguilar, E., 2007. Diseño de procesos en Ingeniería Química. IMP and IPN, 3rd edition, pag. 65-82.

Alcaraz, M. 2015. Internal report of simulation at part-load of 9FB gas turbine in Thermoflow 2013 for Instituto de Investigaciones Electrical (Electrical Research Institute)

Amann, J., Kanniche M., Bouallou, Ch, 2009. Reforming natural gas for CO_2 pre-combustion capture in combined cycle power plant, Clean Techn Environ Policy (2009) 11:67–76.

Asen K., and Eimer, D., 2008. Method for Removing and Recovering Co2 from an Exhaust Gas, Publication number US 20080060346 A1, Original Assignee Norsk Hydro Asa.

ASME paper No. 2000-GT168. Proceedings of ASME International Gas Turbine and Aerorengine Congress and Exhibition, Munich, Germany, 8–11 May 2000.

Annual Energy Outlook, 2007; Energy Information Agency Report No. DOE/EIA-0383; 2007.

Biliyok Ch. and Yeung, H., 2013. Evaluation of natural gas combined cycle power plant for post-combustion CO_2 capture integration. International Journal of Greenhouse Gas Control 19, 396-405

Bolland, O.; Mathieu, P., 1998. Comparison of two CO_2 removal options in combined cycle power plants, Energy Convers. Manage. 39 (16−18), 1653−1663.

Bolland, O., Mathieu, P., 1997. Comparison of Two CO_2 removal Options in Combined Cycle Power Plants. Energy Convers. Manage. 39 (16-18), 1653-1663.

Bolland, O. and Sæther, S., 1992. New concepts for natural gas fired power plants which simplify the recovery of carbon dioxide. Energy Convers. Manage. 1992, 33 (5−8), 467−475.

Bowman M., Sanbor, S., Evulet, E., Ruud, J., 2008. Carbon dioxide capture systems and methods. Patent US 20080011160 A1, Original Assignee General Electric Company

Boyce, M.P., 2006. Gas Turbine Engineering Handbook, 3rd ed., 2006.

Brun, K. and Nored, M, 2008. Application guideline for centrifugal compressor surge control systems, Gas Machinery Research Council. http://www.gmrc.org/documents/GMRCSurgeGuideline_000.pdf.

Canadian Gas Association, 2016 http://www.cga.ca/gas-stats/

CERREY, 2016. http://www.cerreygroup.com/quien.htm

Chakma A. CO_2 Capture Processes – Opportunities for Improved Energy Efficiencies. Energy Conversion and Management 1997; 38(1):51-56.

Charlton, D., 2009. Managing minimum load. Power http://www.powermag.com/managing-minimum-load/

Chemical Engineering index 2013

Cziesla, F., Kremer, H., Much, U., Riemscheneider, J., Quinkertz, R., 2009. Advanced 800+ MW steam power plants and future CCS options, COAL-GEN Europe, September 1-4, 2009, Katowice, Poland

COPAR 2013 (Costos y parámetros de referencia para la formulación de proyectos de inversion del sector eléctrico) Cost and parameter of reference for Project formulation of projects of investment in the electrical sector, 32 edition. Mexican Federal commison of electricity.

Cotton, 1994. Evaluating and Improving Steam Turbine Performance

CTF/TFC 2009. Clean Technology Fund Investment Plant for Mexico. Meeting of the CTF Trust fund Committee. January 29-30 2009. Washington, D.C. Climate Investment Funds CTF/TFC.2/8.

Darie, G., Petcu, H., Negreanu, G., Gherghina, V., 2007. Sliding pressure operation of large conventional steam power units. Proceedings of the 5th IASME/WSEAS Int. Conference on Heat Transfer, Thermal Engineering and Environment, Athens, Greece, August 25-27, 299.

Dávila, M., Jiménez, O., Castro R., Arévalo, V., Stanley, J., and Cabrera, L., 2010. A preliminary selection of regions in Mexico with potential for geological carbon storage. International Journal of Physical Sciences Vol. 5(5), pp. 408-414.

Desideri U., Paolucci A. Performance Modeling of a Carbon Dioxide Removal System for Power Plants. Energy Conversion and Management 1999; 40: 1899-1915.

Ditaranto, M., Hals, H., Bjørge, T., 2009, Investigation on the in-flame NO reburning in turbine exhaust gas. Proceedings of the Combustion Institute.

DOE/NETL, 2013. Cost and Performance Baseline for Fossil Energy Plants Volume 1: Bituminous Coal and Natural Gas to Electricity. US Dept of Energy, National Energy Technology Laboratory, Pittsburgh, PA.

DOE/NETL, 2013. Carbon dioxide transport and storage cost in NETL studies. Annual

DOE/NETL, 2012. Quality Guidelines for Energy System Studies. CO_2 Impurity Design Parameters. DOE (United States Department of Energy)/NETL (National Energy Technology Laboratory).

DOE/NETL, 2007; Energy Information Agency Report No. DOE/EIA-0383; 2007.

DOE/NETL, 2007. Carbon dioxide capture from existing coal-fired power plant.

Dumont N.M., Heyen G., 2004. Mathematical modelling and design of an advanced once-through heat recovery steam generator, Computers and Chemical Engineering 28, pp. 651–660.

ElKady, A. M.; Evulet, A. T.; Brand, A.; Ursin, T. P.; Lynghjem, A., 2008. In Exhaust Gas Recirculation in DLN F-Class Gas Turbines for PostCombustion CO_2 Capture, ASME Turbo Expo 2008: Power for Land, Sea and Air, Berlin, Germany.

Elmasri, M., 2002. Gas turbine components - turbine, Section 9: single pressure HRB/CC Thermodynamics.

e-ON, 2016. Carbon Capture and Storage: A Vital Tool to Help Tackle Climate Change. http://www.eon.com/en/business-areas/power-generation/coal/carbon-capture-and-storage/post-combustion-capture-technology.html

e-ON, 2016. Answers to Frequently Voiced Concerns about CCS. http://www.eon.com/en/info-service/faq/innovation/co2-capture-and-storage.html

Evulet, A., ELKadya A., Branda, A., and Chinnet D., 2009. On the Performance and Operability of GE's Dry Low NOx Combustors utilizing Exhaust Gas Recirculation for Post- Combustion Carbon Capture. Energy Procedia. 1, 3809–3816.

Federal Commission of Electricity, 2014. Programa de obras e inversión del sector eléctrico (POISE) 2014-2028 (Version in Spanish). http://www.amdee.org/Publicaciones/POISE-2014-2028.pdf

Franco, F., Anantharaman, R., Bolland, O., Booth, N., Van Dorst, E., Ekstrom, C., Fernandes, E.S., Macchi, E., Manzolini, G., Nicolic, D., Pfeffer, A., Prins, M., Rezvani, S., Robinson, L., 2012. European best practice guidelines for assessment of CO_2 capture technologies.

Ganapathy, V., ABCO Industries, 1996. Heat-Recovery Steam Generators: Understand the Basics. Chemical Engineering progress.

Gas Turbine World 2013 GTW Handbook. Vol. 30: Pequot Publishing INC, 2013.

Gibbins, J. R., Crane, R.I., 2004. Scope for reductions in the cost of CO_2 capture using flue gas scrubbing with amine solvents. Proceedings of the institution of mechanical engineers, part A. J. Power Energy 218, 231–239.

Glassmann, I., 1996. Combustion, 3rd edition, p. 159, Academic Press Inc.

Goff, G., Rochelle, G., 2004. Monoethanolamine Degradation: O_2 Mass transfer Effects under CO_2 Capture Conditions. Industrial Engineering Chemistry Research 43, 6400-6408.

González-Santaló, J. M., 2013. CCUS in the Mexican electrical sector, Gas Network Meeting from UKCCRC, London, England, May 30-31, 2013.

Gonzalez, J., Gonzalez D. A., Mariño C., 2007. Diagnostics of the operation of power plants, POWER2007 ASME Power 2007 July 17-19, 2007, San Antonio, Texas.

Gorset, O., Knudsen, J.N., Morten O. B., , Askestad, I., 2014. Results from testing of Aker Solutions advanced amine solvents at CO_2 Technology Centre Mongstad, in: procedia, E. (Ed.), GHGT-12, Austin Tx.

Halvorsen, B. J. 2012. Power plant with CO_2 capture based on absorption – part-load performance. Thesis dissertation the Norwegian University of Science and Technology.http://daim.idi.ntnu.no/masteroppgaver/008/8304/masteroppgave.pdf

Hatamiya, S., Araki, H, and Higuchi, S., 2004. An evaluation of advanced humid air turbine system with water recovery. Proceeding of Turbo Expo 2004, 14-17 June 2004, GT 2004-54031.

Hatamiya, S., Yamagishi, M., Yokomizo, O., 2003. Gas turbine electric power generation equipment and air humidifier US 6578354 B2, Hitachi, Ltd.

Hellat, J., and Hoffmann J., 2016. Combined cycle power plant with flue gas recirculation, Publication number US9249689 B2. Original Assignee Alstom Technology Ltd.

Hendriks, C., Wildenborg, T., Feron, P., Graus, W., Brandsma, R., 2003. EC- case carbon dioxide sequestration. TNO / ECOFYS.

Herzog, H., Meldon, J., Hatton, A., 2009. Advanced Post-Combustion CO_2 Capture https://mitei.mit.edu/system/files/herzog-meldon-hatton.pdf

Hone, D., 2016. http://blogs.shell.com/climatechange/category/ccs/

Hu, Y., Li, H., Yan, J., 2012. Techno-economic evaluation of the evaporative gas turbine cycle with different CO_2 capture options. Applied Energy 89, 303-314.

IEAGHG 2012. CO_2 capture at gas fired power plants. International Energy Agency Greehouse Gas. Report number: 2012/8.

IEAGHG, 2011. Retrofitting CO_2 capture to existing power plants.

IEAGHG, 2010. Corrosion and materials selection in CCS system. Report 2010/03.

IEAGHG, 2007. CO_2 capture ready plants. Report 2007/4

Innovative Steam Generator IST, 2012. An Aecon company. http://otsg.com/about/about-otsg/

IPCC AR5, 2013. Climate Change 2013: *The Physical Science Basis* http://www.ipcc.ch/report/ar5/wg1/

IPCC, 2010. CO_2 capture. Special Report on Carbon dioxide Capture and Storage.

IPCC CCS, 2004. Special Report on Carbon Dioxide Capture and Storage https://www.ipcc.ch/pdf/special-reports/srccs/srccs_wholereport.pdf

Irons R., 2013. Aspects of CCS at Maasvlakte 3 (ROAD), e-ON.

Jockenhövel T., Schneider R., Schlüter L., SIEMENS, 2009. Optimal Power Plant Integration of Post-Combustion CO_2 Capture. POWER-GEN Europe 2009, Cologne, Germany May 26-29, 2009. http://www.energy.siemens.com/nl/pool/hq/power-generation/power-plants/steam-power-plant-solutions/coal-fired-power-plants/Optimal-Power-Plant-Integration.pdf

Jonshagen, K., Sipocz, N., Genrup, M., 2011. A novel approach of retrofitting a combined cycle with post combustion CO_2 capture. Journal of engineering for gas turbine and power, vol. 133.

Jordal, K., Marchioro, A.Y., Anantharaman, R., Chikukwa, A., Bolland, O., 2012. Design-point and part-load considerations for natural gas combined cycle plants with post combustion capture. International Journal of Greenhouse Gas Control 11, 271-282.

Karimi, M., Hillestad M., and Svendsen H., 2012. Natural Gas Combined Cycle Power Plant Integrated to Capture Plant, Energy & Fuel, 26, 1805−1813.

Kehlhofer, P., Hannemann, F., Stirninmann, F., and Rukes, B., 2009. Combined-cycle gas and steam turbine power plant, 3rd edition. PennWell corporation.

Kiameh, P., 2003. Power generation handbook: selection, applications, operation, and maintenance. McGRAW-HILL.

Kim, I. and Svendsen, H., 2007. Heat of absorption of carbon dioxide (CO_2) in monoethanolamine (MEA) and 2-(aminoethyl) ethanolamine (AEEA) solutions. Industrial & engineering chemistry research, 2007. 46(17): p. 5803-5809.

Kjaer, S., 1993. The advanced pulverized coal fired power station. Background, status and future. UNIPEDE/IEA Conference on thermal power generation and evironment, Hamburg.

Knudsen, J. N., 2011. Results from test campaigns at the 1 t/h CO2 post-combustion capture pilot-plant in Esbjerg under the EU FP7 CESAR project. In PCCC1 Abu Dhabi, 2011.

Kohl, A., and Nielsen, R., 1997. Gas purification, fifth edition.

Kvamsdal, H.M., Jakobsen, J.P., Hoff, K.A., 2009. Dynamic modelling and simulation of a CO_2 absorber column for post-combustion CO_2 capture. Chemical Engineering and Processing: Process Intensification 48, 135-144.

Lacy, R., 2014. Carbon Capture, Use and Storage. Life Cycle Approach, Gas networking meeting UKCCRC, Cuernavaca, Morelos, Mexico, February, 2014.

Lacy, R., Serralde A., Climent M., V.M., 2013. Initial assessment of the potential for future CCUS with EOR projects in Mexico using CO_2 captured from fossil fuel industrial plants. International Journal of Greenhouse Gas Control 19, 212-219.

Leung, D., Caramanna G., Maroto-Valer M. 2014. An overview of current status of carbon dioxide capture and storage technologies. Renewable and Sustainable Energy Reviews 39 (2014) 426–443

Li, H., Ditaranto, M., Yan, J., 2012. Carbon capture with low energy penalty: Supplementary fired natural gas combined cycles. Applied Energy 97, 164-169.

Li, H., Ditaranto, M., Berstad, D., 2011. Technologies for increasing CO_2 concentration in exhaust gas from natural gas-fired power production with post-combustion, amine-based CO_2 capture. Energy 36, 1124-1133.

Li, H,. Flores S., Hu, Y., Yan, J. 2009. Simulation and optimization of evaporative gas turbine with chemical apsorption for carbon dioxide capture. International journal of green energy 2009; 6(5): 527-39.

Liebenthal, U., and Kather A., 2011. Design and Off-Design Behaviour of a CO_2 Compressor for a Post-Combustion CO_2 Capture Process. 5th International Conference on Clean Coal Technologies, Saragoza, Spain, 8 - 12 May 2011.

Lieuwen, T., and Yang, V., 2013. Gas turbine emission. Cambridge University press.

Lindquist, O. T., Thern, M., and Torisson, T. 2002. Experimental and theoretical results of a humidification tower in an evaporative gas turbine cycle pilot plant. ASME Turbo Expo 2002, Amsterdam, The Netherlands.

Lindquist, T. O., Rosen, P. M., and Torisson, T., 2000. Theoretical and experimental evaluation of the EvGT process, 2000. Proceedings of ASME Advanced Energy Systems Division, Orlando, FL, USA.

Lindquist, T. O., Rosen, P. M., and Torisson, T., 2000. Evaporative gas turbine cycle – a description of a pilot plant and operating experience. Proceedings of ASME Advanced Energy Systems Division, Orlando, FL, USA.

Lombardi, L., 2003. Life cycle assessment comparison of technical solutions for CO_2 emissions reduction in power generation, Energy Conversion and Management 44 (2003) 93–108.

Lucquiaud, M., Gibbins, J., 2011a. Effective retrofitting of post-combustion CO_2 capture to coalfired power plants and insensitivity of CO_2 abatement costs to base plant efficiency. International Journal of Greenhouse Gas Control 5, 427-438.

Lucquiaud, M., Gibbins, J., 2011b. On the integration of CO_2 capture with coal-fired power plants: A methodology to assess and optimise solvent-based post-combustion capture systems. Chemical Engineering Research and Design 89, 1553-1571.

Lucquiaud, M., Gibbins, J., 2009. Retrofitting CO_2 capture ready fossil plants with postcombustion capture. Part 1: Requirements for supercritical pulverized coal plants using solventbased flue gas scrubbing. Proceedings of the Institution of Mechanical Engineers, Part A: Journal of Power and Energy 223, 213-226.

Lucquiaud, M., Chalmers, M., Gibbins, J., 2009. Capture-ready supercritical coal-fired power plants and flexible post-combustion CO_2 capture. Energy Procedia 1, 1411–1418.

LÜDTKE, K.: Process Centrifugal Compressors. Springer-Verlag Berlin Heidelberg, 2004.

McCauley K.J., Weitzel, P.S., McDonald, D.K., Poling C.W., 2012. Deploying Advanced Steam Plants and Integrating Carbon Capture Technologies. Babcock & Wilcox Power Generation Group, Inc. Power-Gen Europe Cologne, Germany June 12-14, 2012

McManus, M., Boyce, D., Baumgarther, R., 2007. Integrated Technologies that Enhance Power Plant Operating Flexibility, – Siemens Power Generation. Power Gen International, New Orleans, USA, December 11–13.

Mechleri, E.D., Biliyok, C., Thornhill, N.F., 2014. Dynamic simulation and control of postcombustion CO2 capture with MEA in a gas fired power plant, Computer Aided Chemical Engineering, pp. 619-624.

Merkel, C.T., Wei, X., He Z., White, L.S., Wijmans J. G., Baker R. W., 2012. Selective Exhaust Gas Recycle with Membranes for CO_2 Capture from Natural Gas Combined Cycle Power Plants, Ind. Eng. Chem. Res. 52(3), 1150-1159.

Mexican Ministry of Energy, 2015. Mexican electric sector prospective 2015-2029. In: Annually Revision of the Mexican electricity sector (Version in Spanish).

https://www.gob.mx/cms/uploads/attachment/file/44328/Prospectiva_del_Sector_Electrico.pdf

Mexican Ministry of Energy, 2014. Mexican electric sector prospective 2014-2028. In: Annually Revision of the Mexican electricity sector (Version in Spanish).

Mexican Ministry of Energy 2014. CCUS technology road map in Mexico. http://www.sener.gob.mx/portal/Default_intermedia.aspx?id=2860

Mexican Ministry of Energy 2012, Mexican electric sector prospective 2012-2026, In: Annually Revision of the Mexican electricity sector (Version in Spanish). http://www.sener.gob.mx/res/PE_y_DT/pub/2012/PSE_2012_2026.pdf

Mexican Ministry of Environment and Natural Resources, 2014. Special Program on Climate Change 2014-2018. (Version in Spanish). http://www.semarnat.gob.mx/sites/default/files/documentos/transparencia/programa_especial_de_cambio_climatico_2014-2018.pdf

Mexican Ministry of Environment and Natural Resources, 2007. Special Program on Climate Change 2009-2012. http://www.preventionweb.net/english/policies/v.php?id=47412&cid=112

Mitsubishi Heavy Industries, 2007. Ltd. Technical Review Vol. 44 No. 4 (Dec. 2007)

Mohammad R. M. Abu Zahra, 2009. Carbon Dioxide Capture from Flue Gas , Development and Evaluation of Existing and Novel Process Concepts. PhD thesis, TU delft http://repository.tudelft.nl/islandora/object/uuid:6d1689f3-7b1a-4355-81b0-af3d19fae469/?collection=research

National Energy Technology Laboratory, 2013. Current and Future Technologies for Natural Gas Combined Cycle (NGCC) Power Plants. DOE/NETL-341/061013, U.S. Department of Energy, Office of Fossil Energy.

National Energy Technology Laboratory (NETL), 2012. Fossil Energy RD&D: Reducing the Cost of CCUS for Coal Power Plants, Revision 1; NETL: Pittsburgh, PA; Report DOE/NETL-2012/1550.

National Energy Technology Laboratory, 2010. Carbon Capture Approaches for Natural Gas Combined Cycle Systems; U.S. Department of Energy Report No. DOE/NETL-2011/ 1470.

National Energy Technology Laboratory (NETL), 2010. Storing CO2 and Domestic Crude Oil with Next Generation CO2-EOR Technology: An Update; NETL: Pittsburgh, PA; Report DOE/NETL-2010/ 1417.

North American Carbon Storage Atlas Organization, 2012. North American Carbon Storage Atlas 2012. http://www.netl.doe.gov/technologies/carbon.seq/refshelf/NACSA2012.pdf

Ogink, M., 2015. Analyses and dynamic modelling of the compressor section in a PCC-process for coal-fired power plants with offshore storage. Master thesis. Delft University. http://delfturbanwater.nl/publications-2/

Oil price, 2014. http://oilprice.com/Energy/Energy-General/Mexico-Shale-Gas-Industry-and-Energy-Reform.html

Ol'khovskii, G., et al, 2013. Thermal Tests of the 9FB Gas Turbine Unit Produced by General Electric, Thermal engineering Vol. 60 No. 9, pp 607-612.

Parsons Brinckerhoff 2013, Electricity generation cost model - 2013 update of non-renewable technologies, Department of Energy and Climate Change, 3512649A.

PECC, 2013. Plan Nacional de Desarrollo 2013-2018. Programa Especial de Cambio Climático 2014-2018 (PECC), Mexico.

Razi, N., Svendsen, H.F., Bolland, O., 2013. Validation of mass transfer correlations for CO_2 absorption with MEA using pilot data. International Journal of Greenhouse Gas Control 19, 478-491.

Reddy, S., Scherffius, J., Freguia, S., Fluor's Econamine FG. 2003. PlusSM Technology: An Enhanced Amine-Based CO2 Capture Process. 2003. Second National Conference on Carbon Sequestration National Energy Technology Laboratory/Department of Energy, Alexandria, VA, May 5–8.

Regulatory Commission of Energy, 2016. Daily report prices of natural gas, liquefied petroleum gas, fuel and oil. (version in Spanish). http://www.cre.gob.mx/documento/3084.pdf

Rezazadeh, F., Galea, W., Hughesb, K., Pourkashania, M., 2015. Performance viability of a natural gas fired combined cycle power plant integrated with post-combustion CO_2 capture at part-load and temporary non-capture operations. International Journal of Greenhouse Gas Control 39 (2015) 397–406.

Roadmap for carbon capture and storage demonstration and deployment in the people's republic of china, November 2015

http://www.adb.org/publications/roadmap-carbon-capture-and-storage-demonstration-and-deployment-prc

Rodriguez De La Garza, 2014. CO_2-EOR Program in Mexico, Gas networking meeting UKCCRC, Cuernavaca, Morelos, Mexico, February, 2014.

Rochelle, G. T. 2009. Amine Scrubbing for CO_2 Capture. Science. Vol. 325, 1652−1654.

Rokke, E., Hustad J. E., 2005. Exhaust Gas Recirculation in Gas Turbines for Reduction of CO_2 Emissions; Combustion Testing with Focus on Stability and Emissions. Industrial Journal of Thermodynamics 8, 167-173.

Rovira, A., Valdes, M., Duran, M., 2010. A model to predict the behaviour at part load operation of once-through heat recovery steam generators working with water at supercritical pressure. Applied Thermal Engineering 30(13):1652-1658.

Rubin, E.S., Short, C., Booras, G., Davison, J., Ekstrom, C., Matuszewski, M., McCoy, S., 2013. A proposed methodology for CO_2 capture and storage cost estimates. International Journal of Greenhouse Gas Control 17, 488-503.

Rubin, E.S., Rao, A.B., 2002. A Technical, Economic and Environmental Assessment of Amine-based CO_2 Capture Technology for Power Plant Greenhouse Gas Control. USDOE.

Sáez, A. 2010. Industrial application of natural gas. Universidad Técnica Federico Santa María Chile. http://cdn.intechopen.com/pdfs-wm/11486.pdf

Salazar-Pereyra, M., Lugo-Leyte, R., Zamora-Mata, J., Ruiz-Ramírez, O., González-Oropeza, R., 2011. Análisis termodinámico de los ciclos rankine supercríticos y subcríticos. CIBIM 10, Oporto, Portugal, 2011.

Sanchez Fernandez, E., Lucquiaud M., Chalmers H., Khakhariab P., Goetheerb E., and Gibbins J., 2016. Operational flexibility options in power plants with integrated post-combustion capture. International Journal of Greenhouse Gas Control.

Sanchez Fernandez, E., Chalmers, H., Naylor, M., Aghani, H., Wettenham, B., Race, J., 2015. Developing CO_2 networks: Key lessons learnt from the first Flexible CCS Network Development (FleCCSnet) project workshop. UKCCSRC.

Sanchez Fernandez, E., Goetheer, E.L.V., Manzolini, G., Macchi, E., Rezvani, S., Vlugt, T.J.H., 2014. Thermodynamic assessment of amine based CO_2 capture technologies in power plants based on European Benchmarking Task Force methodology. Fuel 129, 318-329.

Sanchez Fernandez, E., Heffernan K., van der Ham L., Linders M., Eggink E., Schrama F., Brilman D. W. F., Goetheer E., & Vlugt T., 2013. Conceptual Design of a Novel CO_2 Capture Process Based on Precipitating Amino Acid Solvents. Industrial & Engineering Chemistry Research, 52 (34), 12223-12235.

Satyanarayana, I., Gupta, S., Rajulu, K., Second Law Analysis of Super Critical Cycle. International Journal of Engineering (IJE), Volume(4): Issue(1)

Scottish Power, 2009. Carbon Capture Ready Feasibility Study

Siemens, 2009. CO_2 — Taking the bull by the horns. http://www.energy.siemens.com/co/pool/hq/energy-

topics/venture/downloads/Compression%20solution%20for%20carbon%20capture%20and%20storage.pdf

Siemens, 2006. Introduction to the complementary fired combined cycle power plant, POWER-GEN, Orlando, FL.

Sinclair Knight Merz, 2009. Carrington II Power Station, Carbon capture readiness report. April 2009

Sipocz, N., Jonshagen, K., Assadi, M., Genrup, M., 2011. Novel high-performing single pressure combined cycle with CO2 capture. Journal of engineering for gas turbine and power, vol. 133.

Shiralkar, B., and Griffith, P., 1968. The deterioration in heat transfer to fluids at supercritical pressure and high heat fluxes, Report No. DSR 70332-55, Contract No. Grant-In-Aid American Electric Power, Department of Mechanical Engineering Engineering Projects Laboratory Massachusetts Institute of Technology, June 30, 1968.

Steam its generation and use, 2005. The Babcock & Wilcox Company, 2005. Edition 41.

Swenson, H. S., Carver, J. R., and Kakarala, C. R., 1965. Heat Transfer to Supercritical Water in Smooth Bore Tubes, Journal of Heat Transfer, Trans. ASME, 87, pp. 477-483.

Swisher, J., Bhown A., 2014. Analysis and optimal design of membrane-based CO_2 capture processes for coal and natural gas-derived flue gas. Energy Procedia 63 (2014) 225 – 234

Takahashi, T., Nakao, Y., Koda, E., 2007. Analysis and evaluation about advanced humid air turbine system, International conference on power engineering 2007, Hangzhou, China, pp. 341-344.

Thermoflow, 2013. I. D. 272, propiedad IIE. Inc, http://www.thermoflow.com, 2013.

Thern, M., Lindquist, O. T., and Torisson, T. 2003. Experimental and theoretical evaluation of a plate heat exchanger aftercooler in an evaporative gas turbine cycle. ASME Turboexpo 2003, Atlanta, Georgia, USA.

Valdes, M., Rovira, A., Duran, M.D., 2004. Influence of the heat recovery steam generator design parameters on the thermoeconomic performances of combined cycle gas turbine power plants. Int. J. Energy Res. 28, 1255 - 1267.

Valdes, M., Duran, M.D., Rovira, A., 2003. Thermoeconomic optimization of combined cycle gas turbine using genetic algorithms. Appl. Therm. Eng. 23, 2169-2182.

Van der Wijk, P.C., Brouwer, A.S., Van den Broek, M., Slot, T., Stienstra, G., Van der Veen, W., Faaij, A.P.C., 2014. Benefits of coal-fired power generation with flexible CCS in a future northwest European power system with large scale wind power. International Journal of Greenhouse Gas Control 28, 216-233.

Vermeulen, T. N., 2011. KNOWLEDGE SHARING REPORT – CO_2 Liquid Logistics Shipping Concept (LLSC) Overall Supply Chain Optimization, Global CCS Institute https://hub.globalccsinstitute.com/sites/default/files/publications/19011/co2-liquid-logistics-shipping-concept-llsc-overall-supply-chain-optimization.pdf

Versteeg, G.F., Van Dijck, L.A.J., and Van Swaaij, W.P.M., 1996. On the kinetics between CO_2 and alkanolamines both in aqueous and non-aqueous solutions. An overview. Chem. Eng. Commun. 144: p. 133-158.

Versteeg, G.F. and van Swaaij, W.P.M., 1988. On the kinetics between CO_2 and alkanolamines both in aqueous and non-aqueous solutions-I. Primary and secondary amines. Chem. Eng. Sci.. 43(3): p. 573-585.

Versteeg, G.F. and van Swaaij, W.P.M., 1988. On the kinetics between CO_2 and alkanolamines both in aqueous and non-aqueous solutions-II. Tertiary amines. Chem. Eng. Sci. 43(3): p. 587-591.

Veysey, J., Octaviano C., Calvin, K., Herrera, S., Kitous, A., McFarland, J., Van der Zwaan, B., 2015. Pathways to Mexico's climate change mitigation targets: A multi-model analysis. Energy Economics. http://dx.doi.org/10.1016/j.eneco.2015.04.011

Vitalis B., Riley Power Inc, a subsidiary of Babcock Power Inc, 2006. Constant and sliding-pressure options for new supercritical plants, power, Power, 1-7.

Voleno A., Romano, M., Turia, D., Chiesaa, P., Hob, M., Wileyb, D., 2014. Post-combustion CO_2 capture from natural gas combined cycles by solvent supported membranes. Energy Procedia 63 (2014) 7389 – 7397

World steel prices, 2013. http://worldsteelprices.com/index.htm
http://www.alibaba.com/product-detail/Incoloy-825-UNS-N08825-pipe-tube_2014421910.html

WEO, 2015. World Energy Outlook Special Report: Energy Climate and Change.

Wylie R., 2004. Supercritical combined cycle for generating electric power, U.S. Patent 20040148941 A1, August 05, 2004.

Yagi T., Shibuya H., Sasaki T., 1992. Application of Chemical Absorption Process to CO_2 Recovery from Flue Gas Generated in Power Plants. Energy Conversion and Management 1992; 33(5-8): 349-355.

Yari, M., and Sarabch K., 2005. Modelling and optimization of part-flow evaporative gas turbine cycles. Proc. IMechE Vol. 219 Part A: J. Power and Energy.

Zhai H., and Rubin, E.S., 2013. Comparative Performance and Cost Assessments of Coal- and Natural-Gas-Fired Power Plants under a CO_2 Emission Performance Standard Regulation. Energy Fuels, 27, 4290−4301.

Zhang, N., Liorb, N., 2006. Two novel oxy-fuel power cycles integrated with natural gas reforming and CO_2 capture, Energy 33 (2008) 340–351.

Zhang, Y., Cheng C., 2011. Modeling CO_2 absorption and desorption by aqueous monoethanolamine solution with Aspen rate-based model. Energy Procedia 37 (2013) 1584 – 1596. GHGT-11.

Zeldovich, Y. B., 1946. The oxidation of nitrogen in combustion explosions. Acta Physicochimica U.S.S.R. 21: 577-628.Acad. Sci. USSR. Inst. Chem. Phys., Moscow–Leningrad.

Appendix A

Details of equipment costs for HRSG, ducting and stack; Subcritical steam turbine and auxiliary; cooling water system and BOP (Franco et al (2012)

Plant component	Scaling parameter	Referece erected cost C_0 (M€)[a]	Rerefence size, S_0 [a]	NGCC Reference plant size, w/o capture	NGCC Reference plant size, w capture
HRSG, ducting and stack	U*S	32.6	12.9 MW/K	11.5 MW/K	11.5 MW/K
Subcritical steam turbine, generator and auxiliaries	ST gross power	33.7	200 MW	349 MW	263 MW
Cooling water system and BOP	Q_rejected	49.6	470 MW	487 MW	490 MW

Supercritical SSFCC Reference plant size, w/o capture	Supercritical SSFCC Reference plant size, w capture	Subcritical SSFCC Reference plant size, w/o capture	Subcritical SSFCC Reference plant size, w capture	Scale factor f
3.15 MW/K	3.15 MW/K	8.42 MW/K	8.42 MW/K	0.67
N/A	N/A	634 MW	538 MW	0.67
440 MW	440 MW	480 MW	480 MW	0.67

Appendix B

Mass and energy balance of a conventional NGCC at part-load validation of the NGCC, and CO_2 capture plant

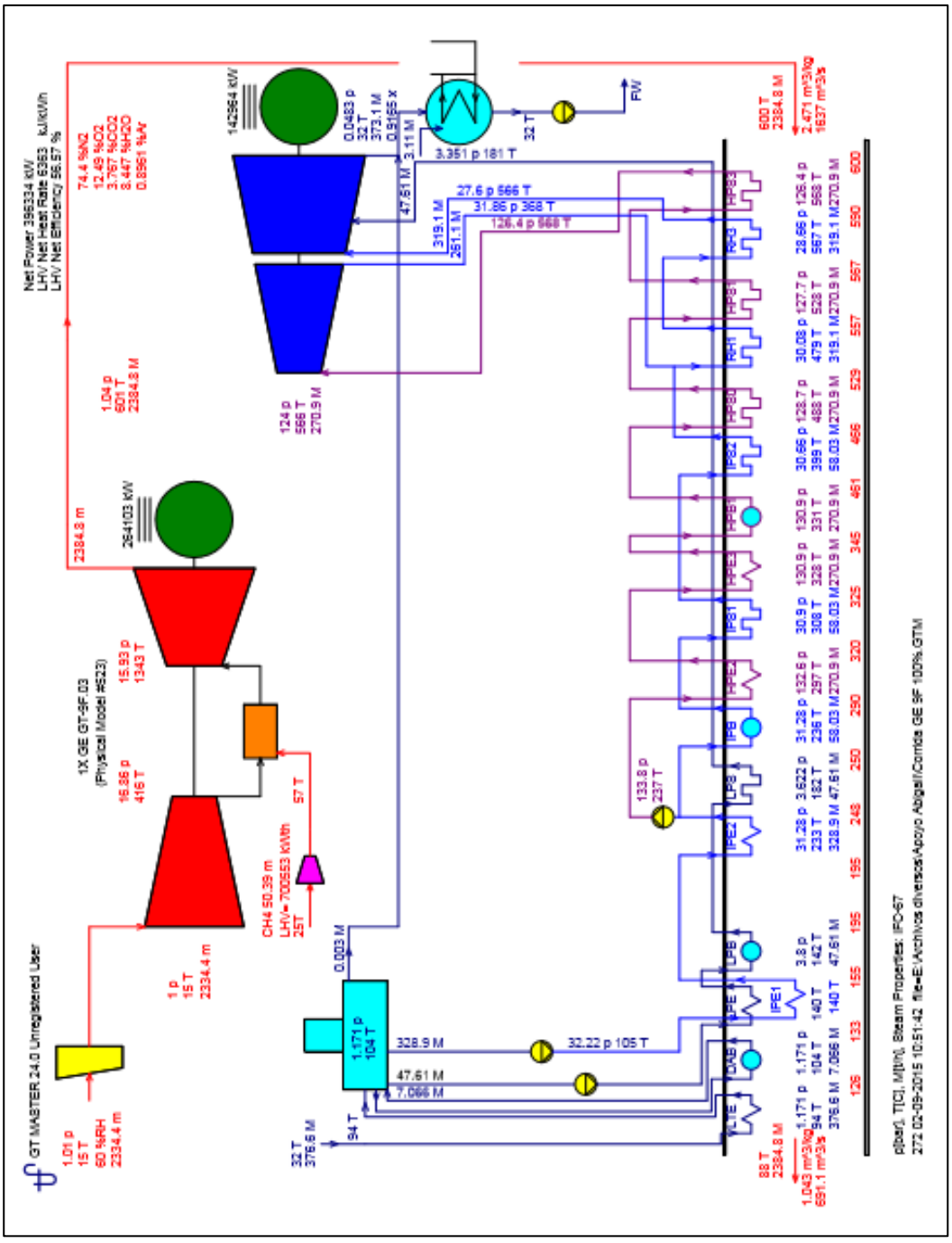

Figure B1. Conventional NGCC at 100% GT load (Alcaraz, 2015)

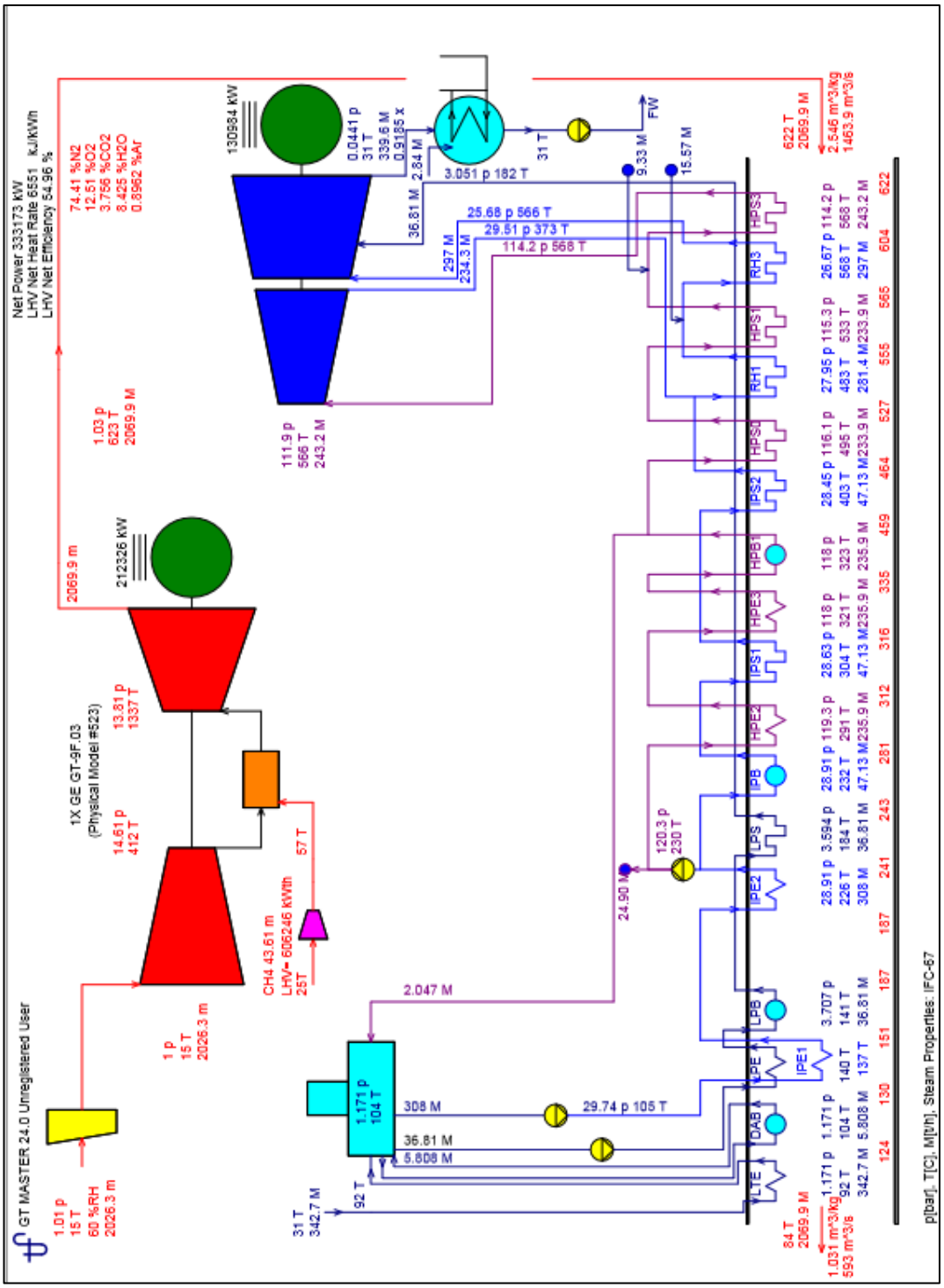

Figure B2. Conventional NGCC at 80% GT load (Alcaraz, 2015)

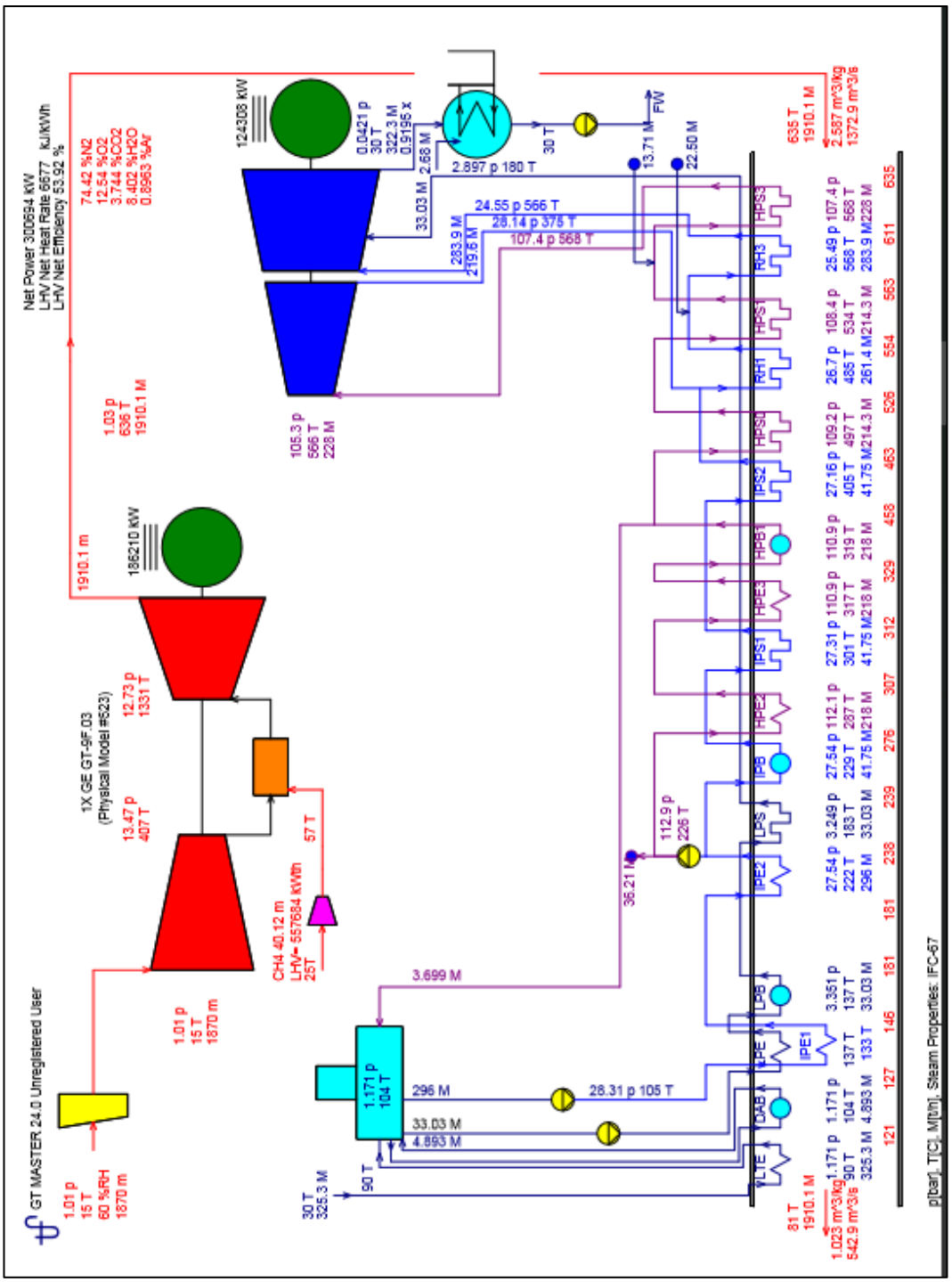

Figure B3. Conventional NGCC at 70% GT load (Alcaraz, 2015)

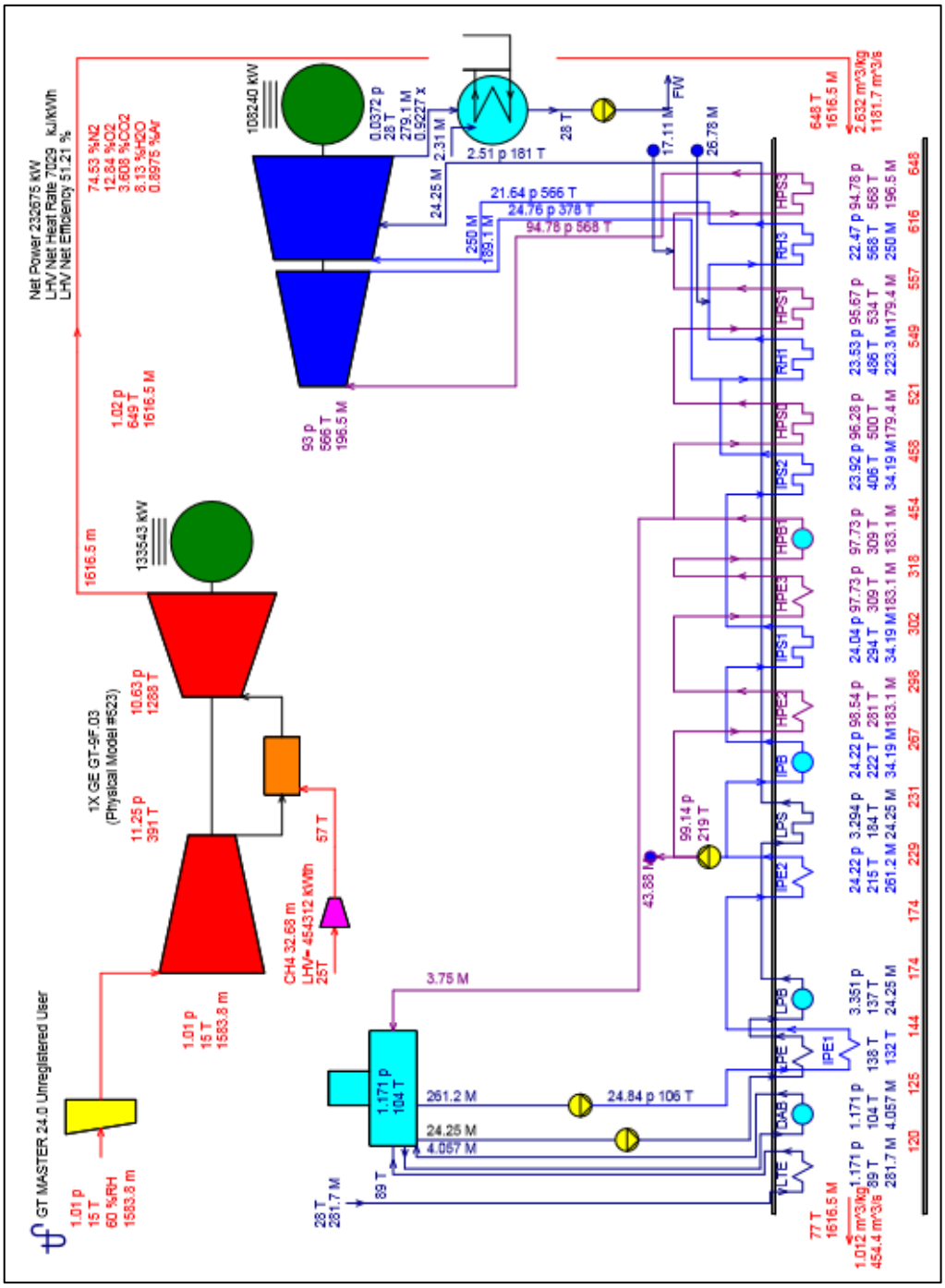

Figure B4. Conventional NGCC at 50% GT load (Alcaraz, 2015)

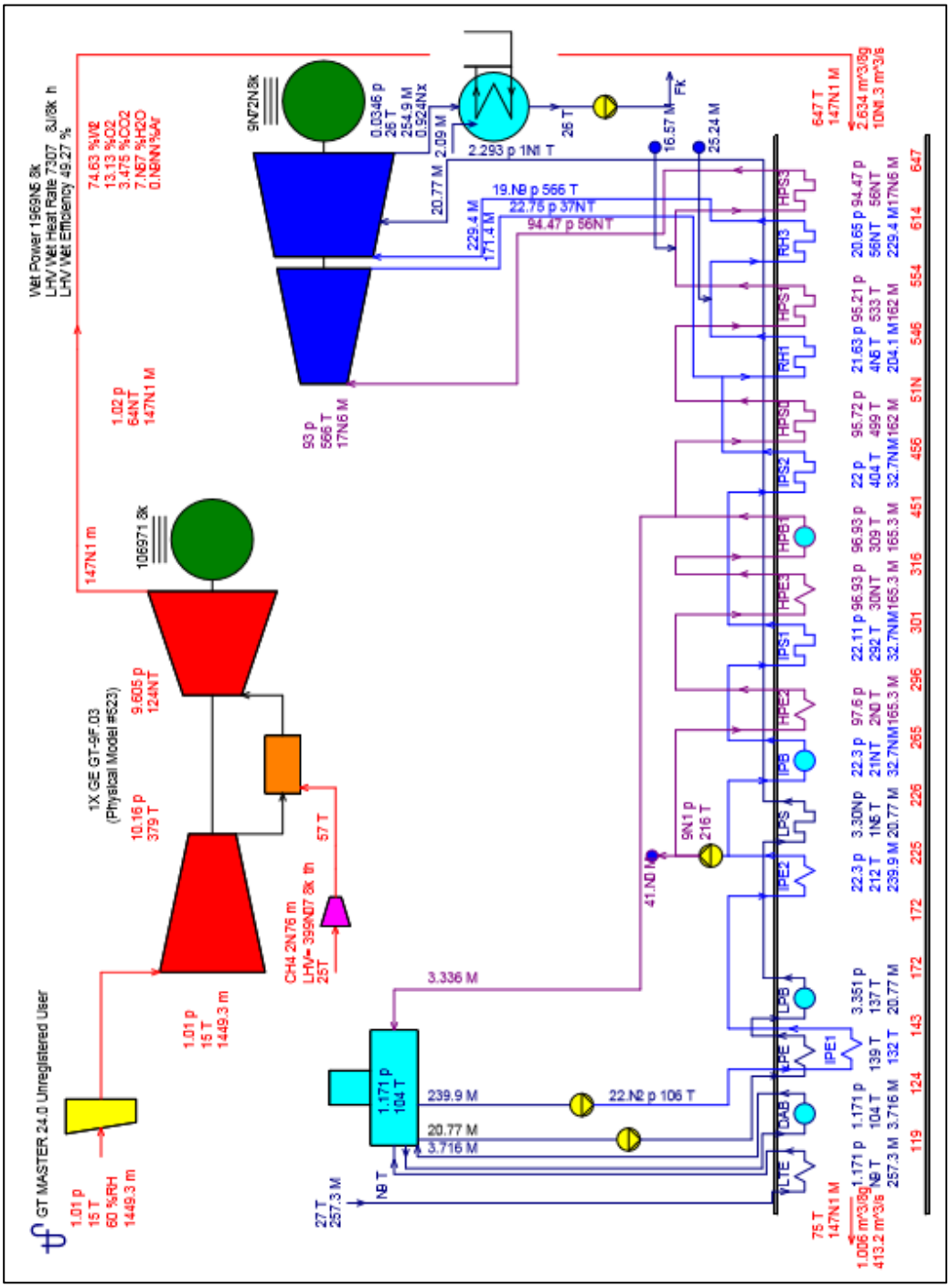

Figure B5. Conventional NGCC at 40% GT load (Alcaraz, 2015)

Appendix C

Deduction of the heat transfer coefficient (Kehlhofer et al., 2009; Jonshagen, 2011)

$$\frac{UA_{op}}{UA_D} = \left(\frac{m_{gop}}{m_{gD}} \right)^{0.61}$$

$$\frac{1}{U_0} = \frac{1}{h_G} + \frac{\delta}{K_M} + \frac{1}{h_m} \tag{1}$$

Vapour side

$$h_v = 0.023 \frac{K_v}{D} \mathrm{Re}_v^{0.8} \mathrm{Pr}_v^{0.4} \tag{2}$$

$$\mathrm{Re}_v = \frac{m_v D}{\mu_v} \tag{3}$$

$$\mathrm{Pr}_v = \frac{Cp_v \mu_v}{K_v} \tag{4}$$

Gas side

$$h_g = 0.4 \frac{K_g}{D} \mathrm{Re}_g^{0.6} \mathrm{Pr}_g^{0..33} \tag{5}$$

$$\mathrm{Re}_g = \frac{m_g D}{\mu_g} \tag{6}$$

$$\mathrm{Pr}_g = \frac{Cp_g \mu_g}{K_g} \tag{7}$$

By combining (2) and (5) in (1)

$$\frac{1}{U} = \frac{1}{0.4 \frac{k_g}{D_T} \mathrm{Re}_g^{0.4} \mathrm{Pr}_g^{0.33}} + \frac{\delta}{K_M} + \frac{1}{0.023 \frac{k_v}{D_T} \mathrm{Re}_v^{0.8} \mathrm{Pr}_v^{0.4}} \tag{8}$$

The heat conductivity through the heat exchanger material is very high compared with h_g and h_v so it can be neglect. In the economizer and evaporator, the heat transfer coefficients on the gas are 0.1 and 0.001 times larger than on the steam side. So equation (8) can be simplified as follow:

$$\frac{1}{U} = \frac{1}{0.4 \frac{k_g}{D_T} \mathrm{Re}_g^{0.4} \mathrm{Pr}_g^{0.33}} \tag{9}$$

Then the expression $\frac{U_{op}A}{U_D A}$ is simplified as follow:

$$\frac{UA_{op}}{UA_D} = \frac{\left(K_g \,\mathrm{Re}_g^{\,0.61}\,\mathrm{Pr}_g^{\,0.33}\right)_{OP}}{\left(K_g \,\mathrm{Re}_g^{\,0.61}\,\mathrm{Pr}_g^{\,0.33}\right)_D} \tag{10}$$

The Prandtl number (Pr) is a dimensionless number depending only on the fluid properties and state of the fluid. The Pr does not vary greatly for different gases, and the temperature dependency is very small. The diameters are fixed and the dynamic viscosity μ can be omitted in most cases.

The expression $\frac{\left(K_g\right)_{OP}}{\left(K_g\right)_D}$ does not vary greatly and depends practically only on the properties of the gas. Equation (10) is simplified as follow:

$$\frac{UA_{op}}{UA_D} = \frac{\left(m_g^{\,0.61}\right)_{OP}}{\left(m_g^{\,0.61}\right)_D} \tag{11}$$

If the heat transfer on both sides is considered in the case for superheaters, because the heat transfer on the steam side is poorer than in the evaporator. The equation 1 is express as follow

$$\frac{1}{U} = \frac{h_v + h_G}{h_v h_G} \tag{12}$$

$\frac{U_{op}A}{U_D A}$ is express as shown in equation (13)

$$\frac{U_{op}A}{U_D A} = \frac{\left(\frac{h_v h_G}{h_v + h_G}\right)_{op}}{\left(\frac{h_v h_G}{h_v + h_G}\right)_D} = \frac{\left(h_v h_G\right)_{op}\left(h_v + h_G\right)_D}{\left(h_v h_G\right)_D\left(h_v + h_G\right)_{OP}} \tag{13}$$

But $\frac{\left(h_g\right)_{op}}{\left(h_g\right)_D} = \left(\frac{m_{gop}}{m_{gD}}\right)^{0.61}$

Then

$$U_{op}A = U_D A\left(\frac{m_{gop}}{m_{gD}}\right)^{0.61}\left(\frac{m_{vop}}{m_{vD}}\right)^{0.8}\frac{\left(h_v + h_G\right)_D}{\left(h_v + h_G\right)_{OP}} \tag{14}$$

The equation (14) is more complicated to solve and it depends on the geometric of the heat exchanger. In order to avoid using the information of the geometric of the heat exchanger,

Aspen plus used a simplified expression equation (15) which depends only with the seam and gas mass flow. It gives a good approximation.

$$U_{op}A = U_D A\left(\frac{m_{gop}}{m_{gD}}\right)^{0.61}\left(\frac{m_{vop}}{m_{vD}}\right)^{0.8} \quad (15)$$

Appendix D

Performance of the compressor stage by stage calculated using Equation 3.2 and Figure 3.15

Subcritical and supercritical SSFCC			Conventional NGCC		
Volumetric flow m^3/h	Pressure ratio (-)	Efficiency (-)	Volumetric flow m^3/h	Pressure ratio (-)	Efficiency (-)
stage 1			**stage 1**		
51,356	2.1260	0.8500	48,459	2.1260	0.8500
44,680	2.1260	0.8288	42,160	2.1260	0.8288
38,517	2.1260	0.8075	36,345	2.1260	0.8075
35,949	2.1260	0.7863	33,922	2.1260	0.7863
31,327	2.1260	0.7650	29,560	2.1260	0.7650
stage 2			**stage 2**		
23,081	2.0287	0.84	18,518	2.0232	0.8400
20,081	2.0287	0.819	16,110	2.0232	0.8190
17,311	2.0287	0.798	13,888	2.0232	0.7980
16,157	2.0287	0.777	12,962	2.0232	0.7770
14,080	2.0287	0.756	11,296	2.0232	0.7560
stage 3			**stage 3**		
11,225	1.8999	0.8300	9,006	1.8951	0.8300
9,766	1.8999	0.8093	7,835	1.8951	0.8093
8,419	1.8999	0.7885	6,754	1.8951	0.7885
7,858	1.8999	0.7678	6,304	1.8951	0.7678
6,847	1.8999	0.7470	5,494	1.8951	0.7470
stage 4			**stage 4**		
5,745	2.0219	0.8200	4,295	2.0173	0.8200
4,998	2.0219	0.7995	3,737	2.0173	0.7995
4,309	2.0219	0.7790	3,222	2.0173	0.7790
4,022	2.0219	0.7585	3,007	2.0173	0.7585
3,504	2.0219	0.7380	2,620	2.0173	0.7380
stage 5			**stage 5**		
2,620	2.0146	0.8100	2,102	2.0114	0.8100
2,280	2.0146	0.7898	1,829	2.0114	0.7898
1,965	2.0146	0.7695	1,577	2.0114	0.7695
1,834	2.0146	0.7493	1,472	2.0114	0.7493
1,598	2.0146	0.7290	1,282	2.0114	0.7290
stage 6			**stage 6**		
1,018	1.8404	0.8000	817	1.8390	0.8000
886	1.8404	0.7800	711	1.8390	0.7800
764	1.8404	0.7600	613	1.8390	0.7600
713	1.8404	0.7400	572	1.8390	0.7400
621	1.8404	0.7200	498	1.8390	0.7200
stage 7			**stage 7**		
530	1.3677	0.7800	425	1.3668	0.7800
461	1.3677	0.7605	370	1.3668	0.7605
397	1.3677	0.7410	319	1.3668	0.7410
371	1.3677	0.7215	298	1.3668	0.7215
323	1.3677	0.7020	259	1.3668	0.7020

Appendix E

Inlet and outlet pressure of steam turbines at part-load

Supercritical SSFCC fixed IGV

Load	%	100		84		74		57		52	
Supercritical steam turbine											
		Inlet	outlet	Inlet	outlet	Inlet	outlet	Inlet	outlet	Inlet	outlet
Pressure	bar	299.71	80.00	222.11	62.44	176.51	52.96	108.00	35.31	95.89	29.80
Pin / Pout		3.75		3.56		3.33		3.06		3.22	
HP steam turbine											
Pressure	bar	79.02	42.64	62.73	34.40	52.41	29.04	34.98	19.94	29.50	16.42
Pin / Pout		1.85		1.82		1.80		1.75		1.80	
IP steam turbine											
Pressure	bar	41.01	4.00	33.15	3.23	28.00	2.73	19.27	1.88	15.84	1.54
Pin / Pout		10.25		10.26		10.26		10.26		10.26	
LP steam turbine											
Pressure	bar	4.00	0.05	3.16	0.04	2.62	0.04	1.23	0.03	0.68	0.03
Pin / Pout		82.82		71.44		63.57		36.45		22.31	

Subcritical SSFCC fixed IGV

Load	%	100		84		74		57		52	
HP steam turbine											
Pressure	bar	172.47	42.64	134.23	33.22	111.54	27.61	77.00	19.06	46.02	11.39
Pin / Pout		4.04		4.04		4.04		4.04		4.04	
IP steam turbine											
Pressure	bar	41.40	4.20	32.23	3.35	26.79	2.75	18.50	1.89	11.06	1.12
Pin / Pout		9.85		9.62		9.74		9.80		9.83	
LP steam turbine											
Pressure	bar	4.21	0.05	3.25	0.04	2.57	0.04	1.21	0.03	-	-
Pin / Pout		87.00		75.70		65.29		37.04			